Brain-Controlled Neuroprosthetic Therapies And Mechanisms Of Recovery After Spinal Cord Injury

THÈSE N^{O} 8075 (2017)

PRÉSENTÉE LE 8 DÉCEMBRE 2017
À LA FACULTÉ DES SCIENCES DE LA VIE
UNITÉ DU PROF. COURTINE
PROGRAMME DOCTORAL EN NEUROSCIENCES

ÉCOLE POLYTECHNIQUE FÉDÉRALE DE LAUSANNE

POUR L'OBTENTION DU GRADE DE DOCTEUR ÈS SCIENCES

PAR

Galyna PIDPRUZHNYKOVA

acceptée sur proposition du jury:

Prof. J. Gräff, président du jury
Prof. G. Courtine, directeur de thèse
Prof. A. Holtmaat, rapporteur
Dr J. Riddell, rapporteur
Dr B. Schneider, rapporteur

ÉCOLE POLYTECHNIQUE
FÉDÉRALE DE LAUSANNE
Suisse
2017

I. SUMMARY

Spinal cord injury (SCI) is the second leading cause of paralysis, which induces abrupt impairments with devastating consequences for the quality of life of patients. Despite significant progress in SCI treatment through neurorehabilitation training and spinal cord stimulation (SCS) techniques, there is still no cure for SCI. Perhaps one of the most impressive achievements in the field of SCI is the recovery of voluntary locomotor function in severely paralyzed rats which underwent neurorehabilitation training combined with electrochemical SCS. Although the neural reorganization underlying this recovery has been shown, the biological mechanisms of plasticity after SCI remain obscure, which may hinder successful translation into patient therapies. My thesis represents a series of studies which investigate the neural mechanisms underlying locomotor recovery after SCI and leverage these findings for the development of brain-controlled neuroprosthetic therapies to enhance the potential of neurorehabilitation therapies.

The first study focused on investigating neural mechanisms underlying locomotor recovery after clinically relevant contusion SCI. During this study, we assessed changes in over a hundred kinematic parameters using gait pattern extraction and principal component analysis. Our results show that the animals learned to step even in the absence of electrochemical enabling factors. Remarkably, we observed a carryover effect of locomotor recovery to the previously unpracticed swimming task. Afterwards, we dissected the neural mechanisms underlying the observed behavioral effect using viral tracing techniques and a double-virus construct allowing targeted pathway inactivation. As a result, we were able to reversibly abolish stepping capacity of rehabilitated rats, suggesting the critical importance of the reticulospinal tract for the recovery from contusion SCI.

These findings gave us the rationale for the second study in which we developed a novel rehabilitation paradigm of brain-controlled stimulation of the mesencephalic locomotor region (MLR). The MLR sends excitatory descending input to reticulospinal neurons in the brainstem. Hence, MLR stimulation could boost the descending locomotor command from the motor cortex that only partially passes through the tissue bridge spared after contusion SCI. We hypothesized that this intervention may lead to improved locomotion in rats after SCI when combined with neurorehabilitation training and electrochemical SCS. We found that brain-controlled MLR stimulation was able to improve kinematic output in rehabilitated animals and to significantly reduce side effects of non brain-controlled MLR stimulation. Thus, this novel neuroprosthetic

paradigm is capable of enhancing existing rehabilitation techniques. However, the long-term effectiveness of this intervention during SCI rehabilitation needs to be further investigated to evaluate its full therapeutic benefit.

Finally, after evaluating the possible beneficial and adverse effects of MLR stimulation in a translational context, we proposed another type of brain-controlled stimulation that directly bypasses the lesion site through an electronic bridge between the brain and the spinal cord. For this, we created a neuroprosthetic system allowing for direct cortical control of spinal cord neuromodulation during gait rehabilitation. This refinement of SCS delivery significantly improved both immediate locomotor output and the long-term recovery of rats after SCI.

In conclusion, this thesis uncovers mechanisms of recovery from SCI and demonstrates the therapeutic potential of brain-controlled neuroprosthetic therapies. Furthermore, it raises important questions and identifies challenges in translating these therapies from the bench to the bedside. Hence, this work constitutes a valuable input for both basic science and the development of clinically relevant interventions.

Keywords: spinal cord injury, neuroprosthetic rehabilitation, brain-controlled neuromodulation, deep brain stimulation, mesencephalic locomotor region, spinal cord stimulation, kinematic analysis, circuitry remodeling, locomotor recovery

II. ZUSAMMENFASSUNG

Die Querschnittlähmung ist weltweit die zweithäufigste Ursache von Lähmungserscheinungen des Körpers, welche einen plötzlichen und traumatischen Einschnitt im Leben von betroffenen Patienten darstellen. Trotz wissenschaftlicher Behandlungsfortschritte mittels Neurorehabilitation und elektrischer Rückenmarksstimulation, konnte bisher kein bleibender Heilungserfolg im Menschen erzielt werden. Ein vielversprechender therapeutischer Ansatz aus der Grundlagenforschung ist die kombinierte elektrisch-pharmakologische Rückenmarksstimulation, welche im Tiermodell der Querschnittlähmung erstmals zu einer Wiederherstellung eines willentlich-gesteuerten Gangbildes führte. Obwohl gezeigt werden konnte, dass diese neuartige Behandlungsform ausgeprägte neurale Reorganisationsprozesse des zentralen Nervensystems bewirkt, blieben die zugrundeliegenen biologischen Mechanismen der neuralen Plastizitätsvorgänge ungeklärt. Dieses fehlende Wissen stellt aktuell ein mögliches Hindernis für die erfolgreiche klinische Translation der Forschungsergebnisse dar. Meine Doktorarbeit setzt hier an und untersucht erstmals neurale Mechanismen, welche im Rahmen der kombinierten elektrisch-pharmakologischen Rückenmarksstimulation im Tiermodell der Querschnittlähmung eine wichtige Rolle spielen. Basierend auf diesen Erkenntnissen, entwickelten wir zudem zwei neuartige Brain-Machine-Interface Systeme, um das therapeutische Potential bestehender Behandlungsverfahren weiter zu verbessern.

Die erste Studie meiner Doktorarbeit befasst sich mit der Untersuchung neuraler Mechanismen der Erholung willentlicher Gangfunktion im Kontusionsmodell der Querschnittlähmung. Während dieser Studie, untersuchten wir therapeutische Effekte in über einhundert kinematischen Parametern mittels automatisierter Gangmuster-Extraktion und anschliessender Hauptfaktoren-Analyse. Unsere Resultate konnten zeigen, dass Tiere nach dem Rehabilitationsvorgang, auch in Abwesenheit elektrisch-pharamkologischer Rückenmarksstimulation, in der Lage waren Schrittbewegungen, unter beibehaltener Gewichtsunterstützung, durchzuführen. Bemerkenswerter Weise, fanden wir auch einen therapeutischen Carry-Over Effekt auf den zuvor nicht trainierten Schwimmtest. Danach untersuchten wir die zugrundeliegenden neuralen Mechanismen des Erholungsvorganges mit viralen Tracing Methoden und der sogenannten Doppel-Virus Technik, welche eine gezielte und reversible Inaktivierung einzelner neuraler Verbindungen des Gehirns ermöglicht. Als Resultat waren wir in der Lage, die Gangfunktion von rehabilitierten Ratten vorübergehend zu blockieren, was eine zentrale Stellung des retikulospinalen Traktes für die Erholung im Kontusionsmodell der Querschnittlähmung nahelegt.

Diese Resultate waren Grundlage für eine zweite Studie, in der wir ein neues Rehabiliationsparadigma, in Form einer neural-gesteuerten tiefen Hirnstimulation der Mesenzephalischen Lokomotor Region (MLR) entwickelten. Die MLR sendet exzitatorische Signale zu den retikulospinalen Neuronen des Hirnstamms. Daher erschien es aus theoretischen Gesichtspunkten plausibel, dass eine Stimulation der MLR durch zusätzliche Aktivierung des retikulospinalen Traktes die verbleibenden, teilweise unterbrochenen, neuralen Signale des motorischen Kortex zum Rückenmark verstärken würde. Unsere Hypothese war es, dass die neural-gesteuerte MLR Stimulation eine verbesserte Gangfunktion in Ratten bewirkt, wenn sie mit Neurorehabilitation und der elektrisch-pharmakologischen Rückenmarksstimulation kombiniert wird. Die Resultate der Studie zeigten, dass die neural-gesteuerte MLR Stimulation in der Lage war Gangparameter in rehabilitierten Ratten unmittelbar zu verbessern, sowie stressbedingte Nebenwirkungen im Vergleich zur nicht neural-gesteuerten MLR Stimulation signifikant zu reduzieren. Zusammenfassend, war es durch diesen neuartigen neuroprosthetischen Ansatz möglich, den Behandlungseffekt existierender Rehabiliationsstrategien weiter zu steigern. Aktuell benötigt es jedoch noch zusätzlicher Untersuchungen um die Wirkung einer langfristigen neural-gesteuerten MLR Stimulation auf die Gangrehabilitation zu evaluieren.

Zuletzt haben wir, in Zusammenschau möglicher Wirkungen und Nebenwirkungen der MLR Stimulation, an einem vereinfachten neuroprosthetischen System gearbeitet, welches die neuralen Signale des Gehirns direkt über eine elektronische Brücke an die Steuerung der elektrischen Rückenmarksstimulation weiterleitet. Diese verfeinerte Anwendung der Rückenmarksstimulation konnte, sowohl unmittelbar als auch langfristig, die Gangrehabilitation in Ratten mit Querschnittlähmung deutlich verbessern.

In Zusammenfassung, hat meine Doktorarbeit neue Einsichten in die Mechanismen der Erholung nach Querschnittlähmung erbracht, und das therapeutische Potential neuartiger neural-gesteuerter neuroprosthetischer Therapien aufgezeigt. Darüber hinaus ergeben sich aus meiner Arbeit wichtige Fragen und Herausforderungen für die erfolgreiche klinische Translation neuroprosthetischer Therapieverfahren. Insgesamt ergibt sich daher aus meiner Forschung sowohl ein wertvoller Beitrag zu Themen der Grundlagenforschung als auch zur Entwicklung neuer, klinisch relevanter Behandlungsformen der Querschnittlähmung.

Suchwörter: Querschnittlähmung, Neuroprosthetik, Neurorehabilitation, Brain-Machine-Interface Systeme, tiefe Hirnstimulation, Mesenzephalischen Lokomotor Region, Rückenmarksstimulation, kinematische Analyse, neurale Reorganisation, Gangrehabilitation

III. ACKNOWLEDGEMENTS

First, I would like to thank my supervisor, Prof. Gregoire Courtine for giving me a chance to work on all the challenging projects revolutionizing the field of spinal cord injury research. It was an exciting adventure trying to solve intellectually stimulating scientific puzzles in a great multidisciplinary team, where all the latest technological innovations are implemented to investigate and fight the devastating spinal cord injury. I believe that the combination of therapies and translational research courageously guided by Gregoire will one day help paralyzed people regain locomotor capacity.

I express my sincere gratitude to the thesis jury and the jury President for their invaluable feedback and time they have put in reviewing my thesis. Thank you, Dr. John Riddell, Dr. Bernard Schneider, Prof. Anthony Holtmaat and Prof. Johannes Gräff for all your contributions and your expert evaluation of my work. Additional thanks goes to my thesis mentor, Prof. Carl Petersen, for following my progress and providing his mentorship during annual evaluations.

I would like to acknowledge the great help I received from the G-lab team, who helped me to start my project. Thank you, Cristina, Natasha and Jean for your help in establishing the surgery procedures, deep brain stimulation technique and starting my initial experiments. Great thanks goes to Lucia and Janine for including me in the contusion study team, introducing me to all the experimental procedures and entrusting me with the responsibility for the double-virus experiments and finalizing the rat contusion study. Additionally, I am grateful to Quentin for his help in planning anatomical investigations, Laeti for the innumerous hours we spent in the behavioral space and Polina for all her help in surgeries and our long secret language conversations. Great thanks to Isabel for introducing me to the kinematic analysis and becoming a great friend, who keeps being as close and supportive years after her graduation as in the good old times. Thanks to Leo for being such an amazing friend and always bringing an easygoing compassionate warmth whenever we see each other, you are a sunshine. Thanks to Mark for being with me from day one until the end, I hope you will always keep your big Californian smile. Great thanks goes to Nick for reviewing my thesis, sharing the tea and bringing Andrea over. My big thanks also goes to Shiqui for the fun times sharing the office and the fruits. Finally, I cannot express enough of my gratefulness to Marco B for all our countless hours establishing the project together, his creativity, bursting energy, endless discussions and becoming the best friend and the best teammate I have ever had a chance to work with.

I wouldn't be myself if I haven't spent most of my free time trying to change the world through working in non-profit associations and connecting with people. It was a great time, where I met amazing friends, who are passionately committed to pursuing common noble causes. Therefore, my bottomless gratitude goes to all the associations and extracurricular project teams, which gave me inspiration and energy to power through the difficult moments. Thank you LSCD and Exposure teams, ShARE, Sandbox and salsa community for all the great projects and times we had together! Special thanks goes to BSNL, which became a part of me and a constant reminder that nobody is perfect, but a team can be.

My scientific journey would be so much less exciting without all the great friends whom I met throughout my life in Ukraine, Germany and Switzerland and who supported me through the hardest moments and celebrated the victories. Thank you, любимые Женя, Алёнка, Ксюша, Оля, Муж и Таманск for the friendship, which resists across all countries and languages. Great thanks to my Tübingen crowd for giving me the feeling of having the second home in Germany and bringing this home feeling along no matter where we meet. Thank you, the KGB crew, Marinochka, Pooja and my Lieblingseinwohners, I am looking forward to discovering new places and adventures with you. Of course, nothing would be possible without the great people, whom I met in the last 4 years in Lausanne. Thank you Dasha and Anya for your genuineness, all the cultural outings and girls' trips. Special thanks goes to Aleks and Daniel for being infinitely reliable, understanding and strong. Thanks to all my friends for challenging and simultaneously supporting me, you inspire me to be a better person.

Finally, nothing would be possible without the precious support and love from my family. Мамочка и папочка, спасибо большое за то, что вы у меня есть - такие вдохновляющие и поддерживающие. Вы меня заразили своим вирусом гиперактивности и неусидчивости, благодаря которому я никогда не устану покорять мир. Спасибо дедушке и бабушке за их любовь и мудрость, и Лёше за Металлист. Огромное спасибо моему братику Димчику за то, что он меня так любит и понимает, и за его силы выдержать всю нашу семейку. Спасибо, что вы всегда со мной где бы я ни была, и за неисчерпаемую любовь и энергию, которая даёт мне силы двигаться вперед. Finally, I cannot thank enough to Niko for all his precious support and understanding, for being my partner and the best friend simultaneously and for all the wonderful moments, we had together. You fill my present with love and my future with purpose.

« Борітеся — поборете! »

Т.Г.Шевченко

IV. TABLE OF CONTENTS

V. ABBREVIATIONS

5-HT	5-hydroxytryptamine, serotonin
8-OH-DPAT	8-hydroxy-2-(dipropylamino)tetralin hydrobromide
AAV	adeno-associated virus
AIS	American Spinal Injury Association impairment scale
AP	anterior posterior (distance from Bregma)
ASIA	American Spinal Injury Association
BDA	biotinylated dextran amine
BMI	brain-machine interface
BSI	brain-spinal interface
BWS	body weight support
CNS	central nervous system
CPGs	central pattern generators
CuN	cuneiform nucleus
DBS	deep brain stimulation
DV	dorsoventral (depth from the surface of the dura mater)
EES	electrical epidural stimulation
EMG	electromyography
eTeNT	enhanced Tetanus Neurotoxin
FB	fastblue
GFAP	glial fibrillary acidic protein
GFP	green fluorescent protein
HiRet	highly efficient gene transfer lentiviral vector
L2	lumbar spinal cord level 2
L-DOPA	Levodopa, L-3,4-dihydroxyphenylalanine
MG	medial gastrocnemius
ML	mediolateral (distance from the longitudinal midline of the scull)
MLR	mesencephalic locomotor region
PBS	phosphate buffered saline
PCA	principal component analysis
PPN	pedunculopontine nucleus
PreCuN	precuneiform nucleus
ROI	region of interest
S1	sacral spinal cord level 1
SD	standard deviation

SEM	standard error of the mean
SCI	spinal cord injury
SCS	spinal cord stimulation
SKF-82197	6-Chloro-7,8-dihydroxy-1-phenyl-2,3,4,5-tetrahydro-1H-3-benzazepine hydrobromide
STN	subthalamic nucleus
TA	tibialis anterior
TRE	tetracycline-responsive element
vGRF	vertical ground reaction forces

1. INTRODUCTION

Spinal cord injury (SCI) is a devastating neurological disorder leading to the complex loss of central control of multiple organs. Locomotion is the most obvious deficit arising from SCI; however, impairments in sensory, bladder, bowel, sexual and autonomic functions also significantly impact quality of life. Functional transmission of neural signals is interrupted due to the degeneration of physical neuronal structures connecting the brain and spinal cord because of the SCI. Depending on the level and severity of SCI, it can lead to complete or partial paralysis below the level of injury. In a minority of cases, the recovery of walking capacity happens spontaneously. However, in the majority of the cases, the locomotor network has to be actively repaired. To assure efficient recovery, the interplay between supraspinal, spinal cord and sensory input circuits has to be effectively reestablished. Therefore, multiple neuroprotective, neuro-repair and neurorehabilitation strategies are being developed and clinically tested worldwide to alleviate the devastating consequences of this neurodegenerative injury.

In the introduction, I will provide an overview of traumatic SCI from the perspective starting with history, epidemiology, and physiological consequences and finish with biological treatment approaches, plasticity mechanisms following SCI and potential developments of neurorehabilitation approaches. During my thesis work, my main goal was to understand the mechanisms of SCI rehabilitation and develop novel neuroprosthetic techniques for facilitating recovery after SCI. Therefore, I will mainly concentrate on locomotor training and electrical stimulation therapies, which were the topic of my thesis research due to the wide use and high translational potential of these techniques.

1.1 Traumatic spinal cord injury: historical perspective, epidemiology and societal burdens

The first description of brain injuries, including two cases of SCI was initially described in an ancient writing "The Edwin Smith Surgical Papyrus" by the great Egyptian physician named Imhotep and is dated around 1700-2500 BC (Hughes, 1988; Feldman and Goodrich, 1999; Donovan, 2007). In these texts, SCI is referred to as "an ailment not to be treated", which in ancient times was considered a fatal and untreatable condition. This attitude persisted for almost 4000 years until the 7th century, when Paul of Aegina introduced the first intervention to relieve SCI consequences through surgical decompression (Goodrich, 2004; Silver, 2005). Since then multiple advances have been made in surgical techniques and acute SCI treatment (Schiller and Mobbs, 2012). However, it was not until the 1940s, when the life expectancy of patients with SCI increased from a few weeks to around a decade. Thanks to the advances made by SCI researchers, this number doubled by the 1950s and continued to grow to close to an average normal life expectancy (Trieschmann, 1988).

Currently the World Health Organization estimates that as many as 2.5 million spinal cord injury (SCI) patients are living worldwide, including 330,000 in the European Union with 11,000 new cases each year ('European Commission : CORDIS, 2016; 'WHO | Spinal cord injury', 2013). Blumer and Quine reported the global prevalence of SCI to be between 110 and 1120 per million in 1995 (Blumer and Quine, 1995), which aligns with the report by Cripps (236-1009) in 2011 (Cripps et al., 2011). Switzerland has one of the lowest SCI incidence rates, with about 15 per million, and the Rhone-Alpes region of France has the lowest global incidence rate of 12.7 per million (Singh et al., 2014). The low SCI rate is likely due to the good economical situation in these regions leading to a peaceful environment.

Depending on socioeconomic factors and a country's development, causes and incidences of SCI vary significantly. In a retrospective study analyzing SCI from 1975 to 2009, the following main traumatic SCI causes were reported: traffic accidents (42.5%), falls (33%), sport/leisure (19%) and the remaining 5.5% happened due to violence & other causes (Knútsdóttir et al., 2012). The same study found that man-women ratio of SCI patients was approximately 2 to 1 (Knútsdóttir et al., 2012). Finally, in addition the devastating impact on the lives of individuals, the costs associated with SCI impose large expenses on society.

Depending on the severity of SCI, the estimated annual costs per patient in the US are from $16.8 thousand to $28.3 thousand and add up across a lifetime to between $1.5-4.7 million per patient (‘WHO | Spinal cord injury’, 2013; McDonald and Sadowsky, 2002). Altogether, the high prevalence of SCI, its dramatic physical and economical consequences creates a strong humanitarian incentive to understand SCI-triggered mechanisms to develop new treatments that can improve patients’ lives.

1.2 Consequences and mechanisms of spinal cord injury

Traumatic SCI is not a short-term event; its consequences result in pathophysiological changes that extend from minutes to years after the injury (Schwab and Bartholdi, 1996). In real life, the most common SCI is due to contusion or compression of the spinal cord by a blunt force (DeVivo et al., 2002), which begins a process called “primary damage”. From the first moments after SCI, the mechanical injury leads to a cascade of bodily reactions termed “secondary injury”, which include cell death, haemorrhage and ischemia, followed by excitotoxic cell death and immune response lasting hours to days (Bareyre *et al.*, 2004a). In the next months the injury becomes chronic, forming a characteristic glial scar and a cyst around the injury site, followed by chronic demyelination, adhesions and fibrosis (Cramer et al., 2005). Although promising advances have been made in basic research of SCI, as discussed in the previous chapter, this neurological disorder is still far from being cured (Adams and Cavanagh, 2004; Silva et al., 2014). Therefore, throughout my thesis I researched mechanisms and potential treatments of a clinically relevant contusion SCI.

The spinal cord is a communication channel between the brain and peripheral organs and is an extremely important structure for locomotion (Kiehn, 2006; Nógrádi and Vrbová, 2013). It relays information from the brain and subcortical structures to the respective organs as shown in **Figure 1.2.1** (Ahuja et al., 2017). The descending motor pathways are generally called based on their origin, for example, the corticospinal and rubrospinal pathways originate in the cortex and red nucleus, respectively, and bring information about locomotion initiation and modulation through the tracts running in the white matter of the spinal cord (Cho, 2015). Following the same logic, the upstream sensory pathways are named the spinothalamic and spinocerebellar pathways because they bring afferent information to the thalamus and cerebellum, respectively.

Although the rat spinal cord is comprised of 35 segments as opposed to the 31 of humans, segmental functions are quite similar (Nógrádi and Vrbová, 2013). Depending on the spinal segment where the injury occurs, its severity and applied treatment post-SCI, all the downstream and upstream projections between the brain and spinal cord may be disrupted, which leads to the impairment or complete loss of sensory and motor functions (Freund et al., 2013). Throughout my research, I studied severe contusion SCI at the T9/T10 level, which only leaves a small ridge of spared tissue on the ventral side of the spinal cord and leads to permanent hindlimb paralysis.

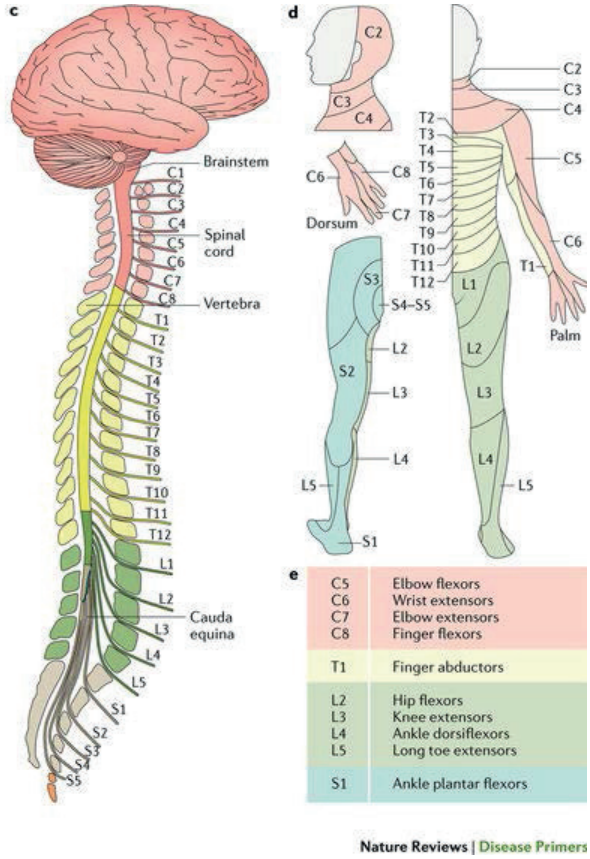

Figure 1.2.1 | Anatomy and function of the spinal cord column. Adapted from (Ahuja et al., 2017).

Clinically, the level of injury is determined based on the lowest dysfunctional spinal segment. The higher the level of the injury is, the worse the consequences of SCI, because more organs become denervated (Kirshblum *et al.*, 2011). **Figure 1.2.1** adapted from Ahuja and colleagues (Ahuja et al., 2017) summarizes the relationships between segmental anatomy and function, and must be read such that damage of a spinal segment leads to impairments in lower segments as well, negatively impacting functioning of the downstream projections from the brain. For example, tetraplegia is a neurological disorder resulting from a SCI at a cervical level and leading to paralysis or loss of motor and/or sensory function of all four extremities. Correspondingly, paraplegia, which I studied in my thesis, is caused by an SCI at a thoracic or lower level of the spinal cord and is characterized by impairments in trunk, legs and pelvic organs (Kirshblum *et al.*, 2011).

1.3 Prognostic factors and spontaneous recovery

As discussed previously, paraplegia leads to the disturbance of lower limb movements and malfunctioning of the organs innervated by the segments below the injury. Restoration of walking is one of the highest priorities of paraplegic patients, along with sexual and bladder functions (Anderson, 2004; Ditunno et al., 2008). However, very few SCI patients are able to regain normal locomotor function. Their recovery largely depends on lesion completeness (Daverat *et al.*, 1988), its neurological level (Stover, 1995; Kirshblum and O'Connor, 1998), but not on the lesion cause (Iseli *et al.*, 1999). Individuals with complete SCI do not regain the ability to walk; however, incomplete injuries exhibit an extensive degree of spontaneous plasticity (Daverat et al., 1988).

In 1969, Frankel et al published an SCI classification system, where they described a severity scale ranging from A to E (Frankel *et al.*, 1969). This provided the foundation of the modern American Spinal Injury Association (ASIA) impairment scale (AIS), which is widely used by clinicians. Currently AIS (**Table 1.3.1**) is an international standard for neurological classification of SCI and is used to determine its functional consequences (Kirshblum *et al.*, 2011).

The American Spinal Injury Association (ASIA) impairment scale	
GRADE	**DEFINITION**
A	**COMPLETE:** no motor or sensory function is preserved in the sacral segments S4-5
B	**SENSORY INCOMPLETE:** sensory (but not motor) function is preserved below the neurological level and extends through the sacral segments S4-S5 AND no motor function is preserved more than three levels below the motor level on either side of the body.
C	**MOTOR INCOMPLETE:** motor function is preserved below the neurological level, and the majority of key muscles below the neurological level have muscle grade less than 3
D	**MOTOR INCOMPLETE:** motor function is preserved below the neurological level, and the majority of key muscles below the neurological level have a muscle grade greater than or equal to 3
E	**NORMAL:** motor and sensory function are normal in all segments of the patients, who had prior deficits

Table 1.3.1 | The American Spinal Injury Association Impairment Scale (AIS). The letters A to E are used to denote degrees of functional impairment. Adapted from the http://asia-spinalinjury.org/information/downloads/.

The AIS provides a substantially accurate assessment of sensorimotor impairments of SCI patients during the first examination and remains the most relevant prognostic factor for their future functional recovery (Scivoletto *et al.*, 2014).

Spontaneous recovery from SCI, that is, restoration of motor, sensory and/or autonomic functions, happens on average in 40% of both humans and animals with SCI (Onifer *et al.*, 2011). According to the AIS scale, 80% of the most severely affected AIS A patients remain as AIS A, with only about 10% converting to AIS B. In turn, AIS B conversion to AIS C is between 15 and 40%, AIS B conversion to AIS C reaches 40% and between 60 and 80% of AIS C patients convert to AIS D by regaining their motor function (Fawcett *et al.*, 2007). Despite lesion level and severity, age, post-SCI care and other clinical examinations, like delayed plantar response (Scivoletto *et al.*, 2014) and task-dependent MEPs (Diehl *et al.*, 2006) are additional predictors of functional recovery, which is very important for healthcare planning (Ditunno *et al.*, 2008).

The mechanisms underlying recovery from SCI have been largely investigated in the past half century (Bareyre *et al.*, 2004a; Ballermann and Fouad, 2006; Courtine *et al.*, 2008; Zörner *et al.*, 2014). However, many unanswered questions remain and translation of approaches developed in animal studies is still complicated (Dietz and Curt, 2006).

1.4 Approaches for treatment of traumatic paralysis

In the majority of SCI cases, there is no spontaneous recovery, and patients require extensive post-injury care and rehabilitation treatment (Fawcett *et al.*, 2007). In fact, modern neurorehabilitative approaches are multifactorial, largely vary from one rehabilitative center to another and often lack solid evidence of their effectiveness (Dietz and Fouad, 2014). Development of most evidence-based clinical neurorehabilitative paradigms for individuals with incomplete SCI began in animal models (Barbeau and Rossignol, 1994; de Leon et al., 1998; Edgerton et al., 2004; Girgis et al., 2007; Courtine et al., 2009) and only later was translated into clinical practices.

During the treatment of incomplete SCI, rehabilitation strategies primarily pursue three main goals: i. Activation of the locomotor circuits below the lesion; ii. Enhancement of plasticity through the lesion cavity and important locomotor centers; iii. Reestablishment of brain to spinal cord connectivity through multiple therapeutic approaches aiming to improve rehabilitation outcomes (Silva *et al.*, 2014). In this section, I will elaborate on the interventions developed for accessing the sublesional spinal circuits and combinatorial therapies for SCI treatment. I will later discuss potential plasticity changes in the context of my thesis work, which may be induced by the treatments and neuroprosthetic interventions described in this section.

1.4.1 *Gaining access to sublesional locomotor circuits and neurorehabilitation paradigms*

Thoracic SCI is characterized by paraplegia of various severity degrees depending on lesion completeness and the number of spared supraspinal connections. The most common and widely used rehabilitation paradigm is locomotor training, which even in chronic patients with incomplete SCI can lead to an improvement of locomotor functions (Wirz *et al.*, 2005; Hubli and Dietz, 2013). However, individuals with severe SCI, for example, AIS A, are not able to regain full independence after rehabilitation training and remain dependent on manual support and/or braces for the rest of their life (Dietz and Fouad, 2014). Additionally, training is restricted to task-specific rehabilitation (Girgis *et al.*, 2007), which has a limited carryover effect. This creates a big burden for the doctors, physiotherapists and patients themselves, who have to define the training approach and decide which tasks are the most important for their everyday life.

The second approach to gain access to preserved locomotor networks below the injury is spinal cord stimulation (SCS). SCS can be done with different degrees of invasiveness, each coming with a tradeoff of the selectivity of recruitment of different muscle groups, ease, safety of use at home and in clinics and adverse effects due to implantation. Various attempts of SCS were shown to be effective both in animal models and in patients. These include epidural electrical stimulation (EES) (Iwahara *et al.*, 1992; Gerasimenko *et al.*, 2003; Courtine *et al.*, 2009; Harkema *et al.*, 2011; Wenger *et al.*, 2016), intraspinal stimulation (Barthélemy *et al.*, 2007; Mushahwar *et al.*, 2007) and transcutaneous stimulation (Hofstoetter *et al.*, 2014; Mayr *et al.*, 2016). All of these methods are better than direct muscle stimulation (Thrasher and Popovic, 2008; Everaert *et al.*, 2010) due to increased endurance and reduced muscle fatigue. This beneficial effect of SCS is explained by a more natural SCS-induced activation of muscle synergies as compared to direct muscle stimulation following a triggered spinal cord efferent signal. There are, of course, challenges associated with the more invasive methods, such as infections during EES and intraspinal electrode implantation, which can lead to damage of the healthy spinal cord around the implantation site.

Already almost half a century ago, promising results in animal models led to the translation of EES into human SCI (Richardson and McLone, 1978; Richardson *et al.*, 1979) and were recently repeated (Minassian *et al.*, 2004; Harkema *et al.*, 2011). The findings of Harkema et al. show that after EES rehabilitation combined with training, the patient was able to voluntarily control some individual joint movements in his previously fully paralyzed leg. The mechanism of the reported effect is most probably the facilitating effect of EES when combined with training, which enabled the passage of the patient's descending voluntary motor command to the muscles below the injury and therefore allowed for voluntary movements.

Not only electrical, but also pharmacological stimulation has been shown to effectively recruit the spinal circuits below the SCI and facilitate locomotion. Multiple studies showed that L-DOPA, noradrenaline and serotonin are useful for facilitating and evoking locomotion (Jankowska *et al.*, 1967; Barbeau and Rossignol, 1987; Cazalets *et al.*, 1992; Schmidt and Jordan, 2000). However, the translation of pharmacological interventions is tricky due to the variability of reactions to the same pharmacological interventions in different species and possible complications with FDA drug approval for use in patients. The most promising results are coming from the patented combination of buspirone, L-DOPA and carbidopa named Spinalon^{TM}, which passed the Phase I/IIa clinical trial stage and showed safety and preliminary efficacy following a single administration in patients with

SCI (Radhakrishna *et al.*, 2017). While these results are indeed promising, it is still necessary to prove Spinalon's efficacy in a large patient population.

Finally, combinatorial interventions incorporating multimodal treatments have also been extensively studied with various degrees of success. For example, Ichiyama and colleagues showed that a combination of the serotonin agonist quipazine and EES can improve treadmill stepping in rats with complete spinal transection in a dose-dependent manner (Ichiyama *et al.*, 2008). Additionally, locomotor training has been combined with the nogo antibody (Maier *et al.*, 2009), fetal spinal cord tissue (Peterson *et al.*, 2000) and olfactory ensheathing glia (Kubasak *et al.*, 2008; Takeoka *et al.*, 2011). However, the most promising results to date come from the combination of EES, pharmacological interventions and rehabilitation training in rodent models (Courtine *et al.*, 2009; van den Brand *et al.*, 2012). Van der Brand and colleagues have shown that with these techniques, fully paralyzed rats are able to regain weight-bearing voluntary locomotion after the staggered hemisection SCI. The reported recovery was largely caused by corticospinal reorganization, where cortical projections in the spinal cord rerouted between the two hemisection lesions in a way that allowed them to reconnect to the sublesional spinal circuits (**Figure 1.4.1** adapted from (van den Brand *et al.*, 2012)). However, the double-hemisection SCI model does not occur in natural conditions. Therefore, in my thesis I concentrated on researching the mechanisms of recovery after clinically relevant contusion SCI and how to facilitate them.

Extensive knowledge about SCI has been built up over the past century shedding light on the mechanisms underlying recovery enabled by neurorehabilitation. Multiple mechanisms of how functional training increases neuroplasticity have been reported in rodent (Girgis *et al.*, 2007; Edgerton *et al.*, 2008; Courtine *et al.*, 2009) and cat SCI models (Barbeau and Rossignol, 1994; de Leon *et al.*, 1998; Edgerton *et al.*, 2004). Additionally, it's been shown that on the cellular level, locomotor training induces upregulation of neurotrophic factors (BDNF), enhances collateral sprouting, neurogenesis, down-regulates receptors for myelin inhibitors (nogo), up regulates growth associated proteins and refines synaptic connectivity (Fouad and Tetzlaff, 2012). Based on the aforementioned animal studies, training of functional movements (e.g. stepping) was successfully translated to individuals with incomplete spinal cord injury (Wernig *et al.*, 1995; Dietz and Harkema, 2004; Harkema *et al.*, 2012). Overall, substantial progress has been made both for developing interventions for SCI treatment, accessing dormant locomotor circuits below the injury and understanding the mechanisms underlying recovery.

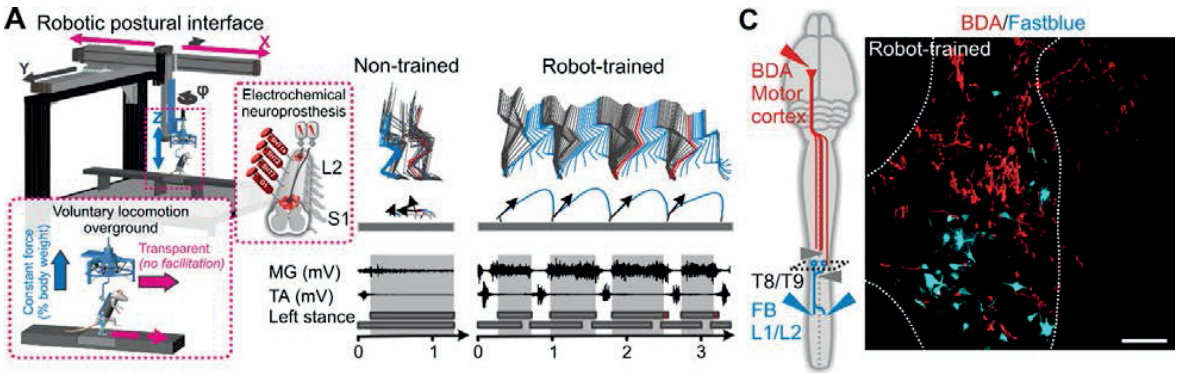

Figure 1.4.1 | Locomotor recovery after double-hemisection injury in rats. (A) Robotic bodyweight support and electrochemical neuromodulation of spinal circuits. Right panel: Kinematic and EMG recordings obtained in a non-trained and trained rat under stimulation and robotic support. **(C)** Formation of intraspinal relays through training. Adapted from (van den Brand *et al.*, 2012).

However, there is still no cure for SCI, and new treatments have to be developed to achieve effective translation into clinics and bring meaningful outcomes for patients. Given the success of the approach so far, future approaches must combine training with plasticity-enhancing treatments, such as pharmacological and electrical stimulation-based approaches (Chen *et al.*, 2006; Courtine *et al.*, 2009; Cortes *et al.*, 2011; Lamy and Boakye, 2011), which have a high potential for triggering beneficial neuroplasticity. Additionally, more realistic SCI models should be used for finding translational approaches. For example, recovery from severe spinal cord contusion which spares less than 10% of spinal cord tissue has never been reported either in humans or in animal models. Therefore, understanding of the mechanisms underlying recovery from clinically relevant contusion SCI can provide valuable scientific insights and aid in developing new therapies and neurorehabilitation paradigms for clinical translation.

1.4.2 *Physiology and history of MLR locomotion*

The forebrain plays a modulatory role during locomotion in higher animals (Beloozerova and Sirota, 1993; Drew *et al.*, 1996), but basic locomotion is initiated and maintained by subcortical structures including the midbrain, brainstem, and the spinal cord itself (Armstrong, 1988). There are several locomotor regions in the brain, which are able to initiate and modulate movements.

Proceeding rostrocaudally, the most important locomotor regions are: the subthalamic (diencephalic) locomotor region in the lateral hypothalamic area, the mesencephalic locomotor region (MLR), corresponding to the cuneiform and pedunculopontine nuclei in the dorsal midbrain, the cerebellar locomotor region located close to the fastigial nuclei in the cerebellar midline, and the pontine locomotor region in the pontomedullary reticular formation (Jahn *et al.*, 2008). While all these regions seem to be important for inducing locomotion, MLR plays a key role (see **Figure 1.4.2** adapted from (Le Ray *et al.*, 2011)) in the downstream locomotor pathway from the basal ganglia to the reticulospinal neurons, and is also involved in gait initiation in humans (Masdeu *et al.*, 1994; Hathout and Bhidayasiri, 2005). Therefore, in what follows, I will concentrate only on the MLR region, its role for locomotion and its potential as a DBS target after SCI.

Early studies in cats showed that the mesencephalic locomotor region (MLR) delivers the command to initiate locomotion in decerebrate animals (Shik *et al.*, 1969; Steeves *et al.*, 1975; Steeves and Jordan, 1980). So far, this has been confirmed in all vertebrate species including birds, salamanders, rodents and primates, among others (Le Ray *et al.*, 2011). The MLR is a functionally defined structure in the midbrain where electrical or chemical stimulation produces bouts of locomotion with a short latency (Le Ray *et al.*, 2011). The anatomical substrate for the MLR has long been debated, but according to the majority of sources, the MLR is considered to be composed of the cuneiform nucleus (CuN), the pedunculopontine nucleus (PPN), and, in some sources, the precuneiform nucleus (PreCuN) (Garcia-Rill and Skinner, 1987; Garcia-Rill, 1991). Although there are some discrepancies about whether the whole PPN and CuN are considered to form an MLR, for the sake of completeness of my literature review, I will consider any evidence about PPN and CuN to be MLR-related. My statement is based on the fact that PPN and CuN are consistently attributed to MLR across all the literature, while the other nuclei are more controversial and vary from one source to another (Le Ray *et al.*, 2011; Ryczko and Dubuc, 2013).

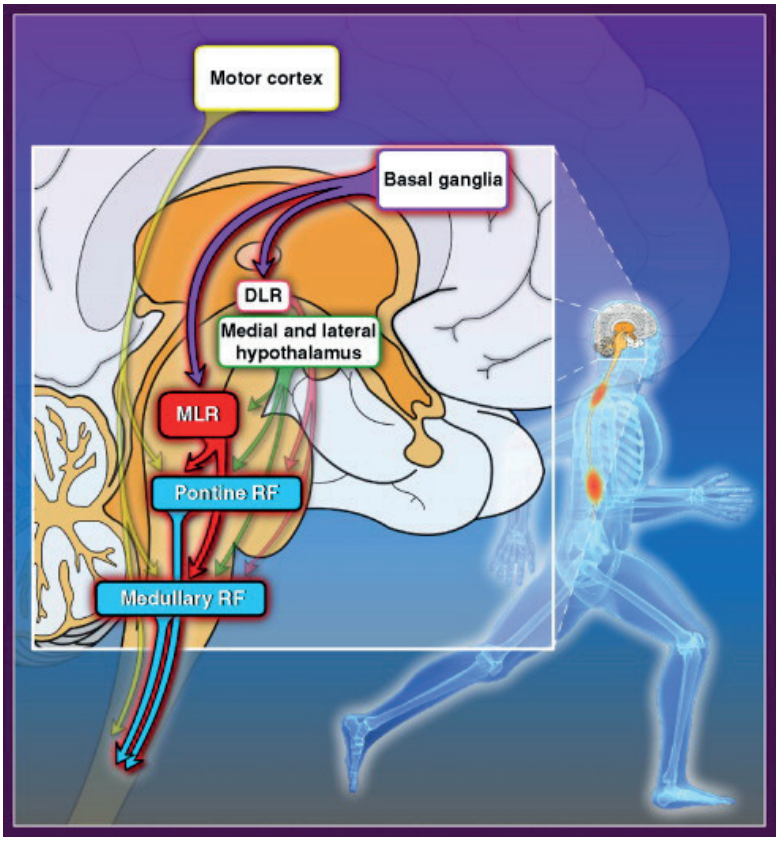

Figure 1.4.2 | The supraspinal control of locomotion. The general organization of the supraspinal control of locomotion has been described in mammals and the most relevant structures and their connections are schematically illustrated on a sagittal view of the forebrain and brainstem. DLR, diencephalic locomotor region; MLR, mesencephalic locomotor region; RF, reticular formation. Adapted from (Le Ray *et al.*, 2011).

The MLR does not project directly to the spinal cord, but instead activates hindbrain reticulospinal cells that in turn project to the spinal cord locomotor networks (Steeves and Jordan, 1984; Garcia-Rill *et al.*, 1987; Garcia-Rill and Skinner, 1987; Rossignol, 2010). Several studies indicate that the MLR projections to reticulospinal neurons are monosynaptic (Ryczko *et al.*, 2013). One study clearly shows this connection by electrically stimulating the MLR and observing evoked short-latency post synaptic potentials in the reticulospinal neurons that are maintained during repetitive MLR stimulation at high frequency (Brocard and Dubuc, 2003). Another remarkable feature of the MLR is that the locomotor speed increases with stimulation frequency of the MLR (Shik *et al.*, 1969). This has been found in all animal species investigated, during both walking and swimming.

To understand the mechanism of MLR action, it is also worth looking at the chemical nature of the MLR itself and its projections to other brain structures. Overall the MLR contains glutamatergic, GABAergic and cholinergic neurons (Martinez-Gonzalez *et al.*, 2011) with multiple neurotransmitters, including glutamate, acetylcholine, GABA, dopamine and noradrenaline (Le Ray *et al.*, 2011). Although cholinergic and glutamatergic MLR inputs to reticulospinal cells have been clearly identified in lampreys (Le Ray *et al.*, 2003), the neurochemical identity of the MLR reticulospinal inputs in other vertebrate species still needs to be investigated.

It has been proposed that the MLR elicits locomotion in three different contexts and could therefore be subdivided into three main functional areas: “an exploratory system,” “an appetitive system,” and “a defensive system” (Sinnamon, 1993). Although the anatomical separation between these three MLR sub-parts is still not clear, all of them may have an important role in the “fight-or-flight response” and are worth investigating in detail.

Recently, Roseberry et al. did the most targeted MLR DBS study to date by optogenetically selectively exciting only glutamatergic MLR neurons, see **Figure 1.4.3** adapted from (Roseberry *et al.*, 2016). The researchers were not only able to elicit short-latency locomotion with the selective optogenetic activation of glutamatergic neurons, but also found correlation of these neurons’ firing with the speed of locomotion. This provides an additional demonstration of MLR’s important involvement in locomotion and shows that it is possible to elicit characteristic locomotor initiation through the specific targeting of descending glutamatergic projections. We managed to replicate this effect in rats by selectively infecting their MLR with the AAV5 /CamKIIa--C1V1 virus and stimulating it optogenetically. However, the biggest optogenetic stimulation intensity failed to elicit the characteristic locomotor response post-SCI (data not shown).

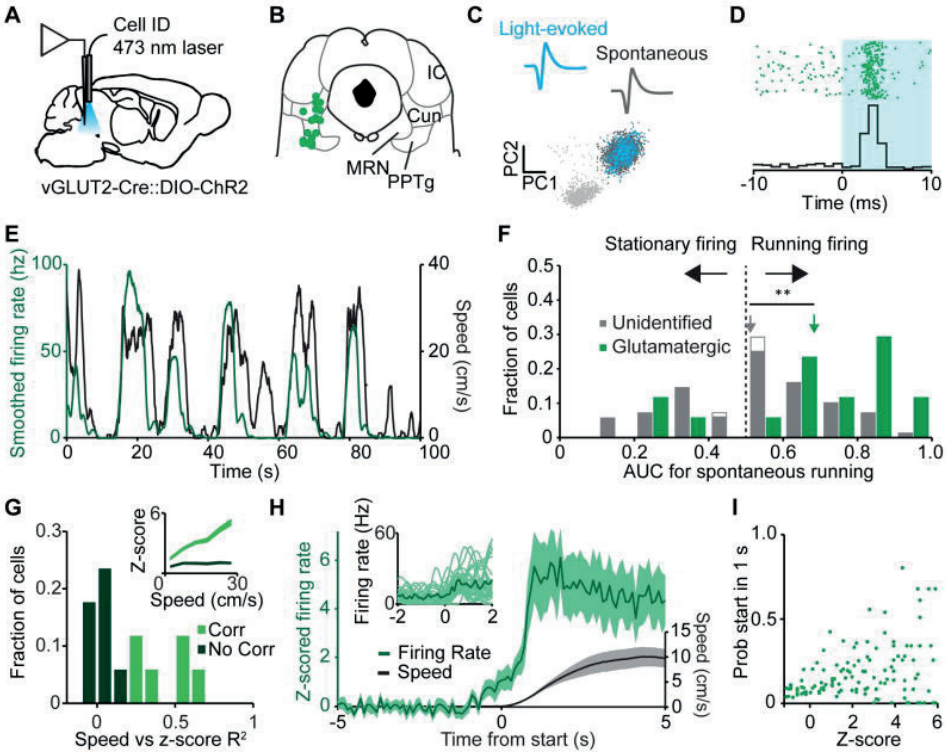

Figure 1.4.3 | Characterization of MLR glutamatergic neurons. (A-D) Identification of glutamatergic MLR neurons. **(E-I)** recording of the single unit firing rate of MLR glutamatergic neurons and its correlation with locomotor speed. Adapted from (Roseberry *et al.*, 2016).

MLR DBS has recently been suggested to be a potential therapeutic intervention for treatment of severe SCI (Bachmann *et al.*, 2013). Namely, the authors reported that MLR DBS of varying intensities induces significant improvements in the quadrupedal stepping task of paralyzed rats, when they are stimulated a month after a severe cut SCI. However, these data only report acute improvements in locomotion, and they did not perform long-term training with MLR DBS. Based on these findings and unpublished data from the laboratoy of Prof. Schwab, a new clinical trial has started aiming to investigate safety and efficacy of MLR DBS in patients with chronic incomplete SCI (L.H. Stieglitz, A Curt, 2017). While the findings of Bachmann's study remain the strongest evidence to date that MLR DBS is beneficial for locomotion after SCI, there are many unanswered questions and limitations, as mentioned before, which may negatively impact clinical outcomes. Therefore, such early translation into clinical trials seems to be unjustified and potentially dangerous for the well-being of patients with SCI.

On the other side, an improved MLR/PPN activity recorded by fMRI has been shown in DBS of the subthalamic nucleus (STN) ON condition in patients with Parkinson's disease, who performed better at a locomotor imagery task as compared to the STN DBS OFF condition (Weiss *et al.*, 2015). Additionally, MLR DBS combined with STN DBS has been reported to help patients with locomotor deficits due to Parkinson's disease, especially for locomotion initiation (Stefani *et al.*, 2007), supporting the idea that MLR is involved with locomotion initiation. However, a complex setup including stimulation of two brain structures at different times prevented the researchers from clearly distinguishing between the benefits produced by STN and MLR DBS.

Together, the cumulative knowledge about the function of the MLR in animals and humans, especially with respect to its role in inducing and facilitating locomotion, provides a strong base for the further investigation of the mechanisms underlying its action during MLR DBS (Mazzone *et al.*, 2016). Potentially, these insights can lead to the development of novel neuroprosthetic platforms using the MLR DBS as a prospective treatment for restoring locomotor function after SCI and other motor disorders, which I will discuss in more detail in the later **Section 1.6.2**.

1.5 Mechanisms of neural reorganization following spinal cord injury and plastic effects induced by treatment

Despite the long-existing belief that damaged axons do not regenerate (Ramón y Cajal and May, 1928), there are multiple examples of spontaneous recovery from SCI hinting at plastic changes occurring even in adult neuronal tissue (Fawcett *et al.*, 2007; Curt *et al.*, 2008). Derived from the Greek word *plassein*, plasticity refers to the ability to be altered or remodeled (Silva *et al.*, 2014). It is worth noting that this remodeling can occur at different levels of neuronal structures from cellular to circuitry rewiring and is not necessarily associated with beneficial functional effects (Holtmaat and Svoboda, 2009; Beauparlant *et al.*, 2013).

The first famous example of plasticity in the central nervous system (CNS) comes from the Canadian physiologists Hubel and Wiesel, who deprived kittens of binocular vision and reported a reversible blindness caused by the maladaptive plasticity of visual cortex in the absence of visual input from one eye (Hubel and Wiesel, 1959). They also observed that the reported neuronal changes could be reversed only during a short timeframe, which Hubel and Wiesel defined as a critical period of plasticity. Later, mechanisms of plasticity were described by Donald Hebb in his book on the organization of behavior (Hebb, 1949) and further studied in detail by Eric Kandell, who received the Nobel prize in 2000 for discovering the mechanisms of learning and neural signal transduction.

In the context of SCI, circuit reorganization plays a pivotal role in recovery and rehabilitation of sensory and motor dysfunction (Bareyre *et al.*, 2004b; Rosenzweig *et al.*, 2010; Onifer *et al.*, 2011; Fouad and Tetzlaff, 2012). The absence of appropriate rehabilitation can lead to maladaptive plastic changes (Beauparlant *et al.*, 2013) and loss of functional capabilities after stroke (Nudo *et al.*, 1996). The changes also result in altered neuronal properties (Murray *et al.*, 2010), anatomical modifications such as collateral sprouting (Fouad *et al.*, 2001; Weidner *et al.*, 2001), complex reorganizations of cortical (Bruehlmeier *et al.*, 1998; Fouad *et al.*, 2001) and spinal cord circuitry (Edgerton *et al.*, 2008; Rossignol *et al.*, 2008). These SCI-induced changes happen at different levels of the CNS, including cortical, brainstem and spinal cord (Bruehlmeier *et al.*, 1998; Jurkiewicz *et al.*, 2007; Onifer *et al.*, 2011), which I will discuss later in this chapter.

Before I start this chapter, I would like to outline the key introductory points, which will be explained throughout this section:

- Plasticity is occurring on all levels (cortical, brainstem and spinal)
- Plasticity can be maladaptive if not steered
- Plasticity can be manipulated in a beneficial way (rehabilitation & pharmacological agents)
- Meaningful rewiring needs activity (i.e., training)

Although many mechanisms of plasticity following SCI have been reported in the past century, there is a need to further understand the exact mechanisms that are underlying plasticity, their time course, interactions with therapeutic approaches and their role at different stages of recovery from SCI. This understanding may provide us with valuable information to help steer neuronal plasticity in the most effective way for facilitating locomotor recovery after SCI, which I tried to do throughout my research by using DBS and EES.

1.5.1 *Motor cortex involvement in locomotion and cortical plasticity following SCI*

There is an ongoing debate between researchers and clinicians about motor cortex involvement in locomotion in health and disease. Therefore, I will shortly describe the evidence in the existing literature and discuss its possible implications for this argument. The first question is whether the motor cortex is necessary for locomotion at all.

Already over half a century ago, Penfield was trying to understand what supraspinal regions are involved in the direct activation and control of locomotor behavior. Together with Jasper, Penfield removed the precentral gyrus and observed motor deficits on the contralateral body side, which recovered after a few weeks with the exception of digital dexterity movements (Penfield and Jasper, 1954). This led him to the conclusion that motor cortex function can be substituted by other brain areas. Additionally, experiments in non-human primates showed that a pyramidotomy lesion of the corticospinal tract leads to impairment of only fine hand movements, while grasping remains normal (Lawrence and Kuypers, 1965). The same group reported that 3 weeks after a corticospinal tract lesion, monkeys' locomotor movements recover to be independent and close to normal (Lawrence and Kuypers, 1968; Lemon *et al.*, 2012). These findings also hint towards the

conclusion that motor cortex is not necessary for imprecise hand and leg movements. Finally, another argument for why the motor cortex does not play a key role in locomotion is that many animals without a motor cortex are still able to perform well-coordinated locomotion, including birds, fish and salamanders (Webster and Steeves, 1988). However, the absence of the involvement of cortex in locomotion in lower animals does not mean it does not contribute in humans.

On the contrary, there are multiple counter-arguments to consider. Primary of these isthe involvement of motor cortex in recovery after neuromotor disorders. Specifically, motor cortex plasticity is correlated with recovery after stroke (Nudo *et al.*, 1996) and SCI (Fouad *et al.*, 2001), cortical maps change in a use-dependent manner (Sanes and Donoghue, 2000) and intracranial microstimulation of the primary motor cortex helps recovery after cortical lesions (Nishibe *et al.*, 2010). Moreover, motor cortex lesions lead to impaired stepping capabilities on the contralateral body side in mice (Ueno and Yamashita, 2011), abolish spontaneous recovery and significantly diminish rehabilitation effects in a specific reaching task (Krajacic *et al.*, 2010). Thus, there is also prevailing evidence suggesting that motor cortex is important and its reorganization plays a beneficial role in recovery from neurological disorders. However, more studies have to be performed to define the exact role of the motor cortex for locomotion in health and disease.

While motor cortex seems to play a less important role in stereotypical locomotion of healthy individuals, its role becomes more significant when the movement is visually guided, especially after SCI (Beloozerova and Sirota, 1993; Drew *et al.*, 1996; Nardone *et al.*, 2013; DiGiovanna *et al.*, 2016). This is likely due to two main reasons: 1- the motor cortex is trying to compensate for the impairments; 2- in the case of the corticospinal tract lesion, motor cortex still needs to control initiation and stopping of movement, which might happen through reorganization of cortical projections to the other supraspinal structures.

Furthermore, cortical representations dynamically change depending on our age, activities, their intensities and practice, and many other factors. Thus, logically SCI also leads to cortical map changes both in animal models and in patients (Bruehlmeier *et al.*, 1998; Fouad *et al.*, 2001; Mikulis *et al.*, 2002; Turner *et al.*, 2003; Jurkiewicz *et al.*, 2007). Rehabilitative training can facilitate recovery after SCI through expanding motor maps and increasing neurotropic factor release (Girgis *et al.*, 2007; Krajacic *et al.*, 2009). The recovery after corticospinal tract lesion in monkeys is critically dependent on the rubrospinal tract reorganization, which takes over the function of a

lesioned corticospinal tract because of their functional similarity and partial redundancy (Lemon *et al.*, 2012).

Overall, motor cortex seems to play an important role in locomotor recovery after SCI. Therefore, we should not neglect to study its contribution to recovery from neuromotor disorders. However, the exact mechanisms of cortical reorganization and the reorganization of its relays to other subcortical structures needs to be investigated in more detail. In the future, a better understanding of cortical changes underlying functional improvements can help us to develop more targeted therapies driving pathway-specific sprouting through other supraspinal centers, which we will exploit in the next section.

1.5.2 ***Reorganization of the reticulospinal system and its contribution to recovery***

The brainstem is an important brain region for the transmission of information between the brain and the rest of the body, especially for the maintenance of basal body functions, such as breathing, heartbeat, sleep-wake cycles, etc. A large body of evidence suggests that the projections from the brainstem to the spinal cord, known as the reticulospinal pathway, are important for both the initiation of stepping rhythm through activation of spinal networks of the lumbar spinal cord (Rossignol, 1996) and voluntary movement control, although the latter is predominantly mediated by the corticospinal and rubrospinal systems in rats (Muir and Whishaw, 2000). In fact, Steeves & Jordan argue that locomotion does not need any cortical input and can be fully performed through activation of the reticulospinal tract alone (Steeves and Jordan, 1980). Moreover, the reticulospinal system is important for the execution of precise finger and hand movements (Davidson and Buford, 2006; Alstermark and Isa, 2012) and contributes to gross hand function after incomplete SCI (Baker *et al.*, 2015; Baker and Perez, 2017). Additionally, its role in activating CPGs has been widely demonstrated in lesion (Steeves and Jordan, 1980; Schucht *et al.*, 2002) and electrophysiological studies (Jordan, 1998; Mori *et al.*, 1998). However, despite its key position and role in relaying descending locomotor drive, very little is known about brainstem plasticity and its contribution to recovery from SCI.

The reticulospinal tract is a heterogeneous tract originating from several nuclei in the reticular formation. It descends mainly ipsilaterally in dorso- and ventrolateral funiculi (Jones and Yang, 1985). Anatomical studies have demonstrated that, following SCI, sparing of only a small unilateral portion of the ventrolateral funiculus is sufficient for spontaneous locomotor recovery (Brustein and Rossignol, 1998; Little *et al.*, 2013). The temporal profile of reticulospinal tract reorganization is also similar to that of locomotor recovery, which is consistent with a causal role in functional rehabilitation (Mori *et al.*, 1992; Jordan, 1998). Further support for this interpretation is provided by a study which showed that sparing of reticulospinal fibres after contusion injury was found to be associated with a better functional outcome (Basso *et al.*, 2002).

As I have discussed previously, midbrain, pons and the medulla oblongata contain key locomotor areas necessary for locomotion initiation (Shik *et al.*, 1969; Jahn *et al.*, 2008). An extensive connection between MLR and reticulospinal nuclei, particularly the gigantocellular nucleus, was found in all healthy vertebrates tested to date (Garcia-Rill *et al.*, 1987; Ryczko and Dubuc, 2013). The descending fibers from reticulospinal neurons in turn project downstream to the spinal pattern

generators (Garcia-Rill and Skinner, 1987; Shaw *et al.*, 2010). Interestingly, in rats with a unilateral hemisection, increased projections from MLR to ipsilateral gigantocellular nucleus were reported, which further showed a double-crossing pattern in a way that the downstream MLR command was reaching the ipsilateral sublesional spinal cord as shown in **Figure 1.5.1** adapted from (Zörner *et al.*, 2014).

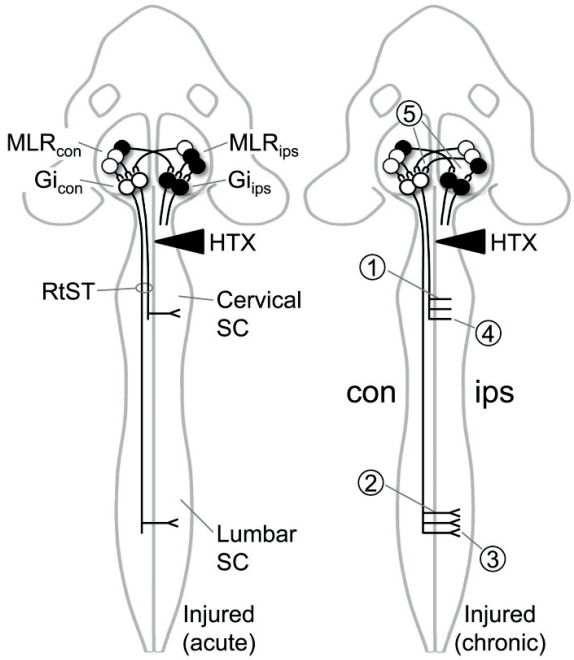

Figure 1.5.1 | MLR-reticulospinal reorganization after a unilateral hemisection SCI. Reorganization of supraspinal connectivity and downstream projections on the ipsilateral lesion side. Adapted from (Zörner *et al.*, 2014).

On the cellular level, BDNF release caused by SCI has been shown to promote regeneration and collateral sprouting of raphespinal, rubrospinal and reticulospinal motor axons and proprioceptive sensory axons (Bregman *et al.*, 1997; Jain *et al.*, 2000; Kwon *et al.*, 2002). The best illustrations of subcortical pathway plasticity are illustrated for the rubrospinal pathway in adult (Lemon *et al.*, 2012) and neonatal animals (Z'Graggen *et al.*, 2000). In the case of the reticulospinal reorganization, extensive reorganization has been shown in 13 day old embryonic chicks (Hasan *et al.*, 1993). It is an encouraging finding and can be relevant for human patients if the SCI happens

in newborns. However, the plasticity potential of the adult nervous system is in general largely diminished (Kennard, 1936), so the reorganization potential of the reticulospinal system after SCI in adults remains unknown.

Alltogether, the studies show that reorganization in unlesioned descending pathways is correlated and important for recovery of incomplete SCI. Based on this, many plasticity-boosting interventions are being developed for restoring brain-spinal connectivity (Olivier Raineteau and Schwab, 2001; Courtine *et al.*, 2008; Ghosh *et al.*, 2009) in animal models and will soon enter the clinical stage. However, convincing evidence of the necessity of the reticulospinal pathway and the mechanisms underlying its reorganization post-SCI are still unknown. Moreover, the interplay between cortical and brainstem projections after SCI remain obscure, and their role for locomotor recovery needs to be uncovered.

1.5.3 *Spinal cord plasticity in acute and chronic SCI states*

Evidence for the existence of central pattern generators in the spinal cord in vertebrates has existed for over half a century. The main characteristic of the locomotor CPG is that spinal cord circuitry alone is sufficient to generate the precise timing and phases of locomotion (Hooper, 2001; Kiehn and Dougherty, 2013). The pioneering studies in this field were done in cats and showed that, even with spinal cord transections, cats can initiate basic locomotor patterns (Forssberg *et al.*, 1980). Since then, evidence for the existence of CPGs has also been found in humans (Dimitrijevic *et al.*, 1998). Additionally, thanks to the "fictive locomotion" induced by MLR stimulation in decerebrated cats, it has been shown that sensory feedback is not necessary for locomotor pattern generation (Shik *et al.*, 1969). The supraspinal drive sent to reticulospinal and spinal networks via MLR DBS leads to adaptive locomotor pattern generation with or without sensory input (air stepping). Although the CPGs can produce rhythm and patterns without sensory input, restoring supraspinal input to CPGs after SCI is crucial for the recovery of voluntary locomotion (van den Brand *et al.*, 2012). Moreover, the contribution of afferent information from muscle spindles and skin receptors to actual locomotion is important for adaptation to the environment (Conway *et al.*, 1987; Kriellaars *et al.*, 1994) and recovery after SCI (Takeoka *et al.*, 2014a).

The spinal networks are preserved after the SCI and remain adaptable to varying sensory inputs and, thus, can be trained for different locomotor tasks even in the absence of any brain input. The first evidence of training-induced recovery of full weight-bearing locomotion in spinal cats comes from the group of Edgerton (Lovely *et al.*, 1986). Shortly thereafter, Rossignol and colleagues confirmed this finding (Barbeau and Rossignol, 1987), which led to the establishment of the new field of locomotor training for treating SCI. The reported training effects in spinal cats were observed not only during training, but also in the following months after training, suggesting the long-term importance of this intervention. Additional evidence that the spinal networks learn comes from a more recent study, where the researchers demonstrated that cats recover much faster after the second transection, if they were trained on the treadmill after the first transection (Barrière *et al.*, 2008).

Additionally, the importance of treadmill training is shown by a threefold improved recovery of spinal cats after two months of rehabilitative training compared to the non-trained ones (de Leon *et al.*, 1998). However, treadmill training is not the only way to induce plastic changes in the spinal networks. As discussed in the **Section 1.4** various pharmacological agents and electrical

stimulation were also shown to be able to activate the sublesional dormant spinal networks and facilitate recovery (Curt *et al.*, 2008; Courtine *et al.*, 2009; Silva *et al.*, 2014). Overall, numerous evidences suggest that spinal networks are important actuators in locomotion, can act in a self-sufficient way and are able to adapt to locomotor tasks in a use-dependent manner even in the absence of the central input (Lovely *et al.*, 1986; Barbeau and Rossignol, 1987; Hooper, 2001).

Mechanisms leading to plasticity of spinal circuits following training happen on multiple levels and can be mainly sub-divided into plasticity of pre-existing circuits and formation of new ones (Olivier Raineteau and Schwab, 2001). Both in humans and in animals, it is evident that the younger the animal, the more likely plastic changes are to occur (Kennard, 1936). In line with this theory, Petruska and colleagues demonstrated that stepping can be fully rehabilitated if the spinal cord transection is performed in neonatal rats at P5, which argues for the importance of the "age-at-injury" (Petruska *et al.*, 2007). However, because the majority of SCI cases happen in humans between the ages of 16 and 30 years old, we will discuss plasticity mechanisms which are happening in adults. Edgerton speculated in his review in 2001 that stepping training leads to the reduction of inhibition in spinal cord networks through diminished glycinergic and GABAergic inhibitory action and, thus, enhanced excitability of the spinal networks below the lesion (Edgerton *et al.*, 2001). Additional changes of firing thresholds of motorneurons and increases in neural signal conductivity velocity contributes to a more efficient learning as shown in monosynaptic reflex loops (Wolpaw, 1997). Lastly, it is important to point out that spontaneous recovery can occur in animals due to their self-training in cages, which is not applicable to humans and has to be thoroughly controlled for in experimental protocols (Caudle *et al.*, 2011).

Plasticity of spinal cord networks can also occur through new circuit formation, which is well-known in the context of peripheral nerve lesions (Wilson and Kitchener, 1996). Spinal networks undergo reorganization after SCI, which is largely dependent on the muscle spindle feedback (Takeoka *et al.*, 2014a). However, sprouting is not always beneficial and can lead to maladaptive changes in the absence of training (Beauparlant *et al.*, 2013) or if training is performed too early after SCI (Krajacic *et al.*, 2010). Thus, the timing of rehabilitation, as well as the type of therapeutic approach are the two crucially important factors in determining rehabilitation strategy after SCI.

Overall, immense progress has been made in the last century in our understanding and ability to facilitate locomotor recovery through activation of sublesional spinal circuits. This has already led to the introduction of locomotor training during rehabilitation of patients with SCI, while EES is in the process of being approved for use in SCI patients in clinics. We therefore need a mechanistic

understanding of the interplay between EES and training, their effect on spinal circuits and their plasticity-promoting potential throughout the whole nervous system.

1.5.4 *Reorganization of descending locomotor pathways and its potential in rehabilitation*

Finally, I would like to put all of the above in context and discuss the interplay between the aforementioned circuit reorganization mechanisms in the cortex, brainstem and spinal cord, especially with reference to how they contribute to locomotor recovery post-SCI. Particularly, I will describe how unlesioned descending locomotor pathways reorganize and contribute to improve locomotor output after SCI.

It has been reported that cats with very severe lesions preserving only 10% of spinal cord white matter are able to walk without external support (Windle *et al.*, 1958). Monkeys were able to recover their hindlimb functions with only 25% of spared spinal cord tissue (Eidelberg, 1981). Remarkably, even humans after a surgical incision which removed 50% of the spinal cord had very subtle effects on locomotion (Nathan, 1994). These studies provide evidence that locomotion can be preserved after SCI if a critical rim of spinal cord tissue remains, allowing a passage for unlesioned descending pathways and a substrate for reorganization of the lesioned ones.

Descending locomotor pathway reorganization can happen through collateral formation (see **Figure 1.5.2** adapted from (Bradbury and McMahon, 2006)) and reconnection of descending fibers to other pathways (Lemon *et al.*, 2012), axonal re-routing in the spinal networks (van den Brand *et al.*, 2012) and through reconnection of descending pathways with interneurons (Courtine *et al.*, 2008). Another very important finding is that positive plastic changes following locomotor training persist and in some cases even increase one year after animals (Wernig *et al.*, 1995) and patients (Yilmaz *et al.*, 2005) with SCI undergo rehabilitative training.

Moreover, reorganization of corticospinal and reticulospinal pathways has been shown to play an important role in recovery of motor function after stroke (Baker *et al.*, 2015). A recent study showed that reticulospinal neurons contribute to gross hand function after incomplete SCI in humans (Baker and Perez, 2017). Given the extensive sprouting of reticulospinal neurons into gray matter structures after SCI (Ballermann and Fouad, 2006) and its key role in the control of locomotion and balance in healthy animals (Drew *et al.*, 1986; Mori *et al.*, 2001), it is important to investigate the contribution of the reticulospinal tract to locomotor recovery after SCI.

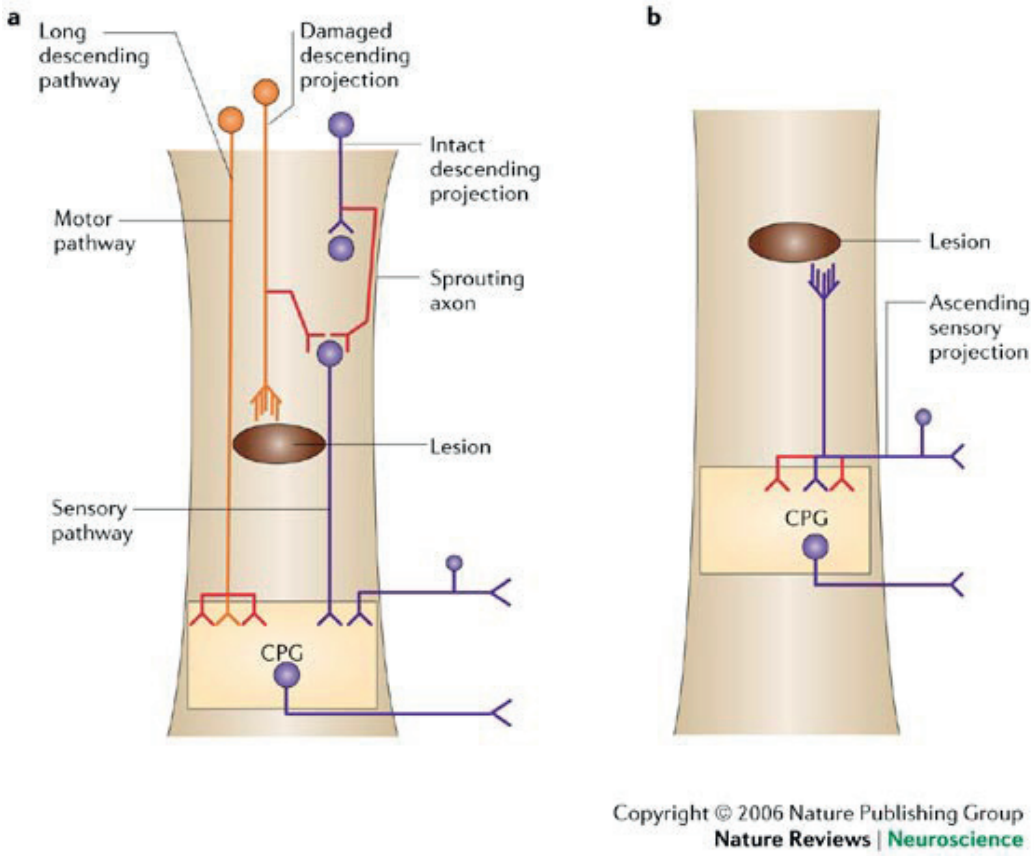

Figure 1.5.2 | Anatomical plasticity of downstream pathways and spinal connectivity lead to functional recovery after SCI. (a) Reorganization of descending system by forming new collateral connections with the propriospanil spinal cord circuits. **(b)** Ascending fiber reorganization allowing for a more effective reconnection with spinal circuits. Adapted from (Bradbury and McMahon, 2006).

To sum up, many plastic changes at multiple CNS levels have been shown after SCI; however, the exact contribution of various descending pathways to recovery and the mechanisms that drive neuronal re-routing and collateral reconnections remain unclear. Understanding of these mechanisms in detail will allow us to effectively stimulate beneficial plasticity and to develop lesion-specific treatment strategies, which is an important step towards personalized medicine.

1.6 Back to the future: what can we learn from the past to develop future translational therapies

To date, the most successful neuroprosthetic application is the cochlear implant, with more than 60 thousand cochlear neuroprotheses implanted in patients worldwide (Middlebrooks *et al.*, 2005). Cochlear implants restore hearing in deaf people through a very specific stimulation of somatotopically organized hair cells in the inner ear, inducing a frequency modulation signal, which in turn evokes a percept similar to the one naturally induced by auditory stimuli. Rapid advances in neurotechnologies and computational power have allowed for the development of novel neuroprosthetic approaches for vision restoration (Lewis *et al.*, 2015), memory enhancement (Hampson *et al.*, 2013) and neuromotor disorders (Leuthardt *et al.*, 2006).

On top of the practical application of brain-machine interfaces (BMIs), which enable patients with neuromotor disorders to communicate with the external environment, BMIs are also interesting from a neuroingineering and basic science perspective. BMI is a useful tool to study neurophysiological mechanisms underlying action planning, plasticity-inducing paradigms and learning (Moxon and Foffani, 2015). Because subjects have a direct readout of their neuronal activity through an actuator, the causal links between neuronal firing and actions can be established better than during the non-BMI neurophysiological experiments, which usually point out correlation and not causation.

Up to now, there have been very few attempts to develop a BMI approach for rehabilitation after SCI (Borton *et al.*, 2013), and of those, most have aimed for a substitutional (Müller-Putz *et al.*, 2005; Alstermark and Isa, 2012; Collinger *et al.*, 2013), as opposed to a therapeutic approach (Capogrosso *et al.*, 2016). Therefore, in this final section, I will summarize developments in the two most promising interventions for SCI treatment: EES and DBS. I will describe their history and application in patients with neuromotor disorders, applications to SCI treatments and BMI in general as a potential ecological approach for improving neuroprosthetic treatments (Courtine and Bloch, 2015).

1.6.1 *History of spinal cord and MLR stimulation in humans with neuromotor disorders*

History of EES in humans

The first example of spinal cord stimulation was performed in 1965 and was described as a new therapy for pain based on the "gate theory" (Melzack and Wall, 1965). The logic behind this application was that it is possible to shut down ascending pain information travelling upstream through excitation of the large sensory A-beta fibers, which in turn activate interneurons subsequently inhibiting the ascending pain information coming from the C-fibers. A few years later, EES was first applied in the dorsal column of a human subject suffering from a terminal cancer condition (Shealy *et al.*, 1967). Since then, there have been multiple improvements in neurotechnologies and additional proofs of concept, which in 1989 led to an FDA approval of EES for pain treatment. Currently, EES is one of the most successful treatments for chronic pain with around 34,000 implantations per year (Krames *et al.*, 2009; Minassian *et al.*, 2016).

Moreover, EES has been used in humans for the treatment of other neurological disorders, such as example multiple sclerosis (Cook and Weinstein, 1973; Cook, 1976). More than 70 patients were implanted with epidural electrodes over their mid-thoracic spinal cord and received 20-50 HZ frequency EES. The patients reported improved spasticity, increased endurance of leg movements, improved voluntary control of movements and autonomic functions. Later Dr. Leon Illis brought these treatment practices to Europe and performed studies on a larger number of multiple sclerosis patients, where he found that only about 30% of patients increased their motor scores (Illis *et al.*, 1980; Illis, 1983). This led him to conclude that EES should be mainly used for improving bladder function and reducing spasticity.

In 1981, Siegfried summarized prior SCS cases for movement disorders including 15 SCI cases, which were used for treatment of multiple neurological disorders, see the **Table 1.6.1** reproduced from (Siegfried *et al.*, 1981).

Spinal cords stimulation for motor movement disorders	
NEUROMOTOR DISEASE	**NUMBER OF PATIENTS**
Multiple sclerosis	616
Cerebral palsy	49
Spasmodic torticollis	33
Dystonia musculorum deformans	25
Brain injury	15
Spinal cord injury	15
Cerebral stroke	13
Amylotrophic lateral sclerosis	9
Friedreich's ataxia	6
Cerebellar ataxia	5
Spastic paraplegia	3
Olivo-pontocerebellar atrophy	2
Pseudobulbar palsy	2
Vascular disorders of spinal cord	1
Transverse myelitis	1
Primary lateral sclerosis	1
Total of cases (March 1980)	796

Table 1.6.1 | Number of patient cases with neuromotor disorders implanted with spinal cord stimulators published between 1973 and 1980. Adapted from (Siegfried *et al.*, 1981).

However, Siegfried's later studies after 1981 reported large variability and no beneficial SCS effects, which led clinicians to abandon EES for multiple sclerosis patients (Siegfried *et al.*, 1981; Waltz, 1997). However, in these experiments there was no patient selection criteria, no attempts to separate responders from non-responders, and the stimulators were implanted above and not below the injury, which naturally did not allow for any stimulation effects below the injury. This mistake was later noticed and the field of SCS was revived thanks to Dimitrijevic and Sherwood (Dimitrijevic *et al.*, 1986).

History of MLR in humans

Since the discovery of the MLR in 1969 (Shik *et al.*, 1969) and many animal studies using MLR DBS for induction of "fictive locomotion" in decerebrated animals, much progress has been made in understanding the physiological importance of this region. However, MLR DBS was only put into clinical practice for patients with Parkinson's disease a few years ago (Mazzone *et al.*, 2005; Plaha and Gill, 2005) and showed promising results of improvement of akinetic symptoms and gait abnormalities (Mazzone *et al.*, 2011). Additionally, faster gait reaction time, reduced freezing and improved posture have been recently reported (Moro *et al.*, 2010; Mazzone *et al.*, 2016).

A few studies compared clinical outcomes between traditional DBS of suthalamic nucleus and the newly introduced PPN DBS. One of the main findings was that PPN DBS, unlike STN DBS, was beneficial for regulating sleep-wake cycles, and specifically for regulating daytime sleepiness (Peppe *et al.*, 2012). However, the role of PPN in the reticular activating system (Garcia-Rill, 2015) is still ambiguous, with some authors arguing that due to its involvement in alertness and attention, PPN DBS is not necessarily the safest approach for treating gait disorders (Winn, 2006).

There are several additional challenges commonly discussed regarding PPN/MLR implantation in humans. The main challenge is defining the implantation target, which arises from a inhomogeneous effect of DBS in different parts of the PPN and leads to large variability in locomotor outcomes and side effects in patients (Ferraye *et al.*, 2009; Moro *et al.*, 2010; Thevathasan *et al.*, 2011; Schrader *et al.*, 2013; Welter *et al.*, 2015). Despite all the complications, MLR is still a very promising target for DBS because of its superior effects compared to STN DBS on improving gait in animal models and patients with Parkinson's disease, and because it is a key location for relaying the downstream motor command coming from the CNS to the spinal cord (Mazzone *et al.*, 2016). However, longterm effects of MLR DBS and its applicability for treatment of other neuromotor disorders, such as SCI, remain to be investigated.

1.6.2 *Spinal cord stimulation and MLR DBS as potential neuroprosthetic targets for SCI treatment*

In the development of translational therapies, it is important to understand the evolution of technologies and treatment approaches to be able to put the future therapies into perspective. Therefore, here I would like to concentrate on SCS and DBS use in patients for SCI treatment specifically.

The first application of SCS in a paraplegic patient was reported by Richardson in 1978, where he showed a 90% reduction of spasticity and an increase in autonomic and bowel functions (Richardson and McLone, 1978). Richardson confirmed this observation in another five patients a year later (Richardson *et al.*, 1979). Later, Barolat and colleagues performed a study on 16 patients and reported a very good outcome of improved spasticity in 14 patients and a robust voluntary rhythmic knee flexion-extension movements with SCS in one patient (Barolat *et al.*, 1988). Thus, the enabling effect of SCS to release spasticity and allow downstream voluntary command has already been shown 30 years ago in SCI patients and even earlier in subjects with multiple sclerosis. These effects were recently replicated by Harkema's group (Harkema *et al.*, 2011), where EES led to voluntary toe and leg movements in a paraplegic patient. Promising results of the combined SCS and locomotor training have been reported by a team from Arizona, where patients improved their treadmill walking speed, needed less body weight support, improved their speed of walking with the walker and had a better endurance with EES (Herman *et al.*, 2002). Altogether, this evidence led to large clinical trials in the US and Switzerland, where the clinical implications of EES for SCI treatment in patients are currently being evaluated.

The mechanisms of EES action and its potential to induce plasticity in the spinal cord have long been debated. Already in 1986, Barolat proposed several explanations of the stimulation effect (Barolat *et al.*, 1988), however more sophisticated computational models of EES action were developed only recently (Rattay *et al.*, 2000; Capogrosso *et al.*, 2013). It is now accepted that EES acts by recruiting large Ia afferent fibers coming from the muscle spindles. These afferent fibers act mainly through indirect connections to motorneurons allowing rhythmic output based on the incoming sensory information. However, EES's potential to induce plastic changes in spinal circuitry and its interaction with training and other neuromodulatory techniques, like pharmacological agents and DBS, is still largely unknown. Additionally, the cost-benefit evaluation of EES treatment for patients and its combinatorial potential should be investigated in detail.

On the other hand, in the past 10 years MLR has been suggested to be a DBS target for treatment of patients with Parkinson's disease (Mazzone *et al.*, 2016). First discovered in 1969 (Shik *et al.*, 1969), it was since extensively studied in various animal models and behavioral paradigms (Ryczko and Dubuc, 2013). MLR receives input from basal forebrain and basal ganglia (Martinez-Gonzalez *et al.*, 2011), while its downstream ipsi- and contralateral motor projections are largely relaying in the gigantocellular reticular nucleus (Steeves and Jordan, 1984; Garcia-Rill and Skinner, 1987; Martinez-Gonzalez *et al.*, 2014). Studies have shown that MLR region is also activated during imaginary gait in humans (Lau *et al.*, 2015), which hints to its importance for locomotion.

As discussed in the previous **Section 1.4**, the importance of the MLR for gait initiation, the ability to control locomotor output with MLR stimulation in an intensity-dependent fashion, as well as its key position in relaying motor signals from higher brain structures down to the brainstem-spinal projections indeed suggests that MLR DBS may be a potential treatment of gait disturbances (Hamani *et al.*, 2011). However, the first decade of MLR DBS in humans has shown ambiguous results; studies have reported MLR DBS effects ranging from limited benefits (Ferraye *et al.*, 2010) to impressive effectiveness in alleviating gait freezing (Thevathasan *et al.*, 2012).

To date, only one group has investigated the effect of MLR DBS after SCI in rodents (Bachmann *et al.*, 2013). Their main findings are illustrated in **Figure 1.6.2 (**adapted from Bachmann *et al.*, 2013) and show that MLR DBS successfully alleviates locomotor deficits caused by severe cut SCI with 10 to 25% spared spinal cord tissue. Notably, they discuss that this effect is only elicited after about a month post-SCI, which they think is due to the reorganization of downstream locomotor pathways happening after the injury. Moreover, in this study only acute MLR DBS effects were reported, and the stimulation was done at only one time point, which leaves critical questions unanswered, such as the importance of stimulation timing, the spinal cord substrate needed for observing this effect and a long-term effects in animals with chronic SCI.

Despite the promising results above, there are still many unanswered questions about the potential of MLR DBS in SCI rehabilitation. For example, the long-term effect of MLR DBS treatment after SCI, its plasticity-inducing potential, and the best electrodes and stimulation parameters have yet to be evaluated. Therefore, an attept for clinical translation of MLR DBS treatment by Dr. Stieglitz et al. at this point seems to be lacking critical evidence from animal models, which might hinder its translation into patients with SCI (L.H. Stieglitz, A Curt, 2017).

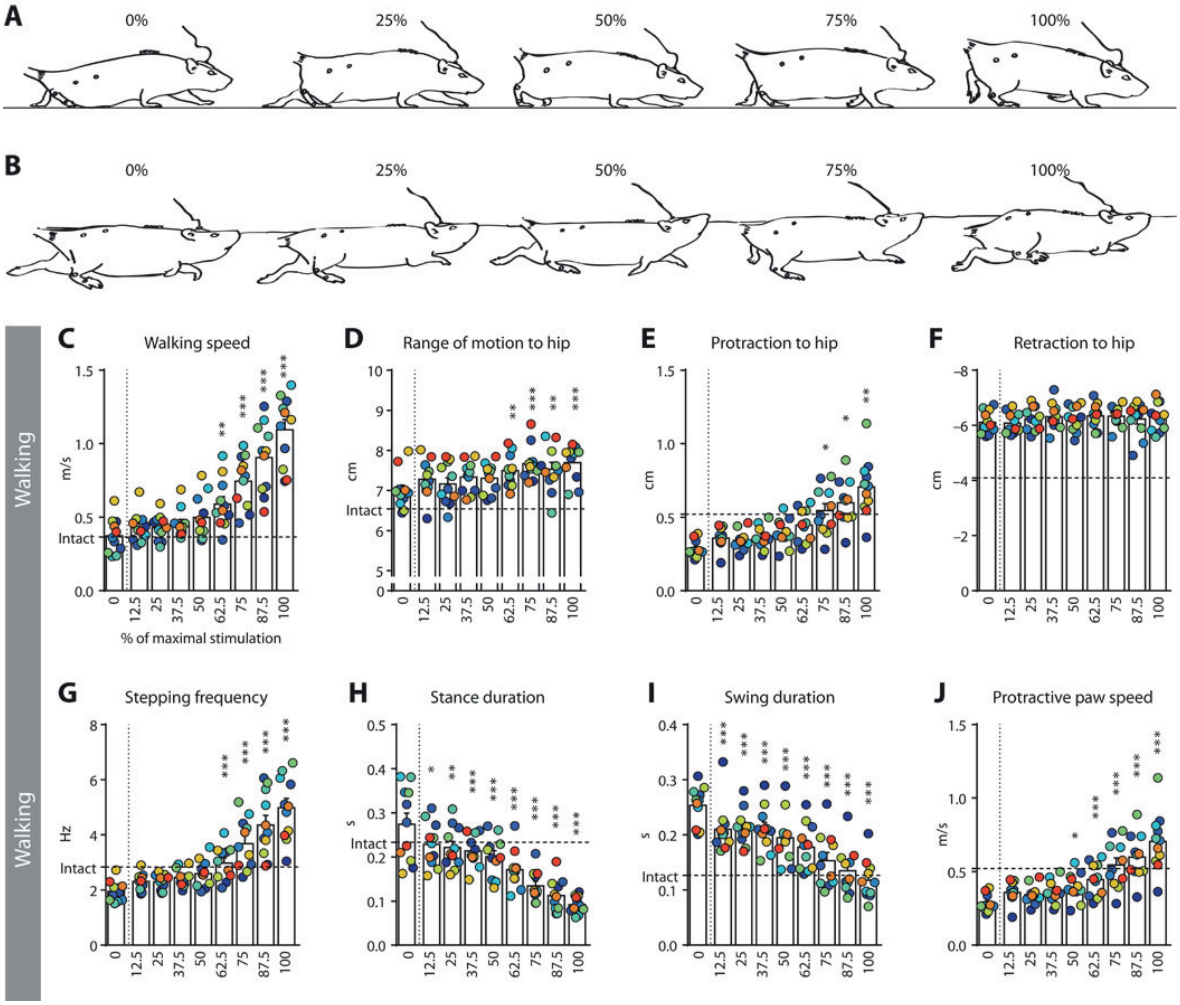

Figure 1.6.2 | Locomotor improvements due to MLR DBS in rats with severe spinal cord injury. (A-B) Graphical demonstrations of locomotor improvements with various MLR DBS intensities. **(C-J)** Improvement of various kinematic parameters with MLR DBS. Adapted from (Bachmann *et al.*, 2013).

Moreover, MLR DBS can induce severe side effects on alertness, including sleep disturbances (Hamani *et al.*, 2016), which is important to minimize in designing neuroprosthetic treatments involving MLR DBS (Courtine and Bloch, 2015). Finally, it will be important to evaluate the combinatorial potential of EES, MLR DBS and locomotor training because combinations of these approaches may have a synergistic effect and promote activity-based plasticity in a more specific manner than any of them alone.

1.6.3 ***Brain machine interface implications for inducing plasticity during rehabilitation***

Currently, neuromodulation of MLR and spinal circuits that restores locomotion after SCI in rats has been triggered externally (**Figure 1.4.1 & 1.6.2**). Hence, the rats have no control over the occurrence of the neuromodulation and subsequent locomotor output. Advances in BMI technology established the conceptual and technological bases for the design of a neuroprosthesis where cortical modulations could recruit midbrain locomotor regions and/or spinal circuits to initiate movement voluntarily (Borton *et al.*, 2013).

Already in 1969 Fetz pioneered closed-loop neural interfaces to promote activity dependent plasticity through neural feedback (Fetz, 1969). For instance, his recent study of precisely timed intraspinal microstimulation triggered by spiking activity of corticospinal neurons during free behavior durably strengthened synaptic connections between the artificially reconnected regions in non-human primates (Nishimura, Perlmutter, Eaton, *et al.*, 2013). A similar neural interface designed to restore communication between motor and somatosensory areas in the cerebral cortex improved motor recovery after experimental stroke in rodents (Guggenmos *et al.*, 2013).

Adaptive DBS in Parkinson's disease showed that closed-loop stimulation is more therapeutically effective than standard DBS both in animals (Rosin *et al.*, 2011) and humans (Little *et al.*, 2013). Closed loop kinematics-based EES delivery paradigms which mimic natural neural activity in the spinal cord during walking were recently developed for SCI treatment (Wenger et al., 2016). However, closed loop DBS protocols after SCI have never been studied before and their potential for inducing activity-dependent plasticity and recovery is as of yet unknown (as illustrated in **Figure 1.6.3)**.

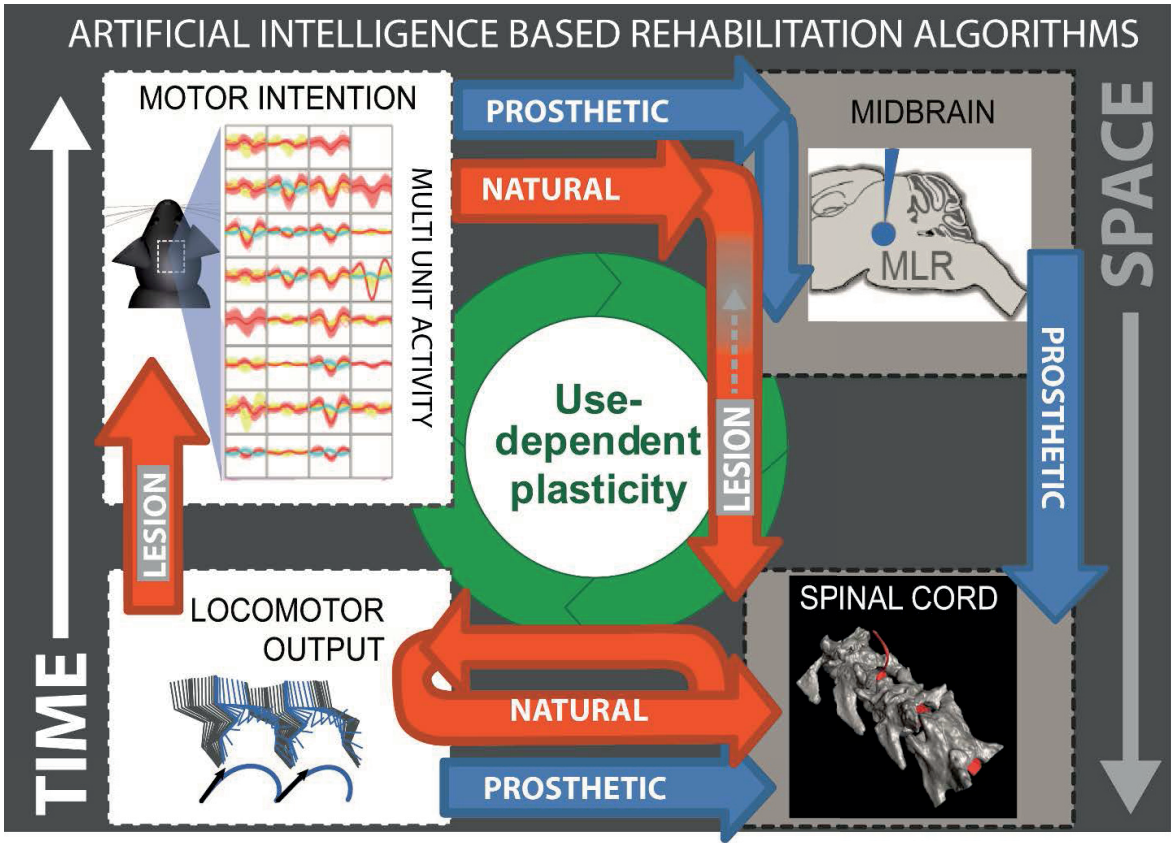

Figure 1.6.3 | Artificial intelligence based rehabilitation algorithms. Motor intention fine-tunes neuromodulation of midbrain, and spinal circuits, and cooperates with residual anatomical connections to promote optimal locomotor states during robot-assisted rehabilitation. The goal is to reprogram spared circuits and residual connections to re-establish walking.

SCI triggers a cascade of neuroplastic changes, as discussed in **Section 1.5** and described in various literature sources (Olivier Raineteau and Schwab, 2001; Bareyre *et al.*, 2004b; Zörner *et al.*, 2014). Therefore, steering these changes with appropriate neurorehabilitative paradigms is beneficial for activity-dependent remodelling (Courtine *et al.*, 2008; Edgerton *et al.*, 2008; Holtmaat and Svoboda, 2009; van den Brand *et al.*, 2012; Fouad and Tetzlaff, 2012) and prevention of maladaptive plasticity (Beauparlant *et al.*, 2013).

The key question is: how can we best stimulate beneficial activity-dependent plasticity? As first hypothesized by Donald Hebb and later confirmed by other researchers, plasticity is reversible and can be succinctly explained as *"Use it or lose it"* (Hebb, 1949; Nudo *et al.*, 1996; Holtmaat and Svoboda, 2009). According to this view, neuronal inactivity leads to shrinkage of unused

connections and, conversely, increased neuronal activity causes strengthening of connections (Murakami *et al.*, 1992). In this context, both EES and MLR DBS have great plastic potential, because electrical stimulation in known to stimulate plasticity in locomotor pathways (Knash *et al.*, 2003; Everaert *et al.*, 2010) and can lead to recovery from corticospinal tract lesions (Carmel *et al.*, 2010). The evidence described above suggests that brain-controlled therapies for neuromotor disorders may have a big potential for both provoking beneficial neural reorganization and facilitating recovery of patients with SCI.

Therefore, in my thesis work I first investigated the mechanisms of recovery after SCI and afterwards developed neuroprosthetic approaches that leverage residual networks and can potentiate locomotor output and recovery through brain-controlled MLR and spinal cord electrical stimulation. Overall, my thesis aims to establish an ecological neuroprosthetic system designed to provide self-driven recruitment of supra- and intraspinal locomotor circuits during rehabilitation training in order to facilitate the recovery process after paralyzing contusion SCI.

2. AIMS OF THE THESIS

2.1 *Help the brain help itself*

SCI is a devastating disorder causing various degrees of paralysis dramatically affecting the quality of life of patients (Scott *et al.*, 2011). The first attempts to treat SCI date only to the beginning of the last century. Despite the tremendous progress in the preclinical SCI research and many therapies currently tested in clinical trials, there is an exceptionally poor conversion rate of these therapies for use in general practice and a lack of understanding of the neurophysiological mechanisms of treatment. Therefore, the main goal running throughout my thesis is to better understand the processes underlying SCI recovery and to learn how we can improve rehabilitation outcomes by facilitating these processes. I hypothesized that it is possible to leverage activity-dependent neuronal plasticity which occurs during SCI rehabilitation, and to boost it by applying brain-controlled electrical stimulation to the supraspinal and spinal structures.

The core of my thesis is composed of three main studies presented in the form of articles, which will follow the logic described below. I will first show how we studied mechanisms underlying recovery from a severe contusion SCI in rodents and identified the routes of communication between the brain and spinal cord that are essential for induced locomotor recovery (***AIM 1***). Second, I will build upon the first finding and describe how we sought to amplify the descending locomotor command through an indirect stimulation of the neuronal pathway which we had identified to be important in the first study (***AIM 2***). Finally, I will describe how we bypassed the brainstem circuits using a brain-controlled neuroprosthetic system acting as an electronic bridge between the brain and spinal cord as well as the effect of this BMI approach on rehabilitation outcomes (***AIM 3***).

AIM 1 | Uncover the mechanisms underlying locomotor recovery after clinically relevant contusion SCI

Chapter 3 ("RESIDUAL RETICULOSPINAL PATHWAYS MEDIATE MOTOR FUNCTION RECOVERY AFTER FUNCTIONALLY COMPLETE SPINAL CORD CONTUSION")

Previous studies have reported a remarkable locomotor recovery after a staggered hemisection lesion, where rats learned to walk again after two months of neuroprosthetic rehabilitation

combined with electrochemical neuromodulation therapies (van den Brand *et al.*, 2012). However, this lesion type never occurs in natural conditions. Therefore, we first set up a clinically relevant contusion spinal cord injury model in our laboratory. Afterwards, we investigated the successes and limitations of our neuroprosthetic interventions to promote recovery after severe contusion SCI and dissected the mechanisms underlying this recovery. To answer these questions, we studied how different combinations of therapy timing and modalities of neuromodulation influence recovery. Behaviorally, we observed that the animals recovered voluntary bipedal locomotion and were even able to climb a staircase. We further investigated anatomical changes underlying this recovery and found an increase in sprouting of motor cortex projections to the reticulospinal neurons in the brainstem. This led us to the hypothesis that the reticulospinal projections play a crucial role in locomotor recovery. To test this hypothesis, we selectively switched off the downstream projection from the reticular formation to the lumbar spinal cord by applying specific viral vectors. This intervention reversibly abolished locomotion in trained animals, suggesting that the reticulospinal pathway is indeed important for the reestablishment of voluntary walking after SCI. These findings shed light on the mechanisms of locomotor recovery after SCI and allow for future development of targeted therapies to boost the reported recovery.

AIM 2 | Leverage reticulospinal circuit remodeling and boost locomotion after severe SCI through the brain-controlled enhancement of the descending supraspinal drive

Chapter 4 ("NEUROPROSTHETIC ENHANCEMENT OF SUPRASPINAL LOCOMOTOR DRIVE ALLEVIATES GAIT DEFICITS AFTER SPINAL CORD INJURY IN RATS")

Previous findings from Prof. Schwab's group (Bachmann *et al.*, 2013) which reported that MLR DBS improves quadrupedal locomotion of rats after SCI inspired us to further study this intervention for SCI rehabilitation. Therefore, for achieving the Aim 2, we developed the surgical procedures, computational infrastructure, and behavioral training paradigms to investigate the potential of neuroprosthetics utilizing MLR DBS to enhance the descending locomotor drive. In particular, we first investigated the interplay between the MLR and motor cortex activity and how it changes following SCI. After SCI, the rats were trained with electrochemical stimulation. Following four weeks of rehabilitation, we report a high degree of control over treadmill stepping output through application of different intensities of MLR DBS. We then took the best stimulation

parameters determined in the treadmill stepping protocol, applied them in an overground walking condition and observed that MLR DBS enhanced locomotor output compared to the no-DBS condition. However, despite improved stepping, MLR DBS turned out to be very stressful for the animals. We came up with the idea to alleviate this stress by introducing a more natural MLR DBS delivery paradigm. Specifically, we decided to use cortically triggered MLR DBS, as opposed to externally triggered stimulation, to amplify the cortically generated movement initiation signal and decrease the stressfulness of the MLR DBS intervention. Indeed, we show that the same locomotor improvements were achieved with additionally improved natural locomotor dynamics, all while decreasing the stressful consequences of the intervention , when MLR DBS was delivered in a more natural brain-controlled way. Altogether, we show a detailed analysis of the effect of MLR DBS on different locomotor tasks after SCI, as well as showing how brain-controlled MLR DBS can produce facilitated locomotion with decreased stressful effects. However, we report important caveats for the translational potential of MLR DBS, including challenges in identifying MLR location, suprathreshold stimulation and critical spinal cord sparing needed for it to be effective. Finally, despite the ability of MLR DBS to alleviate locomotor deficits and our newly developed brain-controlled delivery of MLR DBS, critical questions raised in our paper have to be carefully considered before this method can move to clinical practice.

AIM 3 | Development of brain-controlled spinal neuromodulation to improve locomotor recovery after contusion SCI

Chapter 5 (“BRAIN–CONTROLLED MODULATION OF SPINAL CIRCUITS IMPROVES RECOVERY FROM SPINAL CORD INJURY”)

Our third aim was to develop a neuroprosthetic intervention which reconnects the brain and the sublesional spinal cord though an electronic bridge and to investigate its impact on locomotor recovery after severe SCI. To reach this aim, we researched natural dynamics of motor cortex activation during different walking phases. Afterwards, we developed computational algorithms which allowed us to effectively use cortical activity to proportionally control the intensity of EES delivered to the spinal cord during treadmill and overground walking rehabilitation with electrochemical neuroprosthetics. Finally, we trained two animal groups such that one received the commonly used tonic EES input and the other received brain-controlled EES. We found that the latter group had a significantly better locomotor recovery post-SCI in terms of both time and

quality of locomotion: we observed a faster and better walking capacity already 3 weeks after injury. This study shows that brain-controlled EES delivery induces superior recovery as opposed to the tonic EES, which is an important finding from both the engineering and locomotor science point of view. Activity-dependent plastic changes between cortex and spinal cord induced by our original self-driven neuroprosthetic rehabilitation paradigm need to be further investigated.

3. RESIDUAL RETICULOSPINAL PATHWAYS MEDIATE MOTOR FUNCTION RECOVERY AFTER FUNCTIONALLY COMPLETE SPINAL CORD CONTUSION

Lucia Friedli[1,*], Janine Beauparlant[1,*], Cristina Martinez-Gonzalez[1,*], Galyna Pidpruzhnykova[1], Laetitia Baud[1], Kay Bartholdi[1], Jean Laurens[1], Quentin Barraud[1] and Grégoire Courtine[1]

---

1. Center for Neuroprosthetics and Brain Mind Institute, School of Life Sciences, Swiss Federal Institute of Technology (EPFL), Lausanne, Switzerland

* These authors contributed equally to this work

Corresponding author:
Grégoire Courtine, PhD
Professor, International Paraplegic Foundation Chair in Spinal Cord Repair
Center for Neuroprosthetics and Brain Mind Institute
SWISS FEDERAL INSTITUTE OF TECHNOLOGY (EPFL)
CH-1015 Lausanne
gregoire.courtine@epfl.ch

Original manuscript: “Residual reticulospinal pathways mediate motor function recovery after functionally complete spinal cord contusion” prepared for submission to Nature Neuroscience in May 2015

Lucia Friedli*, Janine Beauparlant*, Cristina Martinez-Gonzalez*, Galyna Pidpruzhnykova, Laetitia Baud, Kay Bartholdi, Jean Laurens, Quentin Barraud and Grégoire Courtine

* These authors contributed equally to this work

My contribution: I was responsible for the latest mechanistic part of the study: I performed all aspects of behavioral experiments for the MLR and double-virus parts, animal care, acquired and analyzed data. I prepared MLR and double-virus figures and finalized all the other figures except for 1.5 and 1.6. I also helped in the manuscript preparation and corrections.

Others contribution: L.F. performed all aspects of behavioral experiments before MLR and double-virus part. J.B., C.M., Q.B. and K.B. analyzed anatomical data and C.M. introduced the double-virus technique. L.B. contributed to behavioral training and data acquisition. J.L. established MLR DBS implantation technique and built DBS electrodes. L.F., J.B., C. M., Q.B., prepared the figures. G.C. conceived the study, wrote the manuscript and all the authors contributed the manuscript editing.

New original manuscript: “Cortico-reticulo-spinal circuit reorganization enables motor recovery after spinal cord contusion” prepared for re-submission to Nature Neuroscience in August 2017

Leonie Asboth[*], Lucia Friedli[*], Janine Beauparlant[*], Cristina Martinez-Gonzalez, Selin Anil, Elodie Rey, Laetitia Baud, Galyna Pidpruzhnykova, Mark A. Anderson, Polina Shkorbatova, Julie Kreider, Bernard L. Schneider, Quentin Barraud, Gregoire Courtine[&]

* These authors contributed equally to this work

Introduced changes: The new manuscript contains an additional set of experiments aiming to optogenetically dissect motor cortex-brainstem circuitry in mice and its contribution to recovery performed by L.A., E.R. and S.A. I was not directly involved in this part of the study and contributed with my experimental results and figures from the first original article described above. Therefore, I will only use the first article for my thesis because of my significant contribution to it.

Other published works: Due to the highly collaborative nature of this study, it was previously partially reported in three PhD theses coming from our laboratory. Namely, the theses of Janine Beauparlant, Lucia Friedli-Wittler and Leonie Asboth.

3.1 Abstract

Spinal cord damage in humans primarily results from contusion injuries. The majority of severe spinal cord contusions spare descending fibers that still connect supraspinal centers to spinal circuits coordinating leg movement, located below the injury. However, these residual descending fibers and spared spinal circuits remain non-functional. Here, we show that electrochemical neuromodulation of lumbar segments immediately reactivates spared spinal circuits. When delivered during robot-assisted rehabilitation, electrochemical neuromodulation progressively restored supraspinal control of hindlimb movements in rats with both acute and chronic functionally complete spinal cord contusions. Using virus-mediated tracing, deep brain stimulation and pathway-specific inactivation experiments, we demonstrate that this recovery relied on the reorganization of residual reticulospinal fibers within specific motor related regions below the injury. Similar therapeutic strategies may improve motor recovery after spinal cord injury in humans.

3.2 Introduction

After a spinal cord injury (SCI), only half of affected individuals recover motor, sensory and/or autonomic functions, with only 10% conversion rate reported in functionally complete patients (Onifer *et al.*, 2011) . However, imaging (Petersen et al., 2012), electrophysiological (Angeli et al., 2014; Barthélemy et al., 2015) and anatomical (Kakulas, 1999) evaluations revealed that functionally complete lesions usually spare regions of white matter that are spared in the outside rim of the spinal cord. These bridges contain residual fibers from mixed populations of projection neurons that maintain a physical connection with lumbar segments, where the neuronal circuits coordinating leg movement reside. Nevertheless, higher brain centers lose the ability to exploit these residual connections to engage spared circuits below injury.

Two main reasons have been identified to account for this failure. First, the interruption of descending pathways suppresses the supraspinal sources of modulation and excitation that are essential to enable functional states of lumbar circuits (Orlovskij et al., 2003; Kiehn, 2006; Jordan et al., 2008; Courtine et al., 2009). Albeit intact, the denervated spinal circuits remain in a non-functional state. Second, the sudden disruption of neural pathways propagates dysfunction throughout the CNS, even in regions distant from the injury (Bachmann *et al.*, 2013). Together with conduction failure (James *et al.*, 2011), this dysfunction contributes to silencing many of the potentially useful descending axons with surviving connections below the injury (Bachmann *et al.*, 2013).

This understanding triggered the development of strategies that target residual descending connections and spared spinal circuits to improve recovery after SCIs (Mushahwar *et al.*, 2007; Courtine *et al.*, 2009; van den Brand *et al.*, 2012; Steuer *et al.*, 2013; Angeli *et al.*, 2014). These interventions act over two time windows. In the short term, the delivery of spinal cord neuromodulation therapies compensates for the interrupted supraspinal inputs, raising the excitability of denervated spinal circuits to a level that enables motor control. For example, individuals with a chronic, functionally complete SCI instantly regained adaptive control over their paralyzed legs during epidural electrical stimulation of lumbar segments (Angeli *et al.*, 2014). In the long term, we exploited robot-assisted rehabilitation (Dominici *et al.*, 2012) to encourage rats to deliver descending drives in the presence of spinal cord neuromodulation therapies. This will-powered training regimen mediated a reorganization of spared neuronal pathways that restored advanced motor control in rats with staggered spinal cord hemisections leading to permanent

paralysis (van den Brand *et al.*, 2012). As observed in paraplegic individuals (Angeli *et al.*, 2014), however, motor control only occurred in the presence of spinal cord neuromodulation therapies.

These experimental developments have been conducted in complete SCI models (Courtine *et al.*, 2009; Steuer *et al.*, 2013), or using cut injuries in order to interrupt specific neuronal pathways (van den Brand *et al.*, 2012). While these well-controlled and reproducible lesion models facilitate conclusive mechanistic studies, they fail to reproduce key functional and anatomical features of natural SCIs. In humans, spinal cord damage primarily results from contusions (Kakulas, 1999; Norenberg *et al.*, 2004). These types of lesion induce highly variable white matter damage. The initial trauma leads to pronounced secondary damage, including the formation of cavities (Basso *et al.*, 1996), inflammatory responses (Silver *et al.*, 2014) and demyelination (James *et al.*, 2011) that impair the functionality of spared neurons and residual fibers in the vicinity of the injury. The situation is even more challenging at extended time points post-injury. In the chronic stage, the window of opportunity for enhanced neuroplasticity extinguishes (O. Raineteau and Schwab, 2001). In parallel, compensatory adaptations occur within spinal circuits below the injury (Beauparlant *et al.*, 2013), leading to neuronal dysfunction that further diminishes the potential for motor recovery (Dietz, 2010).

The ability of spinal cord neuromodulation therapies and rehabilitation to restore motor control after functionally complete spinal cord contusions, both acute and chronic, has never been evaluated. Moreover, the neuronal pathways capable of mediating supraspinal control of leg movement after such injuries are unknown (Angeli *et al.*, 2014). Circuit-level mechanisms enabling immediate control of leg movement during spinal cord neuromodulation and progressive improvement with rehabilitation remain elusive, even though such insight may play a pivotal role in the translation of these interventions into clinical applications.

Here, we modeled a discomplete spinal cord contusion in rats, and demonstrate that will-powered training under robotic assistance and electrochemical neuromodulation reestablished supraspinal control of hindlimb movements. Trained rats exhibited motor control without any neuromodulation, including during an unpracticed swimming task. Due to their ubiquitous localization in the white matter, a subset of reticulospinal fibers systematically survived the injury. Neuroprosthetic rehabilitation triggered a remodeling of these residual fibers into functionally relevant grey matter regions, which was necessary and sufficient to transmit the supraspinal command to spinal circuits coordinating hindlimb movement.

3.3 Materials and Methods

Experimental setup

Experiments were conducted on adult female Lewis rats (~220 g body weight). Animals were housed individually on a 12 h light/dark cycle, with access to food and water *ad libitum*. All animals were handled daily for at least two weeks prior to the first surgeries. Animal care, including manual bladder voiding, was performed twice daily for the first 3 weeks after injury, and once daily for the remaining post-injury period. All procedures and surgeries were approved by the Veterinary Office of the canton of Vaud in Switzerland.

Surgical procedures and post-surgical care

General surgical procedures used have been described previously (van den Brand *et al.*, 2012). Under aseptic conditions and general anesthesia, a partial laminectomy was made at the mid-thoracic level (T9 vertebra) and a 250 kdyn (1 dyn = 10 µN) contusion injury was applied using a force-controlled spinal cord impactor (IH-0400 Impactor, Precision Systems and Instrumentation LLC, USA). The spinal cord displacement induced by the impact was measured for each rat. For positioning epidural stimulation electrodes, a partial laminectomy was performed over spinal segments L2 and S1. Stimulating electrodes were created by removing a small part (~400 µm notch) of insulation from Teflon-coated stainless steel wires (AS632, Cooner Wire, USA), which were subsequently secured at the midline overlying spinal segments L2 and S1 by suturing the wires to the dura. A common ground wire (~1 cm of Teflon removed at the distal end) was inserted subcutaneously over the right shoulder. Bipolar intramuscular electrodes, using the same type of wire, were inserted bilaterally in the medial gastrocnemius (MG, ankle extensor) and tibialis anterior (TA, ankle flexor) muscles to record electromyographic (EMG) activity. All the wires were connected to a percutaneous amphenol connector (Omnetics Connector Corporation, USA) cemented onto the skull of the rat. Early-trained rats were lesioned and implanted with electrodes in the same surgery, while delay-trained rats underwent two surgeries separated by 2 months (**Supplementary Figure S3.1**). Analgesia (buprenorphine Temgesic®, ESSEX Chemie AG, Switzerland, 0.01-0.05 mg per kg, s.c.) and antibiotics (Baytril® 2,5%, Bayer Health Care AG, Germany, 5-10 mg per kg, s.c.) were provided for 3 and 5 days post-surgery, respectively.

Neuroprosthetic rehabilitation

Rats were randomly divided into a non-trained group with 2 or 4 months survival time (n = 8 rats per group), an early-trained group (n = 8) and a delayed-trained group (n = 8) (**Supplementary Figure S3.1**). All the trained rats followed a comprehensive rehabilitation program during 2 months, starting at 7 days or 2 months (9 weeks) post-injury. Rats were trained 6 days per week for 25 min per day. During training, hindlimb motor control was facilitated with electrochemical neuromodulation (van den Brand *et al.*, 2012). Five minutes prior to training, the rats received a systemic (I.P.) administration of quipazine (5-HT2A/C, 0.2 - 0.3 mg/kg) and 8-OH-DPAT (5-HT1A/7, 0.05 - 0.2 mg/kg) that was adjusted daily based on locomotor performance. During training, continuous electrical stimulation (0.2ms, 100-300µA, 40Hz) was delivered through L2 and S1 electrodes to facilitate locomotion. Training was conducted bipedally on a treadmill (11 cm/s) with adjustable robotic bodyweight support against the direction of gravity (Robomedica, USA). Starting 2 weeks after injury, rats were additionally trained overground with the multidirectional robotic bodyweight support system (Dominici *et al.*, 2012). The content of each training session evolved with the actual capacities of the rats and training objectives (van den Brand *et al.*, 2012). Positive reinforcement was used to encourage the rats to perform the requested tasks.

Behavioral evaluations

Hindlimb motor control was evaluated on a treadmill (11 cm/s) along a straight runway and during swimming (**Supplementary Figure S3.1**). Rats were only recorded bipedally to avoid the confounding contribution of the forelimbs in motor performance (Dominici *et al.*, 2012). For both treadmill and overground conditions, a robotic bodyweight support provided optimal vertical and mediolateral supports to the bipedally positioned rats (Dominici *et al.*, 2012). Swimming was recorded in a custom-made swimming pool (dimensions; length 150 cm, width 13 cm, height 40 cm, water depth 24 cm). Rats participated in two sets of behavioral evaluations at 1 and 9 weeks post-injury. The delayed-trained rats were tested at 9 and 17 weeks post-injury (**Supplementary Figure S3.1**). All the rats were evaluated in three experimental conditions independent of their training paradigm: with electrochemical neuromodulation, with electrical neuromodulation only, and without any neuromodulation. To ensure that the specificity of the task was not responsible for their incapacity to initiate and sustain locomotion, non-trained rats practiced overground locomotion with the robotic postural interface for about 10 min per day during 5 sessions before

behavioral recordings. All the trained and non-trained rats equally practiced the swimming task during 5 consecutive days prior to recordings.

Kinematic, kinetic and muscle activity recordings

All procedures used have been detailed previously (van den Brand *et al.*, 2012; Dominici *et al.*, 2012). During both treadmill and overground conditions, bilateral hindlimb kinematics were captured by the high-speed motion capture system Vicon (Vicon Motion Systems, UK), consisting of 12 infrared cameras (T-10, 200 Hz). Reflective markers were attached bilaterally at the iliac crest, the greater trochanter (hip joint), the lateral condyle (knee joint), the lateral malleolus (ankle), the distal end of the fifth metatarsophalangeal (mtp) joint and the tip of the fourth toe. The body was modeled as an interconnected chain of rigid segments, and joint angles were generated accordingly. Ground reaction forces were recorded using a biomechanical force plate (2 kHz; HE6X6, AMTI, YSA) located below the treadmill belt or in the middle of the runway. EMG signals (2 kHz) were amplified, filtered (10-1000 Hz bandpass), stored and analyzed offline to compute the amplitude, duration and timing of individual bursts. For both the left and right hindlimbs, 15 successive step cycles were extracted over several trials on the runway for each rat under each experimental condition and time-point. A 20-s interval was used when no or very minimal hindlimb movements were observed. During swimming, hindlimb kinematics were captured by two Basler cameras (100 Hz; Basler Vision Technologies, Germany). Black dots were drawn on the shaved skin over the same anatomical landmarks of both hindlimbs. Hindlimb movements were reconstructed as a virtual segment connecting the iliac crest and the MTP marker. Kinematracer (Kissei Comtec Co., Japan) motion tracking software was used to obtain 2-D coordinates of hindlimb movements. EMG signals were recorded concomitantly to video acquisition.

Analysis of kinematic, kinetic and muscle activity

A total of 129 parameters quantifying kinematics, kinetics, and muscle activity features were computed for each hindlimb and gait/stroke cycle according to methods described in detail previously (van den Brand *et al.*, 2012; Dominici *et al.*, 2012). All the parameters are reported in **Supplementary Table 1**. To evaluate differences between experimental conditions and groups, as well as the most relevant parameters to explain these differences, we implemented a multi-

step statistical procedure based on PC analysis (Dominici *et al.*, 2012; Takeoka *et al.*, 2014b). The various steps, methods, typical results, and interpretation of the analysis are detailed in **Figure 3.2** and in the **Results** section. PC analyses were applied on data from all individual gait cycles or swim strokes for all the rats together. Data were analyzed using the correlation method, which adjusts the mean of the data to 0 and the standard deviation to 1. This method of normalization allows the comparison of variables with disparate values (large vs. small values) as well as different variances.

Deep brain stimulation of the mesencephalic locomotor region

A monopolar electrode was implanted in the vicinity of the pedunculopontine nucleus to deliver deep brain stimulation of the mesencephalic locomotor region. Custom-made electrodes consisted of 24-gauge stainless steel guiding tubes carrying four 41 AWG teflon coated stainless steel wires (793200, AM Systems, USA). Wires were crimped to a custom-made circular nano-connector (Omnetics Connector Corporation, USA) on one side. The other end was bent 90 deg, fixed with biocompatible glue and cut transversally to expose 4 conductive electrode sites. Two extra wires were attached to the guiding tube as reference electrodes (~1 cm of teflon removed at the end). Implantation coordinates were -7.6 mm to -7.8 mm from Bregma and 2 mm from the longitudinal midline at a depth of 6.0 mm. The coordinates were defined based on the location of cholinergic neurons, which coincides to the pedunculopontine nucleus (**Figure 3.7b**) and functional experiments in pilot studies. To trigger hindlimb movement, continuous monopolar stimulation (0.2 ms, 40 Hz, approximately 150 µA) was delivered at the optimal site. Six trained tats were tested quadrupedally before the lesion, and bipedally under robotic assistance and electrochemical neuromodulation at regular intervals after the injury. Time to initiation of hindlimb movement onset was measured from the onset of stimulation to the moment of paw off. For each day of testing, the total uninterrupted distance travelled by the rats along the runway was measured with and without deep brain stimulation (**Supplementary Figure S3.1**).

Tract-tracing procedures

Non-injured and non-trained rats with chronic contusion injury (9 weeks) received injections of the retrograde tracer FastBlue into the upper lumbar spinal cord. A partial laminectomy was performed

over the L2/L3 spinal segments. Fastblue (FB; 2% in 0.1M phosphate buffer and 2% dimethyl sulfoxide) was infused bilaterally. Three injections of 200 nl Fastblue separated by 1 mm were performed. The injection coordinates were 700 µm lateral of the midline and 1.2 – 1.5 mm below the dorsal surface of the spinal cord.

Anterograde tract-tracing of motor cortex and reticulospinal axonal projections was performed in four groups of rats: no injury, sub-acute injuries (injection at 4 days prior to injury), and chronic injuries (injection at 9 weeks) in both non-trained and trained rats **(Supplementary Figure S3.1**). Two craniotomies were performed over the left motor cortex and bilaterally over the brainstem medulla oblongata. A 10% suspension of BDA 10,000 (10% in 0.01M PBS) was injected into the left motor cortex over 6 sites covering the hindlimb area (coordinates centered -1 mm rostrocaudal and -1.75 mm mediolateral to Bregma, depth 1.5 mm). In the same surgery, an adeno-associated virus serotype 1 (AAV1) expressing green fluorescent protein (GFP) under the cytomegalovirus (CMV) promoter (AAV1-CMV-GFP) was injected in the gigantocellular reticular nucleus of the brainstem. Three injections (300 nl per injection) were made bilaterally (Bregma -11, -11.5, -12 mm) at 8 mm below the surface of the cerebellum. Eleven days later, a partial laminectomy was performed over the L2/L3 segments of the same rats to perform unilateral injections of the retrograde tract tracer Fastblue into the right hemicord, as detailed above.

After an additional survival time of 10 days, all animals were deeply anesthetized by an i.p. injection of 0.5 ml Pentobarbital-Na (50 mg/mL) and transcardially perfused with approximately 80 ml Ringer's solution containing 100'000 IU/L heparin (Liquemin, Roche, Switzerland) and 0.25% $NaNO_2$ followed by 300 ml of cold 4% phosphate buffered paraformaldehyde, pH 7.4 containing 5% sucrose. The brain and spinal cord were removed and postfixed in the same fixative before they were transferred to 30% sucrose in phosphate buffer (PB) for cryoprotection. The tissue was embedded in Tissue Tek O.C.T (Sakura Finetek Europe B.V., The Netherlands), frozen at -40°C, and cut to a thickness of 40 µm.

Immunohistochemistry

For immunohistochemistry experiments, sections used for 5HT staining were pretreated with 0.03% H_2O_2. Mounted or free-floating sections were washed 3 times in 0.1M PBS and blocked in 5% (5HT, NeuN) or 10% (GFAP, GFP) normal goat serum containing 0.3% Triton. Sections were then incubated in primary antibody diluted in the blocking solution overnight at 4°C (GFAP, NeuN,)

or room temperature (GFP, 5HT). Primary antibodies used were rabbit anti-GFAP (1:1000, Dako, USA) or anti-5HT (1:5000, Sigma Aldrich, Germany), mouse anti-NeuN (1:300, Chemicon, Millipore Corporation, USA), chicken anti-GFP (1:500, Life Technologies, USA), anti-vGLUT1 (1:2000, Chemicon, Millipore corporation, USA), anti-vGLUT2 (1:5000, Chemicon, Millipore corporation, USA) and goat anti-ChAT (1:500, Chemicon, Temecula, CA, USA). Sections were again washed 3 times in 0.1M PBS and incubated with the appropriate secondary antibody (Alexa fluor® 488 or Alexa fluor® 555; Molecular Probes, Life Technologies, USA) in blocking solution. Tyramide System Amplification (TSA)-Cyanine 3 kit (PerkinElmer, USA) was used to visualize BDA-labeled fibers. Sections were first washed and endogenous peroxidase activity was quenched by 30 min incubation in 0.1% H_2O_2. After overnight incubation at 4°C with streptavidin-horseradish peroxidase (1:200) in 0.1M PBS-Triton (1%), sections were again washed and incubated in TSA Cyanine 3 (1:100) for 45 sec (spinal cord sections) or 3 min (brainstem sections), respectively. NeuroTrace™ (Life Technologies, USA) was used as a Nissl counterstain at a dilution of 1:50 in 0.1M PBS. Slides were finally washed, air-dried and coverslipped with Mowiol.

Evaluation of spinal cord contusion

The extent and location of spinal cord damage was evaluated in each experimental rat. The lesion cavity was cut in serial coronal sections (40 µm) that were stained using GFAP and NeuN antibodies. The entire extent of the lesion cavity was reconstructed in three-dimensions using Neurolucida (MBF Bioscience, USA). The maximal projection surface was generated for each rat in order to visualize the spared white and grey matter regions. For each lesion, we calculated the spared spinal cord surface with respect to the distance from the epicenter of the lesion, the spared area at the epicenter, and the total volume of damaged spinal cord tissue.

Neuromorphological evaluations

Fiber density (BDA, GFP, 5HT) was measured using 3 to 5 confocal image stacks per region per rat. Images were acquired with standard imaging settings and analyzed using custom-written Matlab (MathWorks, USA) scripts according to previously described methods (van den Brand *et al.*, 2012). Confocal output images were binarized by means of an intensity threshold and divided into square regions of interest (ROI). Densities were computed within each ROI as the ratio of

traced fibers (number of pixels) per ROI area. Axon length was calculated using the same Matlab scripts and skeletonized confocal image stacks. Image acquisition was performed using a Leica TCS SPE or SP5 laser confocal scanning microscope and the LAS AF interface (Leica Microsystems, Germany) and stacks were processed offline using the Imaris software (Bitplane, USA) and Image J (National Institute of Health (NIH), USA). Axon caliber was computed as the ratio between axon density and axon length.

Virus-mediated inactivation experiments

We reversibly prevented synaptic release from reticulospinal neurons with projections to upper lumbar segments using a double virus construct (Kinoshita *et al.*, 2012). We injected a highly efficient retrograde gene transfer lentiviral vector (HiRet-TRE-EGFP.eTeNT; 5 x $10^{\wedge 9}$ vg/mL) carrying enhanced tetanus neurotoxin light chain (eTeNT) and the enhanced GFP (EGFP) downstream of the tetracycline-responsive element (TRE). We placed 4 injections of 250 nl of HiRet-TRE-EGFP.eTeNT per hemicord in the spinal segments L2/L3. Injection sites were located at 800 µm from the midline and separated by 1 mm rostrocaudally. Injection depth was set at 1.5 mm from the dorsal aspect of the spinal cord. In a second surgery, separated by 14 days, rats received injections of AAV2/1-CMV-rtTAV16 (4 x $10^{\wedge 12}$ vg/mL) bilaterally in the gigantocellular region of the reticular formation. Injection coordinates and volumes delivered were identical to the AAV1-CMV-GFP injections used to label the reticulospinal tract. AAV2/1-CMV-rtTAV16 is an adeno-associated virus serotype 1 in an envelope from an adeno-associated virus serotype 2 (AAV2/1) vector carrying the Tet-on sequence, a variant of the reverse tetracycline transactivator (rtTAV16) under the control of the cytomegalovirus (CMV) promoter. Seven days after the second injection, the administration of doxycycline was initiated to induce the expression of eTeNT. Doxycycline was administered i.p. (10 mg/kg) using saline solution as a vehicle. Trained rats (n = 4) were tested overground under robotic assistance and electrochemical neuromodulation before doxycycline administration (baseline), during doxycycline administration (5 days after initiation) and 7 days after the cessation of doxycycline administration. Doxycycline was administered a second time during 5 days prior to terminating the rats in order to ensure expression of GFP in inactivated neurons. In all the experimental rats, we counted the number of neurons expressing GFP through the entire extent of the injected brainstem region.

Statistical procedures

All data are reported as mean values ± s.e.m. Statistical evaluations were performed using one-way ANOVA for neuromorphological evaluations, and one- or two-way repeated-measures ANOVA for functional assessments (Prism, GraphPad Software, USA). The *post hoc* Tukey's or Fisher LSD test was applied when appropriate. Pearson's correlation coefficients were used to evaluate univariate correlations. The significance level was set as $p < 0.05$.

3.4 Results

Functionally complete spinal cord contusion model

We delivered a force feedback controlled controlled contusion at thoracic segment T9 (**Supplementary Figure S3.1**). The impact force was set to 250 kdyn (255.5 ± 1.3 kdyn) to induce a maximum amount of damage while ensuring minimal white matter sparing. This lesion led to the progressive formation of a cystic cavity that expanded over several millimeters (6.10 ± 0.15 mm; **Figure 3.1**). 3D lesion reconstructions revealed a minimal rim of tissue sparing located in the ventrolateral white matter, which amounted to 8.79 ± 0.74 % of healthy cross-sectional tissue (**Supplementary Figure S3.2**). While no differences in lesion size were found between experimental groups ($p = 0.10$), each rat exhibited a distinct pattern of white matter sparing that reproduced the variability of spinal cord damage in humans (Norenberg *et al.*, 2004).

To evaluate hindlimb motor control, we established a robot-assisted testing paradigm that constrained the rats to engage their hindlimbs in order to move towards a food reward (**Figure 3.1a**). To eliminate the confounding contribution of the intact forelimbs, the rats were positioned upright (Dominici *et al.*, 2012; van den Brand *et al.*, 2012). The robotic interface provided adjustable postural assistance in the vertical and mediolateral directions (Dominici *et al.*, 2012). One week after injury, all rats ($n = 16$) failed to activate the muscles below injury, which resulted in flaccid paralysis of both hindlimbs. To reactivate spinal circuits, we applied electrochemical neuromodulation consisting of a serotoninergic replacement therapy and epidural electrical stimulation at segments L2 and S1 (**Figure 3.1a**). Electrochemical neuromodulation immediately promoted alternating plantar stepping on a treadmill, but these movements were involuntary (Courtine *et al.*, 2009). All rats failed to initiate hindlimb movements overground under robotic assistance. Without electrochemical neuromodulation, none of the rats exhibited supraspinal control of hindlimb movement at 2 months post-injury, indicating the presence of a functionally complete SCI (**Figure 3.1d**). Electrochemical neuromodulation improved motor control capacities, enabling the rats to extend the hindlimbs, lift their hindpaws, and in a subset of rats (35%) to perform a few steps (**Figure 3.1d**).

These results show that the contusion SCI led to profound and irreversible damage of spinal tissue that resulted in a permanent loss of functional hindlimb movements in rats.

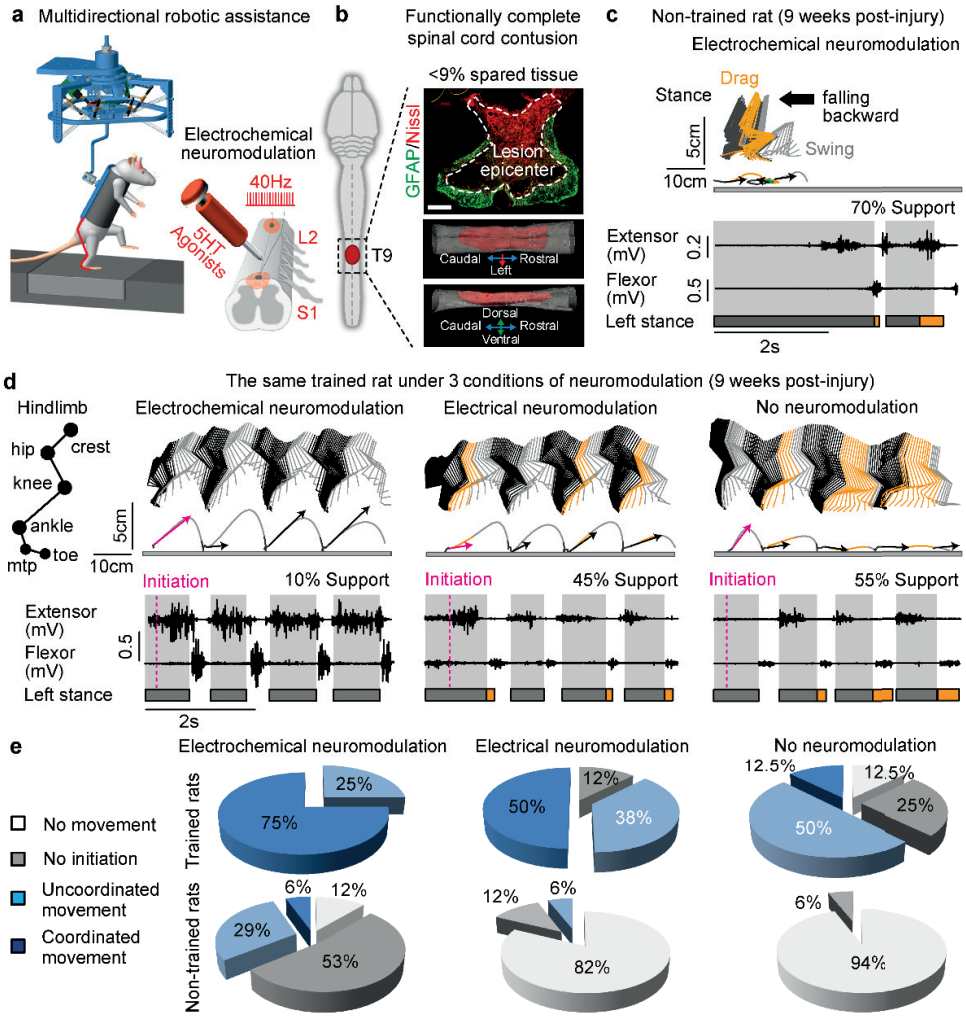

Figure 3.1 | Neuroprosthetic rehabilitation restores hindlimb motor control after functionally complete spinal cord contusion. (a) Evaluation and training of hindlimb motor control in a bipedal posture with multidirectional robotic assistance and electrochemical neuromodulation of lumbosacral circuits. **(b)** Representative section through the injury epicenter, including a 3D reconstruction of the lesion cavity. Scale bar, 500μm. **(c)** Stick diagram decomposition of left hindlimb movement together with endpoint trajectory and electromyographic activity of the medial gastrocnemius (extensor) and tibialis anterior (flexor) muscles. The arrows represent the direction and intensity of the foot velocity vector at swing onset. Grey and yellow bars indicate the duration of stance and drag, respectively. **(d)** Representative executions of the same trained rat under 3 different conditions of neuromodulation, as indicated above each panel. **(e)** Circular plots reporting the gross hindlimb motor performance of non-trained and trained rats under the different conditions of neuromodulation. mtp, metatarsophalangeal joint.

Early delivery of neuroprosthetic rehabilitation restores hindlimb motor control

Rats were subjected to an active training regimen under robotic assistance and electrochemical neuromodulation (van den Brand *et al.*, 2012), starting one week after injury (**Supplementary Figure S3.1**). To encourage the rats to deliver will-powered descending drives, they were motivated with a food reward. After 2 months, all trained rats regained robust hindlimb movements that allowed them to cross the runway uninterruptedly and repeatedly during the entire duration of training sessions (**Figure 3.1d**). The rats were able to support up to 22.5 ± 2 % of their entire body weight on their hindlimbs.

We next tested the respective contribution of chemical and electrical neuromodulation in the same trained rats (**Figure 3.1e**). Under electrical neuromodulation only (no chemical), 88% of the trained rats were still able to produce hindlimb movements that allowed them to reach the reward. In the complete absence of neuromodulation, more than half of the trained rats remained capable of moving forward, albeit gait patterns were impaired (**Figure 3.1e**).

To quantify hindlimb motor control, we conducted kinematic, kinetic and muscle activity analyses. We computed numerous parameters (n = 129, **Supplementary Table 1**) across more than 1'300 steps to establish a comprehensive assessment of performances. To weigh the relative importance of parameters, we used an objective statistical method based on principal component (PC) analysis (Takeoka *et al.*, 2014b) (**Figure 3.2**). For each rat, all computed parameters were averaged across conditions, and a PC analysis was applied to the entire dataset. We visualized gait patterns in the new space created by PC1-3, where PC1 explained the highest amount of variance (38%) and differentiated rats that produced hindlimb movements from rats that failed to exhibit steps (**Figure 3.2a**). Analysis of scores on PC1 revealed that this axis captured the effects of neuroprosthetic rehabilitation ($p < 0.001$; **Figure 3.2a**). PC2 segregated neuromodulation conditions ($p < 0.01$; **Supplementary Figure S3.3**). Parameters that highly correlated (factor loadings) with PC1 and PC2 were extracted, and regrouped into functional clusters corresponding to basic movement features (**Figure 3.2b**). This analysis revealed that trained rats tested under electrochemical neuromodulation produced gait patterns that share many features with those observed in intact rats (**Figure 3.2c**). Parameters clustering on PC2 indicated that the removal of chemical neuromodulation led to decreased muscle activation ($p < 0.01$) and reduced weight-bearing capacities ($p < 0.01$). These same parameters were further affected without neuromodulation ($p < 0.01$; **Figure 3.1** and **Supplementary Figure S3.3**).

These results demonstrate that the early delivery of neuroprosthetic rehabilitation enabled rats with functionally complete spinal cord contusion to regain hindlimb motor control capacities that persisted in the absence of any neuromodulation therapy.

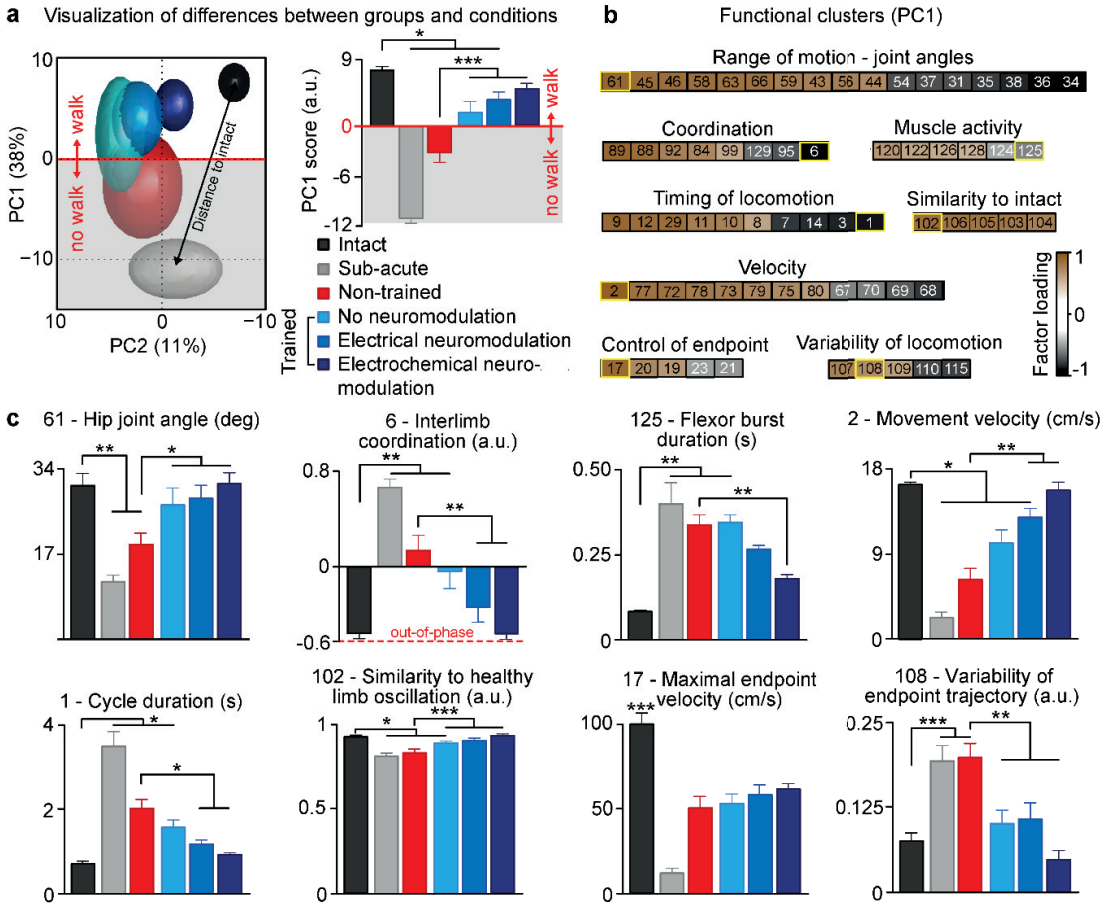

Figure 3.2 | Quantification of hindlimb motor control. (a) A PC analysis was applied on 127 parameters measured over 1300 step cycles across experimental groups and conditions. Hindlimb movement patterns are displayed in the new reference frame created by PC1-3. A least square elliptic fitting was applied to differentiate the clusters related to each group and experimental condition. The bar graphs report the mean values of scores on PC1, which captured the ability to perform hindlimb movements allowing forward progression versus stepping in place or over limited distance. **(b)** Factor loadings were extracted for PC1, and regrouped into functional clusters that are named for clarity. The numbers refer to individual parameters reported in **Supplementary Table 1**. **(c)** The bar graphs report parameters showing high correlations with PC1, highlighted with the yellow frames in the functional clusters. *, P < 0.05; **, P < 0.01; ***, P < 0.001. Error bars, s.e.m.

Transfer of hindlimb motor control capacities to unpracticed motor behavior

We next tested the rats during swimming across a straight pool of water. We implemented this new behavioral task because of four benefits. First, this water prevents rats from utilizing the inertia of the robotic interface to propel themselves forward without supraspinal control (Sławińska *et al.*, 2012). Second, swimming enables evaluations of hindlimb motor control under gravity-reduced conditions when rats cannot support their entire bodyweight (Bachmann *et al.*, 2013). Third, swimming eliminates weight-bearing sensory input that may dissimulate supraspinal contribution (Takeoka *et al.*, 2014b). Fourth, rats rush to escape the water, displaying hindlimb movement that may not be exposed during overground quadrupedal locomotion (Smith *et al.*, 2009; Dominici *et al.*, 2012).

Intact rats produced robust power and return stroke cycles with reciprocal activation of antagonist muscles, and alternative oscillations of the left and right hindlimbs (**Figure 3.3a-b**). Injured rats were tested without neuromodulation at 2 months post-lesion. Non-trained rats displayed minimal hindlimb movements, including occasional uncoordinated strokes or spasms associated with a pronounced co-activation of antagonist muscles ($p < 0.01$; **Figure 3.3a-c**). In contrast, trained rats generated powerful hindlimb movements with alternating activity of extensor and flexor muscles (**Figure 3.3a-c**). Despite significantly reduced velocity ($p < 0.001$; **Figure 3.3c**), the range of hindlimb movements was similar in intact and trained rats (**Figure 3.3a-c**). However, trained rats did not recover interlimb coordination. The left and right hindlimbs oscillated at different frequencies ($p < 0.001$), which resulted in a broad range of interlimb coordination patterns, including periods of synchronized stroke cycles ($p < 0.001$; **Figure 3.3c**).

These results demonstrate that neuroprosthetic rehabilitation restored hindlimb motor control without neuromodulation in an unpracticed motor behavior that relies on a supraspinal drive.

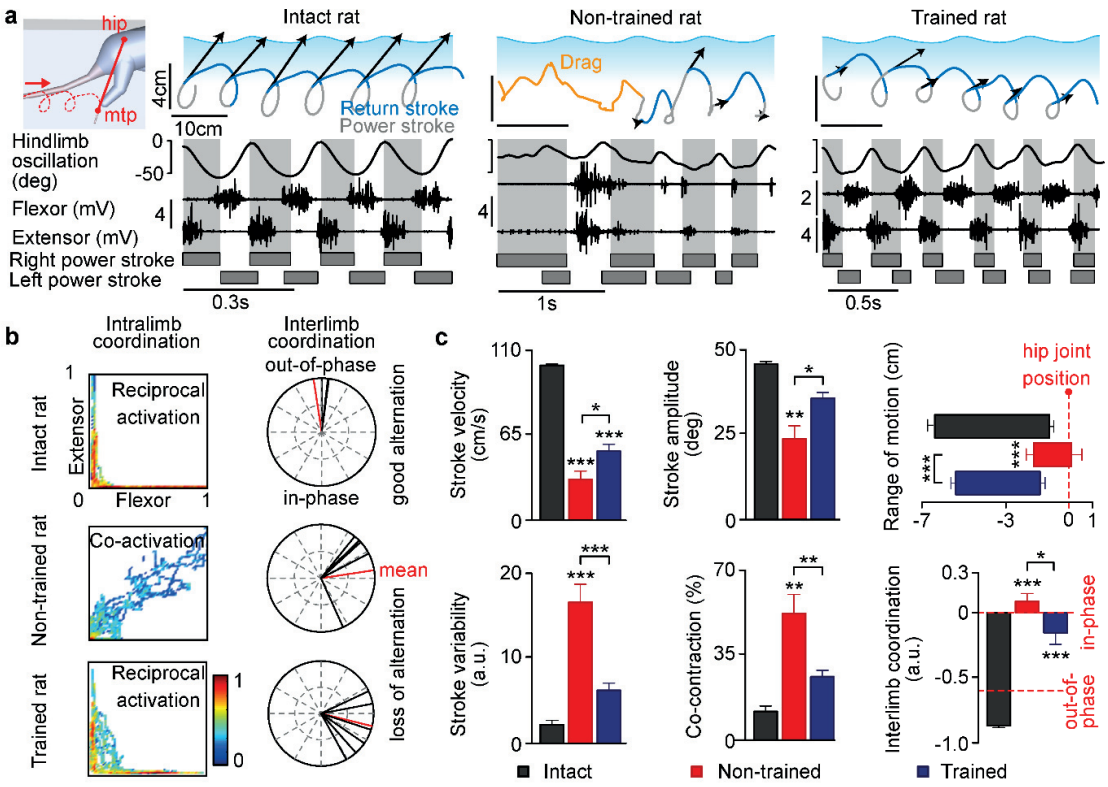

Figure 3.3 | Neuroprosthetic rehabilitation restores hindlimb motor control in an unpracticed swimming task. (A) Color-coded trajectory of the hindlimb endpoint and hindlimb oscillations during power and return stroke together with electromyographic activity of antagonistic ankle muscles during swimming in a straight pool of water. Conventions are the same as in **Figure 3.1**. Injured rats were tested without neuromodulation. **(b)** Normalized density plots displaying the coordination between antagonistic ankle muscles throughout a trial, reflecting intralimb coordination. Polar plot representations illustrating interlimb for each stroke cycle (black lines). **(c)** Bar graphs reporting mean values for representative parameters. *, P < 0.05; **, P < 0.01; ***, P < 0.001. Error bars, s.e.m.

Delayed delivery of neuroprosthetic rehabilitation restores hindlimb motor function

We next tested whether neuroprosthetic rehabilitation was capable of improving hindlimb motor control when delivered in the chronic stage of injury. Rats (n = 8) received the same lesion as early-trained rats. They followed the same neuroprosthetic rehabilitation program for 2 months, but the onset was delayed by 9 weeks (**Supplementary Figure S3.1**).

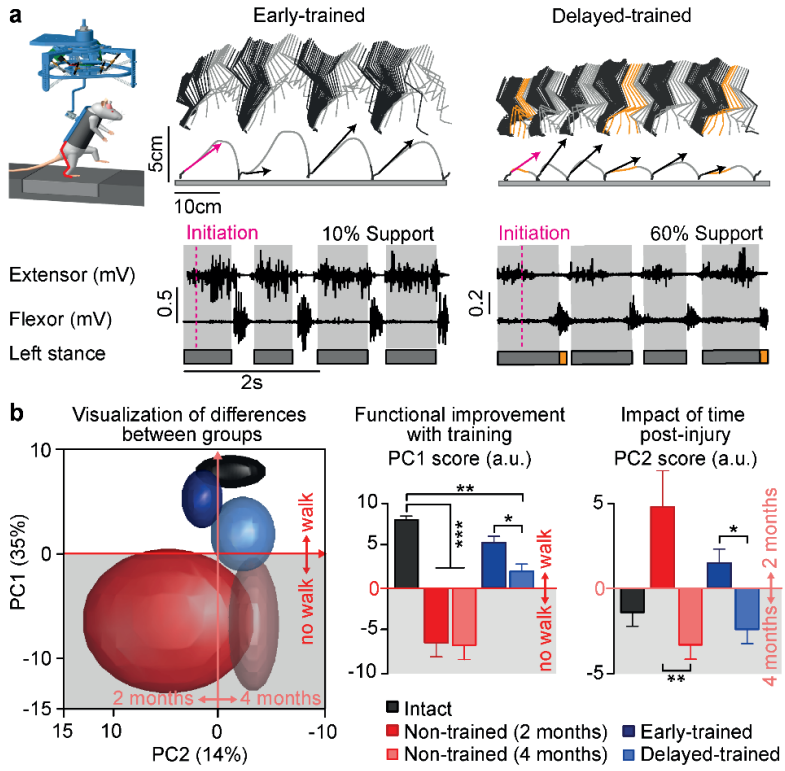

Figure 3.4 | Neuroprosthetic rehabilitation restores hindlimb motor control in delayed-trained rats, but to a lesser extent. (a) Evaluation of hindlimb motor control overground in a bipedal posture under robotic assistance and electrochemical neuromodulation. Representative executions of an early-trained and delayed-trained rats, tested after completion of the rehabilitation program. Conventions are the same as in **Figure 3.1**. **(b)** A PC analysis was applied on the same set of parameters as in **Figure 3.1** for the different groups of rats. Hindlimb movement patterns are displayed in the new reference frame created by PC1-3. The bar graphs report the mean values of scores on PC1 and PC2, which captured functional improvement with training and the impact of time post-injury. The parameters loading on PC1 and PC2, which explain these differences, are reported in **Figure S3.3**. Error bar, sem. *, P < 0.05; **, P < 0.01; ***, P < 0.001.

All delayed-trained rats regained the ability to cross the entire length of the runway on their hindlimbs, but only in the presence of electrochemical neuromodulation (**Figure 3.4**). PC analysis

applied on kinematic, kinetic and muscle activity parameters revealed that the recovery of hindlimb motor control was significantly reduced in delayed-trained rats compared to early-trained rats ($p < 0.05$, **Figure 3.4c**). Delayed-trained rats exhibited slower speed of motion, reduced muscle activity, lower step height, and limited hip joint extension ($p < 0.05$, **Figure 3.4d-e** and **Supplementary Figure S3.4**). Overall, the meta-analysis of all contused animals trained with similar neurorehabilitation protocols lead to the overall recovery of voluntary locomotion in 73.5% of 49 rats and 100% of 8 acutely trained rats scored by two blinded experimenters (**Supplementary Figure S3.10**).

These results show that neuroprosthetic rehabilitation restored supraspinal control of hindlimb movement when delivered in the chronic stage of a functionally complete spinal cord contusion, but performances were reduced compared to early onset of training and motor control only occurred during electrochemical neuromodulation.

Neuroprosthetic rehabilitation promotes reorganization of residual brainstem pathways

We conducted a retrograde tract-tracing study from lumbar segments to identify the neural pathways that maintained a connection across the injury. The contusion completely interrupted axonal projections from neurons located in thoracic and cervical segments above the injury, and in the motor cortex (**Supplementary Figure S3.5**). Only a subset of brainstem projection neurons located in the parapyramidal and gigantocellular regions of the reticular formation retained connections to lumbar segments, which amounted to 8.9 % of neurons counted in healthy rats (**Figure S3.5**).

We next performed an anterograde tract-tracing study from these identified brainstem regions in intact and injured rats, both at sub-acute and chronic stages post-injury (**Supplementary Figure S3.1**). Reticulospinal fibers were labeled with bilateral injections of an adeno-associated virus (AAV1) expressing green fluorescent protein (GFP) under the cytomegalovirus (CMV) promoter (AAV1-CMV-GFP) into the gigantocellular reticular formation. We additionally labeled axonal projections from serotoninergic neurons using immunohistochemistry. Reticulospinal axons are located throughout the ventral and lateral aspect of the spinal cord white matter (**Supplementary Figure S3.6a-b**). Consequently, the lesion systemically spared a subset of these axons,

regardless of the exact and inherently variable location of spinal cord damage (**Supplementary Figure S3.6c**).

We quantified the density of reticulospinal fibers in spinal segments above and below the injury. Compared to intact and sub-acute rats, both non-trained and trained rats showed a significant increase in reticulospinal fiber density above the injury, which specifically occurred in the medial and ventral grey matter ($p < 0.05$, **Figure 3.5a-b**). Trained rats also exhibited a robust increase in reticulospinal fiber density immediately below the injury (**Figure 3.5c,e**) and within mid-lumbar segments (**Figure 3.5d**). While mid-lumbar remodeling was also observed in non-trained rats, the extent was significantly reduced and highly variable compared to trained rats ($p < 0.05$).

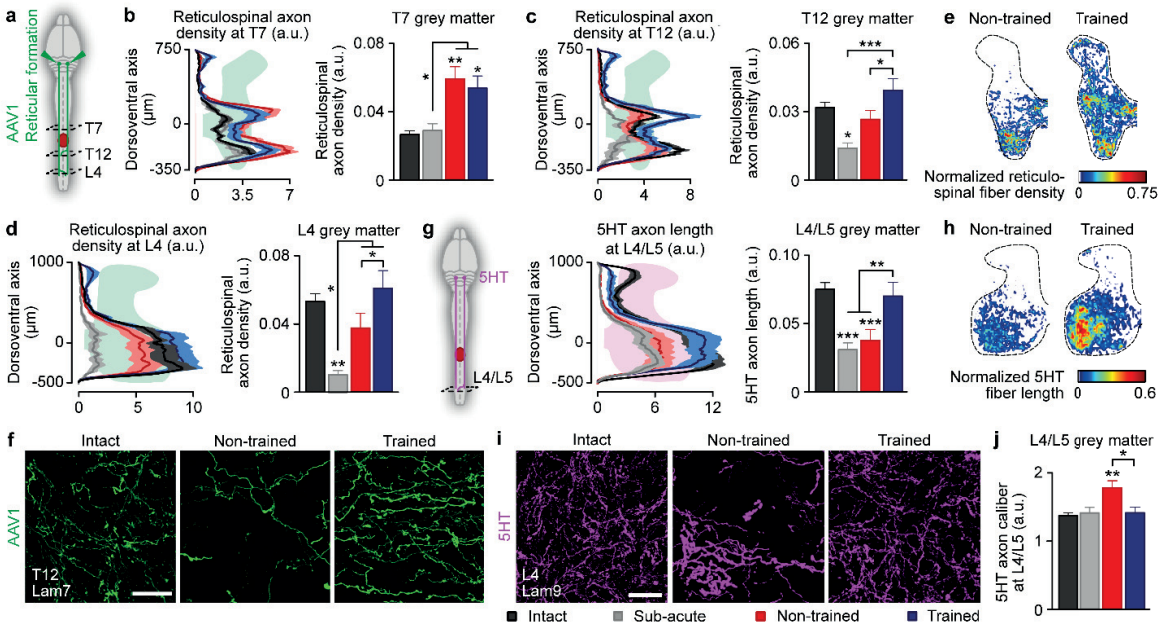

Figure 3.5 | Neuroprosthetic rehabilitation triggers a pronounced remodeling of residual reticulospinal pathways into specific spinal cord regions. (a) Diagram illustrating AAV1-mediated tracing of axonal projections from neurons located in the gigantocellular regions of the reticular formation. Density plot along the dorsoventral extent and bar graphs reporting the mean density of AAV1-labeled reticulospinal axons. These quantifications are shown for segments located **(b)** above, and at the **(c)** thoracic and **(d)** lumbar levels below the injury. **(e)** Representative heatmaps of AAV1-labeled reticulospinal axons, visualized at T12. **(f)** Representative images of AAV1-labeled reticulospinal axons in the lamina 7 of T12 segment. **(g)** Density plot along the dorsoventral extent and bar graphs reporting the mean length of 5-HT axons at L4/L5. **(h)** Representative heatmaps of 5HT axons, visualized at L4/L5. **(i)** Representative images of 5HT axons in the lamina 9 of L4 segment. **(j)** Bar graphs reporting the mean caliber of 5-HT axons at L4/L5. Scale bars, 25µm. *, $P < 0.05$; **, $P < 0.01$; ***, $P < 0.001$. Error bars, s.e.m. Lam, lamina.

At each of the examined spinal levels below the injury, the reorganization of reticulospinal axonal projections occurred within specific regions. In thoracic segments immediately below injury, the density of reticulospinal fibers increased in the intermediate laminas, where spinal projection neurons connected to lumbar motor centers (**Figure 3.6d**) and hindlimb motoneurons (Ni *et al.*, 2014) reside. These neurons relay and amplify the descending locomotor command (Cowley *et al.*, 2008; Juvin *et al.*, 2012). We found close appositions between glutamatergic excitatory synapses of residual reticulospinal fibers and these projection neurons (**Figure 3.6d**). At the mid-lumbar level, the remodeling of residual reticulospinal fibers instead took place into the ventral laminas, which contain motor related interneurons and motoneurons innervating hindlimb muscles (Tripodi *et al.*, 2011) (**Figure 3.6e**).

Spared serotoninergic fibers below the injury did not display increased length in non-trained rats compared to sub-acute evaluations ($p < 0.001$; **Figure 3.5g**). Instead, these fibers exhibited a significant increase in caliber ($p < 0.001$; **Figure 3.5j**), which was previously linked to axonopathy (Müllner *et al.*, 2008). Neuroprosthetic rehabilitation prevented this pathological swelling ($p < 0.05$; **Figure 3.5j**). In contrast, trained rats exhibited a pronounced remodeling of these fibers that was specifically directed to the ventral grey matter containing hindlimb motoneurons (**Figure 3.5h** and **Figure 3.6e**). This remodeling reconstituted the original length and projection patterns observed in healthy rats (**Figure 3.5g**).

These anatomical evaluations reveal that neuroprosthetic rehabilitation mediated a pronounced reorganization of residual reticulospinal and serotoninergic fibers within specific spinal cord regions that are highly relevant for hindlimb motor control.

Motor cortex axonal projections invade regions containing neurons with residual connections

We next evaluated the reorganization of axonal projections from the hindlimb motor cortex. We labeled these fibers using injections of biotinylated dextran amine (BDA). The contusion completely interrupted corticospinal tract projections below the injury (**Figure Supplementary S3.5-6**). In the thoracic segments above the injury, we did not detect changes in corticospinal tract fiber density in either non-trained or trained rats compared to healthy rats (**Figure Supplementary S3.7a-b**). We then evaluated the density of motor cortex axonal projections in the brainstem regions that contained neurons with residual connections below the injury.

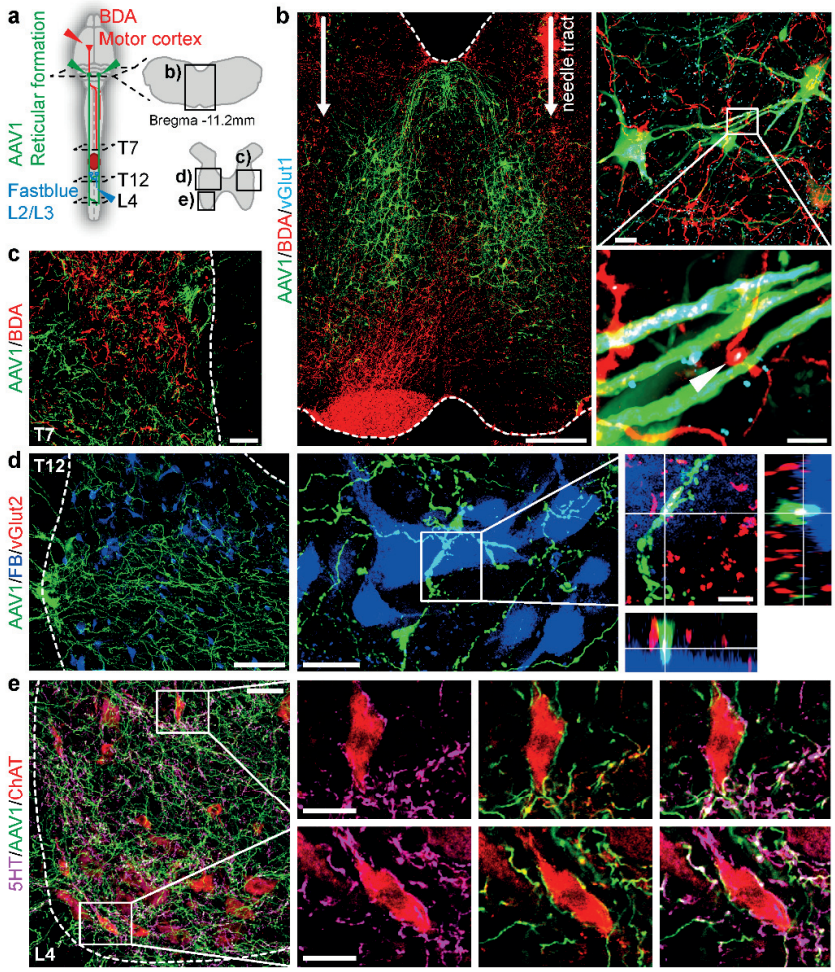

Figure 3.6 | Connectivity of residual reticulospinal pathways below the functionally complete spinal cord contusion in trained rats. (a) Scheme of anatomical experiments. **(b)** BDA-labeled motor cortex axonal projections established vGlut1-positive appositions with AAV1-labeled neurons in the gigantocellular region of the reticular formation (medulla oblongata). Scale bars; 500 µm for overview, 20 µm top right and 5µm bottom right. **(c)** Density of BDA-labeled corticospinal tract axons and AAV1-labeled reticulospinal axons in the thoracic grey matter (T7), above the injury. Scale bar; 50µm. **(d)** AAV1-labeled reticulospinal axons established vGlut2-positive appositions with spinal projection neurons located in the intermediate grey matter of thoracic segments immediately below the injury (T12), which were retrogradelly labeled with FastBlue (FB) from upper lumbar segments (L2/L3). Scale bar; 100 µm for overview, 20 µm middle and 5 µm right. **(e)** AAV1-labeled reticulospinal axons and 5-HT axons entwined motoneurons innervating hindlimb muscles, labeled with anti-choline acetyltransferase (ChAT) antibodies. Scale bar; 50 µm for overview and 20 µm insets.

We found a three-fold increased fiber density in the parapyramidal and the gigantocellular regions of the reticular formation in both non-trained and trained rats compared to intact and sub-acute rats ($p < 0.05$; **Supplementary Figure S3.7**).

These combined anatomical results suggest that reticulospinal neurons with residual synaptic projections below the injury contributed to delivering the supraspinal command to spinal circuits controlling hindlimb movement in trained rats. To establish causality between residual reticulospinal fibers and hindlimb motor control, we conducted both activation and inactivation experiments.

Indirect activation of reticulospinal neurons triggers hindlimb movement in trained rats

Neurons located in the mesencephalic locomotor region project extensively to both the parapyramidal and gigantocellular regions of the reticular formation (Garcia-Rill and Skinner, 1987; Bachmann *et al.*, 2013). Deep brain stimulation of the mesencephalic locomotor region triggers locomotion through the recruitment of these neurons (Bachmann *et al.*, 2013; Ryczko and Dubuc, 2013). We thus tested whether this stimulation was capable of eliciting hindlimb movement during motor recovery in trained rats. We identified the mesencephalic locomotor region anatomically and functionally. Healthy rats (n = 6) received 4 custom-made electrodes in the pedunculopontine nucleus (Ryczko and Dubuc, 2013), which we identified based the location of cholinergic neurons (**Figure 3.7a-b**). Electrical stimulation (40 Hz, 200 µs, 100-200 µA) through the most effective electrode triggered locomotion with a time to initiation of 3.37 ± 1 s (**Figure 3.7c**). The contusion abolished these responses at one week after injury (**Figure 3.7d**). The response progressively reappeared during rehabilitation, in parallel with the recovery of supraspinal control (**Figure 3.7d**). Increasing the stimulation intensity significantly enhanced the robustness of hindlimb movements compared to voluntary executions (n = 4, $p < 0.01$; **Supplementary Figure S3.8**), although the body posture and behavior suggested signs of discomfort.

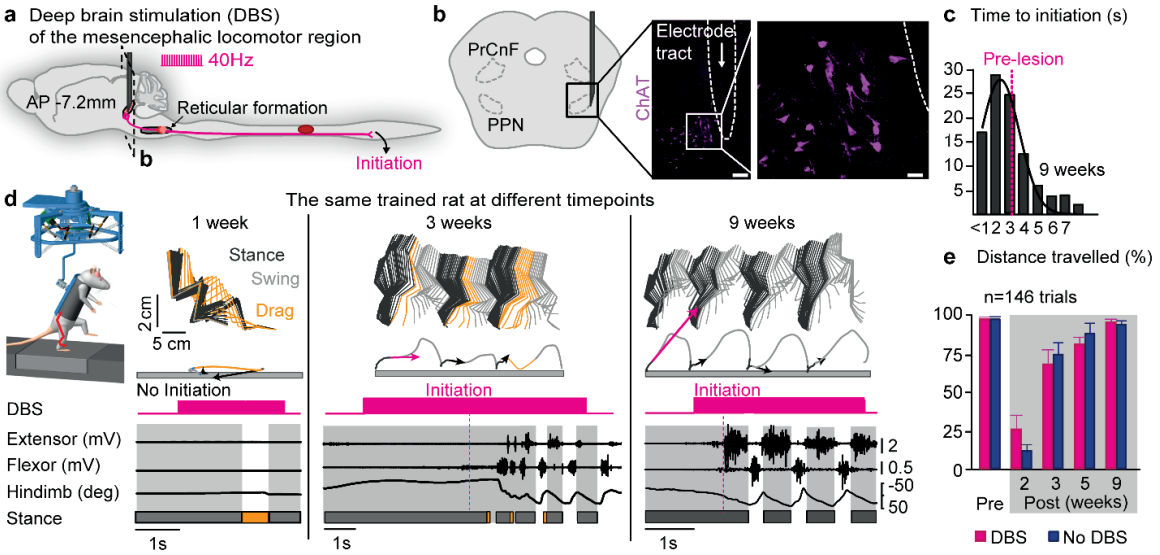

Figure 3.7 | Deep brain stimulation of the mesencephalic locomotor region triggers initiation of hindlimb movement in trained rats. (a) Scheme of anatomical and electrophysiological experiments. **(b)** Location of cholinergic (ChAT) neurons in the pedunculopontine nucleus (PPN), where the deep brain stimulation (DBS) electrodes were implanted. Scale bar; 100 µm and 50 µm for inset. (c) Distribution of the times from DBS onset to initiation of hindlimb movement in trained rats (n = 6 rats), calculated at 9 weeks post-injury. The vertical dotted line indicates the average time to initiation calculated before the injury. **(d)** Representative executions of the same trained rat at 1, 3 and 9 weeks post-injury. Conventions are the same as in **Figure 3.1**. **(e)** Bar graphs reporting the mean uninterrupted distance travelled over the length of the runway during trials with and without DBS for trained rats (n = 6). Error bars, s.e.m. PrCnF, pre-cuneiform nucleus.

Inactivation of residual reticulospinal fibers abolishes hindlimb motor control

We used a doxycycline-inducible tetanus toxin technique (Kinoshita *et al.*, 2012) that allowed the reversible inactivation of reticulospinal neurons with surviving synaptic projections to lumbar segments (**Figure 3.8a**). We injected the highly efficient retrograde gene transfer lentivector HiRet carrying enhanced tetanus neurotoxin light chain (eTeNT) with an enhanced GFP downstream of a tetracycline-responsive element (TRE) into the upper lumbar segments of trained rats. Two weeks later, we injected an AAV2/1 vector carrying the reverse tetracycline transactivator (rtTAV16, Tet-on) bilaterally into the gigantocellular region of the reticular formation (**Figure 3.8b**). Only reticulospinal neurons with synaptic projections below the injury contained both transgenes, which we confirmed histologically (**Figure 3.9c**). Therefore, doxycycline induced the tetanus toxin expression in these neurons only, specifically blocking the synaptic release from these fibers. All

the trained rats (n = 4) had recovered supraspinal control of hindlimb movement during electrochemical neuromodulation (**Figure 3.8d**). Administration of doxycycline during 5 consecutive days suppressed these motor capacities ($p < 0.001$; **Figure 3.8d-e**). Rats repeatedly attempted to activate hindlimb muscles, displaying extensive activation of the trunk musculature and forelimb movements, but they failed to lift their hindpaws and propel their body forward. Hindlimb motor control completely recovered after the cessation of doxycycline administration ($p > 0.2$; **Figure 3.8d-e** and **Supplementary Figure S3.9)**.

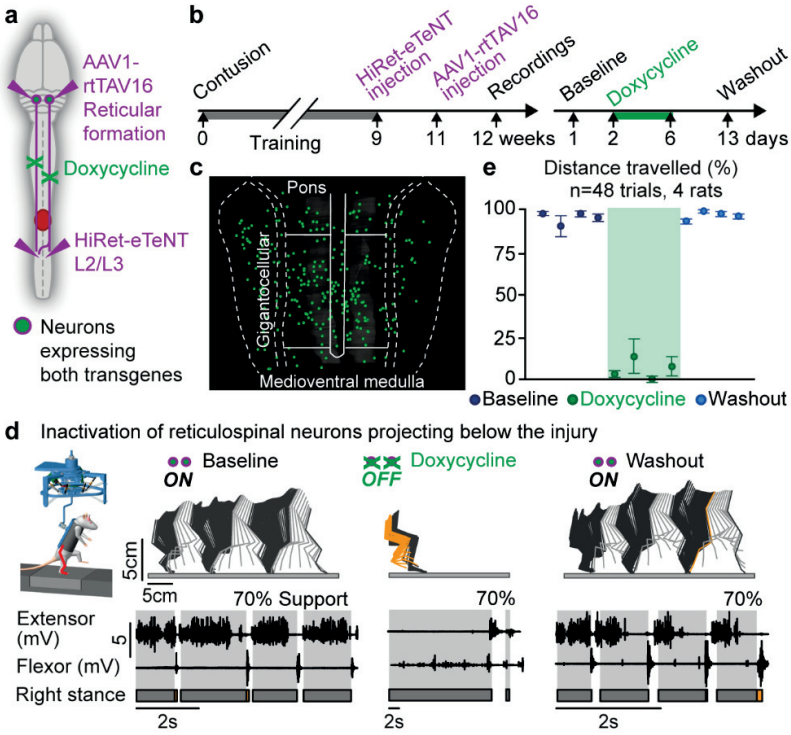

Figure 3.8 | Inactivation of reticulospinal neurons projecting below the injury abolishes hindlimb motor control in trained rats (a) Schematic diagram illustrating virus-mediated inactivation of reticulospinal neurons projecting to L2/L3 spinal segments. **(b)** Timeline of the experiments. **(c)** Reconstruction of all the neurons expressing both transgenes. **(d)** Hindlimb motor control was evaluated in a bipedal posture with robotic assistance and electrochemical neuromodulation. Representative executions of the same trained rat before, during and after doxycycline administration. Conventions are the same as in **Figure 1.1**. **(e)** Bar graphs reporting the mean distance travelled over the length of the runway during trials performed before, during, and after doxycycline administration. Each dot represents mean values for a trained rat. Error bars, s.e.m.

These inactivation and activation experiments establish causal relationships between recovery and reticulospinal neurons with synaptic projections below the injury. Other supraspinal pathways failed to compensate for the blocked synaptic transmission, indicating that these specific reticulospinal neurons were necessary to mediate hindlimb motor control after injury in trained rats.

3.5 Discussion

We modeled a functionally complete spinal cord contusion that reproduced the highly variable damage observed in paraplegic individuals. Will-powered training under electrochemical neuromodulation and robotic assistance restored hindlimb motor control in 73.5% of 49 rats from all the studies performed to date in our laboratory. Our results revealed that the supraspinal command was transmitted through residual reticulospinal pathways that profusely expanded into specific, functionally relevant grey matter territories below the injury. We discuss the implications of these findings for SCI models, spinal cord repair mechanisms, and the clinical translation of neuroprosthetic rehabilitation.

Functionally complete spinal cord contusion model

Neuroprosthetic rehabilitation promoted an extensive remodeling of neuronal pathways that restored hindlimb motor control after staggered thoracic hemisections in rats (van den Brand et al., 2012). However, spinal cord damage in humans primarily results from contusion injuries, which lead to more complex functional and anatomical outcomes than cut injuries (Basso et al., 1996; James et al., 2011; Silver et al., 2014). Consequently the relevance of these findings for paraplegic individuals remained speculative (Sławińska et al., 2012). To remedy this limitation, we modeled a functionally complete spinal cord contusion. In the chronic stage, injured rats exhibited extensive hindlimb movements when moving around quadrupedally in an open field, as previously documented (Basso et al., 1996). Similarly, individuals with a functionally complete SCI can generate vigorous leg movements in response to sensory information during standing and manually assisted stepping (Dietz and Harkema, 2004). However, these movements are produced by motor circuits below the injury, without contribution from supraspinal centers (Edgerton et al., 2008). To circumvent this confounding factor, we tested the rats during swimming and in a robot-assisted bipedal posture. The suppression of weight-bearing information in the water increases the relative contribution of the supraspinal drive (Zagoraiou *et al.*, 2009; Bachmann *et al.*, 2013; Takeoka *et al.*, 2014b), while the bipedal posture forces the rats to activate hindlimb muscles to move forward (Dominici et al., 2012). Both experimental conditions revealed that our SCI model permanently abolished supraspinal control of hindlimb movement, indicating the presence of a functionally complete spinal cord contusion. While this terminology is prone to controversy, it reflects the motor control capacities of the rats, and corresponds to a relevant clinical

classification. In turn, these results reinforce the importance of establishing more refined testing paradigms than the classically used open field conditions to evaluate hindlimb motor control in rodent SCI models.

Residual reticulospinal pathways mediate motor recovery after neuroprosthetic rehabilitation

Higher brain centers produce lower limb movements through various brainstem pathways and spinal interneurons that establish an exquisitely organized motor-circuit communication matrix (Esposito et al., 2014). Spinal cord damage interrupts this connectivity matrix, yielding extraordinary challenges for regaining motor control. Due to the regenerative failure of severed axons (Tuszynski and Steward, 2012), recovery can only occur through the reorganization of the components embedded in the residual tissue. This reorganization necessarily depends on the location and extent of the spinal cord damage. For example, previous work showed that recovery of basic motor capacities after cut injuries involves the establishment of detour circuits reconnecting propriospinal neurons to denervated motor circuits below the lesion (Bareyre *et al.*, 2004a; Courtine *et al.*, 2008; van den Brand *et al.*, 2012; Takeoka *et al.*, 2014b; Zörner *et al.*, 2014). Due to their anatomical location, however, the axons of propriospinal neurons did not survive contusion SCI (Conta Steencken and Stelzner, 2010), preventing this mechanism from contributing to recovery after such lesions. Instead, reticulospinal axons display ubiquitous projection patterns in the ventral and lateral regions of the white matter (Nathan et al., 1996; Ballermann and Fouad, 2006; Jordan et al., 2008). Consequently, the contusion SCI systematically spared a subset of these axons, regardless of the exact location of spinal cord damage. We found that neuroprosthetic rehabilitation triggered a pronounced sprouting of these residual reticulospinal fibers into motor related regions of the thoracic and lumbar grey matter, both above and below the injury. The functional and anatomical reorganization of reticulospinal pathways has been well documented after moderate SCIs in rodents (Ballermann and Fouad, 2006; Zörner et al., 2014) and primates (Zaaimi et al., 2012). Here, we confirmed this remarkable ability after more severe injuries, and extend previous findings by showing that remodeling takes place into specific grey matter territories and is necessary and sufficient for motor execution in trained rats. We therefore propose that will-powered training under electrochemical neuromodulation establishes a novel motor-circuit communication matrix whereby the supraspinal

command is transmitted to specific spinal circuits through reticulospinal neurons with residual synaptic projections below the injury.

Spinal cord repair mechanisms

The circuit-level mechanisms and molecular cues underlying the remodeling of the motor circuits and their connections after injury remain poorly understood. We recently demonstrated that muscle spindle feedback is a key neuronal substrate to direct circuit rearrangement after SCI (Takeoka *et al.*, 2014b). Computer simulations (Capogrosso *et al.*, 2013) and experimental studies (Sayenko *et al.*, 2014) showed that electrochemical neuromodulation facilitates motor control through the recruitment of muscle spindle feedback pathways. Strikingly, we found that the remodeling of reticulospinal fibers precisely occurred in the target grey matter laminas of muscle spindle feedback projections, both at the thoracic (Ni *et al.*, 2014) and lumbar (Tripodi *et al.*, 2011) levels. These observations open the possibility that activity-dependent release of growth factors from muscle spindle afferents promotes this circuit-specific reorganization. For example, the amount of physical activity influences BDNF expression in the spinal cord after SCI (Ying *et al.*, 2008), an effect that may be mediated by muscle spindle feedback (Takeoka *et al.*, 2014b). We thus propose a model in which the interplay between top-down supraspinal drives elicited by will-powered signals and bottom-up activation of muscle spindle feedback with electrochemical neuromodulation triggers a reorganization of the motor-circuit communication matrix at the locations where both inputs converge. While this conceptual framework remains speculative, it opens new avenues for studying spinal cord repair mechanisms and developing therapeutic strategies.

Limitations and therapeutic potential of neuroprosthetic rehabilitation

Neuroprosthetic rehabilitation restored hindlimb motor control in all the trained rats. However, this recovery presented several limitations. Only a subset of rats displayed supraspinal control of movement without neuromodulation. Moreover, balance maintenance was insufficient to enable quadrupedal locomotion without frequent falls. The recovery was even more restricted after chronic injuries. While all the delayed-trained rats regained weight-bearing hindlimb movements, motor control only occurred during electrochemical neuromodulation, and the performance was

moderate compared to early-trained rats. These results stress the importance of devising strategies combining neuroprosthetic rehabilitation, tissue replacement, and growth-promoting interventions in order to create an environment supporting robust functional recovery after the most severe forms of SCI.

Despite these inherent limitations, our results establish a therapeutic framework to improve motor recovery after SCI, especially when delivered in the early phase after injury. Anatomical and functional features of reticulospinal pathways have been well conserved during mammalian evolution (Nathan *et al.*, 1996; Ryczko and Dubuc, 2013; Grillner and El Manira, 2015). As observed in rats, these fibers are scattered in the lateral and ventral aspects of the human spinal cord (Nathan *et al.*, 1996), suggesting that natural spinal cord damage often spares a subset of these axons (Kakulas, 1999; James *et al.*, 2011). We surmise that the immediate recovery of voluntary leg movement during epidural electrical stimulation in individuals with motor complete paraplegia (Angeli *et al.*, 2014) may rely on the recruitment of these spared reticulospinal fibers.

The implementation of neuroprosthetic rehabilitation in clinical settings requires the design of several innovative technologies. These developments include multidirectional robotic support systems and more refined neuromodulation paradigms using spinal implants and pulse stimulators that are tailored for this application. These technological developments are progressing at a fast pace. While challenges lie ahead, neuroprosthetic rehabilitation may progressively become a medical practice to improve functional recovery after SCI.

3.6 Supplementary material

Table 1. Kinematic, kinetic and EMG parameters

#	Computed parameter
	Gait timing
1	**Cycle duration**
2	Movement velocity
3	**Stance duration**
4	Swing duration
5	**Stance duration in percentage of whole cycle**
6	Interlimb coordination
7	**Double stance (in percentage of gait cycle duration)**
8	Stride length
9	**Step length**
10	Step height
11	**Step height normalized to stance height**
12	Path length
	Endpoint trajectory shape
13	**Stance width**
14	Body weight support by the postural prosthesis
15	**Maximal backward position of the foot**
16	Maximal forward position of the foot
17	**Maximal endpoint velocity**
18	Timing of the maximal enpoint velocity
19	**Endpoint acceleration**
20	Endpoint velocity
21	**orientation of the velocity vector at swing onset**
22	Drag duration
23	**relative drag duration (percent of swing duration)**
	Stability
24	**Amplitude of lateral trunk position**
25	Sagital trunk movement
26	**Sagital trunk velocity**
27	Variability of vertical hip-midpoint oscillation
28	**Variability of medio-lateral hip rotation**
29	Forward movement of the center of mass
30	**Lateral oscillation of the center of mass**
	Joint angles and limb segment oscillations
31	**Crest oscillation (minimal elevation)**
32	thigh oscillation (minimal elevation)
33	**Shank oscillation (minimal elevation)**
34	Foot oscillation (minimal elevation)
35	**Toe oscillation (minimal elevation)**
36	Whole limb oscillation (minimal elevation)
37	**Crest oscillation (maximal elevation)**
38	thigh oscillation (maximal elevation)
39	**Shank oscillation (maximal elevation)**
40	Foot oscillation (maximal elevation)
41	**Toe oscillation (maximal elevation)**
42	Whole limb oscillation (maximal elevation)
43	**Hip joint angle (maximal)**
44	Knee joint angle (maximal)
45	**Ankle joint angle (maximal)**
46	MTP joint angle (maximal)
47	**Whole limb adduction**
48	Foot adduction
49	**Hip joint angle (minimal)**
50	Knee joint angle (minimal)
51	**Ankle joint angle (minimal)**
52	MTP joint angle (minimal)
53	**Whole limb abduction**
54	Foot abduction
55	**Crest oscillation**
56	Thigh oscillation
57	**Shank oscillation**
58	Foot oscillation
59	**Toe oscillation**
60	Whole limb oscillation
61	**Hip joint angle**
62	Knee joint angle
63	**Ankle joint angle**
64	MTP joint angle
65	**Whole limb medio-lateral oscillation**
66	Foot rotation
	Velocity
67	**Whole limb angle velocity (minimal)**
68	Hip joint anlge velocity (minimal)
69	**Knee joint angle velocity (minimal)**
70	Ankle joint angle velocity (minimal)
71	**MTP joint angle velocity (minimal)**
72	Whole limb angle velocity (maximal)
73	**Hip joint anlge velocity (maximal)**
74	Knee joint angle velocity (maximal)
75	**Ankle joint angle velocity (maximal)**
76	MTP joint angle velocity (maximal)
77	**Whole limb angle velocity**
78	Hip joint anlge velocity
79	**Knee joint angle velocity**
80	Ankle joint angle velocity
81	**MTP joint angle velocity**
	(Intra-limb) coordination
82	**Temporal coupling between crest and thigh oscillation**
83	Temporal coupling between thight and shank oscillation
84	**Temporal coupling between shank and foor oscialltion**
85	Temporal coupling between foot and toe oscillation
86	**correlation of crest and thigh oscillation**
87	Correlation of thigh and leg oscillation
88	**Correlation of leg and foot oscillation**
89	Correlation of foot and toe oscillation
90	**Correlation of hip and knee oscillation**
91	Correlation of knee and ankle oscillation
92	**Correlation of ankle and MTP oscillation**
93	Timing of crest-thigh (minimal)
94	**Timing of crest-thigh (maximal)**
95	Timing of thigh-shank (minimal)
96	**Timing of thigh-shank (maximal)**
97	Timing of shank-foot (minimal)
98	**Timing of shank-foot (maximal)**
99	Degree of linear coupling between joint oscillations (PC1)
100	**Degree of linear coupling between joint oscillations (PC2)**
101	Degree of linear coupling between joint oscillations (PC3)
	Similarity to healthy gait
102	**Correlation between limb oscillation of healthy and injured leg**
103	Correlation between hip oscillation of healthy and injured leg
104	**Correlation between knee oscillation of healthy and pathological leg**
105	Correlation between ankle oscillation of healthy and injured leg
106	**Correlation between MTP oscillation of healthy and injured leg**
	Variability of gait
107	**Variability of foot trajectory in the forward direction**
108	Variability of foot trajectory in the sagital place
109	**Variability of foot trajectory in the 3-dimensioal room**
110	Variability of gait cycle duration
111	**Variability of stride length**
112	Variability of double stance duration
113	**Variability of step height**
114	Variability of path length
115	**Variability of max endpoint velocity**
	Kinetics
116	**vertical ground reaction force**
	Muscle activity parameters
117	**Burst onset of extensor**
118	Burst end of extenson
119	**Burst duration of extensor**
120	Mean amplitude of extensor
121	**Integral of extensor activity**
122	Root mean square of extensor activity
123	**Burst onset flexor**
124	Burst end of flexor
125	**Burst duration of flexor**
126	Mean amplitude of flexor
127	**Integral of flexor activity**
128	Root mean square of eflexor activity
129	**Co-contraction of the flexor and extensor muscle**

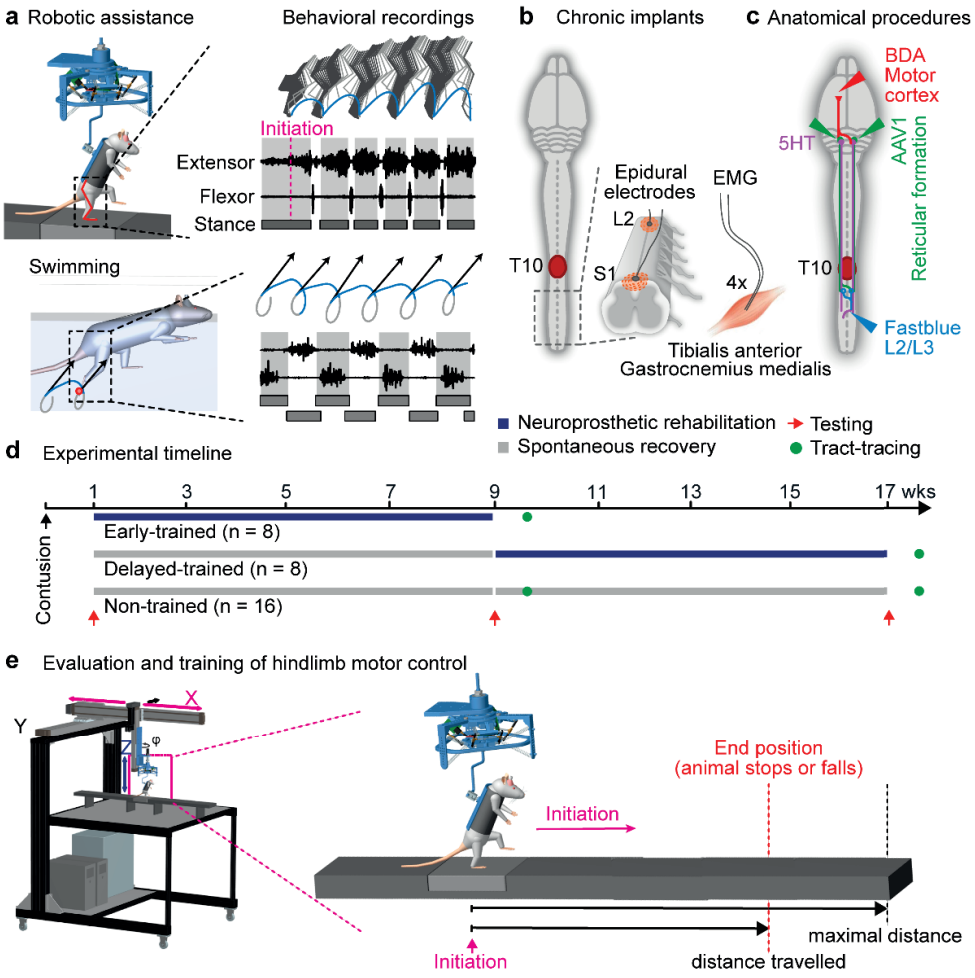

Figure S3.1 | General methods and experimental groups. (a) Representative kinematic and EMG recordings of hindlimb movements in a bipedal posture under robotic assistance and during swimming in an intact rat. **(b)** Electrodes were chronically implanted into the left and the right medial gastrocnemius and tibialis anterior muscles to record EMG activity, and over the dorsal aspect of spinal segments L2 and S1 to deliver electrical neuromodulation. **(c)** Schematic overview over anatomical experiments that were used to evaluate reorganization of neuronal pathways. **(d)** Experimental timeline for the main groups of rats. **(e)** Behavioral task to evaluate and train hindlimb motor control. The distance travelled was measured as the relative distance (%, length of the runway: 140 cm) from the initiation of hindlimb movement to the cessation of the forward progression for at least 2 s.

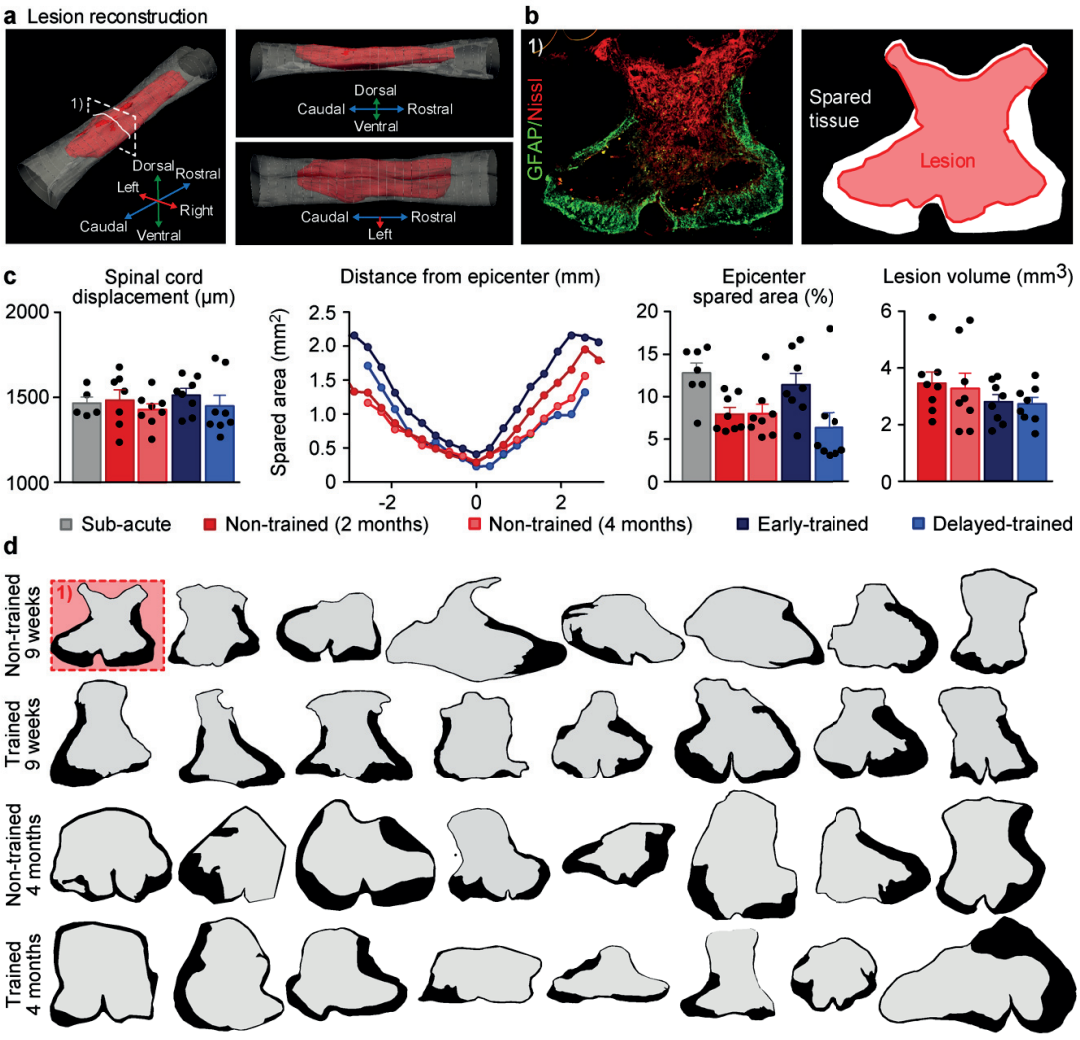

Figure S3.2 | Morphological quantification of the spinal cord contusion injuries in all the experimental rats. (a) 3D reconstruction of a functionally complete spinal cord contusion. **(b)** Epifluorescent image showing a transverse view of the spinal cord reconstructed in (a) at the lesion epicenter, which was used to trace the contour of the lesions, as illustrated. Scale bar, 500μm. **(c)** Bar graphs reporting the amount of spinal cord displacement during the robotic impact for each experimental rat, the mean area of spared tissue at the lesion epicenter, and the volume of the lesion cavity for the different experimental groups. The linear plot reports the mean area of spared tissue with respect to the distance from the lesion epicenter for the different groups of rats, with the exception of the sub-acute group that had not developed cavities at the evaluated time-point. **(d)** Representation of the lesion contours for all the main experimental rats. Error bars, s.e.m.

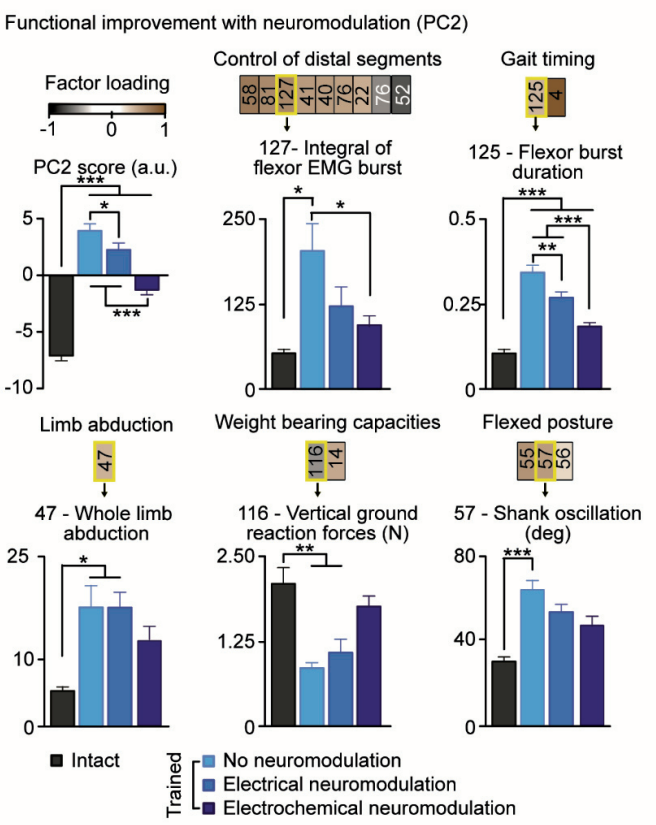

Figure S3.3 | Quantification of functional improvement in early-trained rats with different neuromodulation conditions. Bar graphs reporting mean values of factor loadings on PC2, which captured the differences between neuromodulation conditions. The parameters loading on PC2 were extracted and regrouped into functional clusters that are named for clarity. The numbers refer to individual parameters reported in **Supplementary Table 1**. The bar graphs report mean values for a parameter showing a high correlation with PC2, highlighted with the yellow frames for each functional cluster. *, P < 0.05; **, P < 0.01; ***, P < 0.001. Error bars, s.e.m.

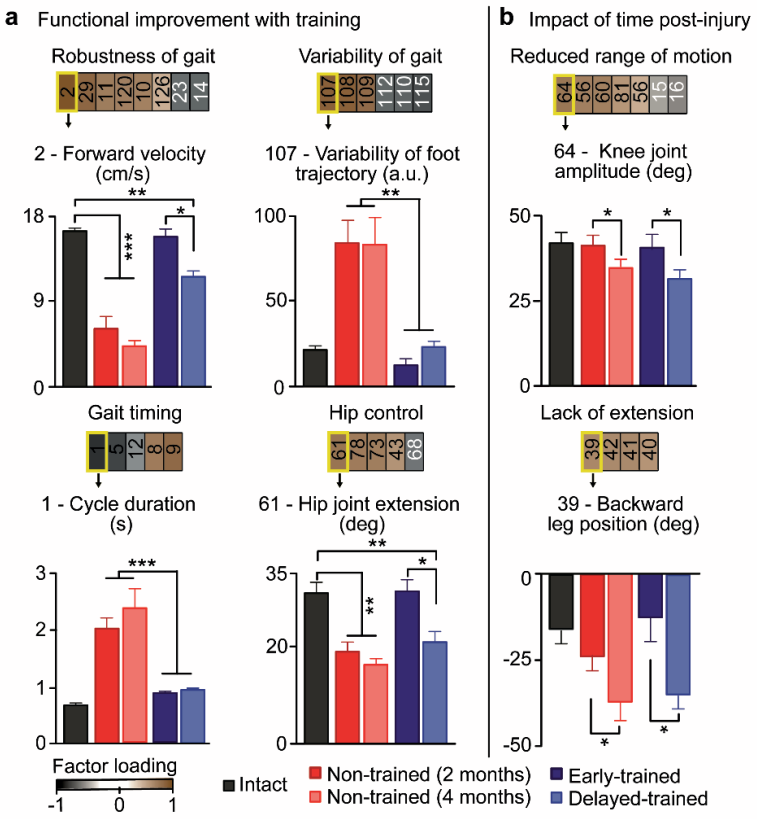

Figure S3.4 | Quantification of hindlimb motor control in early-trained versus delayed-trained rats. (a) Factor loadings were extracted for PC1, which captured the functional improvement with training, and regrouped into functional clusters that are named for clarity. The numbers refer to individual parameters reported in **supplementary Table 1**. The bar graphs report mean values for a parameter showing a high correlation with PC1, highlighted with the yellow frames for each functional cluster. **(b)** The same representations are shown for PC2, which captured the impact of time post-injury on hindlimb motor control features.. *, $P < 0.05$; **, $P < 0.01$; ***, $P < 0.001$. Error bars, s.e.m.

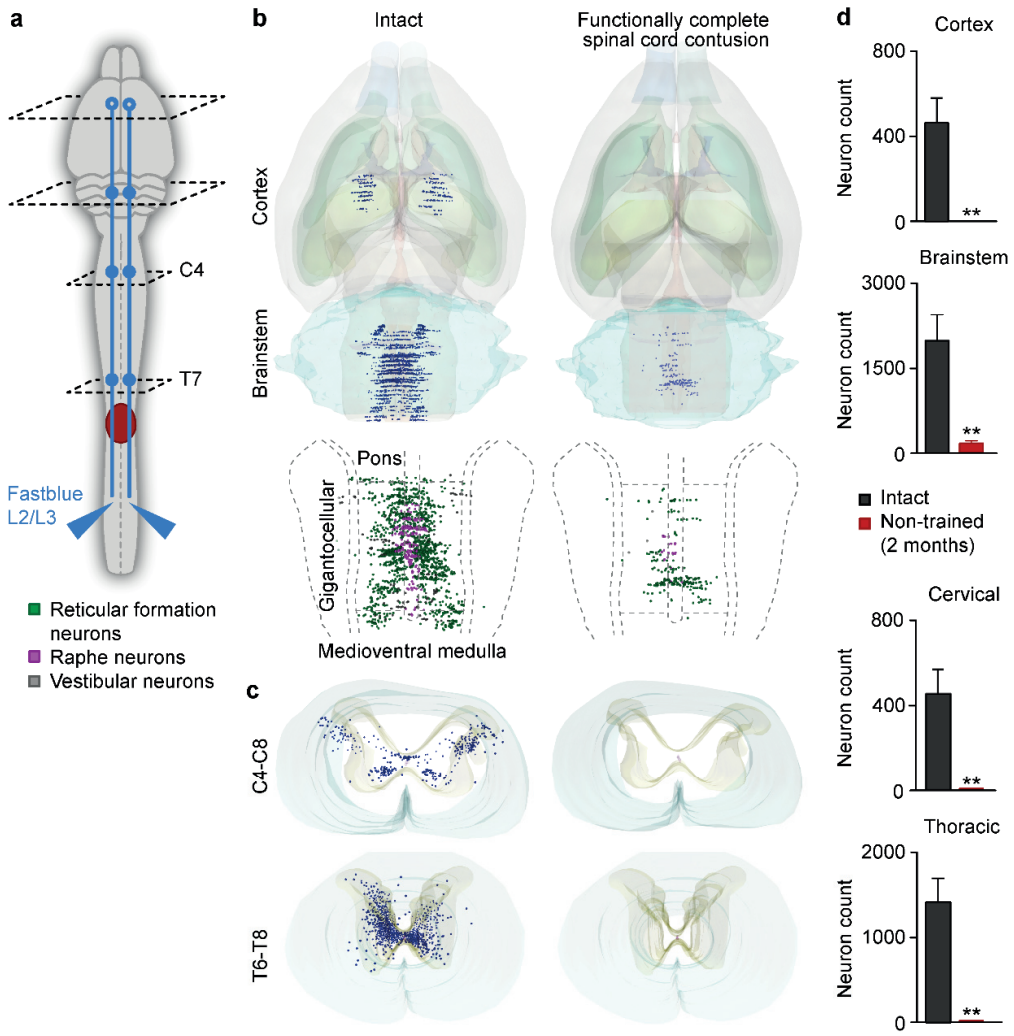

Figure S3.5 | Retrograde tract-tracing from upper lumbar segments identifies projections neurons with residual connection below the injury. (a) Diagram illustrating anatomical experiments. **(b)** 3D reconstruction of retrogradelly labeled neurons in the cortex and brainstem of an intact rat, and a rat traced 2 months after a functionally complete spinal cord contusion. The insets show the reconstruction of retrogradelly labeled neurons in the reticular formation, the raphe, and vestibular nuclei for both rats. **(c)** 3D reconstruction of retrogradelly labeled neurons in cervical (C4-C8) and thoracic (T6-T8) segments. **(d)** Bar graphs reporting the mean number of retrogradelly labeled neurons counted in the cortex and brainstem, as well as in thoracic (T6-T8) and cervical (C4-C8) segments for intact (n = 4) and non-trained injured rats, traced at 2 months post-injury (n = 4). **, P < 0.01. Error bars, s.e.m.

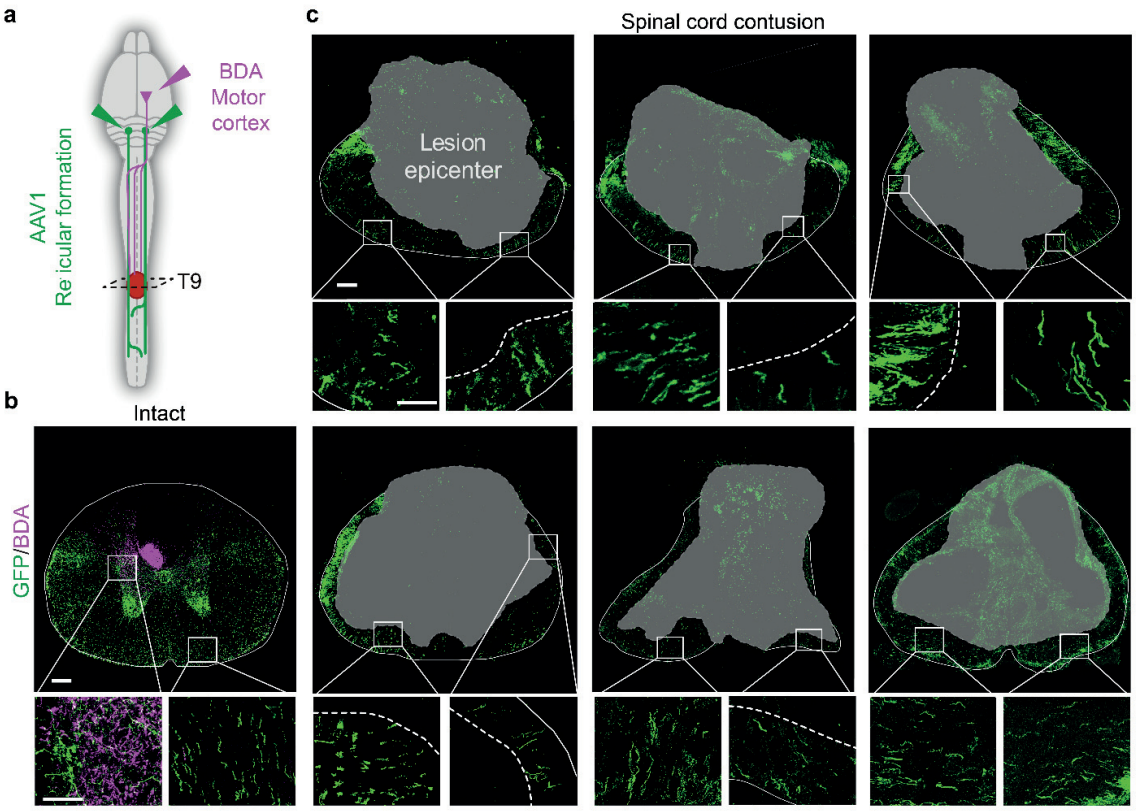

Figure S3.6 | Residual reticulospinal axonal projections in the vicinity of the lesion epicenter. (a) Diagram illustrating anatomical experiment. **(b)** Representative transverse section of thoracic segment T9 showing axonal projections from neurons located in the gigantocellular region of the reticular formation in an intact rat, and in **(c)** various chronically injured rats illustrating the intrinsic variability of contusion injuries. Scale bar, 200 µm for overviews, and 100 µm for insets.

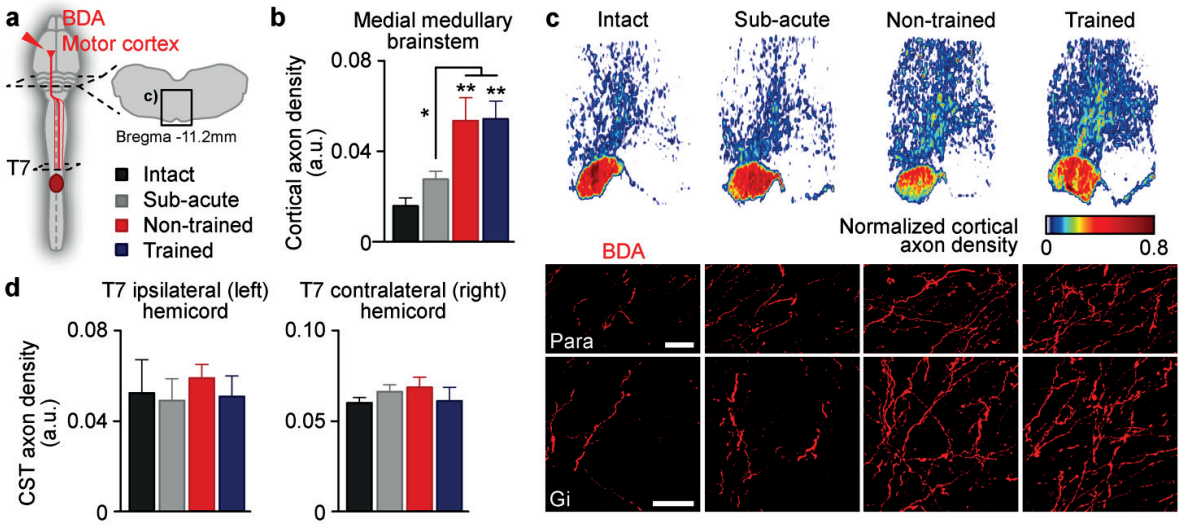

Figure S3.7 | Remodeling of motor cortex axonal projections in the brainstem but not in the spinal cord. (a) Diagram illustrating anatomical experiments. **(b)** Bar graph reporting the mean density of motor cortex axons in the gigantocellular region of the reticular formation. **(c)** Representative heatmaps of motor cortex axonal projections in the gigantocellular region of the reticular formation, together with representative images showing the density of motor cortex axon projections in the parapyramidal (Para) and gigantocellular (Gi) regions of the reticular formation. Scale bar, 25μm. **(d)** Bar graph reporting the mean density of corticospinal tract (CST) axons in the grey matter of T7 spinal segment, both ipsilateral and contralateral to BDA injections.*, $P < 0.05$; **, $P < 0.01$. Error bars, s.e.m.

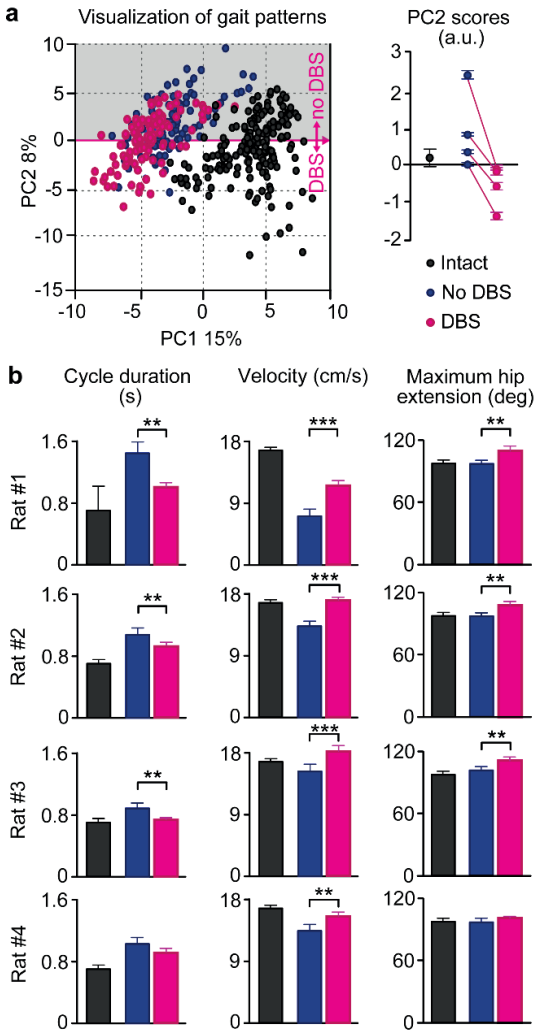

Figure S3.8 | Deep brain stimulation of the mesencephalic locomotor region enhances the robustness of hindlimb movement in trained rats. (a) PC analysis applied on the same set of parameters as in **Figure 1.1**. Each dot corresponds to a gait cycle. For each tested rat (n = 4 for this condition), the plot reports the mean values of scores on PC2, which captured the functional effects of DBS on hindlimb movement patterns of trained rats. **(b)** bar plots reporting, for each tested rat individually, the changes in the mean values of parameters loading on PC2. *, P < 0.05; **, P < 0.01. Error bars, s.e.m.

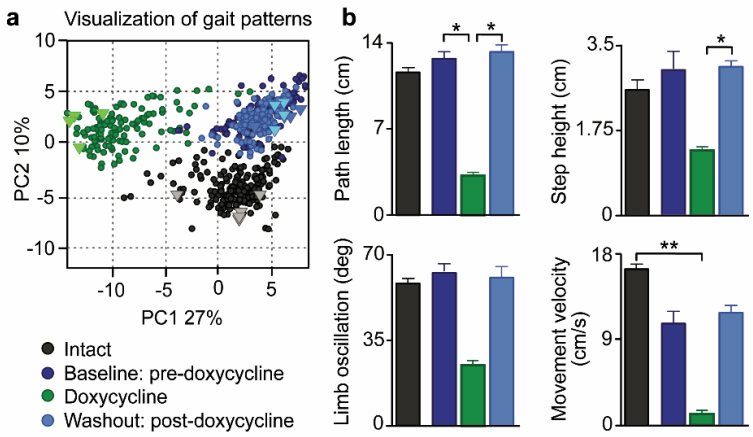

Figure S3.9 | Quantification of hindlimb motor control during inactivation of reticulospinal neurons projecting below the injury in trained rats. (a) PC analysis applied on the same set of parameters as in **Figure 1.1**. Each dot corresponds to a gait cycle, while the triangles represent the mean values for each rat in each condition. **(b)** Bar graphs reporting the mean values of parameters loading on PC1, which captured the impact of the inactivation of reticulospinal neurons on hindlimb motor control. *, P < 0.05; **, P < 0.01. Error bars, s.e.m.

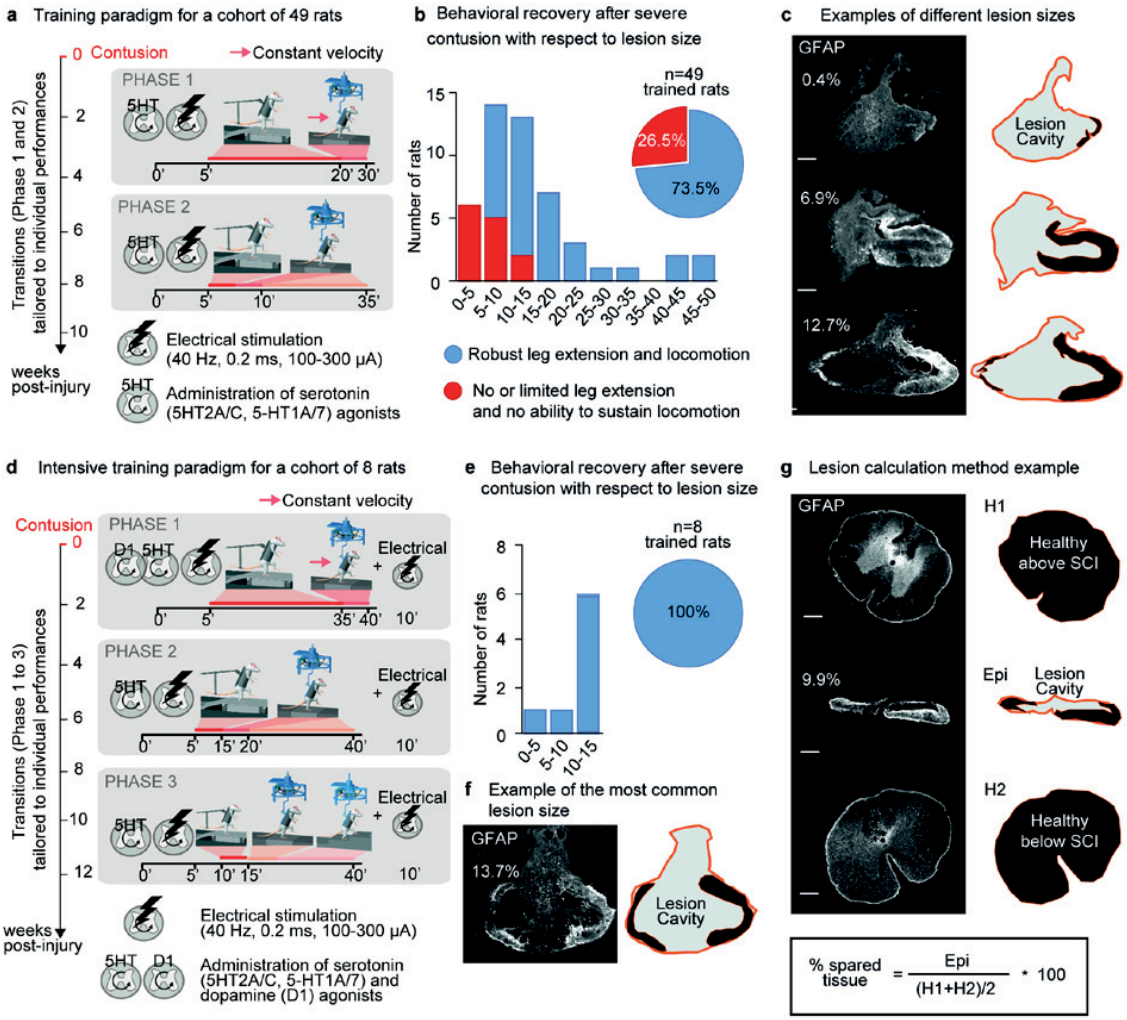

Figure S3.10 | Neuroprosthetic rehabilitation restores hindlimb motor control after functionally complete spinal cord contusion (meta-analysis of 49+8 rats). (a,d) Design of the task-specific training regimen throughout the period of recovery, including the transition from automatic stepping on a treadmill to overground walking with robotic assistance. The variations and time-dependent adaptations of the electrochemical neuromodulation therapy are shown at the bottom. Briefly, the type and concentration of administered chemicals is constantly adjusted to the current motor performance of the rats. The overall aim is to reduce the chemical neuromodulation therapy over time. **(b,e)** Bar graphs reporting the number of rats that recovered robust voluntary stepping scored by a blinded experimenter. **(c,g)** Examples of lesion sizes and computational quantification of spared tissue ridge. **(f)** Representative example of the common lesion size.

4. NEUROPROSTHETIC ENHANCEMENT OF SUPRASPINAL LOCOMOTOR DRIVE ALLEVIATES GAIT DEFICITS AFTER SPINAL CORD INJURY IN RATS

Galyna Pidpruzhnykova [1*], Marco Bonizzato[2*], Natalia Pavlova[1,3], Polina Shkorbatova[1,3], Silvestro Micera[2,4,&] and Gregoire Courtine[1,&]

---

1. Center for Neuroprosthetics and Brain Mind Institute, School of Life Sciences, Swiss Federal Institute of Technology (EPFL), Lausanne, Switzerland
2. Bertarelli Foundation Chair in Translational Neuroengineering, Center for Neuroprosthetics and Institute of Bioengineering, School of Bioengineering, EPFL, Lausanne, Switzerland.
3. Motor Physiology Laboratory, Pavlov Institute of Physiology, St. Petersburg, Russia
4. The BioRobotics Institute, Scuola Superiore Sant'Anna, Pisa, Italy.

* contributed equally to this work

& contributed equally to this work

Corresponding author:
Grégoire Courtine, PhD
Professor, International Paraplegic Foundation Chair in Spinal Cord Repair
Center for Neuroprosthetics and Brain Mind Institute
SWISS FEDERAL INSTITUTE OF TECHNOLOGY (EPFL)
CH-1015 Lausanne
gregoire.courtine@epfl.ch

Manuscript in preparation: “Neuroprosthetic enhancement of supraspinal locomotor drive alleviates gait deficits after spinal cord injury in rats” prepared for submission to Brain in fall 2017

Galyna Pidpruzhnykova*, Marco Bonizzato*, Natalia Pavlova, Polina Shkorbatova, Silvestro Micera[&] and Gregoire Courtine[&]

* this authors contributed equally to this work
[&] this authors contributed equally to this work

My contribution: I was fully responsible for the study: I planned, coordinated, performed all aspects of behavioral experiments, established and performed MLR DBS implantation surgeries, acquired and analyzed behavioral and anatomical data. I prepared and finalized all the figures and wrote the manuscript.

Others contribution: M.B. developed neural decoders, implanted cortical electrodes, contributed equally to all behavioral experiments, data analysis and figure preparation. N.P. and P.S. performed the EES and EMG surgeries. G.C. and S.M. conceived the study, provided supervision and feedback on figures and the manuscript.

Other published works: This study was reported in a PhD thesis of Marco Bonizzato, who is an equally contributing first author.

4.1 Abstract

Deep brain stimulation of the mesencephalic locomotor region (MLR) improves locomotion in rats with severe cut spinal cord injury (SCI), but its impact on locomotion after clinically relevant contusion SCI and on the stress level of the animals remains unknown. Here, we investigated the effect of MLR DBS during different behavioral tasks in rats which had undergone four weeks of neuroprosthetic rehabilitation. We found that although forced MLR DBS leads to an increased locomotor output in rehabilitated rats, it dramatically elevates stress levels of the animals during the voluntary walking task. To address this issue, we developed a brain-controlled MLR DBS interface, whereby the MLR DBS was delivered only during elevated primary motor cortex (M1) states. Our newly developed M1-to-MLR interface reflected the temporal activation pattern of M1 and MLR during natural walking initiation before and after SCI. In line with our hypothesis, we found that the M1-to-MLR interface combined with neuromodulation strategies improved rats' locomotion after SCI, while preserving natural locomotion dynamics and reducing stress levels as compared to externally triggered MLR DBS. However, it is important to note that this superior locomotor performance could only be obtained by applying suprathreshold MLR DBS. Moreover, both forced and M1-triggered MLR DBS were more stressful for the animals then the no DBS condition. Overall, these results demonstrate that brain-controlled delivery of neuromodulation can be effective in alleviating adverse DBS effects and raise important questions for its potential translation.

Keywords: spinal cord injury; neuroprosthetic rehabilitation; brain-controlled interface; deep brain stimulation; kinematic analysis

Abbreviations: SCI = spinal cord injury, DBS = deep brain stimulation, MLR = Mesencephalic locomotor region, M1 = hindlimb motor cortex

4.2 Introduction

Spinal cord injury (SCI) is a devastating disorder that, depending on the injury site and severity, leads to various forms of paralysis and dramatically decreases patients' quality of life (Sekhon and Fehlings, 2001; Simpson *et al.*, 2012; Silva *et al.*, 2014). Among other consequences, SCI disrupts voluntary command coming from the brain to the spinal locomotor centers (Kokotilo *et al.*, 2009; Krassioukov *et al.*, 2012) and can lead to permanent paralysis. Although the spinal cord undergoes substantial reorganization after SCI (Calancie *et al.*, 1996; Bareyre *et al.*, 2004a), some of the plastic changes lead to detrimental consequences, particularly in the absence of physiotherapy rehabilitation (Beauparlant *et al.*, 2013) or sensory feedback (Takeoka *et al.*, 2014b). These destructive changes continue for many years after injury (Bramlett and Dietrich, 2007; Dietz *et al.*, 2009) and complicate the rehabilitation of patients with chronic SCI (Houle and Tessler, 2003).

Various attempts have been made to develop neuroprosthetic interventions and to facilitate recovery after SCI (Thuret *et al.*, 2006; Field-Fote, 2009), including: i. promoting fiber growth across the injury site (Toft *et al.*, 2007; Cregg *et al.*, 2014; Tsintou *et al.*, 2015; Anderson *et al.*, 2016); ii. using non-invasive and invasive spinal cord stimulations (Ragnarsson, 2007; Hamid and Hayek, 2008); iii. combinations of treatments (Courtine *et al.*, 2009; Fong *et al.*, 2009; Musienko *et al.*, 2009) and iv. substitution therapies, like exoskeleton (del-Ama *et al.*, 2012). Deep brain stimulation, on the contrary, has rarely been applied for paralysis treatment post-SCI, despite its widespread use for treatment of other neuromotor disorders, like Parkinson's disease (Benabid *et al.*, 2009; Hamani *et al.*, 2016). One promising piece of evidence suggesting that DBS may be effective for SCI treatment comes from a recent animal study, where DBS of the mesencephalic locomotor region (MLR) improved quadrupedal stepping of rats with severe SCI (Bachmann *et al.*, 2013). The MLR indeed seems to be a promising DBS stimulation target because of its approved use in patients with Parkinson's disease and a function of supraspinal locomotor center playing an important role for locomotion initiation (Ryczko and Dubuc, 2013; Mazzone *et al.*, 2016). The MLR provides excitatory input to the spinal cord and drives controlled locomotion in spinal animals (Shik *et al.*, 1969; Mazzone *et al.*, 2011; Ryczko and Dubuc, 2013); however, the mechanisms of MLR action post-SCI and its interplay with the volitional command coming from hindlimb motor cortex (M1) after SCI remain unknown. Therefore, the clinical translation of this treatment approach into SCI patients at this stage seems to be unjustified because it is lacking preclinical evidence of longterm effectiveness of MLR DBS for SCI treatment and approaches to minimize potential side effects (L.H. Stieglitz, A Curt, 2017).

Brain machine interfaces (BMI) were already successfully used to improve behavioral parameters in Parkinson's disease (Little *et al.*, 2013), are able to induce plastic changes (Nishimura, Perlmutter, Eaton, *et al.*, 2013) for restoring upper limb function in paretic monkeys and alleviate gait deficits after SCI in non-human primates (Capogrosso *et al.*, 2016). Yet the degree to which MLR DBS can improve locomotion and its effect on the behavioral state of the animal is poorly understood. Therefore, investigating MLR DBS mechanisms of action and its potential use in a BMI-controlled manner could provide a basis for novel rehabilitation paradigms after SCI and potentially improve patients' lives in the future (Courtine and Bloch, 2015).

With this in mind, we first studied the natural interplay of M1-MLR activity in healthy and post-SCI rats. We then hypothesized that by applying this pattern for delivering a brain-controlled MLR DBS, we could enable improved locomotion with more comfort for the animals suffering from severe contusion injury. Indeed, we achieved improved locomotion in rats five weeks after severe SCI and managed to alleviate the stressful consequences of forced MLR DBS by applying it in a BMI-driven manner through an open loop brain-controlled MLR DBS. As a result, we report the most ecological way of MLR DBS delivery developed up to date and discuss its implications, advantages and caveats for developing this system further for human patients.

.

4.3 Materials and methods

Experimental setup

Experiments were conducted on adult female Lewis rats (200-220g body weight). The rats were housed individually in transparent cages with access to food and water *ad libitum*. The room was kept on a 12h light/dark cycle at 22 degrees Celsius ambient temperature. Prior to surgery, all the rats were handled and trained to freely walk along the runway. Animal care, including manual bladder voiding, was performed twice per day throughout the whole post-injury period. All experimental procedures were approved by the Veterinary Office of the Canton Vaud, Switzerland.

Surgical procedures and post-surgical care

All surgical procedures and post-operative care for SCI rats have been previously described in detail (Courtine *et al.*, 2009; Scheff and Roberts, 2009; Dominici *et al.*, 2012). Overall, the animals underwent two surgeries: electrode implantation followed by contusion spinal cord injury one week later. During the first surgery, in aseptic conditions and under general anesthesia, each rat was implanted with a 32-channel microelectrode array (Tucker-Davis-Technologies, USA) into layer V of the hindlimb area of the right motor cortex (van den Brand *et al.*, 2012). Additionally, during the same surgery, we implanted a 16-channel single-shank multielectrode array (CM16LP, NeuroNexus, USA) in the left MLR (contralateral to the implanted motor cortex). We used coordinates (Paxinos and Watson, 2004) that spanned the PreCuN, CuN, and PPN nuclei, which were -7.8 to -8.2 mm from Bregma: anterior-posterior (AP), 2 mm from the midline: medio-lateral (ML) and at a depth of -5.6 to -7.5 mm: dorso-ventral (DV). Ground and reference wires from both arrays were attached to screws fixated to the skull. Bipolar intramuscular electrodes were inserted in the contralateral medial gastrocnemius (MG, ankle extensor) and tibialis anterior (TA, ankle flexor) muscles to record electromyographic (EMG) activity (Courtine *et al.*, 2009). Two stimulating wire electrodes were sutured to the dura at the lumbar (L2) and sacral (S1) spinal levels (Courtine *et al.*, 2009). A common ground wire (~1 cm of Teflon removed at the distal end) was inserted subcutaneously over the right shoulder. After a week of recovery from the first surgery, all rats received a 250 kdyn (1 dyn = 10 μN) contusion spinal cord injury at T9/T10 spinal level induced with a force-controlled impactor (IH-0400 Impactor, Precision Systems and Instrumentation LLC, USA) (Scheff and Roberts, 2009). Analgesia (buprenorphine Temgesic®, ESSEX Chemie AG,

Switzerland, 0.01-0.05 mg per kg, s.c.) and antibiotics (Baytril® 2,5%, Bayer Health Care AG, Germany, 5-10 mg per kg, s.c.) were provided for 3 and 5 days post-surgery, respectively.

Locomotor training

Rats were divided in two groups (n=3 per group) and trained 5 days per week for 30 minutes per day starting from day 7 post-injury. Five minutes prior to each training session, the rats received an intraperitoneal injection of quipazine (5-HT2A/C, 0.2 - 0.3 mg/kg) and 8-OH-DPAT (5-HT1A/7, 0.05 - 0.2 mg/kg) adjusted daily based on locomotor output (van den Brand *et al.*, 2012). Locomotor training was performed by first positioning the rat bipedally on a treadmill moving at 11 cm/s with partial vertical support (Robomedica, USA), and later transferring the rat for training overground on a linear runway with a postural robotic interface (Dominici *et al.*, 2012). The duration of the training started from 25 min on the treadmill and 5 min overground and was gradually adjusted to 5 min on treadmill and 25 min overground, depending on the animal's performance. During all training sessions, monopolar stimulation pulses were delivered tonically at L2 and S1 electrodes (40 Hz, 50-350 µA, 0.2 ms) (Courtine *et al.*, 2009).

Kinematic and EMG recordings and analysis

Locomotor performance was evaluated during walking on the treadmill (11 cm/s) and along a straight runway. Optimal body weight support was provided and maintained constant during all recorded conditions: electrochemical neuromodulaction, forced MLR stimulation and brain-controlled MLR stimulation. Kinematic (12 infrared and 2 digital video cameras, 200 Hz) and EMG recordings (2 kHz, 10–1000 Hz bandpass filtered) were performed using an integrated motion capture system (Vicon, UK). Procedures for kinematic data collection and analysis have been described previously in detail (Musienko *et al.*, 2011). To quantify locomotor performance, we isolated single gait cycles, extracted relevant kinematics parameters and applied a principal component (PC) analysis (Courtine *et al.*, 2009; Musienko *et al.*, 2011) on 63 computed variables, whose list is available in Supplementary Table S4.1.

MLR-DBS evaluation and characterization

Following a 6-day recovery period after the electrode implantation, we tested behavioral responses to MLR stimulation (40 Hz train of 200 μs long biphasic pulses, with an amplitude of 50-250 μA). Only the animals who had a typical short-latency locomotion initiation response were used for the study because their implantation was considered successful according to the functional definition of MLR (**Supplementary Figure S4.1**). We report the following implant success rates:

- Pilot animals, 6/12 functional with custom built 2-channel electrodes;
- Pilot animals, 5/5 functional with commercial 16;
- This study, 7/7 functional (16-channel).

Five weeks after spinal cord injury, rats were positioned bipedally on a treadmill, and spinal locomotion was elicited with pharmacological and electrical epidural stimulation, with MLR-DBS initially switched off. The maximum intensity of MLR stimulation without eliciting pain-related behavioral effects (orbital tightening, squeaking) for each animal was detected by progressively incrementing the stimulation pulses amplitude (Max MLR-DBS). Medium and Low MLR-DBS stimulation parameters were defined as 66% and 33% of the maximum amplitude.

MLR recordings

Extracellular voltage signals were pre-amplified, digitalized, sampled at 24 kHz and stored using a BioAmp processor (Tucker-Davis Technologies, USA). The channel average was subtracted offline from each trace to remove common mode noise. MLR multi-unit activity (MUA) consisted of all field potential stochastic events that crossed the threshold value of three standard deviations of the potential signal. For all offline analyses, spike counts were binned using windows of 10ms. To compute the MLR encoding of locomotor speed, both traces were low pass filtered with a 200ms moving average.

Cortex-MLR interface

Intracortical voltage signals were pre-amplified, digitalized and sampled at 24kHz, then bandpass filtered online (0.7-3 kHz), all by means of a real-time BioAmp processor (Tucker-Davis

Technologies, USA). Cortical multi-unit activity (MUA) consisted of all field potential stochastic events that crossed a threshold value. Spike count was collected in bins of 10ms and crossed a Finite Impulse Response (FIR) filter with Gaussian sample decay of 80% in 40ms. A single trial of overground walking between the two extremes of the runway (quadrupedal or bipedal, robot-assisted gravity support) featured an approximately even balance of idle standing time and walking time (usually 5 to 10s of data for quadrupedal walking and 10 to 40s for bipedal). A Self-Organizing Map (SOM) with four output nodes (Matlab function selforgmap([4 1])) was used to segregate the cortical activity recorded during the calibration trial in four ordered clusters, based on the statistical properties of the cortical signal. A cluster value of one was assigned to the state featuring the highest mean spike count across the cortical population, the second was assigned 2/3, the third 1/3, while the last was assigned the value of 0.

A time vector **Y** was created (**Y: 1xt**), where each sample holds the value of the observed cluster. The **Y** vector is then smoothed with a moving window of 500ms length. A linear combination **y=wn** of the MUA of all 32 channels was used as a normalized control variable in online testing (**y**: 1x1 current control variable value, **w**: 1x32 weights, **n**: 32x1 current MUA sample). The weight vector w was computed from data acquired during the calibration trial as the least square solution of **wn=Y**. Thus, **w=Y(n)†**, where (**†**) represents the Moore-Penrose pseudoinverse.

During online testing, whenever **y=wn** crossed a fixed detection threshold in the range 0.7-0.8, the real-time processor would instantly deliver MLR-DBS. Conversely, when y crossed a threshold positioned at a fixed value in the range 0.2-0.3, stimulation was turned off (**Supplementary Figure S4.3**). MLR-DBS parameters were set at the maximal non-painful level identified during treadmill characterization experiments. The acquisition of data presented to the unsupervised learning algorithm and its processing typically required 5min at the beginning of an experimental session. The hard-real-time program was run with cycles of 12kHz.

Cortical raster plots

Spike occurrence time diagrams were obtained by offline analysis. Intracortical voltage data were bandpass filtered (700-3000 Hz) and z-scored. Each event crossing the threshold at -3 standard deviations was added to the neuronal spike count (multi-unit activity).

Immunohistochemistry and neuromorphological evaluation

The rats were deeply anesthetized by an i.p. injection of 0.5 ml Pentobarbital-Na (50 mg/mL) and transcardially perfused with approximately 80 ml Ringer's solution containing 100 kIU/L heparin (Liquemin, Roche, Switzerland) and 0.25% $NaNO_2$ followed by 300 ml of cold 4% phosphate buffered paraformaldehyde, pH 7.4 containing 5% sucrose. The brain and spinal cord were removed and postfixed in the same fixative overnight and later transferred to 30% sucrose in phosphate buffer (PB) for cryoprotection. After 3 days, the tissue was embedded in Tissue Tek O.C.T (Sakura Finetek Europe B.V., The Netherlands), frozen at -40°C, and cut to a thickness of 40 μm. For immunohistochemistry experiments, sections used for GFAP and Nissl staining were directly mounted, washed 3 times in 0.1M PBS and blocked in 10% (GFAP) normal goat serum containing 1% Triton. Sections were then incubated in primary antibody diluted in the blocking solution overnight at 4°C (GFAP). The primary antibody used was rabbit anti-GFAP (1:1000, Dako, USA). Sections were again washed 3 times in 0.1M PBS and incubated with the appropriate secondary antibody (Alexa fluor® 488) in blocking solution. NeuroTraceTM (Life Technologies, USA) was used as a Nissl counterstain at a dilution of 1:50 in 0.1M PBS. Slides were finally washed, air-dried and coverslipped with Mowiol. We used ChAT staining for visualizing post-hoc MLR location through proximity to cholinergic neurons. First, the hindbrains were sliced into series of 40μm-thick slices. The tissue samples were then blocked on a shaker for 60 minutes in PBS 10% NDS and 0.3% Triton X100. Subsequently, the goat anti-ChAT primary antibody (1:100 in PBS 0.1M with 5% NDS and 0.3% Triton X100) was added overnight at 4°C on the shaker. Finally, the donkey anti-goat secondary antibody (Alexa fluor® 647, Life Technology A2 1432) was added at a dilution of 1:300 in 0.1M PBS with 3% NDS and 0.3% Triton X100 for 90 minutes at room temperature on the shaker. Lastly, slides were washed, air-dried and coverslipped with Mowiol.

Evaluation of spinal cord contusion

The extent and location of spinal cord damage was evaluated in each experimental rat. The lesion cavity was cut in serial coronal sections (40 μm) that were stained using GFAP and Nissl staining. Spared tissue was measured using three fluorescent image stacks per rat, from the lesion epicenter going to the first rostral and caudal intact sections, acquired with Olympus Slide Scanner VS120-L100 microscope at 10x magnification and analyzed offline using custom-written Matlab scripts. Slide scanner output images were divided into square regions of interest (ROI). Files were

color-filtered and binarized by means of intensity thresholds, set empirically and maintained across sections. Finally, the amount of tissue spared by the SCI was computed as the ratio of traced fibers (amount of pixels) at the epicenter and the average traced fiber count at the intact sections.

Stressfulness of intervention assessment

For each trial, a picture of the experimental animal was taken at the exact moment it touched a horizontal bar, which was positioned at the end of the runway to indicate the end of the task. The level of stress experienced by the experimental animal was then evaluated using an adapted version of the Rat Grimace Scale (RGS) (Sotocinal et al., 2011), modified to fit experimental protocol and recording setup and include posture in exchange of the "whisker change" parameter. This component was indeed less identifiable from the lateral angle, where the picture was taken. The pictures were then shuffled, blinded and presented to two independent evaluators. Each of the parameters: orbital tightening, nose/cheek flattening, whisker deflection and posture were scored on the scale from 0 to 2, with 0 being normal and 2 signifying the most abnormal state, respectively. Observers' scores were later analyzed and reported in percentage values and averaged across all rats (n=6).

Statistics

Average cortical ensemble firing rates are reported as mean values ± SEM to display the distribution of the mean of the neural variable. All other data are displayed as mean values ± SD. Paired statistical evaluations were performed using Student's t-test or the non-parametric Wilcoxon signed-rank test when at least one of the populations could not be assumed to be normally distributed (after applying the one-sample Kolmogorov-Smirnov test). The Kruskall-Wallis test was applied to all non-paired populations of samples.

4.4 Results

M1 activation precedes locomotor initiation in healthy rats, followed by MLR activation

We first recorded M1 and MLR activity during quadrupedal locomotion in healthy rats (**Figure 4.1A**). The M1 implants (n=8) targeted layer V of hindlimb motor cortex (AP_{ant} = 0.32±0.37; AP_{post}=-2.11±0.46; DV= 1.75±0.36; ML_{centr}= 1.32±0.78; ML_{lat}= 2.7±0.36) and MLR electrodes (n=6) were implanted in the PreCun, CuN and PPN nuclei, according to its anatomical definition, which corresponded to AP=-8.26±0.26, DV=-6.42±0.62, ML=2.07±0.07. The 3D electrode reconstructions revealed that all M1 and MLR electrodes were within the region of interest (**Figure 4.1B**). Additionally to anatomical definition, we determined correct MLR electrode placement functionally by delivering electrical stimulation through one of 16 channels (40 Hz, 200 µs, of 50-250 µA) and observing short-latency 5.78±3.8 s locomotor responses (**Figure 4.4F**). Only the rats with characteristic responses (n=8) were further tested.

We found that both M1 and MLR neuronal populations exhibit an increased firing rate during voluntary quadrupedal locomotion (**Figure 4.1C-E**). We considered the region "activated" at the moment when the ensemble firing rate crossed a threshold of 2 standard deviations above the baseline. As expected, M1 activity consistently preceded locomotor onset by 147±63ms (n=7). Interestingly, despite the ability of MLR to induce involuntary locomotor response, in the voluntary condition it only became activated with a 101±44ms delay after the first hindpaw off movement (**Figure 4.1D**). Overall, the delay between M1 and MLR activations was 250ms (p=0.0005) (**Figure 4.1D**). Moreover, we found that the MLR firing rate was directly proportional to the speed of locomotion in all animals (n=7) with a correlation coefficient of $R^2 > 0.2$ in 53% of the channels **(Fig 4.1F)**, which provides evidence that this region is important for locomotion in healthy rats.

These results show that M1 anticipates locomotion onset and MLR follows, providing supraspinal input modulated by the speed of locomotion in healthy rats.

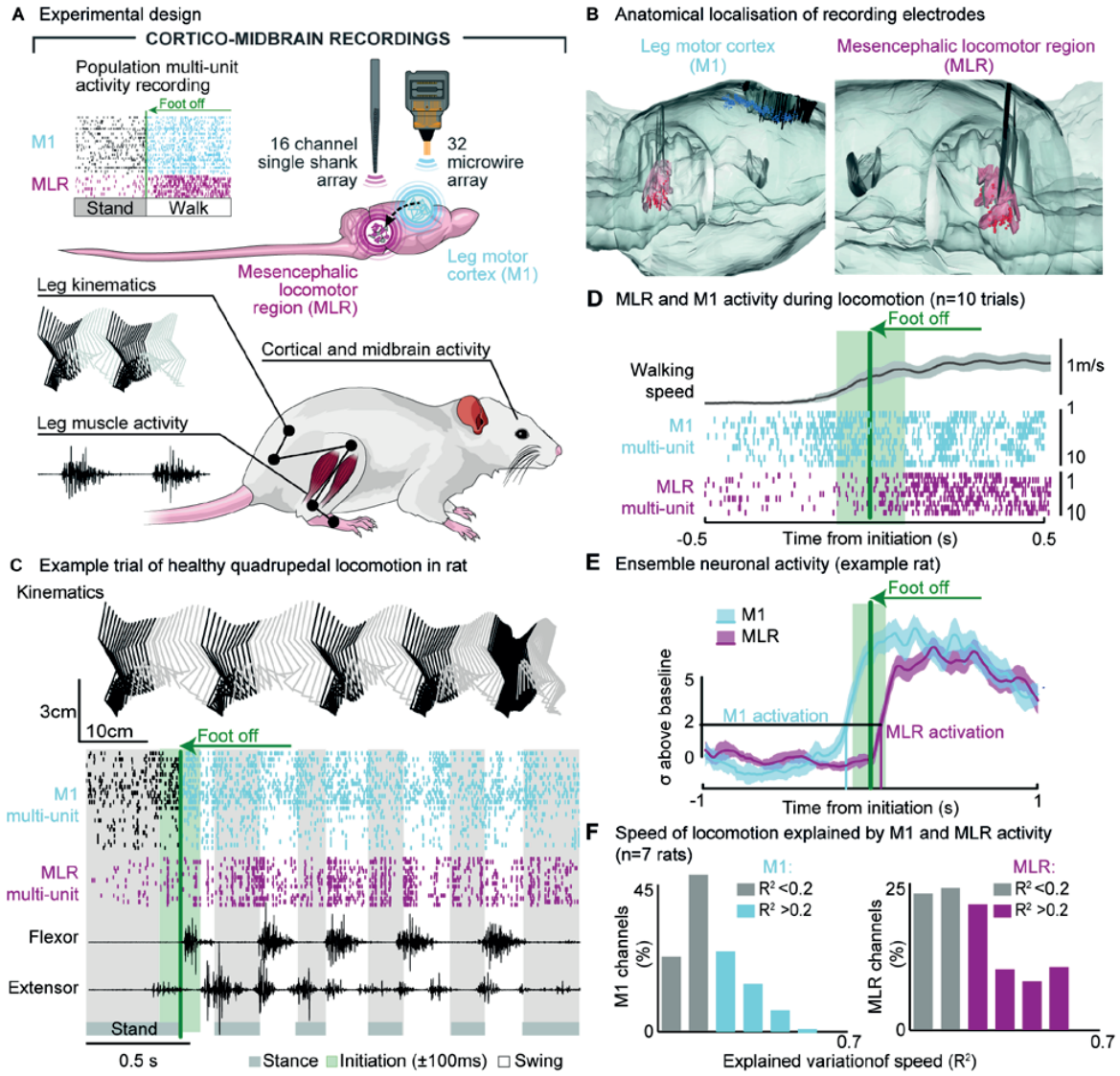

Figure 4.1 | Natural activation of leg motor cortex (M1) precedes locomotion initiation and mesencephalic locomotor region (MLR) activation follows during quadrupedal walk. **(A)** Experimental setup depicting neuronal recordings from the M1 (32 channels) and MLR (16 channels) regions. Leg kinematics and muscle activity were recorded simultaneously with brain activity. **(B)** Combined 3D visualization of M1 and MLR electrode locations in all experimental animals. **(C)** Stick diagram decomposition of left hindlimb movement together with electromyographic activity of leg muscles and multi-unit activity in M1 and MLR regions. **(D)** Example of one MLR channel whose activity was modulated with walking speed across 10 trials in a healthy rat. **(E)** Normalized ensemble M1 and MLR multiunit activity synchronized to locomotor initiation in a healthy rat. **(F)** Speed encoding by MLR and M1 neuronal activity across all rats (n=7).

M1-MLR activation timing remains the same after contusion SCI

After we performed recordings in healthy animals, all the animals underwent a severe contusion injury at thoracic segment T9/T10 with a force impactor set to 250 kdyn.

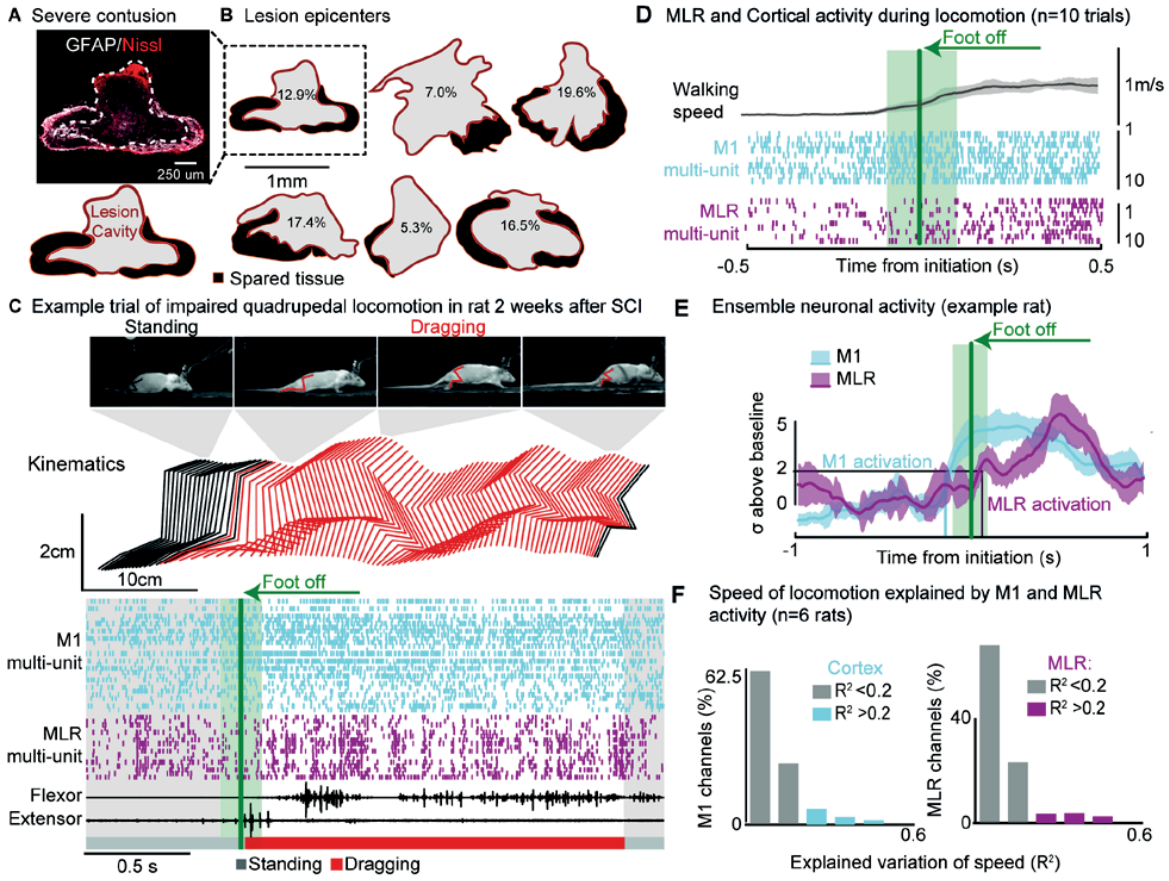

Figure 4.2 | Spinal cord injury disrupts both M1 and MLR activity during quadrupedal locomotion two weeks after severe contusion SCI. (A) Representative section through the injury epicenter, including a graphical visualisation of the lesion cavity. Scale bar, 250µm. **(B)** Representation of the lesion contours for all the main experimental rats. **(C)** Photographical representation of quadrupedal walking after SCI together with the stick diagram decomposition of left hindlimb movement, electromyographic activity of leg muscles and multi-unit activity in M1 and MLR regions. **(D)** Example of one MLR channel whose activity was modulated with walking speed across 10 trials after SCI in the same rat as in **Figure 4.1.D**. **(E)** Normalized ensemble M1 and MLR multiunit activity synchronized to locomotor initiation after SCI in the same rat as in **Figure 4.1.E**. **(F)** Disruption of speed encoding by MLR and M1 neuronal activity after SCI across all rats (n=6).

The injury led to a complete lesion of spinal cord grey matter with a spared ridge of white matter tissue of on average 13.1±5.3 % of healthy cross-sectional tissue, as analyzed by a custom-written matlab software (**Figure 4.2A-B**).

This clinically relevant contusion injury model exhibited similar patterns of spinal cord damage to humans by forming a lesion of a highly variable size. Two weeks after injury, when the formation of the contusion cavity stabilized, we performed quadrupedal behavioral recordings while electrophysiologically recording M1 and MLR activity (**Figure 4.2C**), using the same settings as in healthy rats. At this time point, the animals were completely paraplegic, which meant that the rats were continuously dragging their hindpaws and we observed no plantar stepping in the quadrupedal condition. However, even in the absence of avert hindlimb movements, both M1 and MLR displayed increased firing rate during locomotion (**Figure 4.2C-E**).

We found that the brain signals of both M1 and MLR were severely disrupted by the injury with a significant increase in variability of neural trajectory (**Figure 4.3E**). Further analysis of M1 and MLR activity showed that, surprisingly, the timing of activation between these two regions remained unchanged (**Figure 4.3A**). In the same quadrupedal task, M1 became activated 172±74ms before the first displacement of the foot from the resting position with subsequent activation of MLR 59±43ms after movement onset. The M1-MLR activation delay (n=6, p=0.0011) ranges within the same timings as in the healthy case (**Figure 4.3A**). The relationship between MLR activation and speed deteriorated after SCI with no significant correlation between MLR and locomotor activity found after lesion (**Figure 4.2F**).

These neuronal recordings reveal that SCI leads to drastic decrease in M1 and MLR activity, and disrupts the MLR-speed relationship, while, surprisingly, preserving the M1-MLR temporal pattern of activation.

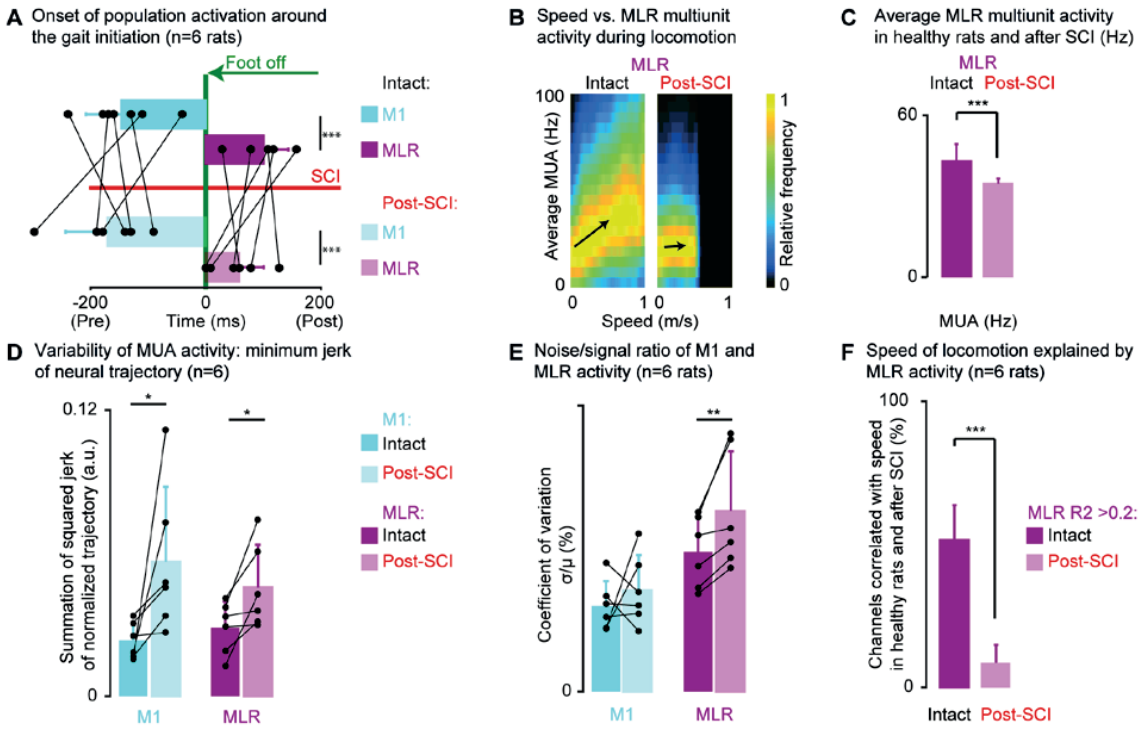

Figure 4.3 | Temporal relationship between M1 and MLR during quadrupedal locomotion remains the same despite neuronal trajectories being severely disrupted. (A) Quantification of onset of cortical activity before and MLR activity after locomotion initiation. **(B)** Correlation between the speed of locomotion and multi-unit activity in M1 and MLR before and after SCI. **(C)** Decrease in the average multi-unit activity of MLR region after SCI. **(D)** The variability of MUA neural trajectory increases in terms of minimum jerk after SCI. **(E)** Cortex retains comparable signal modulation in the idle to walk transition, while locomotor state-dependent information in the MLR decreases after SCI. **(F)** The number of MLR channels correlated with speed of locomotion decreases after SCI. *, $P < 0.05$; **, $P < 0.01$; ***, $P < 0.001$. Error bars, s.d., s.e.m. in F.

Deep brain stimulation of MLR enhances locomotion during treadmill stepping

We trained n=5 rats using a neurorehabilitation paradigm developed in our laboratory (van den Brand *et al.*, 2012), during which the animals received 30 min rehabilitation training 5 days a week with tonic epidural electrical stimulation at segments L2 and S1 and serotoninergic replacement therapy. After the initial training, we recorded the effect of varying MLR DBS on involuntary treadmill stepping (40 Hz, 200 µs, 50-250 µA).

Our hypothesis was that applying MLR DBS after contusion SCI would lead to enhanced locomotor output, which was in line with the existing literature (Bachmann *et al.*, 2013). We observed that delivery of MLR-DBS indeed increased the kinematic output 5 weeks after injury (**Figure 4.4B**), but not at an early stage (**Supplementary Figure S4.2**). Moreover, incremental increase of MLR DBS intensity led to a proportional increase in characteristic locomotor parameters (**Figure 4.4D**). Principal component analysis (PCA) over 63 parameters representing each single gait cycle revealed that forced MLR DBS indeed induced progressive modulation of locomotor output towards a more powerful kinematic state as DBS amplitude was increased (**Figure 4.4C**). In particular, step height and hip excursion displayed a significant progressive increment with larger amplitudes. This modulation seems better represented in distal segments (**Figure 4.4D**). Additionally, we determined the maximum intensity of MLR stimulation which would not cause adverse effects but could disrupt the movement of the animals. We determined suitable parameters by progressively incrementing the stimulation pulse amplitude (Max MLR-DBS) in the treadmill condition, which we then carried over to the runway stimulation. We defined Medium and Low MLR-DBS stimulation parameters for treadmill stimulation as 66% and 33% of the maximum amplitude, respectively (**Figure 4.4D**).

These results show that MLR can be used as a subcortical control center for providing a supraspinal locomotor signal to sublesional spinal cord, which induces modulation of treadmill stepping proportional to the injected charge. Additionally, we also used this modulation to determine optimal stimulation parameters, which will be further translated into the voluntary walking condition.

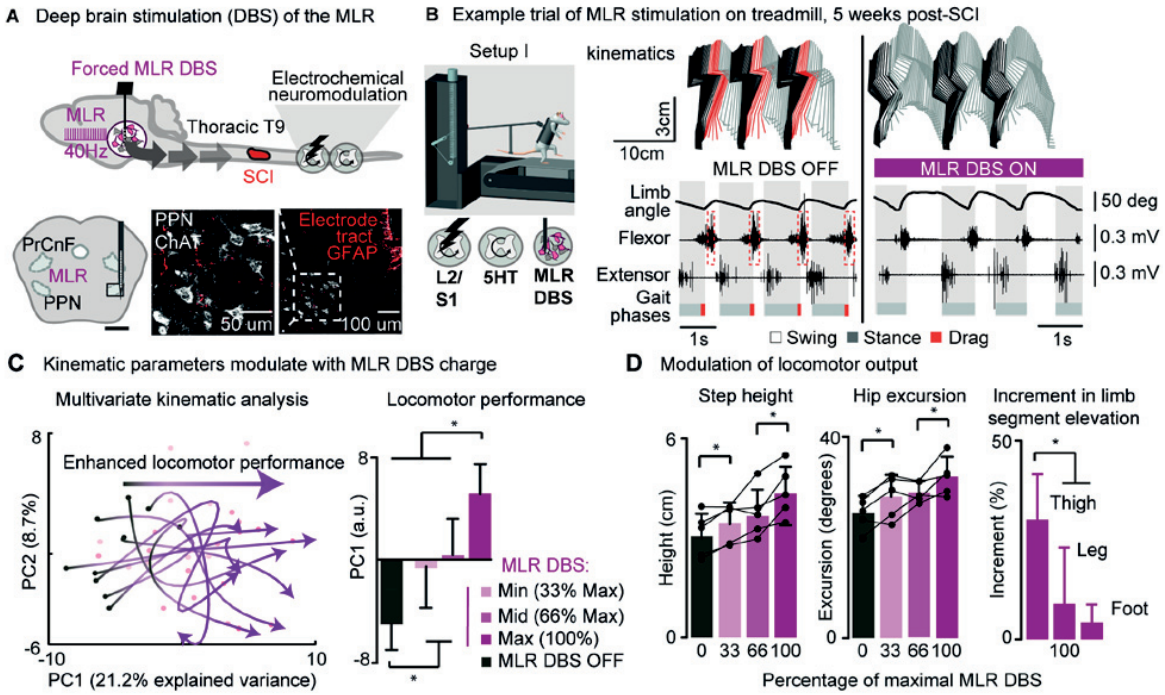

Figure 4.4 | Forced deep brain stimulation of the MLR triggers immediate increase in locomotor performance during passive treadmill walking task in trained rats. **(A)** Upper panel: experimental setup and illustration of MLR DBS delivery. Lower panel: location of cholinergic (ChAT) neurons in the pedunculopontine nucleus (PPN) in the vicinity of the DBS electrode implantation site. Scale bar; 100 µm and 50 µm for inset. **(B)** Setup I: evaluation of MLR DBS effect on kinematic output during treadmill stepping task. Stick diagram of locomotor output combined with endpoint trajectory and electromyographic recordings in two conditions (MLR DBS OFF and ON) **(C)** Principal component (PC) analysis applied on 63 parameters measured over the average step cycle across n=5 animals, 2 hindlimbs per animal and 4 experimental conditions. Hindlimb movement patterns are displayed in the new reference frame created by PC1-2. The lines interpolate dots representing the same animal in four conditions with different DBS intensity levels. The bar graphs report the scores on PC1 across conditions, which captured the enhancement of locomotor output with increasing MLR DBS intensity. **(D)** Increase in step height (left) and hip excursion (center) across all animals. Proximal hindlimb segments display the strongest increase in the extent of elevation (right). *, P < 0.05; **, P < 0.01; ***, P < 0.001. Error bars, s.d.

Forced MLR DBS alleviates locomotor deficits and increases stress in rats during voluntary walk

After determining the most favorable stimulation parameters, we proceeded to test the effects of MLR-DBS during a voluntary locomotor task on the runway. The rats were positioned in a robotic system (Dominici *et al.*, 2012) providing the necessary body weight support in a vertical direction and no horizontal force. The rats had to voluntarily step forward to reach the end of the runway and obtain a resting reward. After five weeks of rehabilitative training, all the animals were able to perform the task successfully and reach the end of the runway.

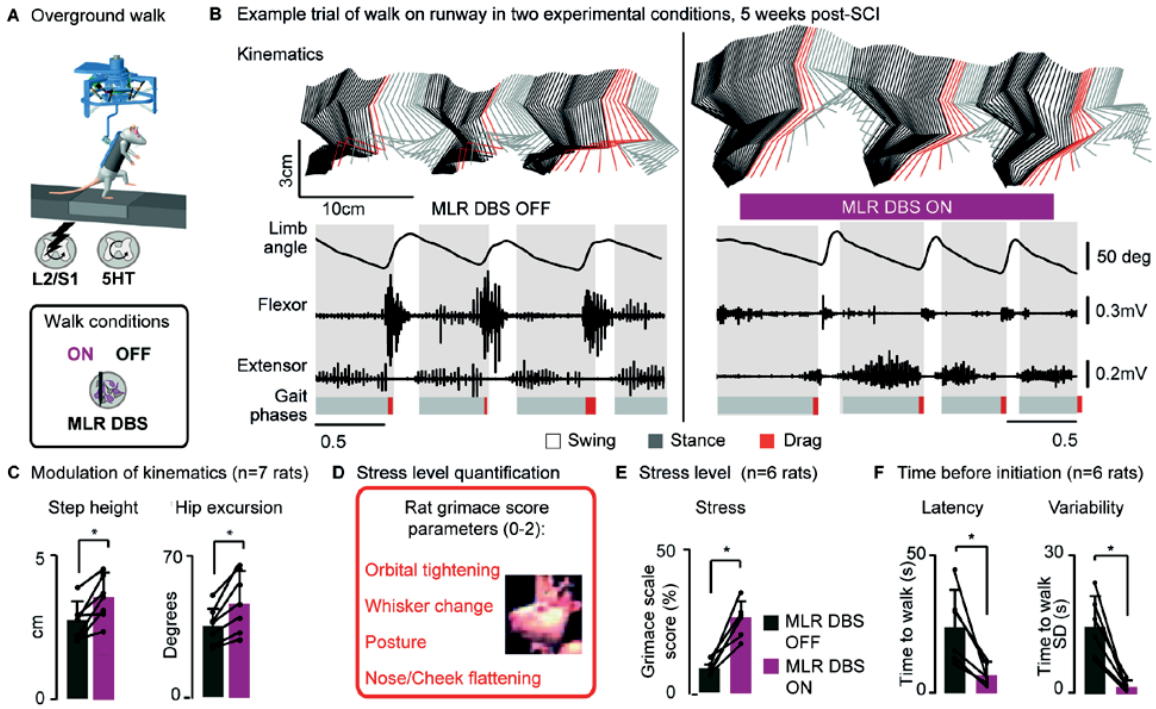

Figure 4.5 | Forced MLR DBS enhances locomotor performance in voluntary runway task, however, behavioral assessment shows increased stress in rats during forced MLR DBS. **(A)** Setup II: evaluation of MLR DBS effect on kinematic output during voluntary runway walking task in the presence of electrochemical neuromodulation. **(B)** Stick diagram of locomotor output combined with endpoint trajectory and electromyographic recordings in two conditions (MLR DBS OFF and ON). **(C)** Increased step height and hip excursion with MLR DBS continuously delivered throughout the walking task in all rats (n=7). **(D)** A scheme of behavioral state evaluation according to the Rat Grimace Scale at the end of trials with MLR DBS OFF and ON conditions. **(E)** Increased stress level when forced MLR DBS is ON in all rats (n=6). **(F)** Forced walking induced by MLR-DBS is characterized by an abnormally low time-to-go and high response predictability (n=6).

In this task, we compared MLR-DBS trials with no DBS trials, while all the other neuromodulation parameters remained the same, meaning that serotonin agonists and EES were present in equal amounts in both conditions (**Figure 4.5A-B**).

We found that MLR DBS stimulation led to increased locomotor output towards a higher kinematic state characterized with increased step height and hip excursion (**Figure 4.5B-C**), similarly to what we observed on the treadmill. Indeed, step height increased on average by 30.6%, while hip excursion rose on average by 31.8% (**Figure 4.5C**).

We further evaluated temporal walking dynamics and the adapted grimace scale to understand how MLR DBS influences overground walking and the general stress level of animals, respectively. We found that MLR DBS dramatically increased the stress level of the animals by 209.6 ± 102.5% in the MLR DBS condition, corresponding to an increment of 16.9 ± 6.8% points on the grimace scale, as corroborated by two independent blinded observers (**Figure 4.5D-E**). We also found that the overground walking dynamics are significantly disrupted due to MLR DBS, resulting in decreased latencies to locomotion initiation, which makes stepping more forced and automatized (**Figure 4.5F**).

These results show that the locomotor output in voluntary stepping after SCI is enhanced by application of MLR DBS with appropriate parameters determined during the treadmill task. However, this intervention seems to strongly increase the stress level of rats and induce a forced, automatized stepping.

Decoding voluntary locomotion intention using unsupervised learning algorithms

Our next step was to develop M1-controlled-MLR DBS interface and test how it affects locomotor performance and the behavioral state of the rats. As we described previously, an active locomotor state correlates with an increase in firing rate across the population of the M1 in healthy rats (**Figure 4.1C-E**). Similarly, as already evaluated in the literature (Dominici *et al.*, 2012; DiGiovanna *et al.*, 2016), rodent M1 is involved in voluntary locomotor tasks after SCI and encodes motor intention (**Figures 4.1E, 4.2E**). Therefore, we thought of decoding the M1 up state and coupling it to MLR DBS to amplify the descending motor command.

Using an unsupervised learning algorithm, we were able to decode the steady walking state with 87.9±8.4% precision across n=7 subjects, while steady idle state was correctly decoded with 90.6±3.5% accuracy (**Supplementary Figure S4.3)**. Analysis of state transition around beginning

and termination of locomotion reveals that walk initiation (first foot-off) features a faster transient in the M1 population activity, captured by a relatively sharper probability of transition to “walk” state for the locomotor intention decoder. Conversely, the stop event, corresponding to the last foot strike, features a slower transient of detection probability (**Supplementary Figure S4.3**).

These results indicate that our decoder has a reliable performance, and can accurately detect onset of M1 activation, interpreted as a “walk intention”.

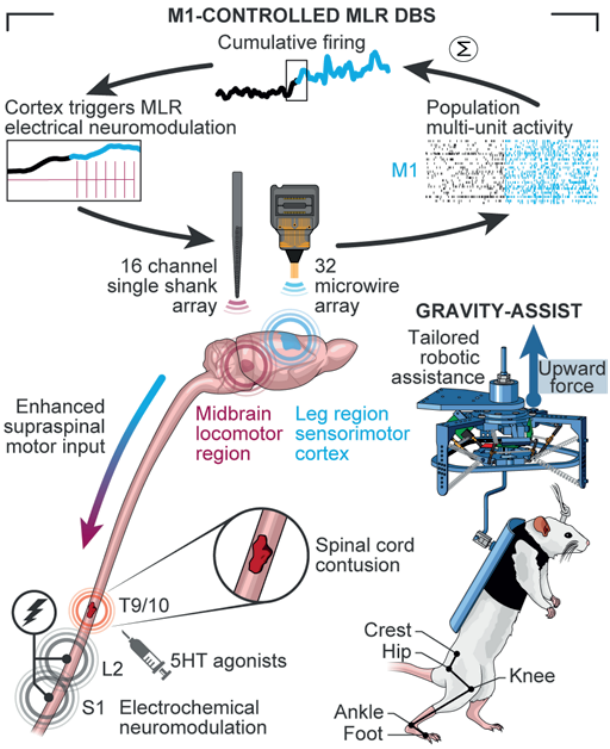

Figure 4.6 | Neuroprosthetic system comprised of M1-controlled MLR DBS for enhancing hindpaw locomotor output after severe contusion spinal cord injury. Experimental setup. **Top panel:** primary leg motor cortex recordings, which trigger MLR DBS when the cumulative firing rate crosses the threshold signaling locomotor command.
Bottom panel: bipedal walking task with gravity-assist providing upward support of the trunk. Simultaneously the brain-triggered MLR is applied (in MLR ON trials) together with the electrochemical modulation below the injury.

M1-controlled MLR DBS leads to enhanced locomotor output with reduced stress levels

We thought to exploit the preserved pattern of M1-MLR activity to enhance the descending locomotor command coming from the M1 by applying MLR DBS as soon as the walk intention in the M1 was decoded (**Figure 4.6**). We implemented this idea in a behavioral platform, where rats were performing the same voluntary locomotor task.

We found that this novel neuroprosthetic approach induced increased kinematic output during the overground bipedal locomotion task (**Figure 4.7B**). In particular, steps were on average 42% higher (n=4) and hip excursion 34% larger as compared to no MLR DBS condition (**Figure 4.7C**). We did not observe a significant increase in locomotor output in n=2 rats, who were excluded from the original group as they failed to recover voluntary motor control. Post-hoc histological analysis of the spinal cord tissue revealed that the contusion SCI was much more severe than in the case of the n=4 tested subjects (**Figure 4.7B**). Indeed, less than 5% of white matter tissue was preserved at the lesion epicenter, while all other subjects had >10% of spared tissue, which allowed a better substrate for cross-lesional connectivity.

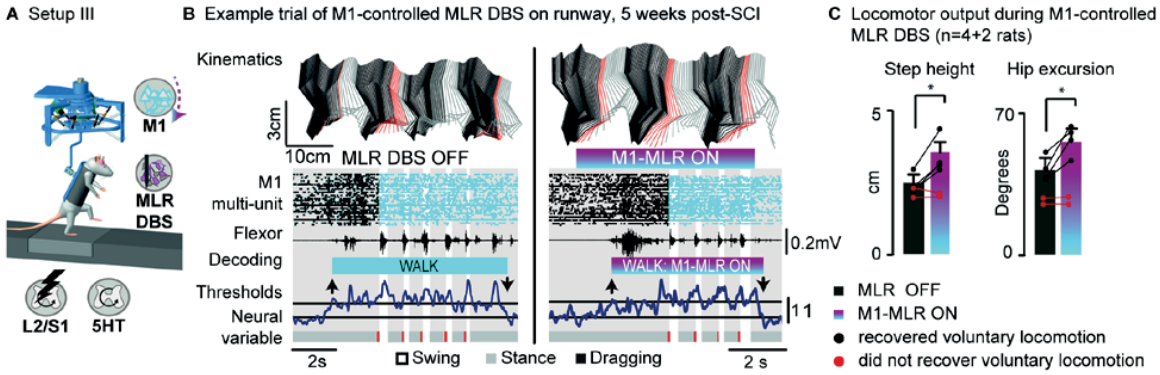

Figure 4.7 | Suprathreshold M1-controlled midbrain stimulation enhances hindpaw motor control after severe contusion spinal cord injury. (A) Setup III: evaluation of M1-controlled MLR DBS effect on kinematic output during voluntary runway walking task in the presence of electrochemical neuromodulation. **(B)** Stick diagram of locomotor output combined with endpoint trajectory and electromyographic recordings in two conditions (forced MLR DBS ON/ BMI OFF and M1-controlled MLR DBS ON/ BMI ON). **(C)** Increased step height and hip excursion with M1-controlled MLR DBS delivered throughout the walking task in all rats (n=6). *, P < 0.05; **, P < 0.01; ***, P < 0.001. Error bars, s.d.

In order to evaluate the immediate therapeutic results of the M1-to-MLR interface, we compared the two conditions (with and without cortical control of MLR-DBS) with the locomotor patterns of n=4 rats that underwent 2 months of rehabilitation. We performed multivariate analysis (using PCA) of over 105 parameters representing the gait cycles in detail. Our results show that when rats received M1-controlled MLR DBS, they display locomotor patterns that are on average 64% closer to rehabilitated rats than those who received only EES stimulation (p=0.03, **Figure 4.8B**).

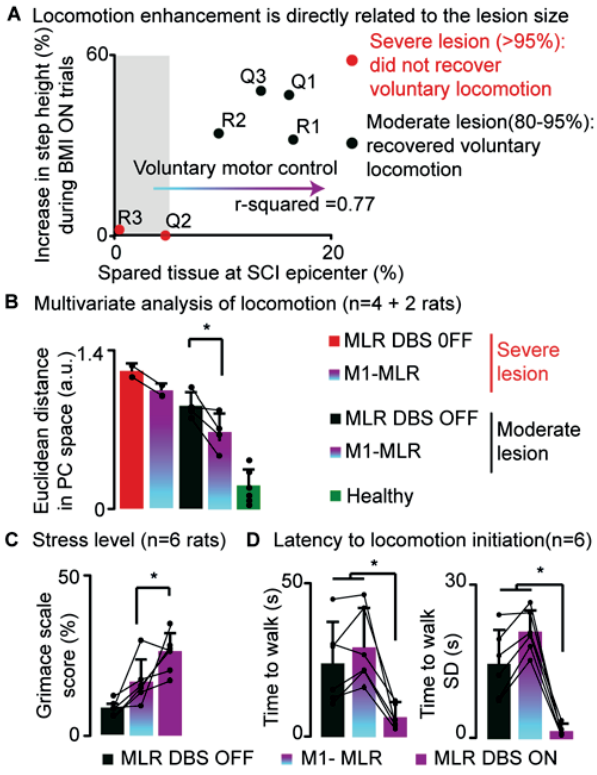

Figure 4.8 | M1-controlled MLR DBS decreases stress level and maintains natural dynamics of locomotion, but superior locomotor performance is only achieved in animals with moderate lesions. (A) Relationship between the level of locomotor output enhancement during brain-controlled MLR DBS condition with the lesion size. **(B)** Euclidian distance in principal component (PC) space between different experimental groups. **(C)** Increased stress level when forced MLR DBS is ON in all rats as compared to the DBS OFF and M1-controlled MLR DBS conditions scored by two blinded experimenters (n=6). **(D)** Disrupted walking dynamics with decreased latency and variability of initiation time with forced MLR DBS in all rats as compared to the DBS OFF and M1-controlled MLR DBS conditions (n=6).

In order to assess whether we can view overground locomotion as “voluntarily” expressed in the M1-controlled MLR-DBS condition (as opposed to forced delivery of DBS, which is known to artificially turn idle states into locomotor ones), we evaluated the “time to walk” parameter and its variability across recording conditions (**Figure 4.8D**). As expected, we found that in all n=6 rats forced MLR-DBS delivery resulted in expression of locomotion within 6.4±3.9s from the trial onset. For each rat, the variability of this characteristic time was very small: the standard deviations across the subjects were 1.5±1.1s. Conversely, both EES and M1-controlled MLR conditions were characterized by over-20s delays for walking initiation (23.9±13.2s and 29.1±12.2s respectively, p=0.02), with very large variabilities (14.7±6.7s and 20.9±4.2s respectively, p=0.02), typical of voluntarily initiated trial execution timings.

Finally, we evaluated the stressfulness for the subject of our novel M1-MLR intervention as compared with forced MLR stimulation. Our results show that M1-controlled MLR DBS application reduces the stress levels of the animals caused by MLR DBS by 44.7±39.7%, when both are compared to the EES condition (n=6, **Figure 4.8C**). This difference corresponds to a decrement of 8.8±10.1 percentage points on the grimace scale scored by two independent blinded observers.

We conducted further analyses to assess whether there is a relationship between the lesion severity and the improvement in locomotor performance during MLR-DBS delivery. We found that our quantification of lesion severity is a predictor of the locomotor performance during M1-MLR-DBS delivery (**Figure 4.8A**). In particular, the relative increase of step height during M1-controlled MLR trials is significantly correlated with the spared tissue at the SCI epicenter (r-sq=0.77). Additionally, spared tissue is also a predictor for both step height (r-sq=0.5) and body-weight support required (r-sq=0.6) during overground locomotion during MLR DBS off trials.

Overall, these results indicate that MLR DBS delivery triggered by M1 activation signal enhances locomotor output in animals with >10% spinal cord spared. The open-loop stimulation paradigm leads to more natural locomotor dynamics and decreased stress levels caused by the intervention, indicating that this neuroprosthetic system could bring additional value to post-SCI rehabilitation methods.

4.5 Discussion

We performed hindlimb motor cortex-midbrain recordings in healthy and injured animals with clinically relevant severe spinal cord contusion injury characterized by highly variable damage similar to that seen in human patients. M1 and MLR activity was strongly reduced by SCI, while the temporal activation pattern remained stable. As MLR is known to be a supraspinal locomotor activation center, we hypothesized that providing MLR DBS in spinal and voluntary locomotion tasks could alleviate gait deficits caused by SCI. Will-powered training under electrochemical neuromodulation and robotic assistance restored hindlimb motor control in four out of six animals, in which we could also enhance locomotion by DBS application. However, the MLR DBS intervention turned out to induce high levels of stress in the animals, which we successfully reduced by applying DBS in a self-driven manner: M1 activity-controlled MLR stimulation. Our results revealed that M1-controlled MLR DBS significantly enhanced locomotor performance to the same level as with the forced-MLR setup, while keeping the stress level of the rats low and preserving natural walk initiation dynamics. We discuss the implications of these developments for SCI models, potential mechanisms of action, and the clinical translation of neuroprosthetic rehabilitation.

M1 and MLR activity deteriorates after spinal cord injury, while the temporal activation pattern remains the same

We developed a behavioral setup that allowed us to simultaneously record electrophysiological signals from M1 and MLR regions during a quadrupedal walking task in awake rats. A few studies have previously investigated MLR (Noga *et al.*, 2017) and M1 (DiGiovanna *et al.*, 2016) activity in awake animals after SCI; however, their activation patterns have never been recorded simultaneously during a behavioral task. As expected, we found that in healthy animals, M1 activity precedes movement onset and serves as a locomotion initiation signal (Capogrosso *et al.*, 2016; DiGiovanna *et al.*, 2016), which we could later use as a DBS trigger. Despite the definition of MLR as a supraspinal locomotor center (Shik *et al.*, 1969; Noga *et al.*, 2003; Ryczko and Dubuc, 2013), we found that activity there follows and does not precede locomotion onset. These results are in line with previously reported findings (Roseberry et al., 2016) and may be due to MLR involvement in the control of posture through muscle tone modulation during locomotion (Mori et al., 1978). However, MLR does not play a key role in natural locomotion initiation in rats because MLR

lesioning does not disrupt locomotion in healthy rats (Dellu *et al.*, 1991, 1991; Steiniger and Kretschmer, 2004; Taylor *et al.*, 2004). Instead, it leads to akinesia in primates (Aziz *et al.*, 1998), which is important to consider for translational prospectives. Additionally, we found a high correlation between MLR multiunit activity and locomotor speed in healthy animals, as has been reported previously (Roseberry et al., 2016). After recordings in healthy animals, the rats underwent severe contusion injury (250 kdyn) at T9/T10 spinal levels, which led to severe paralysis of the hindlimbs. Two weeks after the SCI we recorded M1 and MLR activity and found that neural activity in both regions was significantly disrupted. There is extensive evidence in the literature that M1 activity is disrupted following SCI (Moxon *et al.*, 2014; Frost *et al.*, 2015), but still plays an important role in locomotion (DiGiovanna *et al.*, 2016). Furthermore, we observed a drastic change in MLR speed encoding, which almost disappeared following the SCI. Interestingly, we found that despite the overall loss in activity, the temporal relationship between M1 and MLR activation remains the same, a feature we later took advantage of for initiating MLR DBS. These findings suggest that even after SCI, M1 maintains a relevant neural signal for initiating locomotion and MLR plays a supportive role in the moment of locomotion initiation.

Deep brain stimulation of MLR enhances locomotion after neuroprosthetic rehabilitation

Given our findings that MLR activity decreases following SCI, the fact that MLR DBS improves quadrupedal stepping after severe dorsal column lesion (Bachmann et al., 2013) and is already used in patients for treatment of Parkinson's disease (Stefani et al., 2007; Mazzone et al., 2011), we decided to investigate its potential use in SCI rehabilitation further. We were specifically interested in the degree of controllability that we can get over hindlimb locomotor output through MLR DBS, and prospectively use it for improving impaired voluntary locomotor output after SCI. Our first hypothesis was that MLR DBS leads to stronger locomotion, which is proportionally modulated with DBS intensity in the treadmill stepping task, meaning that increasingly higher current levels applied to the MLR should drive an increase in the frequency of stepping and step height as in previous studies (Shik et al., 1966; Grillner, 2011). All rats underwent 4 weeks of neuroprosthetic rehabilitation (van den Brand et al., 2012) before being treated with MLR DBS. We determined suitable stimulation parameters by varying the amplitude of MLR DBS, while keeping the frequency and pulse width unchanged. Maximal MLR DBS amplitude constituted the highest stimulation intensity below the pain threshold, which we further used for runway MLR DBS

application. In four out of six animals, MLR DBS induced stronger stepping proportionally with increasing DBS intensity. Two remaining animals did not show increased stepping output, which we think is due to two main factors necessary for achieving locomotion rehabilitation and stepping capacity enhancement. First, the sublesional spinal circuits need to be effectively reconnected with the supraspinal regions and second, there has to be a minimum of 5% spinal cord spared to allow enough excitation to pass downstream. Both of these animals had less than 5% of tissue spared, which is not enough neuronal substrate for rehabilitation, and we think this is the main reason that MLR DBS was ineffective in enhancing their stepping. However, MLR DBS effect was strong enough to show a significant enhancement in the full group of animals. Overall, our findings suggest that it is possible to boost voluntary locomotion in moderately rehabilitated rats after SCI by applying appropriate MLR DBS. This is most likely due to the additional excitatory input, which MLR DBS provides through the partially spared reticulospinal pathway (Ryczko et al., 2016), which reorganizes after an incomplete spinal cord injury (Filli et al., 2014). In the future, it would be interesting to see if chronic rehabilitation using MLR DBS leads to sustainable enhancement of downstream reticulospinal pathways promoting better recovery after SCI.

Consequences of MLR DBS intervention and possible ways of stress alleviation

We decided to go beyond evaluation of MLR DBS-induced locomotor effect and evaluate possible side effects induced by this intervention. One of the often reported side effects in patients receiving low-frequency (15–25 Hz) DBS in the PPN is the subjective feeling of “alertness” (Stefani *et al.*, 2007; Hamani *et al.*, 2011). There is evidence for a potential mechanism of this effect because MLR/PPN mediates changes in behavioral state in addition to locomotion, since these two,are naturally recruited in tandem through the interplay between descending (locomotor) and ascending (cortical-state mediating) connections (Lee *et al.*, 2014a). It is generally much harder to assess alertness in animal models because there is no available subjective reports. However, we thought to evaluate the stressfulness of our interventions for the animals by using an adapted rat grimace scale, that has been proven to be a robust method for instantaneous stress level evaluation (Carstens and Moberg, 2000; Sotocinal *et al.*, 2011). Two blind observers reported a twofold increase in stress levels in animals receiving MLR DBS as compared to the same animals in an EES only condition. This strongly suggetss that stress level is an important factor to consider for any potential translation into humans and that it is important to find a way to reduce stressfulness of MLR DBS intervention. The likely mechanism of the observed effect is through

ascending projections to the basal forebrain (Dringenberg and Olmstead, 2003; Martinez-Gonzalez *et al.*, 2011), which are excited by MLR DBS and can also influence cortical states, for example, by sending a signal similar to an efferent copy to the primary visual cortex (Lee *et al.*, 2014a). The brainstem cholinergic system has also been implicated in sensory gating of external inputs (Kobayashi and Isa, 2002), which might contribute to the detected increase in stress level. Lastly, we noticed that locomotion becomes more automated and forced with MLR DBS, characterized by low variability and much shorter initiation times, thus taking away a significant part of the naturally highly variable voluntary locomotion initiation. It would seem that the forced MLR DBS is a stressful intervention heavily influencing volitional control of locomotor initiation, a factor which should be carefully considered during the design of potential translational approaches.

Brain-controlled MLR DBS delivery enhanced locomotion with reduced side effects

To resolve the concerns raised above and provide a more natural method to deliver MLR DBS (Courtine and Bloch, 2015), we hypothesized that a cortically-controlled MLR DBS delivery would alleviate stress and provide a better strategy for delivering MLR DBS. Therefore, we constructed an open-loop system, which uses the M1 signal to drive MLR DBS, which in turn acts as an amplifier for the descending locomotor command coming from M1. To date, several attempts have been made to deliver brain-controlled stimulation (Ethier *et al.*, 2012; Nishimura, Perlmutter, Eaton, *et al.*, 2013), including in monkeys after spinal cord injury (Capogrosso *et al.*, 2016). Many groups reported that brain activity control of DBS delivery shows promising results: it induces spike-time dependent plasticity (Nishimura, Perlmutter, Eaton, *et al.*, 2013), is more efficient and saves battery life of the stimulator in patients with Parkinson's disease (Little *et al.*, 2013). Here we report for the first time that our M1-triggered MLR DBS delivery system enhances locomotion after the SCI while the rats perform a bipedal voluntary locomotor task post-SCI. The M1-MLR DBS induced locomotor enhancement is surprisingly equally as strong as the one observed with forced MLR DBS, despite a smaller continuously applied stimulation current. We believe that this is due to induced potentiation of the descending voluntary control through DBS-induced excitation of reticulospinal pathways (Jahn *et al.*, 2008; Ryczko *et al.*, 2016). Notably, in line with our hypothesis, M1-controlled MLR DBS significantly reduced the level of stress caused by the forced MLR DBS delivery and reversed automated locomotion back to the natural patterns exhibited during the trials with no MLR DBS delivery. We believe that the observed stress reduction was

caused by MLR DBS delivery only during higher locomotor states in a self-driven manner. This stimulation paradigm might release the negative impact produced by forced DBS and turn MLR into an amplifier as opposed to an inducer of the locomotor command, which resembles the natural mechanism of locomotion initiation (Courtine and Bloch, 2015). In sum, we have developed a brain-controlled neuroprosthetic MLR DBS delivery system, which induces the same alleviation of gait deficits post-SCI as the forced MLR, with reduced stress levels and preserved natural locomotor dynamics, which could inspire a novel approach for SCI treatment.

Limitations and therapeutic potential of M1-MLR neuroprosthetic rehabilitation

In this section, we discuss the potential for the M1-MLR neuroprosthetic intervention in the context of current research and therapeutic developments. DBS has been implemented in clinical practice for the past 30 years already and is used for treatment of gait and cognitive dysfunctions (Benabid *et al.*, 2002; Perlmutter and Mink, 2006; Miocinovic *et al.*, 2013). In particular, MLR DBS has been used for alleviation of motor deficits in patients with Parkinson's disease (Mazzone et al., 2011), which makes it feasible to imagine a MLR DBS application for treatment of other disorders such as SCI. Additionally, as discussed before, it has been shown to alleviate locomotor deficits after severe SCI in rats (Bachmann et al., 2013). The MLR DBS most likely acts through continuous excitation of the spared descending reticulospinal circuitry (Noga *et al.*, 2003; Ryczko *et al.*, 2016) leading to more effective use of the tissue. In the long-term this can trigger use-dependent plasticity if it is combined with rehabilitation protocols (Ganguly and Poo, 2013). One downside of MLR DBS is the stress caused by this intervention, both for humans and animals (Shapira *et al.*, 2006). Additionally, the lesion size and location have to be carefully evaluated so that the technique is only applied to subjects, who have enough neural substrate preserved for locomotor enhancement. In our study, we found this threshold to be >5% ventral spinal cord spared in contused rats. Moreover, both our study and that of Bachman et al. observed enhanced locomotion only when the suprathreshold currents were delivered, which has never been done before on human subjects and has to be carefully evaluated (Kringelbach *et al.*, 2007).

Lastly, before subjecting SCI patients to potentially dangerous MLR DBS (L.H. Stieglitz, A Curt, 2017), we have to conduct a careful investigation of long-term effects of MLR DBS. It is crucial to not only determine hypothetical downstream plasticity, but also to investigate possible neural changes induced by the backpropagation of excitatory signals into the cortico-thalamic loop and

basal forebrain. Based on the current literature, potential side effects may include sleep-wake cycle disturbance, increased level of alertness and impaired cognitive abilities (Dringenberg and Olmstead, 2003; Hamani *et al.*, 2016). While MLR stimulation has the potential to induce adverse side effects, by utilizing endogenous M1 activity as a trigger for stimulation we significantly reduce associated side effects, creating a novel neuroprosthetic paradigm capable of enhancing existing rehabilitation techniques.

4.6 Supplementary material

Kinematic and kinetic gait parameters			
Temporal features of gait		**Joint angles and segmental oscillations**	
1	Cycle duration	**32**	Crest elevation angle amplitude
2	Cycle velocity	**33**	Hip elevation angle amplitude
3	Relative stance duration	**34**	Knee elevation angle amplitude
4	Swing duration	**35**	Ankle elevation angle amplitude
5	Relative phases alternation	**36**	Metatarsal elevation angle amplitude
6	Stance duration	**37**	Whole-limb elevation angle amplitude
Limb endpoint trajectory		**38**	Hip joint angle amplitude
7	Stride length	**39**	Knee joint angle amplitude
8	Step length	**40**	Ankle joint angle amplitude
9	3D endpoint path length	**41**	Metatarsal joint angle amplitude
10	Maximum backward position	**42**	Whole-limb abduction amplitude
11	Maximum forward position	43	Foot abduction amplitude
12	Relative step height	**Velocity**	
13	Maximum swing speed	**44**	Crest oscillation velocity amplitude
14	Relative timing of maximum speed during swing	**45**	Thigh oscillation velocity amplitude
15	Acceleration at swing onset	**46**	Leg oscillation velocity amplitude
16	Endpoint velocity	**47**	Foot oscillation velocity amplitude
17	Orientation of velocity vector at swing onset	**48**	Whole limb oscillation velocity amplitude
18	Time of foot dragging	**Limb coordination**	
19	Relative dragging duration	**49**	Temporal coupling between crest and thigh oscillations
20	Relative dragging duration terminal point	**50**	Temporal coupling between leg and thigh oscillations
21	Step height	**51**	Temporal coupling between leg and foot oscillations
Stability		**52**	Correlation between crest and thigh oscillations
22	Foot-pelvis relative position at stance onset	**53**	Correlation between leg and thigh oscillations
23	Stance width	**54**	Correlation between leg and foot oscillations
24	Maximum hip vertical position	**55**	Correlation between hip and knee oscillations
25	Minimal hip vertical position	**56**	Correlation between knee and ankle oscillations
26	Amplitude of hip vertical movement	**57**	Correlation between ankle and metatarsal oscillations
27	Variability of sagittal hip oscillations	**58**	Relative duration between crest and thigh angle minima
Whole body movement		**59**	Relative duration between thigh and leg angle minima
28	Pelvic center of mass forward motion	**60**	Relative duration between leg and foot angle minima
29	Pelvic center of mass mediolateral motion	**61**	Relative duration between crest and thigh angle maxima
30	Pelvic center of mass vertical motion	**62**	Relative duration between thigh and leg angle maxima
31	Pelvic center of mass 3D motion	**63**	Relative duration between leg and foot angle maxima

Table S4.1 | Kinematic and kinetic parameters for PC analysis. Representative kinematic parameters used to assess gait quality in rats.

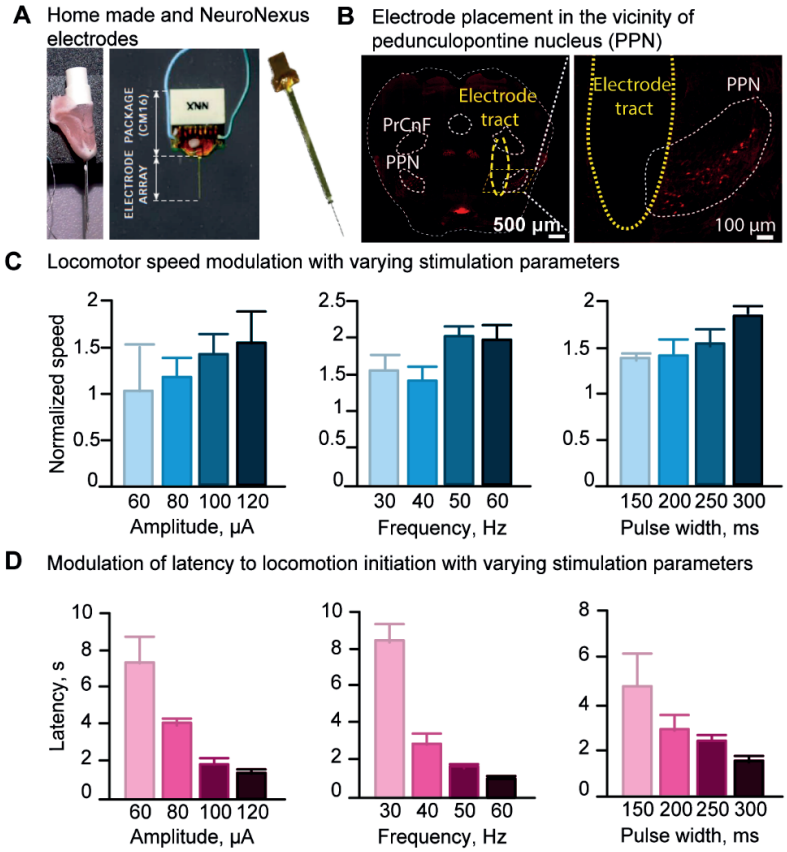

Figure S4.1 | Implantation of the MLR DBS electrodes and characterization of locomotor responses to the MLR DBS. (A) Homemade and custom-made electrodes for the MLR implantation. **(B)** Post-hoc anatomical evaluation of the electrode placement and localization of cholinergic neurons in the rats' PPN. **(C)** Locomotion speed modulation by MLR DBS as a response to different stimulation amplitude, frequency and pulse width. **(D)** Latency of locomotion initiation onset as a response to changing MLR DBS parameters (n=1, representative example animal. Error bars, s.d.).

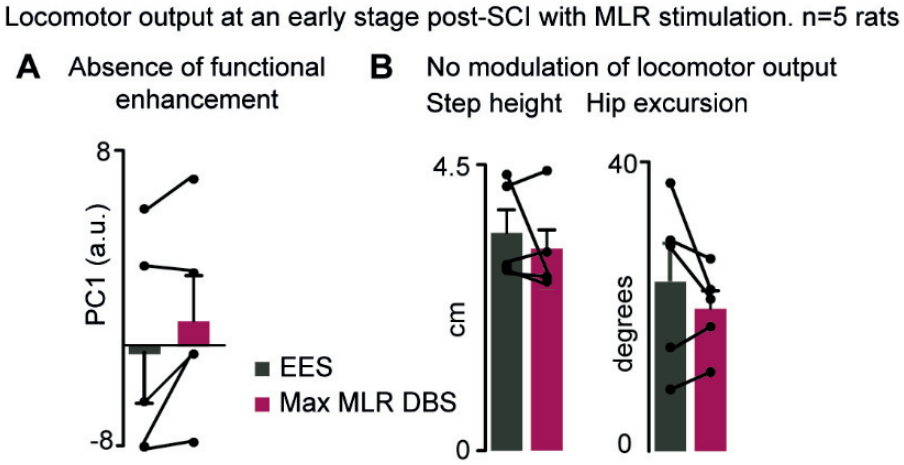

Figure S4.2 | Forced MLR DBS does not trigger increase in locomotor performance during passive treadmill walking task in trained rats two weeks after SCI. (A) Principal component (PC) analysis applied on 63 parameters measured over the average step cycle across n=5 animals, 2 hindlimbs per animal and 2 experimental conditions (MLR DBS OFF and ON). The bar graphs report the scores on PC1 across conditions, which did not capture any enhancement of locomotor output with MLR DBS. **(B)** No increase in step height (left) and hip excursion (right) across all animals early after SCI. Error bars, s.d.

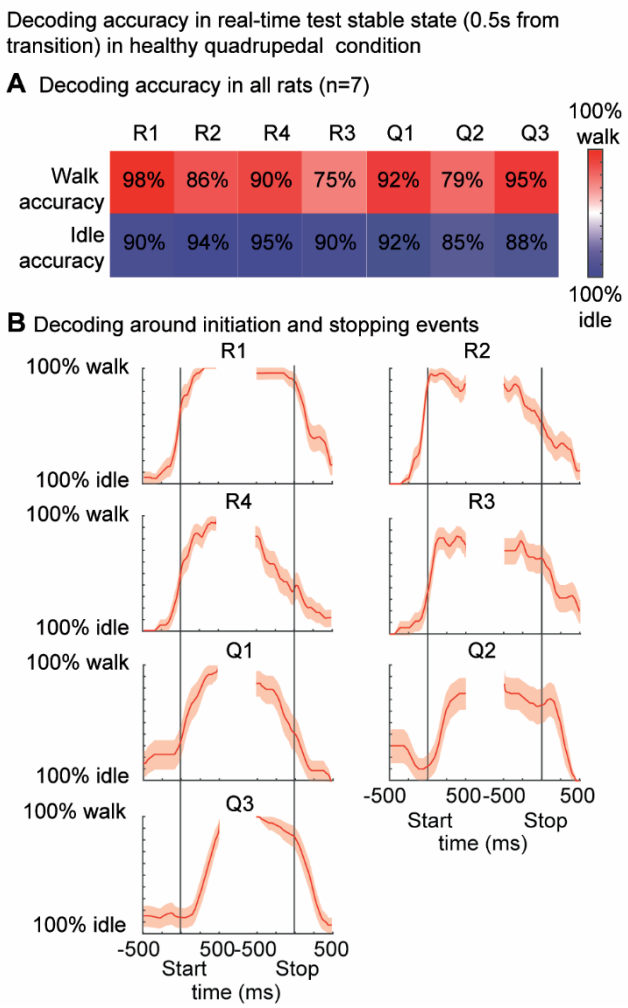

Figure S4.3 | Real-time decoding accuracy in healthy rats performing quadrupedal walking task (n=7). (A) Accuracy of the decoder in capturing walk and idle conditions, where walk initiation is defined as the first foot-off event and walk termination as the last foot strike event. **(B)** Examples of cumulative multiunit activity of motor cortex during walk and idle states. The assessment was performed 0.5s away from state transition.

5. BRAIN–CONTROLLED MODULATION OF SPINAL CIRCUITS IMPROVES RECOVERY FROM SPINAL CORD INJURY

Marco Bonizzato[1], Galyna Pidpruzhnykova[2], Jack DiGiovanna[1], Natalia Pavlova[2,3], Polina Shkorbatova[2,3], Silvestro Micera[1,4,&] and Gregoire Courtine[2,&]

1. Bertarelli Foundation Chair in Translational Neuroengineering, Center for Neuroprosthetics and Institute of Bioengineering, School of Bioengineering, EPFL, Lausanne, Switzerland.
2. Center for Neuroprosthetics and Brain Mind Institute, School of Life Sciences, Swiss Federal Institute of Technology (EPFL), Lausanne, Switzerland
3. Motor Physiology Laboratory, Pavlov Institute of Physiology, St. Petersburg, Russia
4. The BioRobotics Institute, Scuola Superiore Sant'Anna, Pisa, Italy.

[&] contributed equally to this work

Corresponding author:
Grégoire Courtine, PhD
Center for Neuroprosthetics and Brain Mind Institute
SWISS FEDERAL INSTITUTE OF TECHNOLOGY (EPFL)
CH-1015 Lausanne
gregoire.courtine@epfl.ch

Manuscript in preparation: “Brain–controlled modulation of spinal circuits improves recovery from spinal cord injury” prepared for submission to the PNAS in fall 2017

Marco Bonizzato, Galyna Pidpruzhnykova, Jack DiGiovanna, Natalia Pavlova, Polina Shkorbatova, Silvestro Micera[&] and Gregoire Courtine[&]

[&] this authors contributed equally to this work

My contribution: I performed all aspects of behavioral experiments and analyzed all the anatomical and part of the behavioral data, helped in preparation of figures and manuscript editing.

Others contribution: S.M. and G.C. contributed equally to this work. M.B. developed the spinal cord stimulation protocols and brain decoders, performed all the behavioural experiments and analysed the data. N.P., P.S. and M.B. performed the surgeries. M.B., J.D., S.M. and G.C. conceived the study. G.C. wrote the paper and all the authors contributed to its editing.

Other published works: This study was reported in a PhD thesis of Marco Bonizzato.

5.1 Abstract

Growing evidence suggests that brain–controlled neuromodulation therapies augment neuroplasticity and recovery from neurological disorders, but direct proof is still lacking. Here, we show that a direct cortical control of spinal cord stimuation during gait rehabilitation enhanced recovery from spinal cord injury. Rats received a severe spinal cord contusion that led to leg paralysis. We engineered a proportional brain–spine interface whereby cortical ensemble activity continuously determined the intensity of spinal cord stimulation protocols promoting leg flexion during swing. This neural bypass combined with chemical stimulation immediately enabled paralyzed rats to walk overground and adjust foot clearance to climb a staircase. Compared to continuous spinal cord stimulation, brain–controlled stimulation accelerated and enhanced the long–term recovery of locomotion. These results demonstrate the relevance of brain–controlled neuromodulation therapies to augment recovery from motor disorders, establishing important proof–of–concept that warrants clinical studies.

SIGNIFICANCE STATEMENT

Various neural bypasses restored the communication between the brain and paralyzed muscles after neurological disorders, but their potential impact on neural repair remains unclear. In this study, we conceived a neural bypass whereby motor cortex activity continuously determined the intensity of electrical spinal cord stimulation protocols in order to restore locomotion in paralyzed rats. The results show that this neural bypass not only enabled complex locomotor execution immediately, but also accelerated and augmented recovery during rehabilitation in the long-term. This study provides a proof–of–concept on the relevance of neural bypasses for neural repair and recovery from spinal cord injury, warranting clinical studies in the future.

5.2 Introduction

Various neurological disorders compromise the communication between the brain and spinal circuits that produce movement, leading to severe motor deficits. A variety of neural bypasses have been developed to restore this communication (Moritz *et al.*, 2008; Ethier *et al.*, 2012; Bouton *et al.*, 2016; Capogrosso *et al.*, 2016; Ajiboye *et al.*, 2017). For example, brain–controlled neuromuscular stimulation reestablished functional movements of the upper limbs in individuals with tetraplegia (Bouton *et al.*, 2016; Ajiboye *et al.*, 2017). Similarly, our group recently showed that a direct cortical control over the location and timing of electrical spinal cord stimulation enabled nonhuman primates to perform locomotor movements with a paralyzed leg without any prior training (Capogrosso *et al.*, 2016).

While these neural bypasses primarily aimed at restoring lost motor functions with neurotechnologies, there is mounting evidence that the long–term use of these neural bypasses during rehabilitation may augment neuroplasticity and functional recovery (Ethier *et al.*, 2015; McPherson *et al.*, 2015; Krucoff *et al.*, 2016). For example, the strength of neural connections between motor cortex and spinal cord can be modified durably when single corticospinal tract neurons trigger electrical stimulation of the spinal cord (Jackson *et al.*, 2006; Nishimura, Perlmutter and Fetz, 2013; Nishimura, Perlmutter, Eaton, *et al.*, 2013). This activity–dependent stimulation increases the strength of terminal projections from single neurons through spike–timing–dependent plasticity rules. The electrophysiological and molecular mechanisms underlying this Hebbian–like neuroplasticity of connections between two neurons have been extensively documented *in vitro* and *in vivo* (Holtmaat and Svoboda, 2009; Feldman, 2012). It has also been shown that a precisely timed stimulation not only increases the connectivity between the trigger and target sites, but also mediates a reorganisation of the neighbouring neurons (Rebesco *et al.*, 2010). These findings open the intriguing possibility to augment the reorganisation of spared circuits and residual neural pathways between the two regions directly reconnected with neural bypasses and neuronal structures surrounding them. However, the relevance of brain–controlled stimulation for promoting neuroplasticity between cortical and spinal ensemble populations underlying the execution of complex movements after SCI remains hypothetical. Here, we directly tested this concept in a rodent model of severe spinal cord injury.

Our group previously showed that the delivery of epidural electrical stimulations over specific locations and with a precise timing effectively modulate locomotor movements of the paralyzed legs in rats with severe spinal cord injury (van den Brand *et al.*, 2012). However, the rats had no

control over the spinal cord stimulation, and consequently, the stimulation was delivered tonically and did not depend on animals' descending locomotor drive. To remedy this issue, we developed a neural bypass that directly linked cortical activity to the modulation of stimulation protocols. We show that brain–controlled stimulation not only enabled complex locomotor executions such as overground walking and staircase climbing, but also accelerated and improved long-term recovery compared to continuous stimulation when delivered during rehabilitation. These results provide important proof of concept on the relevance of brain–controlled neuromodulation therapies to enhance neural repair and functional recovery from neurological disorders.

5.3 Materials and methods

Animals

Experiments were conducted in adult female Lewis rats (200–220g body weight). All experimental procedures were approved by the Veterinary Office of the Canton Vaud. Each rat was individually housed in a transparent cage with access to food and water ad libitum. The room was kept on a 12h light/dark cycle at 22 degrees Celsius ambient temperature. Prior to surgery, all the rats were acclimatized to walk freely along the runway.

Surgery

All surgical procedures and post–operative care for rats with SCI have been described in detail previously (van den Brand *et al.*, 2012; DiGiovanna *et al.*, 2016; Wenger *et al.*, 2016). Briefly, aseptically and under general anesthesia, a 32–channel microelectrode array (Tucker–Davis–Technologies, USA) was inserted into layer V of the leg region of the right motor cortex, which we previously identified anatomically and electrophysiologically (Krucoff *et al.*, 2016). Bipolar electrodes were inserted into the left (contralateral) tibialis anterior muscles to record electromyographic signals. Two wire electrodes were sutured to the dura over the dorsal aspect of lumbar (L2) and sacral (S1) segments to deliver electrical stimulation (van den Brand *et al.*, 2012). Rats received robotically controlled contusion injury that were delivered at the T9/T10 spinal level using an infinite horizontal impactor (Precision Systems and Instrumentation, USA). The impact force was set at 250 kdyn. Two rats were excluded from the study since they did not show modulation of the cortical activity during locomotion. Post–mortem evaluation of tissue damage revealed an out-of-range SCI injury in these rats (**Supplementary Figure S5.2B**).

Groups

Multiple groups of rats participated to these experiments. The list of experimental procedures conducted on the animals is available on **Supplementary Table ST5.2**.

Locomotor training

Five minutes prior to each training session, rats received an intraperitoneal injection of Quipazine and subcutaneous injection of 8–OH–DPAT (van den Brand *et al.*, 2012). The rats were trained on a treadmill (11 cm/s) and overground in a bipedal posture that encourages volitional control of the legs to walk forward toward a food reward. During training, electrical stimulation was delivered continuous over the L2 and S1 electrodes (monopolar pulses, 40 Hz, 50–350 μA, 0.2 ms). Each training session lasted 30min and took place 5 day per week, starting from 7 days post–injury.

Recordings of kinematic and muscle activity

Procedures for kinematic and muscle activity recordings data collection have been described in detail previously (van den Brand *et al.*, 2012; DiGiovanna *et al.*, 2016; Wenger *et al.*, 2016). Briefly, bilateral leg kinematics were captured using the high–speed motion capture system Vicon (12 infrared and 2 digital video cameras, 200 Hz; Vicon, UK). Electromyographic signals were recorded (2 kHz, 10–1000 Hz bandpass filtered) using the same system.

Analysis of kinematic and muscle activity

A total of 55 parameters quantifying kinematic features were computed for each leg and gait cycle according to methods described in detail previously (van den Brand *et al.*, 2012; DiGiovanna *et al.*, 2016; Wenger *et al.*, 2016). All the parameters are reported in **Supplementary Table ST5.1**. To evaluate differences between experimental groups (rehabilitation), we implemented a statistical procedure based on principal component (PC) analysis. PC analyses were applied on data from all individual gait cycles for all the rats together. Data were analysed using the correlation method, which adjusts the mean of the data to 0 and the standard deviation to 1. This method of normalization allows the comparison of variables with disparate values (large vs. small values) as well as different variances. Locomotor performance was quantified as the Euclidian distance from intact rats in the PC space defined by the first three PCs.

Cortical recordings

Intracortical voltage signals were sampled at 24kHz, pre-amplified, digitalized and filtered online (bandpass filtered, 0.7–3 kHz) using the real–time BioAmp processor from Tucker–Davis Technologies (USA). We calculated multi–unit activity (MUA) from all field potential stochastic events that crossed a threshold value defined visually for each channel. Spike counts were collected in bins of 10 ms and then smoothed with a Finite Impulse Response (FIR) filter with Gaussian sample decay of 80% in 40 ms.

Spinal cord stimulation

Epidural electrical stimulation (0.2 ms, 100-300 μA, 40 Hz) was delivered through the chronically implanted electrodes at L2 and S1 segments using the system used for neural recordings (Tucker–Davis Technologies, USA). During experiments with the brain–spine interfaces, the stimulation delivered over the S1 segment was maintained constant (continuous stimulation).

Cortical decoding

For each rat, we identified the 6 channels with the MUA that correlated most with the envelope (rectified and low–pass filtered at 5 Hz) of the tibialis anterior muscle. We then built a linear combination of the normalized MUAs from these 6 channels termed *normalized cumulative firing*. This variable was used as the control variable for both brain–spine interfaces. The hard–real–time controller operated within cycles of 12 kHz.

Binary brain–spine interface

Whenever *the normalized cumulative firing* crossed a manually selected control threshold corresponding to a latency of 100 ms prior to foot–off event, the controller delivered a stimulation burst (200 ms) over the electrode located at L2. A refractory period of 800 ms and 600 ms was set before the next event detection on the treadmill and runway, respectively. During locomotion along the runway, an additional silent period of 2 s was inserted after the first event detection (initiation) in order to account for the time required for gait initiation. When evaluating decoder

accuracy, all flexion detections occurring within a window of [-200, 100] ms around foot-off (roughly 25% of the average step cycle) where considered as true positives. A false negative is reported in case no detection occurs within this window. True negatives are scored for lack of detections in the timespan between two flexion windows, false positives otherwise. The ROC of the decoding rules is computed by Monte Carlo method, as the average performance of the decoding algorithm to a white noise input, for different noise power amplitude (e.g., a flat zero noise input would lead to 100% true negatives and no correct foot-off detection).

Proportional brain–spine interface

We built a linear relationship between the *normalized cumulative firing* and the amplitude of stimulation delivered to the L2 segment. The currents were constrained with a range of functional values that were identified based on behavioural recordings. Specifically, the lower and upper bounders were defined as the lower and higher current amplitudes capable of mediating stable locomotion on a treadmill while avoiding dragging (lower) or co–contraction of antagonist muscles (upper), respectively. This tuning required 2 to 5 min prior to each experimental session, although these thresholds remain globally stable over time. All the parameters were kept constant across the recording sessions.

Immunohistochemistry and neuromorphological evaluation

All the procedures have been described in detail previously (van den Brand *et al.*, 2012; DiGiovanna *et al.*, 2016; Wenger *et al.*, 2016). Briefly, rats were deeply anesthetized using an i.p. injection of 0.5 ml Pentobarbital–Na (50 mg/mL) and transcardially perfused with approximately 80 ml Ringer's solution containing 100 kIU/L heparin (Liquemin, Roche, Switzerland) and 0.25 % NaNO2 followed by 300 ml of cold 4% phosphate buffered paraformaldehyde, pH 7.4 containing 5% sucrose. The brain and spinal cord were removed, post–fixed overnight, and later transferred to 30% sucrose in phosphate buffer (PB) for cryoprotection. After 3 days, the tissue was embedded in Tissue Tek O.C.T (Sakura Finetek Europe B.V., The Netherlands), frozen at – 40 °C, and cut to a thickness of 40 µm. All the sections were stained using anti–GFAP (1:1000, Dako, USA) and Nissl antibodies in order to visualise the borders of the contusion injury.

Analysis of spinal cord damage

The extent and location of spinal cord damage was evaluated in each rat. Three image stacks were acquired per rat: lesion epicentre and the first intact sections immediately rostral and caudal to the injury. Images were acquired with the Olympus Slide Scanner VS120–L100 microscope at 10x magnification and analyzed offline using custom–written scripts. Slide scanner output images were divided into square regions of interest (ROI). Files were color–filtered and binarized by means of intensity thresholds, set empirically and maintained across sections. The amount of spared tissue was computed as the ratio between the number of pixels at the epicenter and in the intact sections.

Statistics

All other data are displayed as mean values ± SEM. Paired statistical evaluations were performed using Student's t–test or the non–parametric Wilcoxon signed–rank test when at least one of the populations could not be assumed to be normally distributed. The Kruskall–Wallis test was applied to all non–paired populations of samples.

5.4 Results

Technological platform to implement the brain–spine interface

We aimed at restoring the communication across a severe spinal cord contusion using a brain–spine interface that directly links cortical activity to the modulation of epidural electrical stimulation applied to lumbar segments during gait rehabilitation. Due to the critical importance of a rapid link between neural recordings and stimulation protocols, we developed a real–time control system capable of reading multiunit activity, decoding gait events, configuring stimulation parameters, and triggering stimulation protocols within iteration loops remaining below 10 ms (**Figure 5.1**).

Spinal cord stimulation restores leg movement and cortical modulation

Five rats were implanted with a 32–element microwire array into the leg region of the left motor cortex to record multiunit activity from neuronal ensembles (DiGiovanna *et al.*, 2016). To stimulate the spinal cord electrically, we implanted chronic electrodes over the dorsal aspect of lumbar (L2) and sacral (S1) segments. We also monitored the motor responses elicited by this stimulation using bipolar electromyographic electrodes chronically inserted into the flexor muscle of the left ankle (tibialis anterior) (**Figure 5.1**). In the same surgery, the rats received a severe contusion of the spinal cord using a robotically controlled impact onto thoracic segments T9/T10 (250 kdyn).

To evaluate the rats without confounding contribution of the intact forelimb, we positioned them bipedally in a robotic postural interface that provides a gravity–assist optimised for each subject (van den Brand *et al.*, 2012; Mignardot *et al.*, 2017). At 10 days post–injury, all the rats showed complete paralysis of both legs, associated with quiescent activity of leg muscles (**Figure 5.2A**). During these evaluations, we did not detect relevant modulations of motor cortex population responses (**Figure 5.2A**).

The combination of serotonin agonists (van den Brand *et al.*, 2012) and continuous epidural electrical stimulation applied to L2 and S1 segments (40 Hz, 0.1–0.4 mA, 0.3 ms) immediately enabled automated locomotion of the paralyzed legs. However, a systematic dragging of the paws occurred at the beginning of the swing phase (18.2 ± 5.3 %). Under these conditions, the spiking activity recorded from the right motor cortex displayed cyclic modulations that were phase–locked to the automated (involuntary) locomotor movements of the left leg (**Figure 5.2A**).

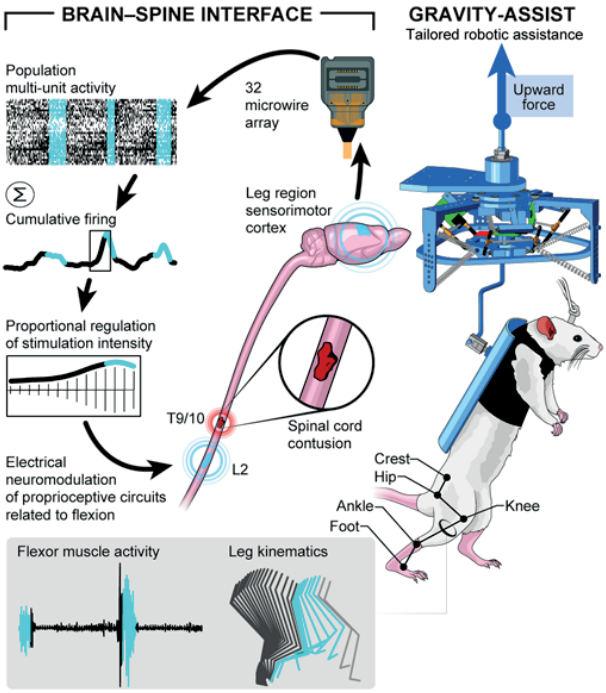

Figure 5.1 | Conceptual and technological design of the brain–spine interface. The rats were implanted with a microwire array (32 wires) into the leg area of the right motor cortex. The raster plot shows neural recordings over three successive gait cycles. Each line represents spiking events identified from one electrode, while the horizontal axis indicates time. Stance and swing are coloured in black and blue, respectively. Two types of brain–spine interface were tested. First, a decoder anticipated the onset of the swing phase, which triggered the delivery of stimulation protocols applied to the lumbar spinal cord, wherein motoneurons innervating flexor muscles reside. Second, the cumulative firing calculated from multi–unit activity was directly linked to the intensity of stimulation protocols delivered to the same location. Shaded region: electromyographic activity of a flexor muscle (tibialis anterior) together with a stick diagram decomposition of leg movements during the stance (dark grey) and swing (light grey) phases of gait. The occurrence of the stimulation is highlighted in blue. During testing, the rats walked in a gravity–assist that personalised the amount of upward force for each rat. Copyright Jemère Ruby (2017).

The depth of modulation of these responses strongly correlated with the amount of spared spinal cord tissue (R^2 = 0.87, **Supplementary Figure S5.1**), suggesting that sensory afferent feedback might be the primary neural input responsible for the modulation of cortical activity. To explore this possibility, we recorded cortical ensemble modulation in response to a cutaneous stimulation

applied to the paw. The strength of the stimulus was adjusted to avoid leg movements. As anticipated, the sensory stimulation led to small, yet reproducible responses in the leg region of the motor cortex ($P < 0.05$; **Supplementary Figure S5.2**).

Decoding of foot–off events from cortical population responses

We then asked whether gait events could be decoded from these modulations. During locomotion enabled by continuous stimulation, we observed that the cumulative firing of cortical ensemble population systematically increased toward the end of stance and peaked during swing (**Figure 5.2A**). We thus sought to decode the onset of the swing phase from these cortical population responses.

We developed a linear classifier based on least–square fit that tracked neural correlates of foot–off events from the cumulative firing of cortical ensemble population (**Supplementary Figure S5.3A**). Evaluations showed that the online decoder accurately predicted foot–off events in real–time over extended periods of locomotion in all the tested rats (n = 5; 90.2 ± 2.4 % correct detections over periods of 120 s). The true–negative rejection rate peaked as high as 92.4 ± 1.4 % (**Figure 5.2B**). This decoding performance lay well above the Receiver Operating Characteristic (ROC) curve of the applied decoding rules (i.e. chance level**; Supplementary Figure S5.3B**).

Locomotion on a treadmill is a highly repetitive task that may inherently lead to high decoding performance without direct relationships with the actual decoded events. To reject this possibility, we compared the intrinsic variability in the timing of foot–off events with the variability of errors in foot–off detections. We found that the variability of errors in foot–off detections was markedly inferior to the intrinsic variability of actual foot–off events across all the recorded gait cycles (**Supplementary Figure 5.3B**).

A brain–spine interface enhancing leg flexion during swing

We next sought to exploit this decoding to engineer a binary (on/off) brain–spine interface through which cortical activity would trigger a spinal cord stimulation protocol targeting flexion components. We previously showed the epidural electrical stimulation applied over upper lumbar segments (L1–L2) primarily modulates muscle synergies related to flexion (Wenger et al., 2016). We thus linked the detection of imminent foot–off events (100 ms anticipation) to the onset of a stimulation burst (200 ms) delivered over the L2 segment.

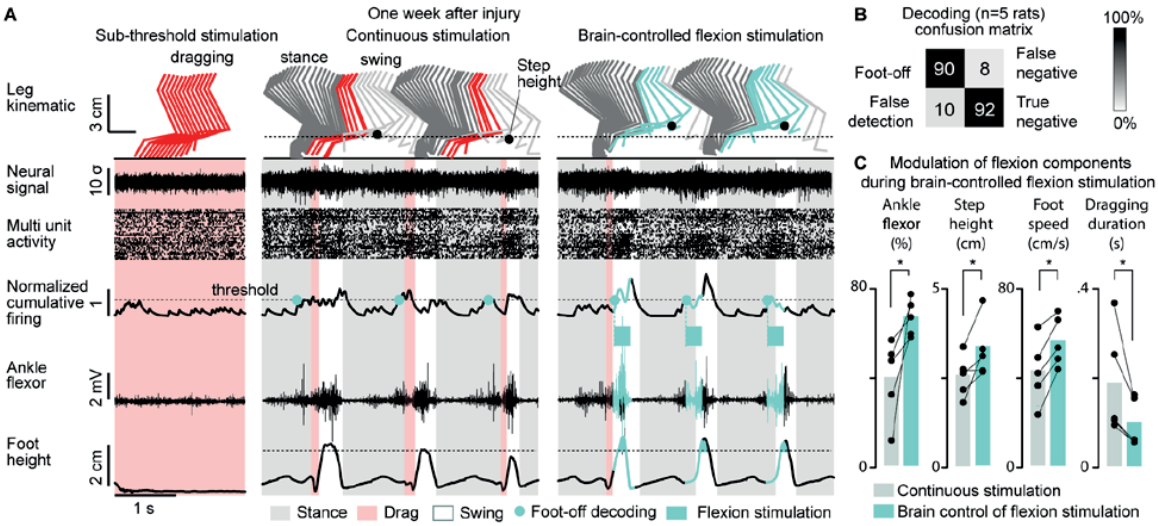

Figure 5.2 | Development and validation of a binary brain–spine interface after contusion. **(A)** Recording performed on a treadmill one week after the severe contusion. From left to right: sub–threshold stimulation of S1 and L2 segments, stimulation of S1 and L2 segments, stimulation of S1 segment plus brain-controlled of L2 segment (flexion stimulation). From top to bottom: color-coded leg kinematics, neuronal signal from a representative channel, multi-unit activity, normalized cumulative firing, electromyographic activity of the tibialis anterior muscle, and vertical displacement of the foot. The gait phases are colour coded. The blue dots indicate swing–off events decoded from cortical population ensemble. The region coloured in blue highlight the occurrence of brain-controlled stimulation over L2. **(B)** Confusion matrix of Foot–off decoding calculated across the 5 rats. **(C)** Bar plots reporting mean values and individual mean values of parameters modulated during continuous stimulation versus brain–controlled stimulation. The relative activation of the tibialis anterior was calculated as a percent of the maximum activity recorded during locomotion. *, $P < 0.05$.

Rats were tested 2 weeks post–injury during locomotion on a treadmill. The binary brain–spine interface reliably triggered the stimulation bursts over the lumbar spinal cord (true positive: 96.2 ± 2.4 %, false–negative rejection: 97.6 ± 2.4 %, **Figure 5.2A**). On the average, the stimulation was triggered 102.2 ± 24.5 ms before foot–off events. Compared to continuous stimulation, brain–controlled stimulation led to a 27.3 ± 10.3 % increase in the amplitude of the electromyographic activity recorded from the tibialis anterior muscle (*P = 0.03;* **Figure 5.2C**). This modulation promoted a significant increase in step height (62.6 ± 22.0%; *P = 0.03*) and speed of foot movement during swing (68.4 ± 15.6%; *P = 0.03*), which led to a 44.7 ± 3.4 % reduction in the duration of foot dragging (*P = 0.03,* **Figure 5.2C**).

The same rats were tested after 3 weeks of gait rehabilitation, when they had recovered the ability to initiate and sustain (voluntary) bipedal locomotion overground with the gravity–assist (van den Brand *et al.*, 2012). Decoding of foot–off events remained highly reliable during this task. On the average, 89.2 ± 3.5 % of foot–off events were correctly identified, with a false–positive rejection rate of 92.2 ± 3.4 % (**Supplementary Figure S5.4**). As observed on the treadmill, brain–controlled stimulation mediated a significant increase in step height (35.8 ± 18.3 %; *P = 0.04*) and speed of foot movement during swing (35.5 ± 10.4 %; *P = 0.02*) compared to continuous stimulation (n = 5, **Supplementary Figure S5.4**).

Cortical ensemble population correlates with step height after gait rehabilitation

The binary brain–spine interface reestablished communication between the motor cortex and lumbar spinal cord below the injury. While this neural bypass alleviated some of the impairments related to flexion during locomotion, the amount of transmitted information remained limited, and consequently, gait deficits persisted. We thus sought to increase the resolution of this communication.

To identify additional information embedded in cortical ensemble population, we studied changes in cortical activity in response to gait rehabilitation. Early after injury, we did not identify correlations between cortical ensemble population and the modulation of gait features such as the step height (0% step height variance explained, **Figure 5.3A–B**).

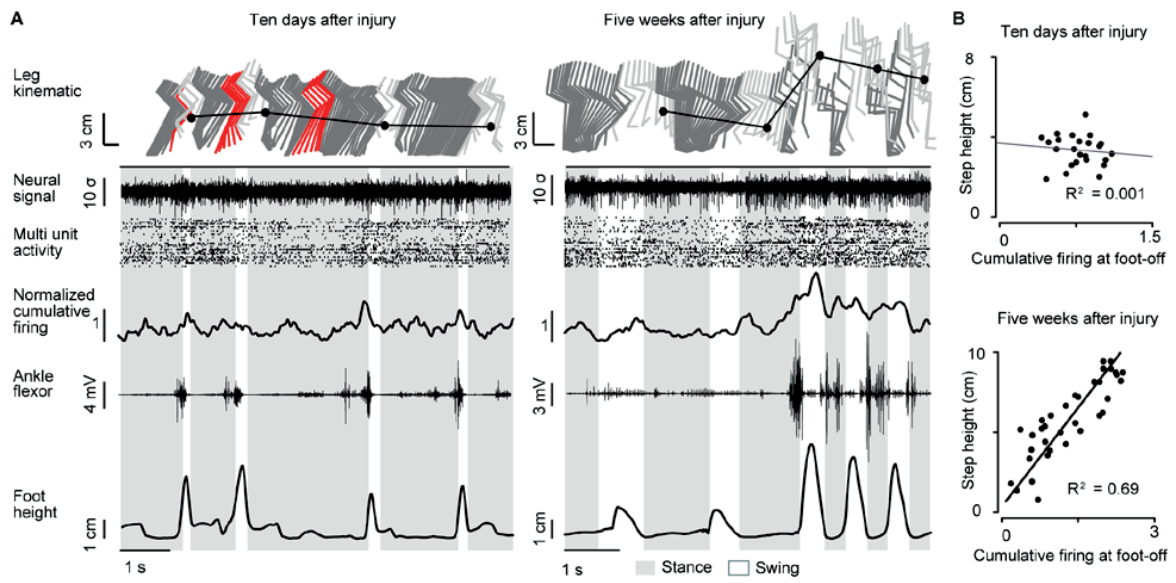

Figure 5.3 | Gait rehabilitation triggers leg flexion encoding in the motor cortex. (A) Bipedal locomotion recorded overground during continuous stimulation at 10 days post–injury. The same rat was recorded after gait rehabilitation, at 5 weeks post–injury. A distractor was presented in front of the rat to encourage variation in foot height. Conventions are the same as in **Figure 5.2**. **(B)** Correlation between cumulative firing at foot–off and the subsequent step height for the rat shown in (A).

When rats had regained the ability to produce robust leg movements after training enabled by the gravity–assist and continuous stimulation, we found a strong linear correlation between the cumulative firing of cortical neurons and the step height. Up to 69% of the variance in step height (49.9 ± 6.9 %) could be predicted from the cumulative firing rate of cortical ensemble population (**Figure 5.3B**, *P = 0.008*). These correlations were consistent with previous findings in healthy rats that associated the peak of cortical activity during swing with the supervision of leg flexion components (Song *et al.*, 2009; Song and Giszter, 2011; Rigosa *et al.*, 2015; DiGiovanna *et al.*, 2016).

Graded modulation of flexion components

We next sought to identify a spinal cord stimulation strategy capable of mediating an increase in the amount of leg flexion during swing that would be proportional to the encoding of step height in

cortical activity. We reasoned that the cumulative firing rate of cortical ensemble population could directly control stimulation protocols that proportionally adjust the amplitude of the step height throughout locomotion.

We previously showed that epidural electrical stimulation applied to upper lumbar segments activates flexor motoneurons pre–synaptically through the recruitment of proprioceptive feedback circuits (Moraud *et al.*, 2016). The activation of these circuits after each pulse of stimulation induces segmental motor responses that can be monitored through electromyographic signals (**Supplementary Figure S5.5A**).

We exploited this property to map the relationships between the amplitude of stimulation applied to L2 segments and the amplitude of flexor muscle activity. For each rat, we found a functional range over which the stimulation elicited motor responses restricted to flexor muscles and proportional to the stimulation amplitude (R^2 = 0.85 ± 0.05 within the functional range ± 50%; **Supplementary Figure S5.5B**).

A proportional brain–spine interface that adjusts step height from cortical activity

We exploited these results to engineer a proportional brain–spine interface that directly and continuously coupled the cumulative firing rates of cortical ensemble population to the intensity of stimulation applied to L2 segment.

A new group of 5 rats participated to these experiments. The animals were tested at 10 days post–injury, when cortical ensemble population associated with locomotion enabled by continuous stimulation showed no correlation with the step height (R^2 = 0 % of explained variance; **Figure 5.4A–B**). In these rats, linking the cumulative firing of cortical neurons to the intensity of stimulation instantly re–established this relationship (**Figure 5.4A–B**). Cortical ensemble activity at foot–off determined 42.2 ± 4.7 % of the variance in the next step (*P = 0.03*, **Figure 5.4B**). This forced link between cortical ensemble population and flexor motoneuron activity mediated the targeted modulation of step height. The proportional brain–spine interface enabled rats tested at 10 days post–injury to produce leg flexion movements with features that reached values close to those recorded in rats after 5 weeks of training enabled by continuous stimulation (R^2 = 49.9 ± 6.9 %; **Figure 5.4B**).

The increased amount of information transmitted across the injury through this proportional brain–spine interface mediated significantly larger improvements of locomotor performance compared to the binary brain–spine interface (on/off only, R^2 = 3.0 ± 3.0 %, *P = 0.03*; **Figure 5.4B**).

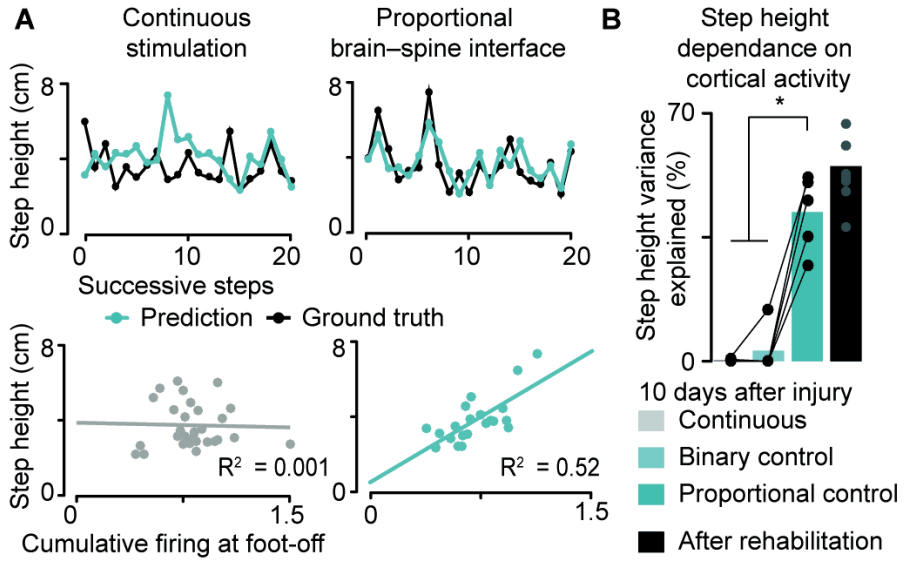

Figure 5.4 | Validation of the proportional brain–spine interface. (A) Actual step heights (black) and predicted step heights (blue) during a continuous sequence of steps with continuous stimulation and the proportional brain–spine interface. The same data is shown in the correlation plots. **(B)** Bar plots reporting the percent of explained variance in step height from the cumulative firing of cortical ensemble population. The same rats (n = 5) were tested with the three conditions of stimulation at 10 days after injury. The same analysis was performed in a group of 8 rats that underwent gait rehabilitation for 5 weeks. *, *P < 0.05*.

To illustrate the functional advantages of this proportional brain–spine interface, we tested the rats during stair climbing, which requires a voluntary increase in foot clearance during swing (**Supplementary Figure S5.6A**). When approaching the staircase, all rats (n = 5) displayed an increase depth of cortical ensemble population activity (*P =0.008*; **Supplementary Figure S5.6B**). This additional activity produced proportional increases in stimulation intensity, which in turn allowed the rats to pass the staircase successfully in a larger number of trials compared to continuous stimulation (*P = 0.04*, **Supplementary Figure S5.6B-C**).

Rehabilitation enabled by the proportional brain–spine interface improved recovery

Finally, we exploited these developments to test our main hypothesis. We evaluated whether gravity–assisted rehabilitation enabled by the proportional brain–spine interface mediated a superior motor recovery compared to the same training regimen with continuous stimulation.

Three groups of rats participated in these experiments. The first group (n = 7) was trained during 5 weeks, 5 times per week for 30 min with continuous stimulation, while the second group (n = 6) was trained the same amount of time with the proportional brain–spine interface. A third group was a control group, which was not trained. For both trained groups, locomotor performance was evaluated weekly overground with the gravity–assist and continuous stimulation. To quantify locomotor performance, we applied a principal component analysis to a large number of parameters calculated from kinematic recordings (n = 55 parameters). Locomotor performance was quantified as the distance from intact rats in the space defined by the first three principal components (explained variance, 62.0 %; **Figure 5.5A**).

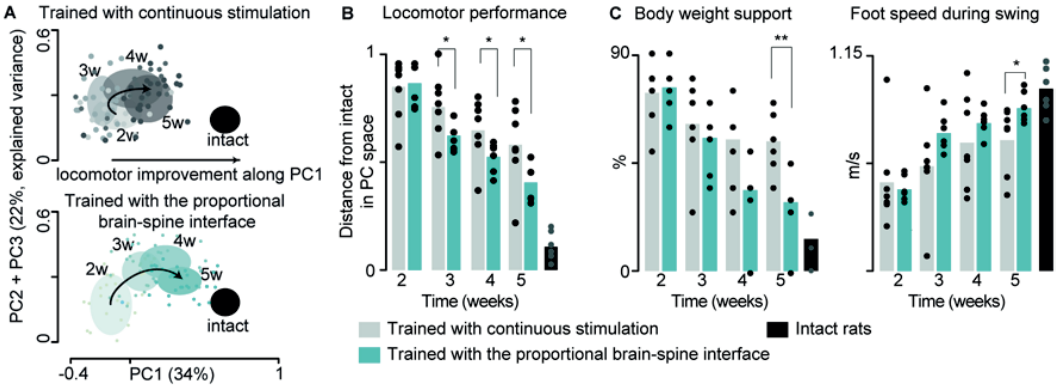

Figure 5.5 | Gait rehabilitation enabled by the proportional brain–spine interface improved recovery. (A) Individual gait cycles recorded during overground locomotion with continuous stimulation every week, from week 2 to week 5, are displayed in the space created by PC1-3 for two rats that are representative of each trained group. The PC analysis was applied on all the gait cycles from all rats at all the time-points. **(B)** Bar plot reporting the mean values of distances between trained rats (n = 6 and 7 rats for the trained group) and intact rats (n = 6) in the PC space over the course of the gait rehabilitation program. This value decreases with improved locomotor performance**. (C)** Bar plots reporting the mean values of body weight support capacities and maximum foot speed during swing. *, *P < 0.05*.

The extent of spinal cord damage was similar across trained rats (tissue sparing, first group: 14.8 ± 5.1 %, second group: 12.0 ± 1.0 %; **Supplementary Figure S5.7**). During the first two weeks post–injury, no difference was detected between both trained groups. Over the course of training, all the rats showed progressive improvements of locomotor performance that contrasted with the absence of voluntary leg movements in non–trained rats ($P < 0.0001$; **Figure 5.5A-B**). However, from the third week and until the end of the rehabilitation program, rats trained with the proportional brain–spine interface exhibited significantly better locomotor performance than rats trained with continuous stimulation ($P = 0.03$; **Figure 5.5B**). Concretely, important gait features such as weight–bearing capacities ($P = 0.01$; **Figure 5.5C**) and foot speed during swing ($P = 0.05$; **Figure 5.5C**) improved significantly more in response to training enabled by the brain–spine interface.

5.5 Discussion

We developed a proportional brain–spine interface that restored communication between the brain and spinal cord located below a severe contusion injury. Brain–controlled stimulation of the denervated spinal cord not only immediately enabled robust movements of the paralyzed legs that supported the execution of complex tasks such as stair climbing, but also improved locomotor recovery compared to continuous stimulation when delivered during rehabilitation. We discuss the implications of these results for the development of brain–spine interface technologies, speculate on the possible mechanisms through which this paradigm enhanced recovery, and consider the next steps for clinical applications.

Next–generation brain–spine interface technologies

In healthy rats, the motor cortex contributes minimally to the production of locomotion (Guo *et al.*, 2015; Kawai *et al.*, 2015). The ablation of the motor cortex only leads to transitory impairments in skilled locomotor behaviors and learning new motor tasks. However, task–dependent leg movements are robustly encoded in the modulation of cortical ensemble population (Song *et al.*, 2009; Manohar *et al.*, 2012; Rigosa *et al.*, 2015; DiGiovanna *et al.*, 2016). Consequently, these cortical signals can be readily exploited to design brain–computer interfaces for locomotor applications (Song and Giszter, 2011; Manohar *et al.*, 2012; Alam *et al.*, 2014).

We confirmed these findings after a severe spinal cord injury. Indeed, we found that the onset of leg flexion could be robustly decoded from cortical ensemble population in rats. In turn, this decoding effectively triggered stimulation protocols that enhanced leg flexion during swing. Moreover, we could maintain a continuous link between the amplitude of cortical population responses and the intensity of stimulation protocols. As early as 10 days after injury, this link allowed paralyzed rats to produce locomotor movements that resembled those observed in rats trained for several weeks. Moreover, the rats effectively exploited the proportional link to increase foot clearance in order to climb a staircase. Importantly, these functional improvements did not require a phase of learning or prior training with the brain–spine interface. Indeed, the neural bypass linked cortical activity that naturally occurs during locomotion to the modulation of proprioceptive feedback circuits that are naturally engaged in the production of locomotion (Moraud *et al.*, 2016). This ecological approach (Courtine and Bloch, 2015) enabled a rapid

calibration of the neural bypass, and its immediate use for the production of adaptive locomotor movements.

We previously developed a wireless brain–spine interface that triggered spinal cord stimulation protocols inducing extension and flexion movements of a paralyzed leg in nonhuman primates (Capogrosso *et al.*, 2016). As observed in rats (Wenger *et al.*, 2016), increasing the amplitude or frequency of stimulation protocols mediated a linear increase in the extent of the extension and flexion of the leg. However, the adjustment of stimulation protocols was pre–programmed. The animals had no control over the parameters of stimulation. Theoretically, the continuous proportional controller developed in rats could translate into phase–dependent control algorithms that continuously modulate the degree of extension and flexion for each leg. Such state–dependent, proportional brain–spine interface has the potential to mediate a markedly more refined prosthetic control of the legs. Future experiments will have to evaluate the viability of this strategy.

Brain–controlled stimulation of the spinal cord enhances motor recovery

Despite its limited contribution to locomotor control, there is growing evidence that the motor cortex of rats play a critical role in motor recovery after injury (van den Brand *et al.*, 2012; Hilton *et al.*, 2016; Hollis *et al.*, 2016; Manohar *et al.*, 2017). Our results are consistent with this model. We observed a progressive recovery of voluntary leg movements in response to gait rehabilitation that coincided with the emergence of strong correlations between cortical ensemble population and leg flexion components. These results suggest that the motor cortex directly contributed to the production of movement following rehabilitation.

However, we speculate that the modulation of motor cortex activity during automated locomotion early after injury was essentially driven by sensory afferent feedback. At this early stage, the electrochemical neuromodulation therapy enables the lumbar spinal cord to interface sensory information with the coordinated recruitment of motor circuits in order to produce locomotion (Manohar *et al.*, 2017). However, supraspinal centers have not been associated with this execution (van den Brand *et al.*, 2012). Therefore, the observed modulation of cortical ensemble population likely resulted from residual neural inputs arising from the spinoparabrachial (Todd, 2010) or spinocerebellar pathways. Due to its anatomical location, these ascending tracts may be partially spared after contusion injuries. Indeed, cutaneous stimulation of the paw produced

reproducible cortical responses in the absence of overt movements, suggesting that sensory pathways mediated the observed modulation of cortical activity (Qi *et al.*, 2014).

We surmise that this property was critical to trigger use–dependent neuroplasticity with the brain–spine interface. In this scenario, the brain–spine interface linked the sensory–driven modulation of cortical ensemble population with stimulation protocols that tuned proprioceptive feedback circuits (Moraud *et al.*, 2016). In turn, this modulation of afferent pathways was directly fed back to cortical ensemble population. Consequently, the neural bypass established a continuous closed–loop connection between cortical and spinal ensemble populations, thus creating the necessary conditions to reinforce the connection between these two populations.

A similar interpretation has been invoked to explain an unexpected neurological recovery in response to a brain–computer interface–based gait rehabilitation (Donati *et al.*, 2016). Paraplegic individuals were trained in an exoskeleton that was actuated based on non–invasive brain recordings. In addition, artificial sensory feedbacks were delivered to both arms in order to feed leg movement–related information to the spinal cord above the injury. Over time, this closed–loop system restored sensation in some of the originally denervated dermatomes.

We propose that, both in rats and humans, these gait rehabilitation programs closing the loop between circuits located above and below the injury increase use–dependent neuroplasticity of residual connections (van den Brand *et al.*, 2012; Nishimura, Perlmutter, Eaton, *et al.*, 2013; McPherson *et al.*, 2015), which enhances functional recovery. Bidirectional spike–timing–dependent plasticity is the most probable mechanism that steers this reorganization (Ethier *et al.*, 2015; McPherson *et al.*, 2015; Krucoff *et al.*, 2016). However, future studies will have to investigate the physiological, anatomical and molecular mechanisms that may support or invalidate our explanation at the level of large neural populations after neurological disorders.

Brain–controlled stimulation of the spinal cord in clinical settings

The proportional brain–spine interface only targeted flexion components and was only tested in rodent models. Despite these limitations, the presents results provide an important proof–of–concept on the relevance of brain–controlled stimulation of the denervated spinal cord to accelerate and augment recovery from spinal cord injury. The ability of the brain–spine interface to restore locomotion in a nonhuman primate model of transient leg paralysis reinforces this

conclusion (Capogrosso *et al.*, 2016). For these previous experiments in primates, our group developed a wireless brain–spine interface integrating intracortical arrays (Hochberg *et al.*, 2012; Collinger *et al.*, 2013), wireless modules (Yin *et al.*, 2014) and pulse generators that have been approved for research applications in humans. Recently, our group also conceived a gravity–assist algorithm that allows gait rehabilitation of paraplegic individuals overground in natural conditions (Mignardot *et al.*, 2017), as implemented in the present study for rodents. This conceptual and technological framework establishes the appropriate conditions to evaluate the therapeutic efficacy of brain–spine interface–based gait rehabilitation for neural repair and recovery in paraplegic individuals.

5.6 Supplementary material

Temporal features of gait
1 Duration of gait cycle
2 Speed of animal during stride
3 Stance duration
4 Swing duration
5 Drag duration

Limb endpoint trajectory
6 Step height
7 Ankle clearance
8 Maximal foot speed during swing
9 Foot acceleration at swing onset
10 Foot speed at swing onset
11 Foot lateral displacement during swing

Stability
12 Stance width
13 Maximum hip vertical position
14 Minimum hip vertical position
15 Hip oscillation amplitude
16 Pelvic center of mass vertical motion

Joint angles
17 Hip joint excursion
18 Knee joint excursion
19 Ankle joint excursion
20 Hip joint speed depth
21 Knee joint speed depth
22 Ankle joint speed depth
23 Foot lateral oscillation

Segmental oscillations
24 Whole-limb excursion amplitude
25 Whole-limb lateral excursion amplitude
26 Whole limb speed depth
27 Crest elevation depth
28 Thigh elevation depth
29 Leg elevation depth
30 Foot elevation depth

Limb coordination
31 Temporal coupling between crest and thigh
32 Temporal coupling between thigh and leg
33 Temporal coupling between leg and foot
34 Correlation between crest and thigh oscillations
35 Correlation between crest and leg oscillations
36 Correlation between crest and foot oscillations
37 Correlation between thigh and leg oscillations
38 Correlation between thigh and foot oscillations
39 Correlation between leg and foot oscillations
40 Relative duration between crest and thigh angle minima
41 Relative duration between crest and leg angle minima
42 Relative duration between crest and foot angle minima
43 Relative duration between thigh and leg angle minima
44 Relative duration between thigh and foot angle minima
45 Relative duration between leg and foot angle minima
46 Phase of Crest maximal contraction
47 Phase of Hip maximal contraction
48 Phase of Knee maximal contraction
49 Phase of Ankle maximal contraction
50 Phase of Foot maximal contraction
51 Lag between crest and thigh maxima
52 Lag between thigh and leg maxima
53 Lag between leg and foot maxima

Robotic assistance required
54 Percentage of body weight supported
55 Robot vertical force

Table ST5.1 | Kinematic and kinetic parameters for PC analysis. Representative kinematic parameters used to assess gait quality in rats.

Animal ID	Binary BSI on treadmill Fig. 2	Binary BSI overground Fig. S4	Cortical modulation vs. spared tissue Fig. S1	Proportional BSI early after SCI Fig. 4	Rehabilitation enabled by proportional BSI Fig. 5	Proportional BSI on staircase Fig. S6	Cutaneous paw stimulation Fig. S2
A1	✓		✓				✓
A2	✓		✓				✓
B1		✓	✓				
B2		✓	✓				
C1			✓				
C2			✓				
D1			✓				
E1	✓	✓	✓				
F1	✓	✓	✓	✓			
F2	✓	✓	✓	✓			
G1				✓			
G2				✓			
G3				✓			
H1					✓		
H2					✓		
H3					✓		
H4					✓		
H5					✓		
H6					✓		
H7					✓		
I1					✓		
I2					✓	✓	
I3					✓	✓	
I4					✓	✓	
I5					✓	✓	
I6					✓	✓	
I1							✓
I2							✓
I3							✓

Table ST5.2 | Experimental groups. Affiliation of animals to experimental groups and an overview of interventions they underwent.

A Variance in step height explained by cortical activity at foot-off

ID animal	Correlation (r value)
A1	0.77
A2	0.83
B1	0.61
B2	0.67
D1	0.35
E1	0.84
F1	0.64
F2	0.79

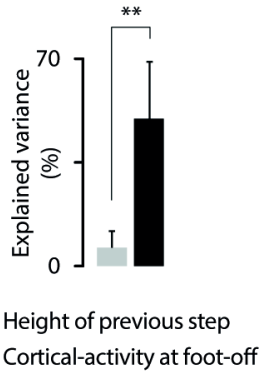

B Modulation of cortical ensemble population increases with the amount of spared tissue

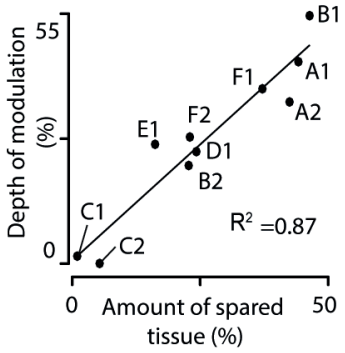

Figure S5.1 | Modulation of cortical ensemble population correlates with step height and depends on the amount of spared tissue. (A) For each rat, the correlation between the cortical activity at foot–off and the step height was calculated. The value of correlation coefficients is reported for each rat. The bar plot reports the mean variance of step height explained by the cortical activity at foot–off measured during the preceding step and for the ongoing step. **, $P < 0.01$. **(B)** Correlation between the amount of spared tissue (%) and the extent of cortical population ensemble modulation during locomotion for all the experimental rats involved in the design of the brain–spine interface. The modulation is expressed in percent of increase of firing rate during locomotion compared to rest. The labels identifying each rat refer to the **Table ST5.1**. Note that rats C1 and C2 were excluded from the study due to the absence of modulation in cortical ensemble population.

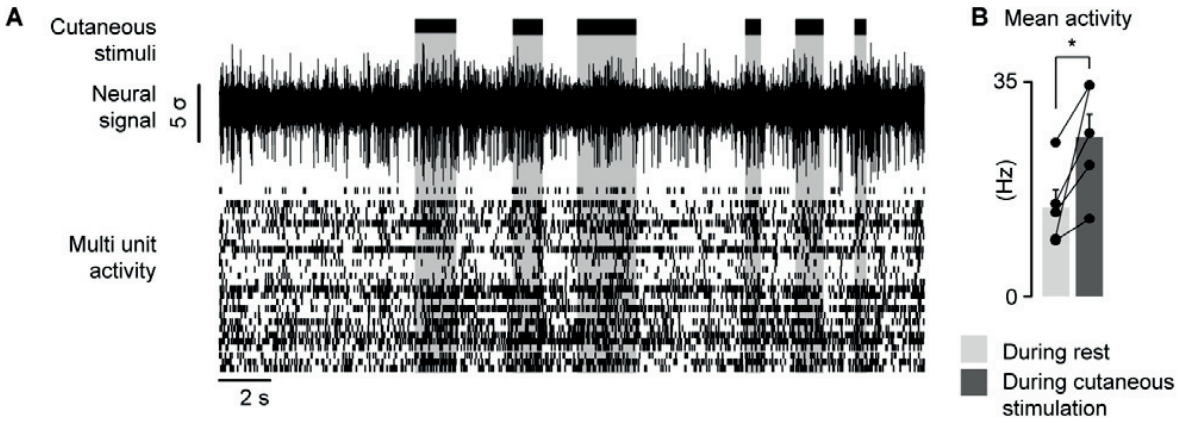

Figure S5.2 | Cortical activity evoked by sensory stimulation of the paw. (A) Example of cortical activity (single channel and multi-unit activity) in response to successive applications of a pressure on the paw contralateral to the recordings. The horizontal bars and shaded region highlight the time windows over which the stimulation was applied. Recordings were performed at 3 weeks post-injury. **(B)** Bar plot reporting the mean activity measured over all the recorded multi-units during rest and over the period of cutaneous stimulation. *, $P < 0.05$.

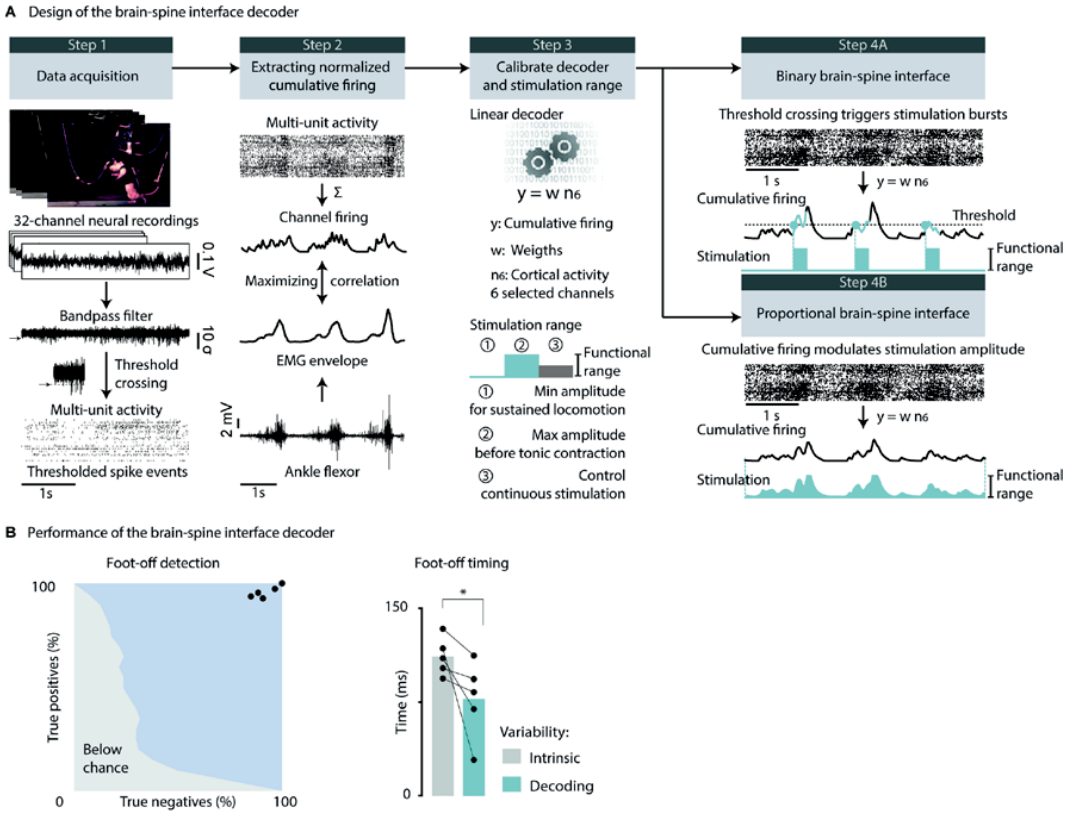

Figure S5.3 | Design of the brain–spine interface decoder. (A) Successive steps involved in the elaboration of the decoders. **Step 1:** Neural signals were synchronized with kinematic and muscle activity recordings during locomotion. Each of the 32 channels from the microwire array implanted into the leg area of the motor cortex was filtered, and then transformed in spiking events. The spiking events were calculated from multi-unit activity, when passing a threshold that was set manually for each channel**. Step 2:** The 6 channels that displayed the largest correlation with the muscle activity measured from the tibialis anterior were isolated. **Step 3**: A linear decoder linking multi-unit activity from the 6 isolated channels with the control variable (step height) was calibrated for each rat. The linear decoder was then implemented in the online processing pipeline. **Step 4A:** The neural recordings were processed online to obtain spike–rate estimates before passing the resulting cumulative firing through the decoder that tracked neural correlates of foot–off events. When the cumulative firing crossed a threshold corresponding to 200 ms before the occurrence of foot–off events, the pulse generator delivered a 200 ms burst of stimulation over the L2 segment. **Step 4B:** The instantaneous values of the cumulative firing continuously (40 Hz) determined the amplitude of the stimulation delivered over the L2 segment. **(B)** Receiver Operating Characteristic (ROC) illustrating the accuracy of foot–off event detections, which lied well above chance level for all the rats (n = 5 rats). Bar plot reporting the variability in the timing of actual and decoded foot–off events across a period of 2 minutes of continuous locomotion. The intrinsic variability of foot–off events was larger than the average error in foot–off event detections.

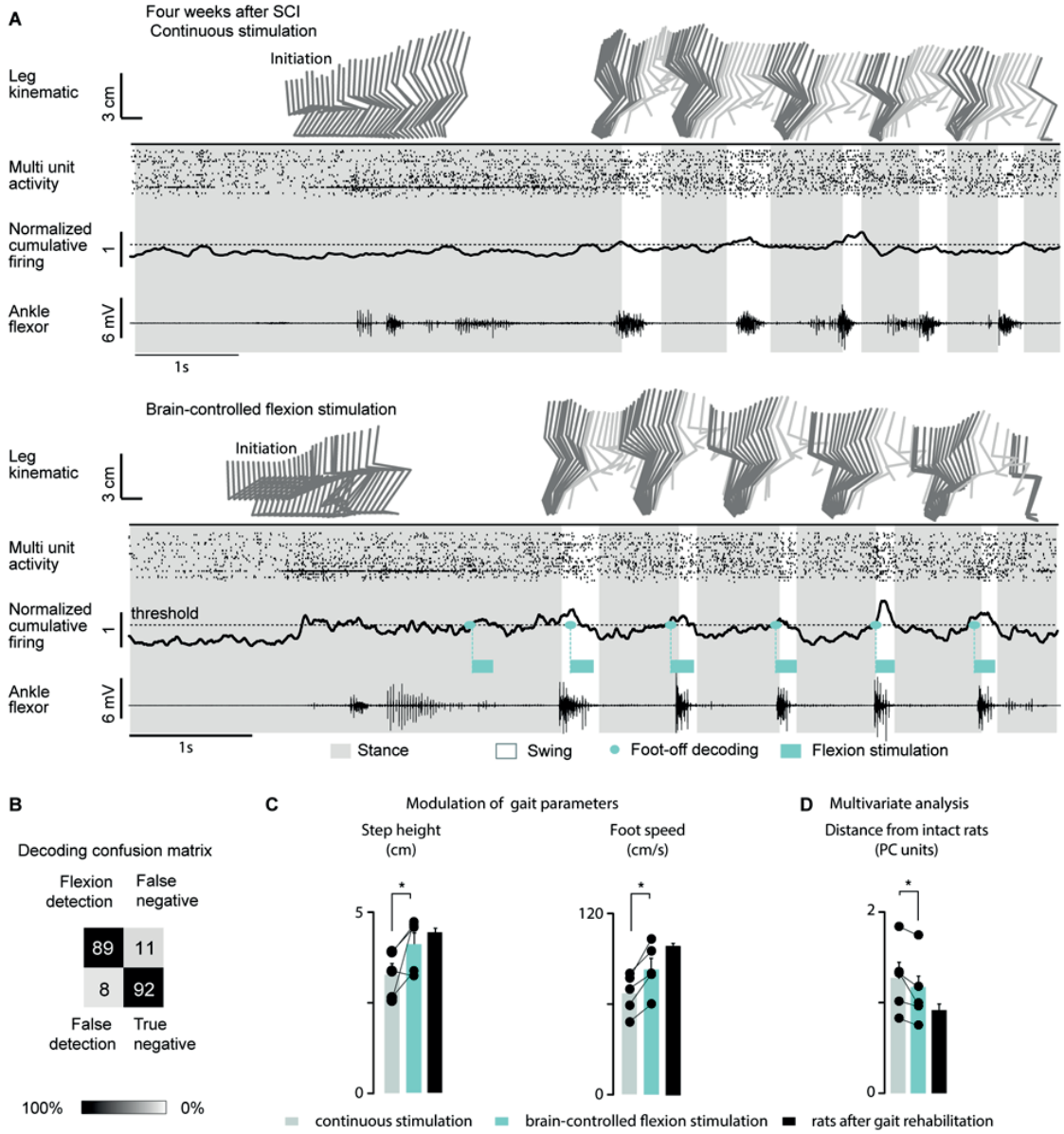

Figure S5.4 | Binary brain–spine interface alleviates locomotor deficits during overground locomotion. (A) Recordings of bipedal locomotion along the runway at 3 weeks post–injury during continuous stimulation and with the binary brain–spine interface. Conventions are the same as in **Fig. 2**. **(B)** Confusion matrix of foot–off event decoding calculated across the 5 rats. **(C)** Bar plots reporting mean values and individual mean values of parameters modulated during continuous stimulation versus brain–controlled flexion stimulation. The values recorded in rats after gait rehabilitation are reported as a reference. **(D)** Bar plot reporting the distance from intact rats in the PC space calculated from 55 gait parameters, which thus quantifies locomotor performance. *, $P < 0.05$.

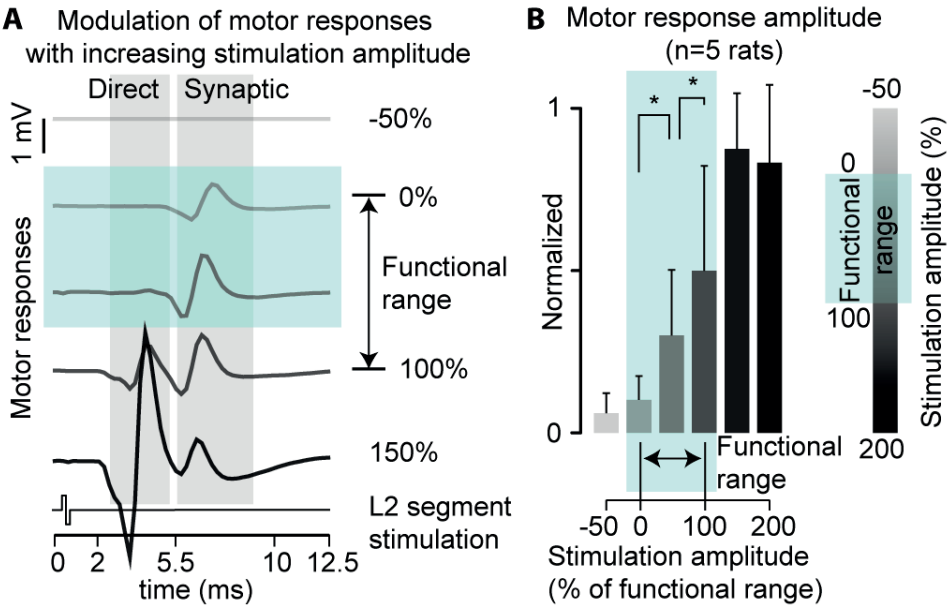

Figure S5.5 | Motor responses following stimulation over the L2 segment. (A) Motor responses recorded from the tibialis anterior muscles following single pulses of stimulation delivered at L2 with increasing amplitudes of stimulation. The value 0 % correspond to the smaller amplitude that was functional to facilitate locomotion. Each response is an average of 10 repetitions. The shaded areas distinguish direct responses (direct stimulation of the motor nerve) from post-synaptic responses, which are elicited from the recruitment of proprioceptive feedback circuits. The blue region highlights the range of amplitudes over which the synaptic responses remained functional, i.e. the stimulation evoked a functional increase in leg flexion components during locomotion without causing co-contraction with other muscles. **(B)** Bar plot reporting the mean amplitude of motor responses over the entire range of tested amplitudes (n = 5 rats). *, $P < 0.05$.

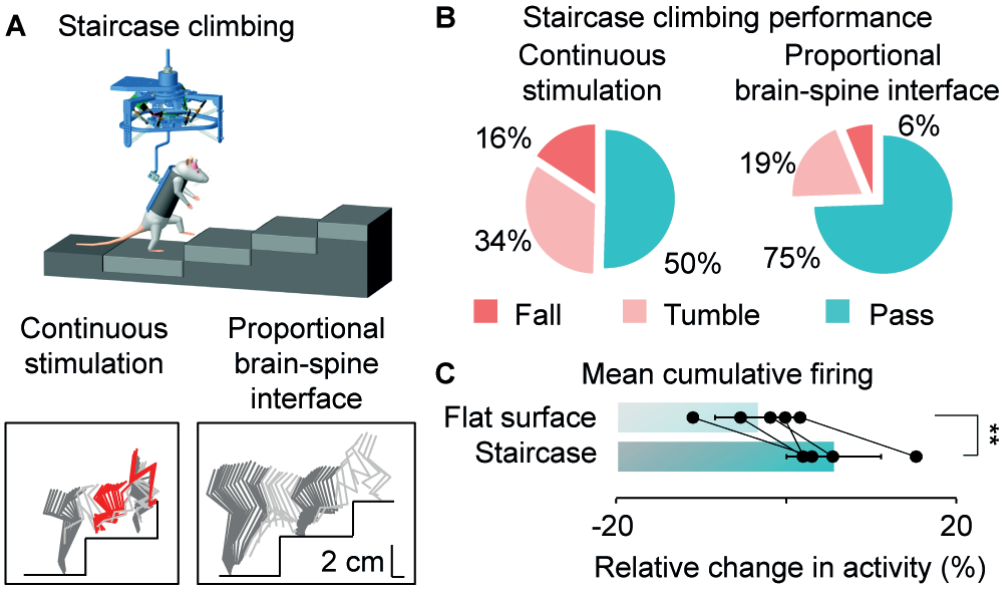

Figure S5.6 | The proportional brain-spine interface improves stair climbing performance. **(A)** Scheme of the locomotor task. **(B)** Circular plots reporting the relative percent of trials with a successful step onto the elevated platform (pass), a tumble and a fall when climbing the staircase with continuous stimulation or proportional brain-spine interface (n = 5 rats). **(C)** Bar plot reporting the mean cumulative firing when progressing along a flat surface and up the staircase. **, $P < 0.01$.

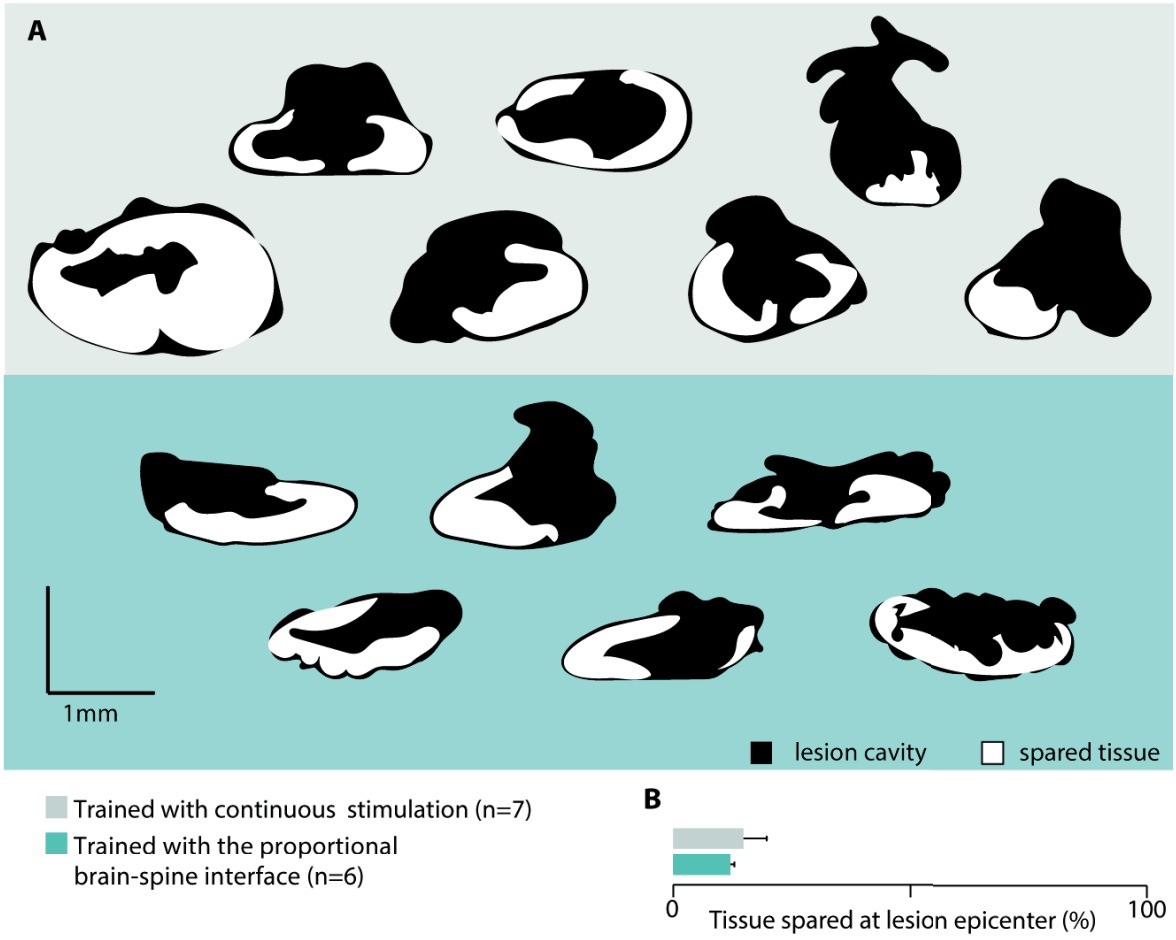

Figure S5.7 | Quantification of the amount of spared spinal cord tissue. (A) Reconstruction of the lesion cavity (black) and spared tissue (white) at the epicentre of the contusion for both trained groups. **(B)** Bar plot reporting the amount of spared tissue for the two trained groups.

6. CONCLUSIONS AND OUTLOOK

This thesis addresses important scientific questions about the potential and limitations of neuroprosthetic treatments to promote locomotor recovery after severe SCI, biological mechanisms underlying this recovery and the possibility to boost these mechanisms through novel neuroprosthetic treatments.

First, we researched the extent to which a combinatorial treatment composed of neurorehabilitation, combinations of EES, pharmacological agents and rehabilitation timing influences locomotor recovery after SCI. To reach this goal, we evaluated the degree of locomotor recovery following different treatment paradigms and locomotor tasks. We further dissected the underlying anatomical mechanisms which enabled this recovery. We identified that the reticulospinal pathway undergoes extensive reorganization after SCI, which contributes to recovery. In particular, we found an increase of projections from the cortex to the reticulospinal pathway in SCI rats as compared to healthy animals. To ascertain the importance of the reorganized reticulospinal pathway, we selectively switched off its descending projections, which led to an immediate impairment of animals' regained ability to walk. Hence, during the first study we successfully enabled locomotor recovery, evaluated the extent to which our neurorehabilitation paradigms are effective and uncovered the biological mechanisms underlying the reported recovery.

We then moved on to develop a neuroprosthetic intervention which would leverage the importance of the reticulospinal pathway and boost the descending supraspinal locomotor command through MLR DBS. To achieve this and to minimize adverse effects caused by MLR DBS, we built an interface where MLR DBS was delivered only when we detected a locomotor command coming from M1. In this study, we achieved superior locomotor output when the rats received M1-controlled MLR DBS as opposed to the no-DBS condition. Additionally, we show that brain-control of MLR DBS was beneficial in relieving the stressful consequences of non-brain-controlled MLR DBS intervention while preserving natural dynamics of locomotion.

Finally, we built another neuroprosthetic system aiming to bypass the SCI and reestablish a direct electronic bridge between M1 and EES delivered to the sublesional spinal cord. This intervention was not only able to promote immediate alleviation of gait disturbances, but was also beneficial for long-term rehabilitation. We report that with our newly developed direct-proportional EES, the

animals recovered their locomotor capacity faster and to a stronger extent than with tonic EES. These findings confirm that reconnecting the sublesional spinal cord and M1 boosts recovery and improves rehabilitation outcomes after SCI. However, the exact mechanisms of the activity-dependent plasticity triggered in this paradigm remain to be uncovered in the future.

Overall, the results presented in my thesis elucidate the mechanisms of locomotor recovery after severe contusion SCI and describe two novel neuroprosthetic techniques aiming to boost activity-dependent plasticity during SCI rehabilitation. In this section I will discuss the main results of my thesis and provide an outlook for future perspectives.

6.1 The role of supraspinal structures in rehabilitation after an incomplete spinal cord injury

Rehabilitation after SCI enhances locomotor recovery through activity-dependent plasticity (Courtine *et al.*, 2008; Edgerton *et al.*, 2008; Lynskey *et al.*, 2008; Fouad and Tetzlaff, 2012). The most impressive recovery to date of full weight-bearing voluntary locomotion was reported after two months of neuroprosthetic rehabilitation combined with electrochemical stimulation (van den Brand *et al.*, 2012). In this study, completely paralyzed rats with a staggered spinal cord hemisection regained their ability to walk due to the reestablishment of brain to spinal cord connections. However, the double-hemisection lesion model never occurs in the natural conditions (Silva *et al.*, 2014). Therefore, in all the studies I did during my thesis, we used a clinically-relevant contusion SCI model (Scheff and Roberts, 2009; Krishna *et al.*, 2013). We first investigated the potential of our neuroprosthetic rehabilitation paradigm and the role of supraspinal structures on recovery after severe contusion SCI, which spares about 10% of spinal cord tissue critically needed for recovery after SCI. Then we moved on to boosting the descending locomotor command through MLR DBS, which we used as an amplifier of the descending locomotor command coming from M1. Overall, in this section I will summarize the main findings of the first two studies presented in my thesis, contextualize them in the existing literature and provide an outlook for the important directions of future research.

6.1.1 *Reticulospinal fibers are essential for relaying the descending locomotor drive*

I argued in the introduction that spontaneous plasticity after SCI occurs at all levels of neural tissue: from reorganization of spinal circuits (Ding *et al.*, 2005; Ballermann and Fouad, 2006) to subcortical and cortical structures (Olivier Raineteau and Schwab, 2001; Jurkiewicz *et al.*, 2007; Rosenzweig *et al.*, 2010). This plasticity is enhanced by training and other neuromodulation strategies (Edgerton *et al.*, 2001; Bradbury and McMahon, 2006). However, the mechanisms underlying recovery after contusion SCI are not yet understood. Therefore, in the first study, we researched the potential and limitations of our neuroprosthetic interventions to promote locomotor recovery after SCI and their mechanisms of action. To investigate this, we introduced rehabilitation in more clinically relevant conditions: chronic and EES-only (no pharmacological treatment) rehabilitation paradigms to closer mimic clinical settings. We found that the animals recovered in all the conditions: acute rehabilitation with full electrochemical neuromodulation, acute rehabilitation with EES only and chronic rehabilitation with full neuromodulation. Remarkably, we found that more than half of the animals from the first group were able to initiate and execute voluntary walking without any neuromodulation after a two month rehabilitation period. Additionally, we observed a carryover effect, which enabled the trained rats to swim in the absence of prior training and with no enabling factors. The other two groups (chronic and EES-only) also regained voluntary stepping capacity, but to a lesser extent than the group trained with full electrochemical neuromodulation starting in an acute phase one week after SCI.

To investigate the mechanisms which enabled this locomotor recovery, we specifically dissected which descending tracts underwent reorganization and probed whether they were indeed essential for the regained voluntary walking capacity. We discovered that activity-dependent plasticity occurred between the motor cortex and the reticulospinal tract, which was partially spared after the dorsal contusion SCI. We then selectively inactivated the reticulospinal connections using a double-virus technique and observed a reversible suppression of the voluntary walking capacity of rehabilitated rats. These results clearly demonstrate that the reorganized reticulospinal pathway is indeed crucial for locomotion of trained rats with severe contusion SCI. Thus, in this study we show that neuroprosthetic rehabilitation combined with electrochemical modulation elicit both behavioral consequences and anatomical remodeling which underlie recovery after SCI. The identified reticulospinal pathway and its importance in the observed recovery provides the groundwork for my second study, which aims to indirectly boost

the supraspinal command descending through the reticulospinal pathway to sublesional spinal circuits.

Further experiments done by another group in our laboratory dissected the role of motor cortex connectivity to the reticulospinal neurons, which constitutes a very important building block in understanding the mechanisms underlying SCI recovery. They found that motor cortex plays an important role in observed locomotor recovery and that optogenetic stimulation of glutamatergic pyramidal neurons in hindlimb motor cortex can facilitate locomotion in mice. In the future, it will also be important to understand the contribution of other supraspinal structures, such as basal ganglia and substantia nigra, to SCI recovery. They are likely to be important actuators because of the descending locomotor drive they produce, the bidirectional projections to the reticular activating system in all vertebrates and their involvement in other neurological disorders (Grillner and Robertson, 2016). Additionally, the extent to which the visual and somatosensory cortices contribute to locomotor recovery needs to be investigated because these structures are strongly affected by motor state (Stryker, 2014; Roseberry *et al.*, 2016). Their contribution can become even more important after SCI, especially in patients, who use their visual system to compensate for the lack of proprioception following SCI (Beloozerova and Sirota, 1993; Drew *et al.*, 1996). Furthermore, it is important to understand how motivational state of the animals contributes to the activity-depending plasticity and locomotor recovery, and whether these mechanisms apply to patients (Bradbury and McMahon, 2006). For example, would motivational stimuli increase rehabilitation outcome in patients? Is there a correlation between activation of nucleus accumbens and effectiveness of rehabilitation and can we boost it? Additionally, we need to understand how pain perception influences rehabilitation and whether blocking it on the spinal or supraspinal level could improve locomotor recovery with training (McMahon *et al.*, 2005). Finally, we have to uncover the mechanisms of recovery and understand which rehabilitation strategies are the most beneficial for facilitating it and promoting activity-dependent plasticity (Silva *et al.*, 2014). Thus, biological changes caused by different interventions, such as neurotropic factors, EES, training, myelin growth-promoting molecules, pharmacological agents and their combinations need to be further investigated in the context of SCI.

6.1.2 *MLR DBS alleviates locomotor deficits post-SCI by utilizing reorganized reticulospinal pathways*

MLR DBS immediately improves locomotion in rats with severe dorsal column lesion (Bachmann *et al.*, 2013) and has been used recently to treat gait deficits in patients with Parkinson's disease (Hamani *et al.*, 2016). Moreover, many studies attribute the STN DBS effect of alleviation of gait disturbances in neuromotor disorders to the MLR (Weiss *et al.*, 2015). This could indeed be a possible mechanism of STN DBS action because of the STN's downstream glutamatergic projections to the MLR (Ryczko and Dubuc, 2013). However, MLR DBS studies in humans have shown variable effects on gait. Moreover some studies have reported adverse effects like alertness and sleep disturbances (Stefani *et al.*, 2007; Thevathasan *et al.*, 2012; Mazzone *et al.*, 2016). Despite extensive research dissecting the role of MLR in locomotion (Ryczko and Dubuc, 2013), there is a clear lack of understanding of how it can be used for SCI treatment. Because of its projections down to the reticulospinal neurons in the brainstem, we hypothesized that the MLR has potential for increasing locomotor output after SCI and promoting activity-dependent plasticity if stimulated during rehabilitation.

Thus, in our second study we investigated how MLR activity is modulated during locomotion before and after SCI. We also studied the impact of MLR DBS on treadmill and overground locomotion using brain-controlled MLR DBS delivery. We found that although MLR DBS induces characteristic forced locomotion initiation in an intensity-dependent way (Shik *et al.*, 1969), natural MLR activity always follows locomotion both in the healthy and post-SCI state. Our findings in healthy animals are in line with a recently published study which also reports MLR activation after locomotor onset and a correlation between MLR activity and speed of locomotion (Roseberry *et al.*, 2016). After the healthy MLR recordings, animals underwent severe contusion SCI and were then trained with the same neurorehabilitation protocol as in the first study. Namely, they received neuroprosthetic training combined with electrochemical neuromodulation for four weeks. Subsequently, we tested modulation of treadmill kinematic parameters with varying MLR DBS intensity and found increased locomotor output with increase in stimulation parameters, similar to other vertebrates (Shik *et al.*, 1969; Ryczko and Dubuc, 2013). The MLR DBS induced incremental increase in step height, which allowed us to find the best stimulation parameters for the overground walking condition. Afterwards, we subjected rats to MLR DBS during the voluntary walking task and found that their locomotor deficits decreased during the DBS ON condition as opposed to DBS OFF. However, this intervention turned out to be stressful for the animals. Therefore, we sought to alleviate these

adverse DBS effects by introducing a brain-controlled DBS delivery paradigm, which I will discuss in the next section along with its potential for inducing activity-dependent plasticity. Overall, our findings provide a proof of concept that MLR DBS indeed alleviates locomotor deficits in rats with severe contusion SCI during a one-time application on both treadmill and overground, such that animals regain their voluntary walking capacity after 4 weeks of rehabilitation.

Despite the significant results on the level of the group, two out of six animals did not show this improvement. These two were the only animals in the study who had less than 5% of their spinal cord tissue spared. The lack of an effect of MLR DBS is most probably due to the lack of neuronal substrate remaining to relay the descending locomotor command. Additionally, we faced many challenges during MLR DBS implantation because anatomical coordinates do not always guarantee the same DBS effect. This is in part due to the fact that MLR is a functionally defined region with inhomogeneous cellular composition (Mazzone *et al.*, 2011). These complications and a critical need to standardize the identification of MLR has been already pointed out in patients (Hamani *et al.*, 2016). Furthermore, we only observed increased kinematic performance when using suprathreshold MLR DBS parameters. This is a critical point which may prevent translation of MLR DBS into patients with SCI. We additionally faced the problem of MLR DBS-induced stress in rats during our study, which has to be largely avoided in clinics. Moreover, we failed to show the effectiveness of MLR DBS in the long term because the MLR DBS kinematic effects disappeared after multiple applications. This could have been caused by a variety of reasons, such as electrode or tissue damage, animals' adaptation to stimulation or rats learning to activate their maximal locomotor capacity even during DBS off trials. Finally, the involvement of the MLR in the regulation of sleep (Stefani *et al.*, 2013), visual responses during locomotion (Lee *et al.*, 2014b), arousal (Garcia-Rill, 2015; Goetz *et al.*, 2016) and reward (Xiao *et al.*, 2016) have to be seriously taken into account during the cost-benefit analysis of MLR DBS implantation in patients.

Nevertheless, there is an ongoing clinical trial researching this intervention in patients with SCI (L.H. Stieglitz, A Curt, 2017). The endpoints and cost-benefit analysis of this clinical study is questionable due to all the complications listed above and the absence of any proof of the longterm MLR DBS effectiveness for SCI treatment. Therefore, investigating longterm effects of MLR DBS and constructing reliable MLR identification procedures are critical steps before translational studies in patients can be performed.

6.2 Brain machine interfaces for promoting locomotor recovery after incomplete SCI

Brain machine interfaces have been proposed as a tool for neuroprosthetic applications to treat neuromotor disorders and to answer basic scientific questions regarding CNS plasticity (Leuthardt *et al.*, 2006; Moxon and Foffani, 2015). Since the pioneering study by Fetz and colleagues, who trained monkeys to increase their brain activity above a threshold to get a reward (Fetz, 1969), immense progress has been made in the field of BMIs. Currently, there has been a decade-long ongoing BrainGate clinical trial (Brower, 2005) to show the safety and efficacy of BMIs for treating tetraplegic patients. The hope is that BMIs will allow these patients to communicate with the external world by interfacing brain decoding with various interventions, such as functional electrical stimulation for reaching and grasping movement restoration (Ajiboye *et al.*, 2017).

Moreover, BMIs have a high potential for driving spike time dependent plasticity because of the possibility to precisely time recorded presynaptic neuron firing with the stimulation of the postsynaptic neuron or neuronal ensembles. For example, BMI induces synaptic plasticity in the corticospinal tract *in vivo* through intraspinal stimulation precisely coupled with the firing activity of pyramidal neurons in the motor cortex (Nishimura, Perlmutter, Eaton, *et al.*, 2013). BMI is also effective in alleviating symptoms of other neurological disorders such as stroke (Guggenmos *et al.*, 2013) and Parkinson's disease (Rosin *et al.*, 2011).

Therefore, the two last studies of my thesis describe how we investigated the effect of brain-controlled MLR DBS (**Chapter 4**) and EES (**Chapter 5**) on locomotor rehabilitation in rats after SCI. Specifically, the first question we tried to answer was whether brain-controlled MLR can be useful for alleviating adverse DBS effects. Afterwards, we investigated the potential of direct-proportional EES in longterm rehabilitation and induction of activity-dependent plasticity. Our findings show that BMI is indeed useful for both alleviating the stressful consequences of MLR DBS and inducing superior locomotor recovery, which I will discuss below along with an outlook for future research directions.

6.2.1 *Brain-controlled MLR DBS and its potential for SCI rehabilitation*

As discussed previously, MLR DBS induces locomotion with short latencies (Shik *et al.*, 1969; Ryczko and Dubuc, 2013) by sending the descending locomotor drive bilaterally to the resticulospinal pathways, which in turn control locomotor neuron pools of proximal and axial muscles (Noga *et al.*, 2003; Matsuyama *et al.*, 2004). MLR DBS has also been used for alleviating gait disturbances in patients with Parkinson's disease (Hamani *et al.*, 2016; Mazzone *et al.*, 2016) and rats with severe SCI (Bachmann *et al.*, 2013). However, some studies report that MLR DBS in patients leads to adverse effects including sleep disturbances and the feeling of alertness (Stefani *et al.*, 2013). Likewise, we found that MLR DBS application dramatically increases the stress level of rats during the voluntary locomotor task and leads to unnatural forced locomotion. Therefore, we investigated whether brain-controlled MLR DBS delivery can be beneficial for locomotor performance and alleviation of stressful DBS consequences as it is in humans (Rosin *et al.*, 2011). Indeed, we found that cortically-triggered MLR DBS evoked stronger kinematic output as opposed to the DBS OFF condition and significantly decreased the stressfulness of intervention compared to the forced MLR DBS. We also found similar locomotor dynamics during M1-triggered MLR DBS and no-DBS conditions, including long and variable initiation latencies characteristic of voluntary locomotion, which suggests that M1-triggered MLR DBS produces more natural stepping dynamics. These results hint that our newly established brain-controlled MLR DBS neuroprosthetic system has a higher translational potential than non brain-controlled MLR DBS delivery. However, the reported side effects and complications, which I discuss in **Chapter 4**, pose important questions about whether MLR DBS should be used in humans and if so, whether brain-controlled MLR DBS delivery is the most reasonable way of doing it.

In the future, it is important to investigate the long-term effects of MLR DBS and its ability to trigger activity-dependent plastic changes during rehabilitation. Additionally, the rapid progress in the field of optogenetics allows targeting precise cell populations, which may be useful for triggering cell-specific activation in the MLR and potentially affecting only locomotor output and not the wakefulness state of the animal. Moreover, it is very important to understand the effectiveness of MLR DBS during repeated applications and the possibility of subthreshold stimulation to induce beneficial plastic changes in the long-term. Furthermore, other possibilities of using M1 input should be considered, for example using the brain signal to proportionally modulate the MLR DBS intensity, as opposed to the ON-OFF DBS delivery. Finally, alternative targets for enhancement

of the descending motor command through the spared fibers of the reticulospinal tract and their potential for promoting plastic changes should be investigated, including the possibility of stimulation of the gigantocellular nucleus itself.

6.2.2 *Direct-proportional BSI for promoting locomotor recovery through activity-dependent plasticity after SCI*

As I described in the introduction, for over half a century SCS has been widely used in patients for treatment of neuromotor disorders (Waltz, 1997), and its synergistic effect with training after SCI has been reported in animals (Edgerton *et al.*, 2008; Courtine *et al.*, 2009). In fact, the mechanisms through which both training and EES act biologically are similar, including both by promoting upregulation of expression of neurotropic factors such as BDNF and by enhancing collateral sprouting of neurons (Bradbury and McMahon, 2006; Udina *et al.*, 2008; Ying *et al.*, 2008). Previous studies have shown that spatiotemporal modulation of EES parameters allows fully transected rats to climb staircases (Wenger *et al.*, 2014) and leads to a much faster and stronger recovery of contused animals (Wenger *et al.*, 2016). On the other hand, BMI is an effective approach to promote specific plastic changes and enhance connections between regions by precisely timing their stimulation application (Guggenmos *et al.*, 2013; Nishimura, Perlmutter, Eaton, *et al.*, 2013). Moreover, a brain spinal interface has recently been reported to induce an acute alleviation of gait deficits in non-human primates with unilateral SCI (Capogrosso *et al.*, 2016). However, the long-term consequences of BSI application in rehabilitation of an incomplete SCI have never been reported before. Thus, in the last **Chapter 5** I describe the neuroprosthetic platform incorporating the brain-controlled EES delivery and its implications for SCI rehabilitation.

Our idea was to use cortically triggered EES to boost the reestablishment of the lost connection between brain and the spinal cord. Namely, we provided self-driven recruitment of spinal locomotor circuits, during which the recorded activity of M1 was proportionally translated into the EES amplitude applied to the dorsal surface of the spinal cord in rats during rehabilitation. For the first time we show a longterm effect of such a system. Namely, rehabilitative training with our newly established direct-proportional EES system facilitated recovery after paralyzing contusion SCI as compared to training with the conventional tonic EES. Although this behavioral recovery is truly important, it is worth investigating the exact biological mechanisms and pathways underlying the observed locomotor improvements. Furthermore, it is important to investigate which temporal

stimulation parameters trigger the most beneficial plastic changes and whether the spatial location of the EES stimulation can be optimized depending on gait phases. Moreover, it would be interesting to study the combinatorial potential of this neuroprosthesis with growth-promoting factors like the nogo and chondroitinase. Finally, it is also worth investigating whether similar effects can be obtained with the non-invasive electrocorticography recordings and transcutaneous SCS, which would make this approach easier to translate to humans.

Overall, both approaches described in this section: cortically-triggered MLR and direct-proportional EES showed beneficial effects for locomotor recovery of rats after SCI. However, questions about how exactly they have to be applied to best trigger the activity-dependent plasticity and recovery after SCI need further investigation. Furthermore, their translational potential and clinically-relevant outcomes need to be thoroughly evaluated before moving into patients, which I will discuss in the next section.

6.3 The future of neurorehabilitation

Since the last century, humanity started a fight against SCI and its devastating consequences, which led to the development of surgical decompression techniques, rehabilitation paradigms and electrical and chemical treatments aiming to decrease inflammation and promote activity-dependent plasticity of locomotor networks after SCI (Kakulas, 1999; Fawcett *et al.*, 2007; Silva *et al.*, 2014). However, to date there is no cure of SCI, and more than half of SCI patients never regain their ability to walk. Therefore, this final chapter will concentrate on promising future directions in the SCI field and will describe the tactics to address remaining questions along with their challenges during translation into clinics.

First of all, the advances in neuroprosthetics have to be mechanistically-driven to allow for better control and predictability of therapeutic outcomes. Thus, understanding the precise mechanisms of neuronal reorganization after SCI and its modulation with training has to be thoroughly investigated before moving into human applications. Importantly, plastic changes at all CNS levels from spinal locomotor network reorganization to changes in other important locomotor structures such as brainstem, MLR, basal ganglia, thalamus and motor cortex need to be dissected in detail. Additionally, the combinatorial potential of different interventions to promote plasticity needs to be further investigated. Finally, treatments for other neuromotor disorders such as stroke may have a high translational potential for SCI treatment and are therefore worth considering (Iseli *et al.*, 1999; Kwon *et al.*, 2016). Overall, the “translation by design approach”, where patients’ needs and translational criteria are applied while planning animal experiments can trigger a more meaningful outcome of early preclinical studies (Curt, 2012; Reier *et al.*, 2012). Therefore, in this section I will discuss the definition of a meaningful outcome, cost-benefit analysis of therapeutic interventions, and how our newly developed neuroprosthethic systems fit into the context of these questions.

6.3.1 ***Lost in translation: key challenges in translating preclinical developments in clinics and ways to solve them***

Multiple advances have been made in developing novel therapies for SCI treatment; however, a cure for this condition continues to elude us. There is an ongoing debate between clinicians and preclinical researchers about what needs to be done to produce research that is clinically relevant and meaningful for patients (Curt, 2012; Wu *et al.*, 2015). Therefore, in this final section, I will discuss and propose possible ways to make a translation from bench to bedside more reliable.

First of all, we need to define goals in terms of a minimally viable outcome and a meaningful test which is sensitive enough to assess it (Wu *et al.*, 2015). Afterwards, the outcome measures have to be robust in assessing the desired achievement for the patient and must be well above the measurement noise (van Hedel *et al.*, 2006). For example, in addition to the standardized 6 minute or 10 meter walking tests, the functional independence measure of the patients has to be assessed and additional goals should be defined with the physiotherapist. Additionally, the rehabilitation should not stop in the clinics, patients have to keep working on their own so that their recovery keeps growing and not reversing after the rehabilitation has finished. Therefore, it is important to perform follow up assessments post-therapy and to aim for long-term improvements.

Second, it is important to define patients' inclusion criteria for specific treatments and determine the best fitting parameters for every therapeutic intervention. For example, when is the best time to start locomotor training? It seems that it is now established that it is best to start rehabilitative training four weeks after the SCI (Curt *et al.*, 2008; Zörner and Schwab, 2010); however, for the EES, DBS and pharmacological treatments the timelines are still unknown. Another question is: Does one treatment fit all? Naturally, it does not, and personalized neuroprosthetic approaches are particularly important in SCI because of its traumatic nature and very variable injury characteristics and consequences. Therefore, a precise definition of patient selection criteria for a particular intervention and robust proof from animal models of the necessary neurobiological substrate for rehabilitation are fundamental. For example, the patient's age, remaining muscle tone, innervation and spared tissue ridge are crucial criteria for selecting a therapeutic intervention and predicting the outcome. Finally, it is very important to perform a comprehensive evaluation of the cost-benefit analysis in terms of both financial burdens and adverse effects, which may be caused by invasive treatments.

6.3.2 *Translational potential of our original brain-controlled neuroprosthetic interventions*

In conclusion, I will discuss our two newly developed neuroprosthetic interventions and their potential for clinical translation according to the crucial criteria outlined above. First of all, there is a common challenge associated with both neuroprosthetic systems because cortical activity undergoes substantial changes after SCI (Moxon *et al.*, 2014). However, despite these changes, we were able to successfully record activity in M1 throughout months of experiments, which was substantial enough to allow the decoding of locomotor intention and modulation.

On our way to establishing cortically-triggered MLR DBS neuroprosthetic rehabilitation from SCI treatment, we detected multiple difficulties of this approach that may make translation to clinics complicated: 1. Surgical targeting of MLR is tricky due to the functional definition of this region. We were only able to achieve consistent implantations with chronically implanted movable electrodes, which are not available for human use; 2. We had to use suprathreshold MLR DBS to induce locomotor effects, and the locomotor effects disappeared with repeated MLR DBS application; 3. MLR DBS turned out to be very stressful for the animals, and even the cortically-triggered MLR DBS delivery lead to increased stress levels as compared to the DBS OFF condition; 4. It was complicated to assess balance-related outcomes due to the use of a rehabilitation model, where rats were always trained and tested with the robotic support, which solves the balance problem. Overall, we concluded that cortically-driven MLR DBS delivery alleviates gait deficits after severe SCI and decreases the stress levels induced by forced MLR DBS. While it is an interesting finding from the scientific perspective, its implication for SCI treatment in humans is less obvious. Therefore, we conclude that MLR DBS is far from being ready for translation into patients with SCI and it is worth identifying a more reliable DBS target with a robust effect on locomotion.

As an alternative, we developed a brain-controlled system, which bypasses the lesion and directly translates cortical activity into EES stimulation amplitude delivered during rehabilitation. The results of this intervention turned out to be promising and showing that our newly developed paradigm applied during rehabilitation leads to a faster and stronger recovery of rats with severe SCI as compared to the tonic EES group. The translational potential of this system is supported by the fact that EES for SCI treatment is already being investigated in two ongoing clinical trials. However, it is hard to imagine the use of invasive cortical recording techniques in patients with incomplete SCI, where our system would have a potential strengthening and rerouting the residual

neuronal pathways for restoring locomotor capacity. Therefore, less invasive techniques and their potential in allowing decoding of cortical activity with sufficient precision for SCI application needs to be investigated. Additonally, we need to keep in mind the challenge of restoring the balance and providing appropriate sensory feedback, which is crucial for rehabilitation during preclinical and clinical investigations.

Overall, the three studies presented in my thesis describe how I tackled the biological mechanisms of SCI recovery and tried to develop translational therapies for its enhancement.

Finally, I do not cease to be amazed by how interesting and ever changing the nervous system is and how many enigmatic mechanisms remain to be uncovered on the way to winning the fight against multiple neurological disorders, including the devastating SCI. I wish a lot of enthusiasm, inspiration and success to all the researchers working hard for this noble cause, and am looking forward to new breakthroughs, which will finally cure patients with SCI.

VI. BIBLIOGRAPHY

Adams M, Cavanagh JFR. International Campaign for Cures of Spinal Cord Injury Paralysis (ICCP): another step forward for spinal cord injury research. Spinal Cord 2004; 42: 273–280.

Ahuja CS, Wilson JR, Nori S, Kotter MRN, Druschel C, Curt A, et al. Traumatic spinal cord injury. 2017; 3: 17018.

Ajiboye AB, Willett FR, Young DR, Memberg WD, Murphy BA, Miller JP, et al. Restoration of reaching and grasping movements through brain-controlled muscle stimulation in a person with tetraplegia: a proof-of-concept demonstration. Lancet Lond. Engl. 2017; 389: 1821–1830.

Alam M, Chen X, Zhang Z, Li Y, He J. A brain-machine-muscle interface for restoring hindlimb locomotion after complete spinal transection in rats. PloS One 2014; 9: e103764.

Alstermark B, Isa T. Circuits for skilled reaching and grasping. Annu. Rev. Neurosci. 2012; 35: 559–578.

del-Ama AJ, Koutsou AD, Moreno JC, de-los-Reyes A, Gil-Agudo A, Pons JL. Review of hybrid exoskeletons to restore gait following spinal cord injury. J. Rehabil. Res. Dev. 2012; 49: 497–514.

Anderson KD. Targeting recovery: priorities of the spinal cord-injured population. J. Neurotrauma 2004; 21: 1371–1383.

Anderson MA, Burda JE, Ren Y, Ao Y, O'Shea TM, Kawaguchi R, et al. Astrocyte scar formation aids central nervous system axon regeneration. Nature 2016; 532: 195–200.

Angeli CA, Edgerton VR, Gerasimenko YP, Harkema SJ. Altering spinal cord excitability enables voluntary movements after chronic complete paralysis in humans. Brain J. Neurol. 2014; 137: 1394–1409.

Armstrong DM. The supraspinal control of mammalian locomotion. J. Physiol. 1988; 405: 1–37.

Aziz TZ, Davies L, Stein J, France S. The role of descending basal ganglia connections to the brain stem in parkinsonian akinesia. Br. J. Neurosurg. 1998; 12: 245–249.

Bachmann LC, Matis A, Lindau NT, Felder P, Gullo M, Schwab ME. Deep brain stimulation of the midbrain locomotor region improves paretic hindlimb function after spinal cord injury in rats. Sci. Transl. Med. 2013; 5: 208ra146.

Baker SN, Perez MA. Reticulospinal Contributions to Gross Hand Function after Human Spinal Cord Injury. J. Neurosci. Off. J. Soc. Neurosci. 2017; 37: 9778–9784.

Baker SN, Zaaimi B, Fisher KM, Edgley SA, Soteropoulos DS. Pathways mediating functional recovery. Prog. Brain Res. 2015; 218: 389–412.

Ballermann M, Fouad K. Spontaneous locomotor recovery in spinal cord injured rats is accompanied by anatomical plasticity of reticulospinal fibers. Eur. J. Neurosci. 2006; 23: 1988–1996.

Barbeau H, Rossignol S. Recovery of locomotion after chronic spinalization in the adult cat. Brain Res. 1987; 412: 84–95.

Barbeau H, Rossignol S. Enhancement of locomotor recovery following spinal cord injury. Curr. Opin. Neurol. 1994; 7: 517–524.

Bareyre FM, Kerschensteiner M, Raineteau O, Mettenleiter TC, Weinmann O, Schwab ME. The injured spinal cord spontaneously forms a new intraspinal circuit in adult rats. Nat. Neurosci. 2004a; 7: 269–277.

Bareyre FM, Kerschensteiner M, Raineteau O, Mettenleiter TC, Weinmann O, Schwab ME. The injured spinal cord spontaneously forms a new intraspinal circuit in adult rats. Nat. Neurosci. 2004b; 7: 269–277.

Barolat G, Myklebust JB, Wenninger W. Effects of spinal cord stimulation on spasticity and spasms secondary to myelopathy. Appl. Neurophysiol. 1988; 51: 29–44.

Barrière G, Leblond H, Provencher J, Rossignol S. Prominent role of the spinal central pattern generator in the recovery of locomotion after partial spinal cord injuries. J. Neurosci. Off. J. Soc. Neurosci. 2008; 28: 3976–3987.
Barthélemy D, Leblond H, Rossignol S. Characteristics and mechanisms of locomotion induced by intraspinal microstimulation and dorsal root stimulation in spinal cats. J. Neurophysiol. 2007; 97: 1986–2000.
Barthélemy D, Willerslev-Olsen M, Lundell H, Biering-Sørensen F, Nielsen JB. Assessment of transmission in specific descending pathways in relation to gait and balance following spinal cord injury. Prog. Brain Res. 2015; 218: 79–101.
Basso DM, Beattie MS, Bresnahan JC. Graded histological and locomotor outcomes after spinal cord contusion using the NYU weight-drop device versus transection. Exp. Neurol. 1996; 139: 244–256.
Basso DM, Beattie MS, Bresnahan JC. Descending systems contributing to locomotor recovery after mild or moderate spinal cord injury in rats: experimental evidence and a review of literature. Restor. Neurol. Neurosci. 2002; 20: 189–218.
Beauparlant J, van den Brand R, Barraud Q, Friedli L, Musienko P, Dietz V, et al. Undirected compensatory plasticity contributes to neuronal dysfunction after severe spinal cord injury. Brain J. Neurol. 2013; 136: 3347–3361.
Beloozerova IN, Sirota MG. The role of the motor cortex in the control of accuracy of locomotor movements in the cat. J. Physiol. 1993; 461: 1–25.
Benabid AL, Benazzous A, Pollak P. Mechanisms of deep brain stimulation. Mov. Disord. 2002; 17: S73–S74.
Benabid AL, Chabardes S, Mitrofanis J, Pollak P. Deep brain stimulation of the subthalamic nucleus for the treatment of Parkinson's disease. Lancet Neurol. 2009; 8: 67–81.
Blumer CE, Quine S. Prevalence of spinal cord injury: an international comparison. Neuroepidemiology 1995; 14: 258–268.
Borton D, Micera S, Millán J del R, Courtine G. Personalized neuroprosthetics. Sci. Transl. Med. 2013; 5: 210rv2.
Bouton CE, Shaikhouni A, Annetta NV, Bockbrader MA, Friedenberg DA, Nielson DM, et al. Restoring cortical control of functional movement in a human with quadriplegia. Nature 2016; 533: 247–250.
Bradbury EJ, McMahon SB. Spinal cord repair strategies: why do they work? Nat. Rev. Neurosci. 2006; 7: 644–653.
Bramlett HM, Dietrich WD. Progressive damage after brain and spinal cord injury: pathomechanisms and treatment strategies. Prog. Brain Res. 2007; 161: 125–141.
van den Brand R, Heutschi J, Barraud Q, DiGiovanna J, Bartholdi K, Huerlimann M, et al. Restoring voluntary control of locomotion after paralyzing spinal cord injury. Science 2012; 336: 1182–1185.
Bregman BS, McAtee M, Dai HN, Kuhn PL. Neurotrophic Factors Increase Axonal Growth after Spinal Cord Injury and Transplantation in the Adult Rat. Exp. Neurol. 1997; 148: 475–494.
Brocard F, Dubuc R. Differential contribution of reticulospinal cells to the control of locomotion induced by the mesencephalic locomotor region. J. Neurophysiol. 2003; 90: 1714–1727.
Brower V. When mind meets machine. EMBO Rep. 2005; 6: 108–110.
Bruehlmeier M, Dietz V, Leenders KL, Roelcke U, Missimer J, Curt A. How does the human brain deal with a spinal cord injury? Eur. J. Neurosci. 1998; 10: 3918–3922.
Brustein E, Rossignol S. Recovery of locomotion after ventral and ventrolateral spinal lesions in the cat. I. Deficits and adaptive mechanisms. J. Neurophysiol. 1998; 80: 1245–1267.

Calancie B, Lutton S, Broton JG. Central nervous system plasticity after spinal cord injury in man: interlimb reflexes and the influence of cutaneous stimulation. Electroencephalogr. Clin. Neurophysiol. Mot. Control 1996; 101: 304–315.
Capogrosso M, Milekovic T, Borton D, Wagner F, Moraud EM, Mignardot J-B, et al. A brain-spine interface alleviating gait deficits after spinal cord injury in primates. Nature 2016; 539: 284–288.
Capogrosso M, Wenger N, Raspopovic S, Musienko P, Beauparlant J, Bassi Luciani L, et al. A computational model for epidural electrical stimulation of spinal sensorimotor circuits. J. Neurosci. Off. J. Soc. Neurosci. 2013; 33: 19326–19340.
Carmel JB, Berrol LJ, Brus-Ramer M, Martin JH. Chronic electrical stimulation of the intact corticospinal system after unilateral injury restores skilled locomotor control and promotes spinal axon outgrowth. J. Neurosci. Off. J. Soc. Neurosci. 2010; 30: 10918–10926.
Carstens E, Moberg GP. Recognizing Pain and Distress in Laboratory Animals. ILAR J. 2000; 41: 62–71.
Caudle KL, Brown EH, Shum-Siu A, Burke DA, Magnuson TSG, Voor MJ, et al. Hindlimb Immobilization in a Wheelchair Alters Functional Recovery Following Contusive Spinal Cord Injury in the Adult Rat. Neurorehabil. Neural Repair 2011; 25: 729–739.
Cazalets JR, Sqalli-Houssaini Y, Clarac F. Activation of the central pattern generators for locomotion by serotonin and excitatory amino acids in neonatal rat. J. Physiol. 1992; 455: 187–204.
Chen Y, Chen XY, Jakeman LB, Chen L, Stokes BT, Wolpaw JR. Operant conditioning of H-reflex can correct a locomotor abnormality after spinal cord injury in rats. J. Neurosci. Off. J. Soc. Neurosci. 2006; 26: 12537–12543.
Cho TA. Spinal cord functional anatomy. Contin. Minneap. Minn 2015; 21: 13–35.
Collinger JL, Wodlinger B, Downey JE, Wang W, Tyler-Kabara EC, Weber DJ, et al. High-performance neuroprosthetic control by an individual with tetraplegia. Lancet Lond. Engl. 2013; 381: 557–564.
Conta Steencken AC, Stelzner DJ. Loss of propriospinal neurons after spinal contusion injury as assessed by retrograde labeling. Neuroscience 2010; 170: 971–980.
Conway BA, Hultborn H, Kiehn O. Proprioceptive input resets central locomotor rhythm in the spinal cat. Exp. Brain Res. 1987; 68: 643–656.
Cook AW. Electrical stimulation in multiple sclerosis. Hosp. Pract. 1976; 11: 51–58.
Cook AW, Weinstein SP. Chronic dorsal column stimulation in multiple sclerosis. Preliminary report. N. Y. State J. Med. 1973; 73: 2868–2872.
Cortes M, Thickbroom GW, Valls-Sole J, Pascual-Leone A, Edwards DJ. SPINAL ASSOCIATIVE STIMULATION: A NON-INVASIVE STIMULATION PARADIGM TO MODULATE SPINAL EXCITABILITY. Clin. Neurophysiol. Off. J. Int. Fed. Clin. Neurophysiol. 2011; 122: 2254–2259.
Courtine G, Bloch J. Defining ecological strategies in neuroprosthetics. Neuron 2015; 86: 29–33.
Courtine G, Gerasimenko Y, van den Brand R, Yew A, Musienko P, Zhong H, et al. Transformation of nonfunctional spinal circuits into functional states after the loss of brain input. Nat. Neurosci. 2009; 12: 1333–1342.
Courtine G, Song B, Roy RR, Zhong H, Herrmann JE, Ao Y, et al. Recovery of supraspinal control of stepping via indirect propriospinal relay connections after spinal cord injury. Nat. Med. 2008; 14: 69–74.
Cowley KC, Zaporozhets E, Schmidt BJ. Propriospinal neurons are sufficient for bulbospinal transmission of the locomotor command signal in the neonatal rat spinal cord. J. Physiol. 2008; 586: 1623–1635.
Cramer SC, Lastra L, Lacourse MG, Cohen MJ. Brain motor system function after chronic, complete spinal cord injury. Brain J. Neurol. 2005; 128: 2941–2950.
Cregg JM, DePaul MA, Filous AR, Lang BT, Tran A, Silver J. Functional regeneration beyond the glial scar. Exp. Neurol. 2014; 253: 197–207.

Cripps RA, Lee BB, Wing P, Weerts E, Mackay J, Brown D. A global map for traumatic spinal cord injury epidemiology: towards a living data repository for injury prevention. Spinal Cord 2011; 49: 493–501.
Curt A. The translational dialogue in spinal cord injury research. Spinal Cord 2012; 50: 352–357.
Curt A, Van Hedel HJA, Klaus D, Dietz V, EM-SCI Study Group. Recovery from a spinal cord injury: significance of compensation, neural plasticity, and repair. J. Neurotrauma 2008; 25: 677–685.
Daverat P, Sibrac MC, Dartigues JF, Mazaux JM, Marit E, Debelleix X, et al. Early prognostic factors for walking in spinal cord injuries. Paraplegia 1988; 26: 255–261.
Davidson AG, Buford JA. Bilateral actions of the reticulospinal tract on arm and shoulder muscles in the monkey: stimulus triggered averaging. Exp. Brain Res. 2006; 173: 25–39.
Dellu F, Mayo W, Cherkaoui J, Le Moal M, Simon H. Learning disturbances following excitotoxic lesion of cholinergic pedunculo-pontine nucleus in the rat. Brain Res. 1991; 544: 126–132.
DeVivo MJ, Go BK, Jackson AB. Overview of the national spinal cord injury statistical center database. J. Spinal Cord Med. 2002; 25: 335–338.
Diehl P, Kliesch U, Dietz V, Curt A. Impaired facilitation of motor evoked potentials in incomplete spinal cord injury. J. Neurol. 2006; 253: 51–57.
Dietz V. Behavior of spinal neurons deprived of supraspinal input. Nat. Rev. Neurol. 2010; 6: 167–174.
Dietz V, Curt A. Neurological aspects of spinal-cord repair: promises and challenges. Lancet Neurol. 2006; 5: 688–694.
Dietz V, Fouad K. Restoration of sensorimotor functions after spinal cord injury. Brain 2014; 137: 654–667.
Dietz V, Grillner S, Trepp A, Hubli M, Bolliger M. Changes in spinal reflex and locomotor activity after a complete spinal cord injury: a common mechanism? Brain 2009; 132: 2196–2205.
Dietz V, Harkema SJ. Locomotor activity in spinal cord-injured persons. J. Appl. Physiol. Bethesda Md 1985 2004; 96: 1954–1960.
DiGiovanna J, Dominici N, Friedli L, Rigosa J, Duis S, Kreider J, et al. Engagement of the Rat Hindlimb Motor Cortex across Natural Locomotor Behaviors. J. Neurosci. Off. J. Soc. Neurosci. 2016; 36: 10440–10455.
Dimitrijevic MM, Dimitrijevic MR, Illis LS, Nakajima K, Sharkey PC, Sherwood AM. Spinal cord stimulation for the control of spasticity in patients with chronic spinal cord injury: I. Clinical observations. Cent. Nerv. Syst. Trauma J. Am. Paralys. Assoc. 1986; 3: 129–144.
Dimitrijevic MR, Gerasimenko Y, Pinter MM. Evidence for a Spinal Central Pattern Generator in Humansa. Ann. N. Y. Acad. Sci. 1998; 860: 360–376.
Ding Y, Kastin AJ, Pan W. Neural Plasticity After Spinal Cord Injury. Curr. Pharm. Des. 2005; 11: 1441–1450.
Ditunno PL, Patrick M, Stineman M, Ditunno JF. Who wants to walk? Preferences for recovery after SCI: a longitudinal and cross-sectional study. Spinal Cord 2008; 46: 500–506.
Dominici N, Keller U, Vallery H, Friedli L, van den Brand R, Starkey ML, et al. Versatile robotic interface to evaluate, enable and train locomotion and balance after neuromotor disorders. Nat. Med. 2012; 18: 1142–1147.
Donati ARC, Shokur S, Morya E, Campos DSF, Moioli RC, Gitti CM, et al. Long-Term Training with a Brain-Machine Interface-Based Gait Protocol Induces Partial Neurological Recovery in Paraplegic Patients. Sci. Rep. 2016; 6: 30383.
Donovan WH. Spinal Cord Injury—Past, Present, and Future. J. Spinal Cord Med. 2007; 30: 85–100.
Drew T, Dubuc R, Rossignol S. Discharge patterns of reticulospinal and other reticular neurons in chronic, unrestrained cats walking on a treadmill. J. Neurophysiol. 1986; 55: 375–401.
Drew T, Jiang W, Kably B, Lavoie S. Role of the motor cortex in the control of visually triggered gait modifications. Can. J. Physiol. Pharmacol. 1996; 74: 426–442.

Dringenberg HC, Olmstead MC. Integrated contributions of basal forebrain and thalamus to neocortical activation elicited by pedunculopontine tegmental stimulation in urethane-anesthetized rats. Neuroscience 2003; 119: 839–853.
Edgerton VR, Courtine G, Gerasimenko YP, Lavrov I, Ichiyama RM, Fong AJ, et al. Training locomotor networks. Brain Res. Rev. 2008; 57: 241–254.
Edgerton VR, de Leon RD, Harkema SJ, Hodgson JA, London N, Reinkensmeyer DJ, et al. Retraining the injured spinal cord. J. Physiol. 2001; 533: 15–22.
Edgerton VR, Tillakaratne NJK, Bigbee AJ, de Leon RD, Roy RR. Plasticity of the spinal neural circuitry after injury. Annu. Rev. Neurosci. 2004; 27: 145–167.
Eidelberg E. Consequences of spinal cord lesions upon motor function, with special reference to locomotor activity. Prog. Neurobiol. 1981; 17: 185–202.
Esposito MS, Capelli P, Arber S. Brainstem nucleus MdV mediates skilled forelimb motor tasks. Nature 2014; 508: 351–356.
Ethier C, Gallego JA, Miller LE. Brain-controlled neuromuscular stimulation to drive neural plasticity and functional recovery. Curr. Opin. Neurobiol. 2015; 33: 95–102.
Ethier C, Oby ER, Bauman MJ, Miller LE. Restoration of grasp following paralysis through brain-controlled stimulation of muscles. Nature 2012; 485: 368–371.
Everaert DG, Thompson AK, Chong SL, Stein RB. Does functional electrical stimulation for foot drop strengthen corticospinal connections? Neurorehabil. Neural Repair 2010; 24: 168–177.
Fawcett JW, Curt A, Steeves JD, Coleman WP, Tuszynski MH, Lammertse D, et al. Guidelines for the conduct of clinical trials for spinal cord injury as developed by the ICCP panel: spontaneous recovery after spinal cord injury and statistical power needed for therapeutic clinical trials. Spinal Cord 2007; 45: 190–205.
Feldman DE. The spike-timing dependence of plasticity. Neuron 2012; 75: 556–571.
Feldman RP, Goodrich JT. The Edwin Smith Surgical Papyrus. Childs Nerv. Syst. ChNS Off. J. Int. Soc. Pediatr. Neurosurg. 1999; 15: 281–284.
Ferraye MU, Debû B, Fraix V, Goetz L, Ardouin C, Yelnik J, et al. Effects of pedunculopontine nucleus area stimulation on gait disorders in Parkinson's disease. Brain J. Neurol. 2010; 133: 205–214.
Ferraye MU, Gerardin P, Debû B, Chabardès S, Fraix V, Seigneuret E, et al. Pedunculopontine nucleus stimulation induces monocular oscillopsia. J. Neurol. Neurosurg. Psychiatry 2009; 80: 228–231.
Fetz EE. Operant conditioning of cortical unit activity. Science 1969; 163: 955–958.
Field-Fote E. Spinal Cord Injury Rehabilitation. F.A. Davis; 2009.
Filli L, Engmann AK, Zörner B, Weinmann O, Moraitis T, Gullo M, et al. Bridging the gap: a reticulo-propriospinal detour bypassing an incomplete spinal cord injury. J. Neurosci. Off. J. Soc. Neurosci. 2014; 34: 13399–13410.
Fong AJ, Roy RR, Ichiyama RM, Lavrov I, Courtine G, Gerasimenko Y, et al. Recovery of control of posture and locomotion after a spinal cord injury: solutions staring us in the face. Prog. Brain Res. 2009; 175: 393–418.
Forssberg H, Grillner S, Halbertsma J. The locomotion of the low spinal cat. I. Coordination within a hindlimb. Acta Physiol. Scand. 1980; 108: 269–281.
Fouad K, Pedersen V, Schwab ME, Brösamle C. Cervical sprouting of corticospinal fibers after thoracic spinal cord injury accompanies shifts in evoked motor responses. Curr. Biol. CB 2001; 11: 1766–1770.
Fouad K, Tetzlaff W. Rehabilitative training and plasticity following spinal cord injury. Exp. Neurol. 2012; 235: 91–99.
Frankel HL, Hancock DO, Hyslop G, Melzak J, Michaelis LS, Ungar GH, et al. The value of postural reduction in the initial management of closed injuries of the spine with paraplegia and tetraplegia. Spinal Cord 1969; 7: 179–192.

Freund P, Curt A, Friston K, Thompson A. Tracking Changes following Spinal Cord Injury. The Neuroscientist 2013; 19: 116–128.
Frost SB, Dunham CL, Barbay S, Krizsan-Agbas D, Winter MK, Guggenmos DJ, et al. Output Properties of the Cortical Hindlimb Motor Area in Spinal Cord-Injured Rats. J. Neurotrauma 2015; 32: 1666–1673.
Ganguly K, Poo M. Activity-Dependent Neural Plasticity from Bench to Bedside. Neuron 2013; 80: 729–741.
Garcia-Rill E. The pedunculopontine nucleus. Prog. Neurobiol. 1991; 36: 363–389.
Garcia-Rill E. Waking and the reticular activating system in health and disease [Internet]. 2015. [cited 2017 Jul 6] Available from: http://search.ebscohost.com/login.aspx?direct=true&scope=site&db=nlebk&db=nlabk&AN=986471
Garcia-Rill E, Houser CR, Skinner RD, Smith W, Woodward DJ. Locomotion-inducing sites in the vicinity of the pedunculopontine nucleus. Brain Res. Bull. 1987; 18: 731–738.
Garcia-Rill E, Skinner RD. The mesencephalic locomotor region. II. Projections to reticulospinal neurons. Brain Res. 1987; 411: 13–20.
Gerasimenko YP, Avelev VD, Nikitin OA, Lavrov IA. Initiation of locomotor activity in spinal cats by epidural stimulation of the spinal cord. Neurosci. Behav. Physiol. 2003; 33: 247–254.
Ghosh A, Sydekum E, Haiss F, Peduzzi S, Zörner B, Schneider R, et al. Functional and anatomical reorganization of the sensory-motor cortex after incomplete spinal cord injury in adult rats. J. Neurosci. Off. J. Soc. Neurosci. 2009; 29: 12210–12219.
Girgis J, Merrett D, Kirkland S, Metz G a. S, Verge V, Fouad K. Reaching training in rats with spinal cord injury promotes plasticity and task specific recovery. Brain J. Neurol. 2007; 130: 2993–3003.
Goetz L, Piallat B, Bhattacharjee M, Mathieu H, David O, Chabardès S. The primate pedunculopontine nucleus region: towards a dual role in locomotion and waking state. J. Neural Transm. 2016; 123: 667–678.
Goodrich JT. History of spine surgery in the ancient and medieval worlds. Neurosurg. Focus 2004; 16: E2.
Grillner S. Control of Locomotion in Bipeds, Tetrapods, and Fish [Internet]. In: Comprehensive Physiology. John Wiley & Sons, Inc.; 2011. Available from: http://dx.doi.org/10.1002/cphy.cp010226
Grillner S, El Manira A. The intrinsic operation of the networks that make us locomote. Curr. Opin. Neurobiol. 2015; 31: 244–249.
Grillner S, Robertson B. The Basal Ganglia Over 500 Million Years. Curr. Biol. CB 2016; 26: R1088–R1100.
Guggenmos DJ, Azin M, Barbay S, Mahnken JD, Dunham C, Mohseni P, et al. Restoration of function after brain damage using a neural prosthesis. Proc. Natl. Acad. Sci. 2013; 110: 21177–21182.
Guo J-Z, Graves AR, Guo WW, Zheng J, Lee A, Rodríguez-González J, et al. Cortex commands the performance of skilled movement. eLife 2015; 4: e10774.
Hamani C, Lozano AM, Mazzone PAM, Moro E, Hutchison W, Silburn PA, et al. Pedunculopontine Nucleus Region Deep Brain Stimulation in Parkinson Disease: Surgical Techniques, Side Effects, and Postoperative Imaging. Stereotact. Funct. Neurosurg. 2016; 94: 307–319.
Hamani C, Moro E, Lozano AM. The pedunculopontine nucleus as a target for deep brain stimulation. J. Neural Transm. 2011; 118: 1461–1468.
Hamid S, Hayek R. Role of electrical stimulation for rehabilitation and regeneration after spinal cord injury: an overview. Eur. Spine J. 2008; 17: 1256–1269.

Hampson RE, Song D, Opris I, Santos LM, Shin DC, Gerhardt GA, et al. Facilitation of memory encoding in primate hippocampus by a neuroprosthesis that promotes task-specific neural firing. J. Neural Eng. 2013; 10: 066013.
Harkema S, Gerasimenko Y, Hodes J, Burdick J, Angeli C, Chen Y, et al. Effect of epidural stimulation of the lumbosacral spinal cord on voluntary movement, standing, and assisted stepping after motor complete paraplegia: a case study. Lancet Lond. Engl. 2011; 377: 1938–1947.
Harkema SJ, Schmidt-Read M, Lorenz DJ, Edgerton VR, Behrman AL. Balance and ambulation improvements in individuals with chronic incomplete spinal cord injury using locomotor training-based rehabilitation. Arch. Phys. Med. Rehabil. 2012; 93: 1508–1517.
Hasan SJ, Keirstead HS, Muir GD, Steeves JD. Axonal regeneration contributes to repair of injured brainstem-spinal neurons in embryonic chick. J. Neurosci. Off. J. Soc. Neurosci. 1993; 13: 492–507.
Hathout GM, Bhidayasiri R. Midbrain ataxia: an introduction to the mesencephalic locomotor region and the pedunculopontine nucleus. AJR Am. J. Roentgenol. 2005; 184: 953–956.
Hebb DO. The organization of behavior: a neuropsychological theory. New York; London; Sydney: John Wiley & Sons; 1949.
van Hedel HJA, Wirz M, Curt A. Improving walking assessment in subjects with an incomplete spinal cord injury: responsiveness. Spinal Cord 2006; 44: 352–356.
Herman R, He J, D'Luzansky S, Willis W, Dilli S. Spinal cord stimulation facilitates functional walking in a chronic, incomplete spinal cord injured. Spinal Cord 2002; 40: 65–68.
Hilton BJ, Anenberg E, Harrison TC, Boyd JD, Murphy TH, Tetzlaff W. Re-Establishment of Cortical Motor Output Maps and Spontaneous Functional Recovery via Spared Dorsolaterally Projecting Corticospinal Neurons after Dorsal Column Spinal Cord Injury in Adult Mice. J. Neurosci. Off. J. Soc. Neurosci. 2016; 36: 4080–4092.
Hochberg LR, Bacher D, Jarosiewicz B, Masse NY, Simeral JD, Vogel J, et al. Reach and grasp by people with tetraplegia using a neurally controlled robotic arm. Nature 2012; 485: 372–375.
Hofstoetter US, McKay WB, Tansey KE, Mayr W, Kern H, Minassian K. Modification of spasticity by transcutaneous spinal cord stimulation in individuals with incomplete spinal cord injury. J. Spinal Cord Med. 2014; 37: 202–211.
Hollis ER, Ishiko N, Yu T, Lu C-C, Haimovich A, Tolentino K, et al. Ryk controls remapping of motor cortex during functional recovery after spinal cord injury. Nat. Neurosci. 2016; 19: 697–705.
Holtmaat A, Svoboda K. Experience-dependent structural synaptic plasticity in the mammalian brain. Nat. Rev. Neurosci. 2009; 10: 647–658.
Hooper SL. Central Pattern Generators [Internet]. In: eLS. John Wiley & Sons, Ltd; 2001. [cited 2017 Jul 6] Available from: http://onlinelibrary.wiley.com/doi/10.1038/npg.els.0000032/abstract
Houle JD, Tessler A. Repair of chronic spinal cord injury. Exp. Neurol. 2003; 182: 247–260.
Hubel DH, Wiesel TN. Receptive fields of single neurones in the cat's striate cortex. J. Physiol. 1959; 148: 574–591.
Hubli M, Dietz V. The physiological basis of neurorehabilitation - locomotor training after spinal cord injury. J. NeuroEngineering Rehabil. 2013; 10: 5.
Hughes JT. The Edwin Smith Surgical Papyrus: an analysis of the first case reports of spinal cord injuries. Paraplegia 1988; 26: 71–82.
Ichiyama RM, Gerasimenko Y, Jindrich DL, Zhong H, Roy RR, Edgerton VR. Dose dependence of the 5-HT agonist quipazine in facilitating spinal stepping in the rat with epidural stimulation. Neurosci. Lett. 2008; 438: 281–285.
Illis LS. Central nervous stimulation in neurological disease. J. R. Soc. Med. 1983; 76: 905–909.
Illis LS, Sedgwick EM, Tallis RC. Spinal cord stimulation in multiple sclerosis: clinical results. J. Neurol. Neurosurg. Psychiatry 1980; 43: 1–14.

Iseli E, Cavigelli A, Dietz V, Curt A. Prognosis and recovery in ischaemic and traumatic spinal cord injury: clinical and electrophysiological evaluation. J. Neurol. Neurosurg. Psychiatry 1999; 67: 567–571.
Iwahara T, Atsuta Y, Garcia-Rill E, Skinner RD. Spinal cord stimulation-induced locomotion in the adult cat. Brain Res. Bull. 1992; 28: 99–105.
Jackson A, Mavoori J, Fetz EE. Long-term motor cortex plasticity induced by an electronic neural implant. Nature 2006; 444: 56–60.
Jahn K, Deutschländer A, Stephan T, Kalla R, Hüfner K, Wagner J, et al. Supraspinal locomotor control in quadrupeds and humans. Prog. Brain Res. 2008; 171: 353–362.
Jain N, Florence SL, Qi H-X, Kaas JH. Growth of new brainstem connections in adult monkeys with massive sensory loss. Proc. Natl. Acad. Sci. 2000; 97: 5546–5550.
James ND, Bartus K, Grist J, Bennett DLH, McMahon SB, Bradbury EJ. Conduction failure following spinal cord injury: functional and anatomical changes from acute to chronic stages. J. Neurosci. Off. J. Soc. Neurosci. 2011; 31: 18543–18555.
Jankowska E, Jukes MG, Lund S, Lundberg A. The effect of DOPA on the spinal cord. 6. Half-centre organization of interneurones transmitting effects from the flexor reflex afferents. Acta Physiol. Scand. 1967; 70: 389–402.
Jones BE, Yang TZ. The efferent projections from the reticular formation and the locus coeruleus studied by anterograde and retrograde axonal transport in the rat. J. Comp. Neurol. 1985; 242: 56–92.
Jordan LM. Initiation of locomotion in mammals. Ann. N. Y. Acad. Sci. 1998; 860: 83–93.
Jordan LM, Liu J, Hedlund PB, Akay T, Pearson KG. Descending command systems for the initiation of locomotion in mammals. Brain Res. Rev. 2008; 57: 183–191.
Jurkiewicz MT, Mikulis DJ, McIlroy WE, Fehlings MG, Verrier MC. Sensorimotor cortical plasticity during recovery following spinal cord injury: a longitudinal fMRI study. Neurorehabil. Neural Repair 2007; 21: 527–538.
Juvin L, Le Gal J-P, Simmers J, Morin D. Cervicolumbar coordination in mammalian quadrupedal locomotion: role of spinal thoracic circuitry and limb sensory inputs. J. Neurosci. Off. J. Soc. Neurosci. 2012; 32: 953–965.
Kakulas BA. A review of the neuropathology of human spinal cord injury with emphasis on special features. J. Spinal Cord Med. 1999; 22: 119–124.
Kawai R, Markman T, Poddar R, Ko R, Fantana AL, Dhawale AK, et al. Motor cortex is required for learning but not for executing a motor skill. Neuron 2015; 86: 800–812.
Kennard MA. AGE AND OTHER FACTORS IN MOTOR RECOVERY FROM PRECENTRAL LESIONS IN MONKEYS. Am. J. Physiol. -- Leg. Content 1936; 115: 138.
Kiehn O. Locomotor circuits in the mammalian spinal cord. Annu. Rev. Neurosci. 2006; 29: 279–306.
Kiehn O, Dougherty K. Locomotion: Circuits and Physiology. In: Neuroscience in the 21st Century: From Basic to Clinical. 2013. p. 1209–1236.
Kinoshita M, Matsui R, Kato S, Hasegawa T, Kasahara H, Isa K, et al. Genetic dissection of the circuit for hand dexterity in primates. Nature 2012; 487: 235–238.
Kirshblum SC, Burns SP, Biering-Sorensen F, Donovan W, Graves DE, Jha A, et al. International standards for neurological classification of spinal cord injury (Revised 2011). J. Spinal Cord Med. 2011; 34: 535–546.
Kirshblum SC, O'Connor KC. Predicting neurologic recovery in traumatic cervical spinal cord injury. Arch. Phys. Med. Rehabil. 1998; 79: 1456–1466.
Knash ME, Kido A, Gorassini M, Chan KM, Stein RB. Electrical stimulation of the human common peroneal nerve elicits lasting facilitation of cortical motor-evoked potentials. Exp. Brain Res. 2003; 153: 366–377.

Knútsdóttir S, Thórisdóttir H, Sigvaldason K, Jónsson H, Björnsson A, Ingvarsson P. Epidemiology of traumatic spinal cord injuries in Iceland from 1975 to 2009. Spinal Cord 2012; 50: 123–126.
Kobayashi Y, Isa T. Sensory-motor gating and cognitive control by the brainstem cholinergic system. Neural Netw. 2002; 15: 731–741.
Kokotilo KJ, Eng JJ, Curt A. Reorganization and Preservation of Motor Control of the Brain in Spinal Cord Injury: A Systematic Review. J. Neurotrauma 2009; 26: 2113–2126.
Krajacic A, Ghosh M, Puentes R, Pearse DD, Fouad K. Advantages of delaying the onset of rehabilitative reaching training in rats with incomplete spinal cord injury. Eur. J. Neurosci. 2009; 29: 641–651.
Krajacic A, Weishaupt N, Girgis J, Tetzlaff W, Fouad K. Training-induced plasticity in rats with cervical spinal cord injury: effects and side effects. Behav. Brain Res. 2010; 214: 323–331.
Krames E, Poree L, Deer T, Levy R. Implementing the SAFE Principles for the Development of Pain Medicine Therapeutic Algorithms That Include Neuromodulation Techniques. Neuromodulation J. Int. Neuromodulation Soc. 2009; 12: 104–113.
Krassioukov A, Biering-Sørensen F, Donovan W, Kennelly M, Kirshblum S, Krogh K, et al. International standards to document remaining autonomic function after spinal cord injury. J. Spinal Cord Med. 2012; 35: 202–211.
Kriellaars DJ, Brownstone RM, Noga BR, Jordan LM. Mechanical entrainment of fictive locomotion in the decerebrate cat. J. Neurophysiol. 1994; 71: 2074–2086.
Kringelbach ML, Jenkinson N, Owen SLF, Aziz TZ. Translational principles of deep brain stimulation. Nat. Rev. Neurosci. 2007; 8: 623–635.
Krishna V, Andrews H, Jin X, Yu J, Varma A, Wen X, et al. A Contusion Model of Severe Spinal Cord Injury in Rats [Internet]. J. Vis. Exp. JoVE 2013[cited 2017 May 5] Available from: http://www.ncbi.nlm.nih.gov/pmc/articles/PMC3855925/
Krucoff MO, Rahimpour S, Slutzky MW, Edgerton VR, Turner DA. Enhancing Nervous System Recovery through Neurobiologics, Neural Interface Training, and Neurorehabilitation. Front. Neurosci. 2016; 10: 584.
Kubasak MD, Jindrich DL, Zhong H, Takeoka A, McFarland KC, Muñoz-Quiles C, et al. OEG implantation and step training enhance hindlimb-stepping ability in adult spinal transected rats. Brain J. Neurol. 2008; 131: 264–276.
Kwon BK, Liu J, Messerer C, Kobayashi NR, McGraw J, Oschipok L, et al. Survival and regeneration of rubrospinal neurons 1 year after spinal cord injury. Proc. Natl. Acad. Sci. U. S. A. 2002; 99: 3246–3251.
Kwon H-M, Lynn MJ, Turan TN, Derdeyn CP, Fiorella D, Lane BF, et al. Frequency, Risk Factors, and Outcome of Coexistent Small Vessel Disease and Intracranial Arterial Stenosis: Results From the Stenting and Aggressive Medical Management for Preventing Recurrent Stroke in Intracranial Stenosis (SAMMPRIS) Trial. JAMA Neurol. 2016; 73: 36–42.
Lamy J-C, Boakye M. Non-invasive tools to promote spinal plasticity in humans. Clin. Neurophysiol. Off. J. Int. Fed. Clin. Neurophysiol. 2011; 122: 2114–2115.
Lau B, Welter M-L, Belaid H, Fernandez Vidal S, Bardinet E, Grabli D, et al. The integrative role of the pedunculopontine nucleus in human gait. Brain J. Neurol. 2015; 138: 1284–1296.
Lawrence DG, Kuypers HG. PYRAMIDAL AND NON-PYRAMIDAL PATHWAYS IN MONKEYS: ANATOMICAL AND FUNCTIONAL CORRELATION. Science 1965; 148: 973–975.
Lawrence DG, Kuypers HG. The functional organization of the motor system in the monkey. I. The effects of bilateral pyramidal lesions. Brain J. Neurol. 1968; 91: 1–14.
Le Ray D, Brocard F, Bourcier-Lucas C, Auclair F, Lafaille P, Dubuc R. Nicotinic activation of reticulospinal cells involved in the control of swimming in lampreys. Eur. J. Neurosci. 2003; 17: 137–148.

Le Ray D, Juvin L, Ryczko D, Dubuc R. Chapter 4--supraspinal control of locomotion: the mesencephalic locomotor region. Prog. Brain Res. 2011; 188: 51–70.
Lee AM, Hoy JL, Bonci A, Wilbrecht L, Stryker MP, Niell CM. Identification of a brainstem circuit regulating visual cortical state in parallel with locomotion. Neuron 2014a; 83: 455–466.
Lee AM, Hoy JL, Bonci A, Wilbrecht L, Stryker MP, Niell CM. Identification of a brainstem circuit regulating visual cortical state in parallel with locomotion. Neuron 2014b; 83: 455–466.
Lemon RN, Landau W, Tutssel D, Lawrence DG. Lawrence and Kuypers (1968a, b) revisited: copies of the original filmed material from their classic papers in Brain. Brain J. Neurol. 2012; 135: 2290–2295.
de Leon RD, Hodgson JA, Roy RR, Edgerton VR. Locomotor capacity attributable to step training versus spontaneous recovery after spinalization in adult cats. J. Neurophysiol. 1998; 79: 1329–1340.
Leuthardt EC, Schalk G, Moran D, Ojemann JG. The emerging world of motor neuroprosthetics: a neurosurgical perspective. Neurosurgery 2006; 59: 1-14; discussion 1-14.
Lewis PM, Ackland HM, Lowery AJ, Rosenfeld JV. Restoration of vision in blind individuals using bionic devices: A review with a focus on cortical visual prostheses. Brain Res. 2015; 1595: 51–73.
L.H. Stieglitz, A Curt. Deep Brain Stimulation in Patients With Incomplete Spinal Cord Injury for Improvement of Gait [Internet]. ClinicalTrials.gov 2017[cited 2017 Aug 14] Available from: https://www.smartpatients.com/trials/NCT03053791
Little S, Pogosyan A, Neal S, Zavala B, Zrinzo L, Hariz M, et al. Adaptive Deep Brain Stimulation In Advanced Parkinson Disease. Ann. Neurol. 2013; 74: 449–457.
Lovely RG, Gregor RJ, Roy RR, Edgerton VR. Effects of training on the recovery of full-weight-bearing stepping in the adult spinal cat. Exp. Neurol. 1986; 92: 421–435.
Lynskey JV, Belanger A, Jung R. Activity-dependent plasticity in spinal cord injury. J. Rehabil. Res. Dev. 2008; 45: 229–240.
Maier IC, Ichiyama RM, Courtine G, Schnell L, Lavrov I, Edgerton VR, et al. Differential effects of anti-Nogo-A antibody treatment and treadmill training in rats with incomplete spinal cord injury. Brain J. Neurol. 2009; 132: 1426–1440.
Manohar A, Flint RD, Knudsen E, Moxon KA. Decoding hindlimb movement for a brain machine interface after a complete spinal transection. PloS One 2012; 7: e52173.
Manohar A, Foffani G, Ganzer PD, Bethea JR, Moxon KA. Cortex-dependent recovery of unassisted hindlimb locomotion after complete spinal cord injury in adult rats. eLife 2017; 6
Martinez-Gonzalez C, Andel J van, Bolam JP, Mena-Segovia J. Divergent motor projections from the pedunculopontine nucleus are differentially regulated in Parkinsonism. Brain Struct. Funct. 2014; 219: 1451–1462.
Martinez-Gonzalez C, Bolam JP, Mena-Segovia J. Topographical Organization of the Pedunculopontine Nucleus [Internet]. Front. Neuroanat. 2011; 5[cited 2017 Jun 7] Available from: http://www.ncbi.nlm.nih.gov/pmc/articles/PMC3074429/
Masdeu JC, Alampur U, Cavaliere R, Tavoulareas G. Astasia and gait failure with damage of the pontomesencephalic locomotor region. Ann. Neurol. 1994; 35: 619–621.
Matsuyama K, Nakajima K, Mori F, Aoki M, Mori S. Lumbar commissural interneurons with reticulospinal inputs in the cat: Morphology and discharge patterns during fictive locomotion. J. Comp. Neurol. 2004; 474: 546–561.
Mayr W, Krenn M, Dimitrijevic MR. Epidural and transcutaneous spinal electrical stimulation for restoration of movement after incomplete and complete spinal cord injury. Curr. Opin. Neurol. 2016; 29: 721–726.

Mazzone P, Filho OV, Viselli F, Insola A, Sposato S, Vitale F, et al. Our first decade of experience in deep brain stimulation of the brainstem: elucidating the mechanism of action of stimulation of the ventrolateral pontine tegmentum. J. Neural Transm. 2016; 123: 751–767.
Mazzone P, Lozano A, Stanzione P, Galati S, Scarnati E, Peppe A, et al. Implantation of human pedunculopontine nucleus: a safe and clinically relevant target in Parkinson's disease. Neuroreport 2005; 16: 1877–1881.
Mazzone P, Scarnati E, Garcia-Rill E. The Pedunculopontine Tegmental Nucleus: from Basic Neuroscience to Neurosurgical Applications Commentary. J. Neural Transm. Vienna Austria 1996 2011; 118: 1391–1396.
McDonald JW, Sadowsky C. Spinal-cord injury. The Lancet 2002; 359: 417–425.
McMahon SB, Cafferty WBJ, Marchand F. Immune and glial cell factors as pain mediators and modulators. Exp. Neurol. 2005; 192: 444–462.
McPherson JG, Miller RR, Perlmutter SI. Targeted, activity-dependent spinal stimulation produces long-lasting motor recovery in chronic cervical spinal cord injury. Proc. Natl. Acad. Sci. U. S. A. 2015; 112: 12193–12198.
Melzack R, Wall PD. Pain mechanisms: a new theory. Science 1965; 150: 971–979.
Middlebrooks JC, Bierer JA, Snyder RL. Cochlear implants: the view from the brain. Curr. Opin. Neurobiol. 2005; 15: 488–493.
Mignardot J-B, Le Goff CG, van den Brand R, Capogrosso M, Fumeaux N, Vallery H, et al. A multidirectional gravity-assist algorithm that enhances locomotor control in patients with stroke or spinal cord injury [Internet]. Sci. Transl. Med. 2017; 9Available from: http://stm.sciencemag.org/content/9/399/eaah3621.abstract
Mikulis DJ, Jurkiewicz MT, McIlroy WE, Staines WR, Rickards L, Kalsi-Ryan S, et al. Adaptation in the motor cortex following cervical spinal cord injury. Neurology 2002; 58: 794–801.
Minassian K, Jilge B, Rattay F, Pinter MM, Binder H, Gerstenbrand F, et al. Stepping-like movements in humans with complete spinal cord injury induced by epidural stimulation of the lumbar cord: electromyographic study of compound muscle action potentials. Spinal Cord 2004; 42: 401–416.
Minassian K, McKay WB, Binder H, Hofstoetter US. Targeting Lumbar Spinal Neural Circuitry by Epidural Stimulation to Restore Motor Function After Spinal Cord Injury. Neurotherapeutics 2016; 13: 284–294.
Miocinovic S, Somayajula S, Chitnis S, Vitek JL. History, applications, and mechanisms of deep brain stimulation. JAMA Neurol. 2013; 70: 163–171.
Moraud EM, Capogrosso M, Formento E, Wenger N, DiGiovanna J, Courtine G, et al. Mechanisms Underlying the Neuromodulation of Spinal Circuits for Correcting Gait and Balance Deficits after Spinal Cord Injury. Neuron 2016; 89: 814–828.
Mori RL, Bergsman AE, Holmes MJ, Yates BJ. Role of the medial medullary reticular formation in relaying vestibular signals to the diaphragm and abdominal muscles. Brain Res. 2001; 902: 82–91.
Mori S, Matsui T, Kuze B, Asanome M, Nakajima K, Matsuyama K. Cerebellar-induced locomotion: reticulospinal control of spinal rhythm generating mechanism in cats. Ann. N. Y. Acad. Sci. 1998; 860: 94–105.
Mori S, Matsuyama K, Kohyama J, Kobayashi Y, Takakusaki K. Neuronal constituents of postural and locomotor control systems and their interactions in cats. Brain Dev. 1992; 14 Suppl: S109-120.
Mori S, Nishimura H, Kurakami C, Yamamura T, Aoki M. Controlled locomotion in the mesencephalic cat: distribution of facilitatory and inhibitory regions within pontine tegmentum. J. Neurophysiol. 1978; 41: 1580–1591.

Moritz CT, Perlmutter SI, Fetz EE. Direct control of paralysed muscles by cortical neurons. Nature 2008; 456: 639–642.
Moro E, Lozano AM, Pollak P, Agid Y, Rehncrona S, Volkmann J, et al. Long-term results of a multicenter study on subthalamic and pallidal stimulation in Parkinson's disease. Mov. Disord. 2010; 25: 578–586.
Moxon KA, Foffani G. Brain-Machine Interfaces beyond Neuroprosthetics. Neuron 2015; 86: 55–67.
Moxon KA, Oliviero A, Aguilar J, Foffani G. Cortical reorganization after spinal cord injury: always for good? Neuroscience 2014; 283: 78–94.
Muir GD, Whishaw IQ. Red nucleus lesions impair overground locomotion in rats: a kinetic analysis. Eur. J. Neurosci. 2000; 12: 1113–1122.
Müller-Putz GR, Scherer R, Pfurtscheller G, Rupp R. EEG-based neuroprosthesis control: a step towards clinical practice. Neurosci. Lett. 2005; 382: 169–174.
Müllner A, Gonzenbach RR, Weinmann O, Schnell L, Liebscher T, Schwab ME. Lamina-specific restoration of serotonergic projections after Nogo-A antibody treatment of spinal cord injury in rats. Eur. J. Neurosci. 2008; 27: 326–333.
Murakami F, Song WJ, Katsumaru H. Plasticity of neuronal connections in developing brains of mammals. Neurosci. Res. 1992; 15: 235–253.
Murray KC, Nakae A, Stephens MJ, Rank M, D'Amico J, Harvey PJ, et al. Recovery of motoneuron and locomotor function after spinal cord injury depends on constitutive activity in 5-HT2C receptors. Nat. Med. 2010; 16: 694–700.
Mushahwar VK, Jacobs PL, Normann RA, Triolo RJ, Kleitman N. New functional electrical stimulation approaches to standing and walking. J. Neural Eng. 2007; 4: S181-197.
Musienko P, Brand R van den, Maerzendorfer O, Larmagnac A, Courtine* G. Combinatory Electrical and Pharmacological Neuroprosthetic Interfaces to Regain Motor Function After Spinal Cord Injury. IEEE Trans. Biomed. Eng. 2009; 56: 2707–2711.
Musienko P, van den Brand R, Märzendorfer O, Roy RR, Gerasimenko Y, Edgerton VR, et al. Controlling specific locomotor behaviors through multidimensional monoaminergic modulation of spinal circuitries. J. Neurosci. Off. J. Soc. Neurosci. 2011; 31: 9264–9278.
Nardone R, Höller Y, Höller P, Thon N, Thomschewski A, Brigo F, et al. The role of the ipsilateral primary motor cortex in movement control after spinal cord injury: a TMS study. Neurosci. Lett. 2013; 552: 21–24.
Nathan PW. Effects on movement of surgical incisions into the human spinal cord. Brain J. Neurol. 1994; 117 (Pt 2): 337–346.
Nathan PW, Smith M, Deacon P. Vestibulospinal, reticulospinal and descending propriospinal nerve fibres in man. Brain J. Neurol. 1996; 119 (Pt 6): 1809–1833.
Ni Y, Nawabi H, Liu X, Yang L, Miyamichi K, Tedeschi A, et al. Characterization of long descending premotor propriospinal neurons in the spinal cord. J. Neurosci. Off. J. Soc. Neurosci. 2014; 34: 9404–9417.
Nishibe M, Barbay S, Guggenmos D, Nudo RJ. Reorganization of Motor Cortex after Controlled Cortical Impact in Rats and Implications for Functional Recovery. J. Neurotrauma 2010; 27: 2221–2232.
Nishimura Y, Perlmutter SI, Eaton RW, Fetz EE. Spike-timing dependent plasticity in primate corticospinal connections induced during free behavior. Neuron 2013; 80: 1301–1309.
Nishimura Y, Perlmutter SI, Fetz EE. Restoration of upper limb movement via artificial corticospinal and musculospinal connections in a monkey with spinal cord injury. Front. Neural Circuits 2013; 7: 57.
Noga BR, Kriellaars DJ, Brownstone RM, Jordan LM. Mechanism for activation of locomotor centers in the spinal cord by stimulation of the mesencephalic locomotor region. J. Neurophysiol. 2003; 90: 1464–1478.

Noga BR, Sanchez FJ, Villamil LM, O'Toole C, Kasicki S, Olszewski M, et al. LFP Oscillations in the Mesencephalic Locomotor Region during Voluntary Locomotion [Internet]. Front. Neural Circuits 2017; 11[cited 2017 Jun 13] Available from: http://www.ncbi.nlm.nih.gov/pmc/articles/PMC5437718/

Nógrádi A, Vrbová G. Anatomy and Physiology of the Spinal Cord [Internet]. Landes Bioscience; 2013. [cited 2017 Jun 29] Available from: https://www.ncbi.nlm.nih.gov/books/NBK6229/

Norenberg MD, Smith J, Marcillo A. The pathology of human spinal cord injury: defining the problems. J. Neurotrauma 2004; 21: 429–440.

Nudo RJ, Wise BM, SiFuentes F, Milliken GW. Neural substrates for the effects of rehabilitative training on motor recovery after ischemic infarct. Science 1996; 272: 1791–1794.

Onifer SM, Smith GM, Fouad K. Plasticity After Spinal Cord Injury: Relevance to Recovery and Approaches to Facilitate It. Neurotherapeutics 2011; 8: 283–293.

Orlovskij GN, Deliagina TG, Grillner S. Neuronal control of locomotion : from mollusc to man. Oxford [u.a.: Oxford Univ. Press; 2003.

Paxinos G, Watson C. The Rat Brain in Stereotaxic Coordinates - The New Coronal Set. Academic Press; 2004.

Penfield W, Jasper HH. Epilepsy and the functional anatomy of the human brain,. Boston: Little, Brown; 1954.

Peppe A, Pierantozzi M, Baiamonte V, Moschella V, Caltagirone C, Stanzione P, et al. Deep Brain Stimulation of Pedunculopontine Tegmental Nucleus: Role in Sleep Modulation in Advanced Parkinson Disease Patients—One-Year Follow-Up. Sleep 2012; 35: 1637–1642.

Perlmutter JS, Mink JW. Deep brain stimulation. Annu. Rev. Neurosci. 2006; 29: 229–257.

Petersen JA, Wilm BJ, von Meyenburg J, Schubert M, Seifert B, Najafi Y, et al. Chronic cervical spinal cord injury: DTI correlates with clinical and electrophysiological measures. J. Neurotrauma 2012; 29: 1556–1566.

Peterson CA, Murphy RJ, Dupont-Versteegden EE, Houlé JD. Cycling exercise and fetal spinal cord transplantation act synergistically on atrophied muscle following chronic spinal cord injury in rats. Neurorehabil. Neural Repair 2000; 14: 85–91.

Petruska JC, Ichiyama RM, Jindrich DL, Crown ED, Tansey KE, Roy RR, et al. Changes in motoneuron properties and synaptic inputs related to step training after spinal cord transection in rats. J. Neurosci. Off. J. Soc. Neurosci. 2007; 27: 4460–4471.

Plaha P, Gill SS. Bilateral deep brain stimulation of the pedunculopontine nucleus for Parkinson's disease. Neuroreport 2005; 16: 1883–1887.

Qi H-X, Reed JL, Gharbawie OA, Burish MJ, Kaas JH. Cortical neuron response properties are related to lesion extent and behavioral recovery after sensory loss from spinal cord injury in monkeys. J. Neurosci. Off. J. Soc. Neurosci. 2014; 34: 4345–4363.

Radhakrishna M, Steuer I, Prince F, Roberts M, Mongeon D, Kia M, et al. Double-Blind, Placebo-Controlled, Randomized Phase I/IIa Study (Safety and Efficacy) with Buspirone/Levodopa/Carbidopa (SpinalonTM) in Subjects with Complete AIS A or Motor-Complete AIS B Spinal Cord Injury. Curr. Pharm. Des. 2017; 23: 1789–1804.

Ragnarsson KT. Functional electrical stimulation after spinal cord injury: current use, therapeutic effects and future directions. Spinal Cord 2007; 46: 255–274.

Raineteau O, Schwab ME. Plasticity of motor systems after incomplete spinal cord injury. Nat. Rev. Neurosci. 2001; 2: 263–273.

Raineteau O, Schwab ME. Plasticity of motor systems after incomplete spinal cord injury. Nat. Rev. Neurosci. 2001; 2: 263–273.

Ramón y Cajal S, May RM. Degeneration & regeneration of the nervous system,. London: Oxford University Press, Humphrey Milford; 1928.

Rattay F, Minassian K, Dimitrijevic MR. Epidural electrical stimulation of posterior structures of the human lumbosacral cord: 2. quantitative analysis by computer modeling. Spinal Cord 2000; 38: 473–489.
Rebesco JM, Stevenson IH, Körding KP, Solla SA, Miller LE. Rewiring neural interactions by micro-stimulation. Front. Syst. Neurosci. 2010; 4
Reier PJ, Lane MA, Hall ED, Teng YD, Howland DR. Translational spinal cord injury research: preclinical guidelines and challenges. Handb. Clin. Neurol. 2012; 109: 411–433.
Richardson RR, Cerullo LJ, McLone DG, Gutierrez FA, Lewis V. Percutaneous epidural neurostimulation in modulation of paraplegic spasticity. Six case reports. Acta Neurochir. (Wien) 1979; 49: 235–243.
Richardson RR, McLone DG. Percutaneous epidural neurostimulation for paraplegic spasticity. Surg. Neurol. 1978; 9: 153–155.
Rigosa J, Panarese A, Dominici N, Friedli L, van den Brand R, Carpaneto J, et al. Decoding bipedal locomotion from the rat sensorimotor cortex. J. Neural Eng. 2015; 12: 056014.
Roseberry TK, Lee AM, Lalive AL, Wilbrecht L, Bonci A, Kreitzer AC. Cell-Type-Specific Control of Brainstem Locomotor Circuits by Basal Ganglia. Cell 2016; 164: 526–537.
Rosenzweig ES, Courtine G, Jindrich DL, Brock JH, Ferguson AR, Strand SC, et al. Extensive spontaneous plasticity of corticospinal projections after primate spinal cord injury. Nat. Neurosci. 2010; 13: 1505–1510.
Rosin B, Slovik M, Mitelman R, Rivlin-Etzion M, Haber SN, Israel Z, et al. Closed-loop deep brain stimulation is superior in ameliorating parkinsonism. Neuron 2011; 72: 370–384.
Rossignol S. Neural control of stereotypic limb movements. Handb. Physiol. Sect. 12 Exerc. Regul. Integr. Mult. Syst. 1996: 173–216.
Rossignol S. Neural Control of Stereotypic Limb Movements [Internet]. In: Comprehensive Physiology. John Wiley & Sons, Inc.; 2010. Available from: http://dx.doi.org/10.1002/cphy.cp120105
Rossignol S, Barrière G, Frigon A, Barthélemy D, Bouyer L, Provencher J, et al. Plasticity of locomotor sensorimotor interactions after peripheral and/or spinal lesions. Brain Res. Rev. 2008; 57: 228–240.
Ryczko D, Auclair F, Cabelguen J, Dubuc R. The mesencephalic locomotor region sends a bilateral glutamatergic drive to hindbrain reticulospinal neurons in a tetrapod. J. Comp. Neurol. 2016; 524: 1361–1383.
Ryczko D, Dubuc R. The multifunctional mesencephalic locomotor region. Curr. Pharm. Des. 2013; 19: 4448–4470.
Ryczko D, Grätsch S, Auclair F, Dubé C, Bergeron S, Alpert MH, et al. Forebrain dopamine neurons project down to a brainstem region controlling locomotion. Proc. Natl. Acad. Sci. U. S. A. 2013; 110: E3235–E3242.
Sanes JN, Donoghue JP. Plasticity and primary motor cortex. Annu. Rev. Neurosci. 2000; 23: 393–415.
Sayenko DG, Angeli C, Harkema SJ, Edgerton VR, Gerasimenko YP. Neuromodulation of evoked muscle potentials induced by epidural spinal-cord stimulation in paralyzed individuals. J. Neurophysiol. 2014; 111: 1088–1099.
Scheff S, Roberts KN. Infinite Horizon Spinal Cord Contusion Model [Internet]. In: M.D JC, M.D ZCX, M.D X-MX, M.D JHZ, editor(s). Animal Models of Acute Neurological Injuries. Humana Press; 2009. p. 423–432.[cited 2017 May 12] Available from: http://link.springer.com/chapter/10.1007/978-1-60327-185-1_36
Schiller MD, Mobbs RJ. The historical evolution of the management of spinal cord injury. J. Clin. Neurosci. Off. J. Neurosurg. Soc. Australas. 2012; 19: 1348–1353.

Schmidt BJ, Jordan LM. The role of serotonin in reflex modulation and locomotor rhythm production in the mammalian spinal cord. Brain Res. Bull. 2000; 53: 689–710.
Schrader C, Seehaus F, Capelle HH, Windhagen A, Windhagen H, Krauss JK. Effects of pedunculopontine area and pallidal DBS on gait ignition in Parkinson's disease. Brain Stimulat. 2013; 6: 856–859.
Schucht P, Raineteau O, Schwab ME, Fouad K. Anatomical correlates of locomotor recovery following dorsal and ventral lesions of the rat spinal cord. Exp. Neurol. 2002; 176: 143–153.
Schwab ME, Bartholdi D. Degeneration and regeneration of axons in the lesioned spinal cord. Physiol. Rev. 1996; 76: 319–370.
Scivoletto G, Tamburella F, Laurenza L, Torre M, Molinari M. Who is going to walk? A review of the factors influencing walking recovery after spinal cord injury [Internet]. Front. Hum. Neurosci. 2014; 8[cited 2017 Jun 29] Available from: http://journal.frontiersin.org/article/10.3389/fnhum.2014.00141/full
Scott JM, Warburton DER, Williams D, Whelan S, Krassioukov A. Challenges, concerns and common problems: physiological consequences of spinal cord injury and microgravity. Spinal Cord 2011; 49: 4–16.
Sekhon LH, Fehlings MG. Epidemiology, demographics, and pathophysiology of acute spinal cord injury. Spine 2001; 26: S2-12.
Shapira NA, Okun MS, Wint D, Foote KD, Byars JA, Bowers D, et al. Panic and fear induced by deep brain stimulation. J. Neurol. Neurosurg. Psychiatry 2006; 77: 410–412.
Shaw AC, Jackson AW, Holmes T, Thurman S, Davis GR, McClellan AD. Descending brain neurons in larval lamprey: Spinal projection patterns and initiation of locomotion. Exp. Neurol. 2010; 224: 527–541.
Shealy CN, Mortimer JT, Reswick JB. Electrical inhibition of pain by stimulation of the dorsal columns: preliminary clinical report. Anesth. Analg. 1967; 46: 489–491.
Shik ML, Severin FV, Orlovskiĭ GN. [Control of walking and running by means of electric stimulation of the midbrain]. Biofizika 1966; 11: 659–666.
Shik ML, Severin FV, Orlovsky GN. Control of walking and running by means of electrical stimulation of the mesencephalon. Electroencephalogr. Clin. Neurophysiol. 1969; 26: 549.
Siegfried J, Lazorthes Y, Broggi G. Electrical spinal cord stimulation for spastic movement disorders. Appl. Neurophysiol. 1981; 44: 77–92.
Silva NA, Sousa N, Reis RL, Salgado AJ. From basics to clinical: A comprehensive review on spinal cord injury. Prog. Neurobiol. 2014; 114: 25–57.
Silver J, Schwab ME, Popovich PG. Central nervous system regenerative failure: role of oligodendrocytes, astrocytes, and microglia. Cold Spring Harb. Perspect. Biol. 2014; 7: a020602.
Silver JR. History of the treatment of spinal injuries. Postgrad. Med. J. 2005; 81: 108–114.
Simpson LA, Eng JJ, Hsieh JTC, Wolfe and the Spinal Cord Injury Rehabilitation Evidence (SCIRE) Research Team DL. The Health and Life Priorities of Individuals with Spinal Cord Injury: A Systematic Review. J. Neurotrauma 2012; 29: 1548–1555.
Singh A, Tetreault L, Kalsi-Ryan S, Nouri A, Fehlings MG. Global prevalence and incidence of traumatic spinal cord injury. Clin. Epidemiol. 2014; 6: 309–331.
Sinnamon HM. Preoptic and hypothalamic neurons and the initiation of locomotion in the anesthetized rat. Prog. Neurobiol. 1993; 41: 323–344.
Sławińska U, Rossignol S, Bennett DJ, Schmidt BJ, Frigon A, Fouad K, et al. Comment on 'Restoring voluntary control of locomotion after paralyzing spinal cord injury'. Science 2012; 338: 328; author reply 328.

Smith RR, Brown EH, Shum-Siu A, Whelan A, Burke DA, Benton RL, et al. Swim training initiated acutely after spinal cord injury is ineffective and induces extravasation in and around the epicenter. J. Neurotrauma 2009; 26: 1017–1027.
Song W, Giszter SF. Adaptation to a cortex-controlled robot attached at the pelvis and engaged during locomotion in rats. J. Neurosci. Off. J. Soc. Neurosci. 2011; 31: 3110–3128.
Song W, Ramakrishnan A, Udoekwere UI, Giszter SF. Multiple types of movement-related information encoded in hindlimb/trunk cortex in rats and potentially available for brain-machine interface controls. IEEE Trans. Biomed. Eng. 2009; 56: 2712–2716.
Sotocinal SG, Sorge RE, Zaloum A, Tuttle AH, Martin LJ, Wieskopf JS, et al. The Rat Grimace Scale: A partially automated method for quantifying pain in the laboratory rat via facial expressions. Mol. Pain 2011; 7: 55.
Steeves JD, Jordan LM. Localization of a descending pathway in the spinal cord which is necessary for controlled treadmill locomotion. Neurosci. Lett. 1980; 20: 283–288.
Steeves JD, Jordan LM. Autoradiographic demonstration of the projections from the mesencephalic locomotor region. Brain Res. 1984; 307: 263–276.
Steeves JD, Jordan LM, Lake N. The close proximity of catecholamine-containing cells to the 'mesencephalic locomotor region' (MLR). Brain Res. 1975; 100: 663–670.
Stefani A, Lozano AM, Peppe A, Stanzione P, Galati S, Tropepi D, et al. Bilateral deep brain stimulation of the pedunculopontine and subthalamic nuclei in severe Parkinson's disease. Brain 2007; 130: 1596–1607.
Stefani A, Peppe A, Galati S, Stampanoni Bassi M, D'Angelo V, Pierantozzi M. The Serendipity Case of the Pedunculopontine Nucleus Low-Frequency Brain Stimulation: Chasing a Gait Response, Finding Sleep, and Cognition Improvement [Internet]. Front. Neurol. 2013; 4[cited 2017 Jun 7] Available from: http://www.ncbi.nlm.nih.gov/pmc/articles/PMC3672779/
Steiniger B, Kretschmer BD. Effects of ibotenate pedunculopontine tegmental nucleus lesions on exploratory behaviour in the open field. Behav. Brain Res. 2004; 151: 17–23.
Steuer I, Rouleau P, Guertin PA. Pharmacological approaches to chronic spinal cord injury. Curr. Pharm. Des. 2013; 19: 4423–4436.
Stover SL. Spinal Cord Injury: Clinical Outcomes from the Model Systems. Aspen Publications; 1995.
Stryker MP. A Neural Circuit That Controls Cortical State, Plasticity, and the Gain of Sensory Responses in Mouse. Cold Spring Harb. Symp. Quant. Biol. 2014; 79: 1–9.
Takeoka A, Jindrich DL, Muñoz-Quiles C, Zhong H, van den Brand R, Pham DL, et al. Axon Regeneration Can Facilitate or Suppress Hindlimb Function after Olfactory Ensheathing Glia Transplantation. J. Neurosci. 2011; 31: 4298–4310.
Takeoka A, Vollenweider I, Courtine G, Arber S. Muscle Spindle Feedback Directs Locomotor Recovery and Circuit Reorganization after Spinal Cord Injury. Cell 2014a; 159: 1626–1639.
Takeoka A, Vollenweider I, Courtine G, Arber S. Muscle spindle feedback directs locomotor recovery and circuit reorganization after spinal cord injury. Cell 2014b; 159: 1626–1639.
Taylor CL, Kozak R, Latimer MP, Winn P. Effects of changing reward on performance of the delayed spatial win-shift radial maze task in pedunculopontine tegmental nucleus lesioned rats. Behav. Brain Res. 2004; 153: 431–438.
Thevathasan W, Cole MH, Graepel CL, Hyam JA, Jenkinson N, Brittain J-S, et al. A spatiotemporal analysis of gait freezing and the impact of pedunculopontine nucleus stimulation. Brain J. Neurol. 2012; 135: 1446–1454.
Thevathasan W, Coyne TJ, Hyam JA, Kerr G, Jenkinson N, Aziz TZ, et al. Pedunculopontine nucleus stimulation improves gait freezing in Parkinson disease. Neurosurgery 2011; 69: 1248–1253; discussion 1254.

Thrasher TA, Popovic MR. Functional electrical stimulation of walking: function, exercise and rehabilitation. Ann. Readaptation Med. Phys. Rev. Sci. Soc. Francaise Reeducation Fonct. Readaptation Med. Phys. 2008; 51: 452–460.
Thuret S, Moon LDF, Gage FH. Therapeutic interventions after spinal cord injury. Nat. Rev. Neurosci. 2006; 7: 628–643.
Todd AJ. Neuronal circuitry for pain processing in the dorsal horn. Nat. Rev. Neurosci. 2010; 11: 823–836.
Toft A, Scott DT, Barnett SC, Riddell JS. Electrophysiological evidence that olfactory cell transplants improve function after spinal cord injury. Brain J. Neurol. 2007; 130: 970–984.
Trieschmann RB. Spinal Cord Injuries: Psychological, Social, and Vocational Rehabilitation. Demos Medical Publishing; 1988.
Tripodi M, Stepien AE, Arber S. Motor antagonism exposed by spatial segregation and timing of neurogenesis. Nature 2011; 479: 61–66.
Tsintou M, Dalamagkas K, Seifalian AM. Advances in regenerative therapies for spinal cord injury: a biomaterials approach. Neural Regen. Res. 2015; 10: 726–742.
Turner JA, Lee JS, Schandler SL, Cohen MJ. An fMRI investigation of hand representation in paraplegic humans. Neurorehabil. Neural Repair 2003; 17: 37–47.
Tuszynski MH, Steward O. Concepts and methods for the study of axonal regeneration in the CNS. Neuron 2012; 74: 777–791.
Udina E, Furey M, Busch S, Silver J, Gordon T, Fouad K. Electrical stimulation of intact peripheral sensory axons in rats promotes outgrowth of their central projections. Exp. Neurol. 2008; 210: 238–247.
Ueno M, Yamashita T. Kinematic analyses reveal impaired locomotion following injury of the motor cortex in mice. Exp. Neurol. 2011; 230: 280–290.
Waltz JM. Spinal Cord Stimulation: A Quarter Century of Development and Investigation. Stereotact. Funct. Neurosurg. 1997; 69: 288–299.
Webster DM, Steeves JD. Origins of brainstem-spinal projections in the duck and goose. J. Comp. Neurol. 1988; 273: 573–583.
Weidner N, Ner A, Salimi N, Tuszynski MH. Spontaneous corticospinal axonal plasticity and functional recovery after adult central nervous system injury. Proc. Natl. Acad. Sci. U. S. A. 2001; 98: 3513–3518.
Weiss PH, Herzog J, Pötter-Nerger M, Falk D, Herzog H, Deuschl G, et al. Subthalamic nucleus stimulation improves Parkinsonian gait via brainstem locomotor centers. Mov. Disord. Off. J. Mov. Disord. Soc. 2015; 30: 1121–1125.
Welter M-L, Demain A, Ewenczyk C, Czernecki V, Lau B, El Helou A, et al. PPNa-DBS for gait and balance disorders in Parkinson's disease: a double-blind, randomised study. J. Neurol. 2015; 262: 1515–1525.
Wenger N, Moraud EM, Gandar J, Musienko P, Capogrosso M, Baud L, et al. Spatiotemporal neuromodulation therapies engaging muscle synergies improve motor control after spinal cord injury. Nat. Med. 2016; 22: 138–145.
Wenger N, Moraud EM, Raspopovic S, Bonizzato M, DiGiovanna J, Musienko P, et al. Closed-loop neuromodulation of spinal sensorimotor circuits controls refined locomotion after complete spinal cord injury. Sci. Transl. Med. 2014; 6: 255ra133.
Wernig A, Müller S, Nanassy A, Cagol E. Laufband therapy based on 'rules of spinal locomotion' is effective in spinal cord injured persons. Eur. J. Neurosci. 1995; 7: 823–829.
Wilson P, Kitchener PD. Plasticity of cutaneous primary afferent projections to the spinal dorsal horn. Prog. Neurobiol. 1996; 48: 105–129.
Windle WF, Smart JO, Beers JJ. Residual function after subtotal spinal cord transection in adult cats. Neurology 1958; 8: 518–521.

Winn P. How best to consider the structure and function of the pedunculopontine tegmental nucleus: Evidence from animal studies. J. Neurol. Sci. 2006; 248: 234–250.
Wirz M, Zemon DH, Rupp R, Scheel A, Colombo G, Dietz V, et al. Effectiveness of automated locomotor training in patients with chronic incomplete spinal cord injury: a multicenter trial. Arch. Phys. Med. Rehabil. 2005; 86: 672–680.
Wolpaw JR. The complex structure of a simple memory. Trends Neurosci. 1997; 20: 588–594.
Wu X, Liu J, Tanadini LG, Lammertse DP, Blight AR, Kramer JLK, et al. Challenges for defining minimal clinically important difference (MCID) after spinal cord injury. Spinal Cord 2015; 53: 84–91.
Xiao C, Cho JR, Zhou C, Treweek JB, Chan K, McKinney SL, et al. Cholinergic Mesopontine Signals Govern Locomotion and Reward through Dissociable Midbrain Pathways. Neuron 2016; 90: 333–347.
Yilmaz F, Sahin F, Aktug S, Kuran B, Yilmaz A. Long-term follow-up of patients with spinal cord injury. Neurorehabil. Neural Repair 2005; 19: 332–337.
Yin M, Borton DA, Komar J, Agha N, Lu Y, Li H, et al. Wireless neurosensor for full-spectrum electrophysiology recordings during free behavior. Neuron 2014; 84: 1170–1182.
Ying Z, Roy RR, Zhong H, Zdunowski S, Edgerton VR, Gomez-Pinilla F. BDNF-exercise interactions in the recovery of symmetrical stepping after a cervical hemisection in rats. Neuroscience 2008; 155: 1070–1078.
Zaaimi B, Edgley SA, Soteropoulos DS, Baker SN. Changes in descending motor pathway connectivity after corticospinal tract lesion in macaque monkey. Brain J. Neurol. 2012; 135: 2277–2289.
Zagoraiou L, Akay T, Martin JF, Brownstone RM, Jessell TM, Miles GB. A cluster of cholinergic premotor interneurons modulates mouse locomotor activity. Neuron 2009; 64: 645–662.
Z'Graggen WJ, Fouad K, Raineteau O, Metz GA, Schwab ME, Kartje GL. Compensatory sprouting and impulse rerouting after unilateral pyramidal tract lesion in neonatal rats. J. Neurosci. Off. J. Soc. Neurosci. 2000; 20: 6561–6569.
Zörner B, Bachmann LC, Filli L, Kapitza S, Gullo M, Bolliger M, et al. Chasing central nervous system plasticity: the brainstem's contribution to locomotor recovery in rats with spinal cord injury. Brain J. Neurol. 2014; 137: 1716–1732.
Zörner B, Schwab ME. Anti-Nogo on the go: from animal models to a clinical trial. Ann. N. Y. Acad. Sci. 2010; 1198: E22–E34.
European Commission : CORDIS : Projects & Results Service : Periodic Reporting for period 1 - MoreGrasp (Restoration of upper limb function in individuals with high spinal cord injury by multimodal neuroprostheses for interaction in daily activities) [Internet]. [cited 2017 Jun 28] Available from: http://cordis.europa.eu/result/rcn/196482_en.html
WHO | Spinal cord injury [Internet]. WHO[cited 2017 Jun 28] Available from: http://www.who.int/mediacentre/factsheets/fs384/en/

VII. CURRICULUM VITAE

Galyna Pidpruzhnykova

Avenue Tivoli 32B, 1007 Lausanne, Switzerland
galyna.pidpruzhnykova@gmail.com
+ 41 (0)786575745
galynapidpruzhnykova (Skype)
Ukrainian, DOB: 25. 04. 1990
Swiss Permit B, 2013-present

Education

Swiss Federal Institute of Technology in Lausanne (EPFL) November 2013- November 2017 (expected graduation)
PhD Neuroscience
PhD thesis: "Brain-controlled neuroprosthetic therapies and mechanisms of recovery after spinal cord injury".
Thesis supervisors: Prof. G. Courtine

Eberhard Karls University of Tübingen, DE October 2011- August 2013
MSc Behavioral and Cognitive Neuroscience, grade: Very Good, 1.4/max 1.0
MSc thesis: "Neural correlates of association learning in carrion crows".
Thesis supervisors: Prof., Dr. rer. nat. A. Nieder

Taras Shevchenko National University of Kyiv, UA September 2007- July 2011
BSc Biology, grade: Excellent, 93.7 / 100
BSc thesis: The role of agonists of D2 dopamine receptors in the pathogenesis of experimental ulcerative colitis.
Supervisor: Dr. A.N. Tolstanova

Lyceum Goloseevskiy №241, Kyiv, UA September 2006- July 2007
School Diploma, Graduated with Honors

Professional experience

Swiss Federal Institute of Technology in Lausanne (EPFL) November 2013- November 2017

PhD student, IRP Chair of Spinal Repair

Designed and executed a 4-year project aiming to revolutionize existing rehabilitation techniques after spinal cord injury. The result of the study was the establishment of a highly innovative brain-controlled neuroprosthetic system, which improved locomotor recovery in rats.

- Innovative: performed planning and development of a complex novel neuroprosthetic platform, developed new methodologies and surgical techniques
- Team player: established collaborations with multidisciplinary teams, performed experiments in a team
- Analytical: performed analysis of behavioral and anatomical experiments in rats
- Success-oriented: the project was successfully delivered on time, and resulted in 4 internship reports, a Master's thesis and a scientific publication (currently in preparation).

Department of Animal physiology, University of Tübingen March 2013-August 2013
Center for Integrative Neuroscience (CIN), Tübingen, DE February 2012-October 2012
Research assistant

- Adaptable and fast learner: dug into the new topic and mastered laboratory techniques in short periods
- Organized: planned, executed and analyzed behavioral and neuronal data in rats and crows
- Independent: developed and implemented novel behavioral paradigms and analytical methods

Bioanalytical laboratory "Clinfarm" LTD (Kyiv, UA) June 2010-August 2011
Internship, Biologist-Analyst
Worked as part of a team on the investigation of pharmacokinetic qualities of the generic drug "Quercetin" to compare its performance with the original compound. The result of this study proved the generic drug's equivalence and resulted in licensing of the product according to EU regulations, allowing its sales in Europe.

- Assisted in planning experimental protocols and writing the manuscript
- Prepared solutions for pharmacokinetic investigations

Extra-curricular projects

BioScience Network Lausanne (BSNL) April 2015- present
Vice-president and President September 2015- present

BioScience Network Lausanne (BSNL) is a non-profit student association striving to bridge the gap between academia and industry and to promote the career development of Life Science students through the organization of networking and career events.

- Leadership: re-structured and established collaborations with companies and educational institutions (McKinsey, AstraZeneca, Innovation Forum)
- Fundraising: prepared proposals and created databases, trained team, monitored progress, performed troubleshooting (Funds raised: 5,000 ChF in 6 months)
- Member of the organizing core team for the Life Science Career Day: 600 participants, 50 speakers from industry plus 15 career coaches

ShARE EPFL (student consulting) October 2015- August 2016
Board member of ShARE EPFL August 2016-present

ShARE is a multicultural, non-profit think tank for students that aims to deepen the understanding of the complexities of socio-economic issues through presentations, conferences and consulting-like projects. I worked in a team of four people to provide a competitor and market analysis of a computer vision start up at an early development stage.

- Developed methodologies to research the market, prepared a literature review of existing technologies
- Performed SWOT analysis for key competitors, presented the results in front of the client (EPFL Technology transfer office and a CEO of an early stage startup)

EPFL Doctoral Program in Neuroscience, PhD student representative September 2015- present

- Introduced a new translational skill course, established collaboration between EPFL and UNIL, negotiated ECTS credits

Organizer of Summer School, Zermatt, CH October 2015- September 2016

- Defined and implemented strategy (proposal preparation, program planning, fundraising, marketing)
- Result: 11 speakers, 30 participants, funds raised: 38,000 ChF

Publications in peer-reviewed journals:

Pidpruzhnykova G*, Bonizzato M*, Pavlova N, Micera S, Courtine G. Brain-controlled midbrain neuromodulation enhances locomotion after spinal cord injury. *In preparation for Brain* (* equally contributed with Bonizzato M)

Bonizzato M, **Pidpruzhnykova G**, Formento E, Pavlova N, Micera S, Courtine G. Brain-controlled modulation of spinal circuits improves locomotor recovery after spinal cord injury. *In preparation for PNAS*

Veit L, **Pidpruzhnykova G**, Nieder A. Learning Recruits Neurons Representing Previously Established Associations in the Corvid Endbrain. J Cogn Neurosci. 2017 May 30:1-13. doi: 10.1162.

Veit L, **Pidpruzhnykova G**, Nieder A. Associative learning rapidly establishes neuronal representations of upcoming behavioral choices in crows. Proc Natl Acad Sci U S A. 2015 Dec 8;112(49):15208-13. doi: 10.1073.

Pidpruzhnykova G.J., Kuharskiy V.M., Dzubenko N.V., Tolstanova G.M. Efficacy of D2 dopamine receptor agonists in experimental ulcerative colitis treatment (UKR) // Poltavskyj Visnyk. – 2010. – № 4. – P. 64-66.

Conference papers and posters:

Pidpruzhnykova G, Bonizzato M, Pavlova N, Martinez-Gonzalez C, Micera S, Courtine G. Brain-controlled neuromodulation of mesencephalic locomotor center to enhance recovery after SCI. [NNBE Summer SChool], (Zermatt. August, 2016).

Pidpruzhnykova G, Martinez-Gonzalez C, Friedli L, Beauparlant J, Baud L, Duis S, Ulrich G, Courtine G. Neuroprosthetic rehabilitation restores supraspinal control of movement after a severe acute and chronic contusion of the spinal cord due to activity-dependent reorganization of reticulospinal neurons. . [OptoDBS], (Geneva. May, 2015).

Pidpruzhnykova G, Martinez-Gonzalez C, Friedli L, Beauparlant J, Baud L, Duis S, Ulrich G, Courtine G. Neuroprosthetic rehabilitation restores supraspinal control of movement after a severe acute and chronic contusion of the spinal cord. [Society For Neuroscience], (Washington DC. November, 2014).

Pidpruzhnykova G, Friedli L, Beauparlant J, Martinez-Gonzalez , Baud L, Duis S, Ulrich G, Courtine G. Neuroprosthetic rehabilitation restores supraspinal control of movement after a severe acute and chronic contusion of the spinal cord [Neurotrauma Summer School], (Toledo. June, 2014)

Brugger D., **Pidpruzhnykova G.,** Schwarz C. Increasing the spatial resolution of cortical microstimulation. [Society For Neuroscience], (New Orleans. October 17, 2012) - P. 65.

Pidpruzhnykova G., Kuharskiy V., Tolstanova G. Role of D2 and D3 dopamine receptors in the pathogenesis of experimental ulcerative colitis: Programme and abstracts [Young physiologists' symposium], (Manchester, England, 28th-29th June 2010). - P. 37-38.

Conference presentations:

Oral presentation "Laminar variability of detection thresholds in rat barrel cortex" 13th Conference of Junior Neuroscientists of Tuebingen, Germany, November 12th, 2012.

Oral presentation "Visual prostetics: biological issues" Heilig Kreuztal seminar, Gratuate Germany, June 2012.

Workshops and Summer schools:

- School on neurophysiology and biomedical engineering – Zermatt, Switzerland — August 2015
- Neurotrauma summer school - Fundación Ortega y Gasset, Toledo, Spain — June 2014
- Electrophysiology lab practical - Graduate Training Center of Neuroscience. Tübingen — August 2012
- Analysis and models in Neurophysiology - Bernstein Center Freiburg, Germany — October 2012

Awards:

- Winner of the "Max Planck Society" Scholarship — 2011 - 2013
- Winner of the "Zavtra.UA" Scolarship from The Victor Pinchuk Foundation — 2011
- Highschool graduation: Silver Medal "For high academic success" — 2007
- Winner of Kyiv Small Academy of Sciences competition: second prize. — 2007
- Winner of Kyiv Olympiad in Biology: third prize. — 2006 - 2007

Technical skills

- **Laboratory techniques:** behavioral training of rats and crows, electrophysiology, optogenetics, various surgeries in rodents, anatomical tissue analysis (immunohistochemistry), fluorescent imaging
- **Computer software:** Microsoft office (Word, Excel, PowerPoint, Outlook), Image processing (Adobe Illustrator), Note sharing (Evernote, Dropbox, Google collaborative software), Project management (Trello, Slack)
- **Data analysis:** Statistics (Prism), Locomotion (Vicon Nexus, Matlab), Histology (OlyVIA, Neurolucida)
- **Languages:** Russian & Ukrainian (native), English (fluent), German C1

Interests and hobbies

Dancing (salsa, bachata, classic ballroom), hiking, snowboarding, cultural travel and extreme sports (sky diving)

Geneva, November 2017